PRODUCTION OF NOVEL MANUFACTURED PLASTIC AGGREGATE AND ITS UTILISATION IN CONCRETE

By

Fahad Khshim Alqahtani

A thesis submitted to the University of Birmingham for the degree of

DOCTOR OF PHILOSOPHY

School of Civil Engineering
College of Engineering and Physical Sciences
University of Birmingham
July 2017

UNIVERSITY OF
BIRMINGHAM

University of Birmingham Research Archive

e-theses repository

This unpublished thesis/dissertation is copyright of the author and/or third parties. The intellectual property rights of the author or third parties in respect of this work are as defined by The Copyright Designs and Patents Act 1988 or as modified by any successor legislation.

Any use made of information contained in this thesis/dissertation must be in accordance with that legislation and must be properly acknowledged. Further distribution or reproduction in any format is prohibited without the permission of the copyright holder.

ABSTRACT

Plastic waste and its low recycling rate make a significant contribution towards the pollution of the environment. Therefore, it is essential that plastic waste is utilised in different applications. One of the applications is its use either as an aggregate or to form aggregate for use in the concrete. New sustainable construction materials (i.e. lightweight aggregates) were developed using plastic waste and by-product or low cost granular materials. These aggregates have a relatively low density and water absorption as compared to conventional aggregates, and were successfully used to produce sustainable or green lightweight concrete.

The new aggregates were used to replace the conventional coarse fraction of either normal weight or lightweight aggregates at full or partial replacements; where both properties of fresh and hardened concrete were investigated. It was found that the effect of the replacement level of the conventional aggregate with the manufactured recycled plastic aggregates (i.e. RP2F1A, RP3F3A) was less prominent on density as compared to the other properties. The hardened concrete showed a reduction in mechanical properties (compressive, flexural, splitting tensile strength, modulus of elasticity), with an increase in the proportions of manufactured recycled plastic aggregates in the mix.

The assessment of durability properties, thermal conductivity and curing temperature was also carried out. The concrete ductility, drying shrinkage, creep strain and thermal conductivity increased as the content of manufactured recycled plastic aggregate increased in the mix. Whilst, the chloride permeability was found to decrease with an increase in the percentage of recycled plastic aggregate. Microscopic investigation was also carried out which demonstrated significant differences in the microstructure of aggregates, alongside different modes of failure between aggregates and cement paste. Finally, models were proposed to predict the mechanical and durability properties utilising the results of this study.

The overall results of this research suggest that two certain types of the produced aggregates exhibited higher potential for use as a main source of coarse aggregate in structural sustainable lightweight concrete mixes.

PUBLICATIONS

From the results of this study, two patents have been granted and two journal papers have been published. The research work was presented in six conferences/exhibitions; where two conference papers were published. These publications are as follows:

- Alqahtani, F. K., Khan, M. I. and Ghataora, G., 2014. Synthetic aggregate for use in concrete. *U.S. Patent 8,921,463.*

- Alqahtani, F. K., Khan, M. I. and Ghataora, G., 2015. Synthetic aggregate for use in concrete. *K.S.A. Patent 3960.*

- Alqahtani, F.K., Ghataora, G., Khan, M.I., Dirar, S., Kioul, A. and Al-Otaibi, M., 2015. Lightweight concrete containing recycled plastic aggregates. *2015-ICMEP*.

- Alqahtani, F. K., Khan, M. I., Ghataora, G. and Dirar, S., 2016. Production of Recycled Plastic Aggregates and Its Utilization in Concrete. *Journal of Materials in Civil Engineering-ASCE*, 04016248.

- Alqahtani, F. K., Ghataora, G., Khan, M. I. and Dirar, S., 2016. Innovative recycled plastic lightweight aggregate. *9th Saudi Student Conference*, Birmingham, UK, Feb 2016.

- Alqahtani, F. K., Ghataora, G., Khan, M. I. and Dirar, S., 2017. Novel lightweight concrete containing manufactured plastic aggregate. *Construction and Building Materials*, 148, 386-397.

PRIZE

- Two acknowledgement letters from the Saudi Arabian Cultural Attaché in London for the publications during the PhD study period.

- Best Paper Award was received in the 9th Saudi Student Conference (Birmingham, UK)

- A silver Medal was awarded in 44th International Exhibition of Inventions of Geneva.

DEDICATION

This thesis is dedicated to the soul of my dear father (may Allah bless him) who encouraged me to achieve my goals and with no doubt, to my beloved mother.

ACKNOWLEDGEMENTS

I am extremely grateful to my mother, brothers and sisters for their encouragement and support during the period of PhD study.

I would like to express my deep thanks to my supervisors, Dr Gurmel Ghataora, Dr Samir Dirar and Prof. M. Iqbal Khan, for their guidance and advice during the period of this study. I am also grateful to King Saud University (KSU) for sponsoring and funding this research project and to the University of Birmingham for academic and supervision assistance. The laboratory staff of KSU and UoB are also acknowledged for their assistance during laboratory work.

In addition, I also extend my appreciations to the SABIC research centre at KSU, particularly to Mr Abdullah Al Otabia; Dr Kioul and Mr Manssor Al Otabia for supporting this research. The procurement of Lytag aggregate by Lytag Limited in the UK was also essential for this research.

Last but not least, my appreciation goes to my friends and colleagues: Mr Abdulaziz Alshahrani; Mr Rshad Al Malki; Mr Hadi Al Asmari; Mr Gunim Al Onazi; Mr Hassan Al Solami; Mr Sharaz Hossain;Mr Shamas Soukat; Mr Essam Sultan; Mr Abullah Alwakeel; Dr Salem Alqahtani; Dr Fahad Al Mutlaq; Dr Walid Zahid; Dr Khalid Alqahtani; Dr Galal Fares; Dr Sami Alsane; Dr Arif Abadal; Mr Fahid Aslam; Mr Saif Alzabeebee; Mr Giulio Vita; Mr Abdulsattar; Mr Jalal Mahjoob; Mr Zafer Qudri; Mr Wasim for their valuable discussion, advice and encouragement.

This thesis was copy edited for the conventions of language, grammar and spelling by Janet's Proofreading Service.

LIST OF ABBREVIATIONS

ACI	American Concrete Institute
ASTM	American Society for Testing and Materials
BS EN	British Standards and European Standards
CA	Coarse aggregate
FA	Fine aggregate
FAF	Fly ash filler
ITZ	Interfacial transition zone
LAC	Concrete made using Lytag aggregate (LYA)
LLDPE	Linear low density polyethylene
LWA	Conventional volcanic lightweight coarse aggregate
LWC	Concrete made using volcanic lightweight aggregate (LWA)
LYA	Lytag coarse aggregate
NA	Normal weight coarse aggregate
NC	Concrete made using normal weight aggregate (NA)
PET	Polyethylene terephthalate
QFF	Quarry fine filler
RP1F1A	Recycled plastic aggregate made using 50 % LLDPE and 50 % RSF
RP1F1C0.5	Concrete mix containing RP1F1A at w/c of 0.5
RP1F1C0.6	Concrete mix containing RP1F1A at w/c of 0.6
RP1F2A	Recycled plastic aggregate made using 50 % LLDPE and 50 % FAF
RP1F2C0.5	Concrete mix containing RP1F2A at w/c of 0.5
RP1F2C0.6	Concrete mix containing RP1F2A at w/c of 0.6
RP1F3A	Recycled plastic aggregate made using 50 % LLDPE and 50 % QFF
RP1F3C0.5	Concrete mix containing RP1F3A at w/c of 0.5
RP1F3C0.6	Concrete mix containing RP1F3A at w/c of 0.6
RP2F1A	Recycled plastic aggregate made using 30 % LLDPE and 70 % RSF
RP2F1C0.5	Concrete mix containing RP2F1A at w/c of 0.5
RP2F1C25	Concrete mix containing RP2F1A at a replacement level of 25%
RP2F1C50	Concrete mix containing RP2F1A at a replacement level of 50%
RP2F1C75	Concrete mix containing RP2F1A at a replacement level of 75%
RP2F1C100	Concrete mix containing RP2F1A at a replacement level of 100%
RP2F2A	Recycled plastic aggregate made using 30 % LLDPE and 70 % FAF
RP2F2C0.5	Concrete mix containing RP2F2A at w/c of 0.5
RP2F3A	Recycled plastic aggregate made using 30 % LLDPE and 70 % QFF
RP2F3C0.5	Concrete mix containing RP2F3A at w/c of 0.5
RP3F1A	Recycled plastic aggregate made using 50 % PET and 50 % RSF
RP3F1C0.5	Concrete mix containing RP3F1A at w/c of 0.5
RP3F2A	Recycled plastic aggregate made using 50 % PET and 50 % FAF

RP3F2C0.5	Concrete mix containing RP3F2A at w/c of 0.5
RP3F3A	Recycled plastic aggregate made using 50 % PET and 50 % QFF
RP3F3C0.5	Concrete mix containing RP3F3A at w/c of 0.5
RP3F3C25	Concrete mix containing RP3F3A at a replacement level of 25%
RP3F3C50	Concrete mix containing RP3F3A at a replacement level of 50%
RP3F3C75	Concrete mix containing RP3F3A at a replacement level of 75%
RP3F3C100	Concrete mix containing RP3F3A at a replacement level of 100%
RP4F1A	Recycled plastic aggregate made using 30 % PET and 70 % RSF
RP4F1C0.5	Concrete mix containing RP4F1A at w/c of 0.5
RP4F2A	Recycled plastic aggregate made using 30 % PET and 70 % FAF
RP4F2C0.5	Concrete mix containing RP4F2A at w/c of 0.5
RP4F3A	Recycled plastic aggregate made using 30 % PET and 70 % QFF
RP4F3C0.5	Concrete mix containing RP4F3A at w/c of 0.5
RPA	Recycled plastic aggregate
RPA Group 1	Recycled plastic aggregate comprising the following types of RPA (RP1F1A, RP1F2A, RP1F3A, RP2F1A, RP2F2A, RP2F3A)
RPA Group 2	Recycled plastic aggregate comprising the following types of RPA (RP3F1A, RP3F2A, RP3F3A, RP4F1A, RP4F2A, RP4F3A)
RPAC-1	Recycled plastic aggregate concrete containing RPA Group 1
RPAC-2	Recycled plastic aggregate concrete containing RPA Group 2
RSF	Red dune sand filler
SLA	Synthetic lightweight aggregate
WPLA	Waste plastic lightweight aggregate
A	Air content
E_c	Modulus of elasticity
f_c	Cylinder compressive strength
f_r	Flexural strength
f_t	Splitting tensile strength
RH	Relative humidity
S_l	Slump
T	Age at any time
t_o	Age at loading
v/s	Volume to surface ratio
W/C	Water to cement ratio
ρ_a	Fine to total aggregate ratio
γ_c	Modification factor
γ_w	Dry density
λ	Ultimate creep coefficient factor

Table of Contents

ABSTRACT ..... **II**

PUBLICATIONS ..... **IV**

DEDICATION ..... **V**

ACKNOWLEDGEMENTS ..... **VI**

LIST OF ABBREVIATIONS ..... **VII**

LIST OF FIGURES ..... **XV**

LIST OF TABLES ..... **XXII**

CHAPTER 1: INTRODUCTION **1**

1.1 BACKGROUND 1

1.2 OVERVIEW OF PLASTICS 4

1.2.1 Plastic production, waste generation and recycling *4*

1.2.2 Limitations of the recycling of plastic *6*

1.2.3 Disposal of plastic waste *7*

1.3 OVERVIEW OF INDUSTRIAL AND MINERAL WASTES OR GRANULAR MATERIALS 9

1.3.1 Fly ash *9*

1.3.2 Quarry fines *11*

1.3.3 Dune sand *12*

1.4 STATEMENT OF THE PROBLEM 14

1.5 AIM AND OBJECTIVES 15

1.6 RESEARCH HYPOTHESES AND INNOVATIVE FEATURES OF THE RESEARCH 16

1.7 THESIS OUTLINE 17

CHAPTER 2: LITERATURE REVIEW **18**

2.1 GENERAL 18

2.2 LIGHTWEIGHT CONCRETE 18

2.2.1 Lightweight concrete using natural lightweight aggregates *20*

2.2.2 Lightweight concrete using synthetic aggregates *21*

2.3 SYNTHETIC PLASTIC 23

2.3.1 Shredded or virgin plastic particles as aggregate *23*
2.3.2 Plastic based aggregates *28*
2.4 FRESH PROPERTIES OF CONCRETE 32
2.4.1 Slump *32*
2.4.2 Fresh density *34*
2.5 HARDENED PROPERTIES OF CONCRETE 36
2.5.1 Dry density *36*
2.5.2 Compressive strength *39*
2.5.3 Splitting tensile strength *42*
2.5.4 Flexural strength *45*
2.5.5 Modulus of elasticity *47*
2.5.6 Poisson's ratio *49*
2.5.7 Stress-strain response and failure mechanism *50*
2.5.8 Abrasion resistance *53*
2.5.9 Microstructure analysis *53*
2.5.10 Drying shrinkage *55*
2.5.11 Creep *56*
2.6 DURABILITY RELATED PROPERTIES 57
2.6.1 Water absorption *57*
2.6.2 Chloride ion penetration *58*
2.7 PHYSICAL PROPERTIES 59
2.7.1 Fire resistance *59*
2.7.2 Thermal conductivity *59*
2.8 SUMMARY OF EXISTING DEVELOPMENTS 60
2.9 GAP OF KNOWLEDGE 61

CHAPTER 3: MATERIALS AND EXPERIMENTAL DESIGN 63

3.1 GENERAL 63
3.2 MATERIALS USED 63
3.2.1 Recycled plastic waste *64*
3.2.2 Filler materials *65*
3.2.3 Coarse and fine aggregates *69*
3.3 RESEARCH METHODOLOGY AND TECHNIQUES USED 71

3.3.1 Research programme in Phase-1 ..... *73*
3.3.2 Research programme in Phase-2 ..... *73*
3.3.3 Research programme in Phase-3 ..... *75*
3.4 CONCRETE MIX DESIGN 78
3.5 MIXING, CASTING AND CURING 81
CHAPTER 4: MANUFACTURE AND CHARACTERISATION OF RECYCLED PLASTIC AGGREGATE 82
4.1 GENERAL 82
4.2 SELECTION, CHARACTERIZATION, OPTIMIZATION AND PREPARATION OF MATERIALS USED 82
4.2.1 Selection and characterization of recycled plastic and filler types *82*
4.2.2 Optimizing the mixing proportions *83*
4.2.3 Preparation of composite mix *84*
4.3 TECHNIQUES USED FOR MANUFACTURING OF RECYCLED PLASTIC AGGREGATE 85
4.3.1 General *85*
4.3.2 Using a heating mixer technique *85*
4.3.3 Using an extrusion technique *87*
4.3.4 Compression moulding press technique *89*
4.4 CHARACTERIZATION OF MANUFACTURED RECYCLED PLASTIC AGGREGATE 95
4.4.1 Shape and texture *99*
4.4.2 Particle size distribution *101*
4.4.3 Fineness modulus *105*
4.4.4 Bulk specific gravity *106*
4.4.5 Water absorption *108*
4.4.6 Unit weight *110*
4.4.7 Aggregate void content *112*
4.4.8 Strength *113*
4.4.9 Microscopic investigation *115*
4.4.10 Ash test *118*
4.5 COST ANALYSIS OF RECYCLED PLASTIC AGGREGATE 119
4.6 SUMMARY 121

CHAPTER 5: INVESTIGATION FOR RECYCLED PLASTIC AGGREGATE OPTIMIZATION 123

5.1 GENERAL 123
5.2 FRESH PROPERTIES OF RECYCLED PLASTIC AGGREGATES CONCRETE 125
5.2.1 Slump 125
5.2.2 Fresh density 128
5.3 HARDENED PROPERTIES OF RECYCLED PLASTIC AGGREGATES CONCRETE 131
5.3.1 Dry density 131
5.3.2 Compressive strength 133
5.3.3 Flexural strength 138
5.3.4 Microscopic investigations 142
5.3.5 Mechanism of failure 145
5.4 DURABILITY RELATED PROPERTIES OF RECYCLED PLASTIC AGGREGATES CONCRETE 146
5.5 OPTIMIZATION OF WATER TO CEMENT RATIOS 150
5.6 SELECTION OF RPA CONCRETE OPTIMIZED MIXES 150
5.6.1 Optimized mix selected from RPAC-1 150
5.6.2 Optimized mix selected from RPAC-2 152
5.7 SUMMARY 153

CHAPTER 6: INVESTIGATION OF FRESH AND HARDENED PROPERTIES OF OPTIMIZED CONCRETE MIXES 154

6.1 GENERAL 154
6.2 FRESH PROPERTIES OF RP2F1C AND RP3F3C MIXES 155
6.2.1 Slump 155
6.2.2 Fresh density 157
6.3 HARDENED PROPERTIES OF RP2F1C AND RP3F3C MIXES 159
6.3.1 Dry density 160
6.3.2 Compressive strength 162
6.3.3 Flexural strength 165
6.3.4 Splitting tensile strength 167
6.3.5 Modulus of elasticity 169
6.3.6 Stress-strain behaviour 171

6.3.7 Poisson's ratio *173*
6.3.8 Abrasion resistance *175*
6.3.9 Microscopic investigation *177*
6.4 CORRELATION BETWEEN MECHANICAL PROPERTIES 180
6.4.1 Correlation between splitting tensile strength and compressive strength *180*
6.4.2 Correlation between flexural strength and compressive strength *183*
6.4.3 Correlation between modulus of elasticity and compressive strength *186*
6.5 SUMMARY 189

CHAPTER 7: INVESTIGATION OF DURABILITY AND PHYSICAL PROPERTIES OF OPTIMIZED CONCRETE MIXES 191

7.1 GENERAL 191
7.2 DURABILITY RELATED PROPERTIES OF RP2F1C AND RP3F3C MIXES 192
7.2.1 Water absorption *192*
7.2.2 Chloride permeability *194*
7.2.3 Drying shrinkage *196*
7.2.4 Creep *199*
7.3 PHYSICAL PROPERTIES OF RP2F1C AND RP3F3C MIXES 202
7.3.1 Thermal conductivity *202*
7.3.2 Curing temperature *203*
7.4 CORRELATION OF DURABILITY PROPERTIES 205
7.4.1 Correlation between chloride permeability and compressive strength *205*
7.4.2 Correlation between creep coefficient and time *206*
7.5 SUMMARY 212

CHAPTER 8: CONCLUSIONS AND RECOMMENDATIONS FOR FURTHER STUDIES 214

8.1 GENERAL 214
8.2 CONCLUSIONS 214
8.3 RECOMMENDATIONS FOR FURTHER WORKS 218

REFERENCES 221

APPENDICES 242

APPENDIX A1: TESTS CONDUCTED ON COARSE AGGREGATE 242
APPENDIX A2: TESTS CONDUCTED ON CONCRETE 244
A2.1 General *244*
A2.2 Fresh properties *244*
A2.3 Hardened properties *246*
A2.4 Durability properties *251*
A2.5 Physical properties *256*
APPENDIX A3: SAMPLE CALCULATIONS OF MIX DESIGN 259
APPENDIX A4: INVESTIGATING OF SPECIMEN SIZE EFFECT 263

LIST OF FIGURES

Figure 1.1: Burning of plastic waste (Deccan Chronicle, 2016) 8
Figure 1.2: Disposal Plastic waste into open land (Shutterstock, 2017) 8
Figure 1.3: Dumping plastic waste into seas and oceans (BBC, 2014) 8
Figure 1.4: Heaps of fly ash (Irvin, 2010) 10
Figure 1.5: Landfill with fly ash (Rankin, 2017) 10
Figure 1.6: Quarry fines heaps at Gritstone quarry (Mitchell, 2016) 12
Figure 1.7: Road blocking due to the movement of dune sand (SoilSolutions, 2017) 13
Figure 1.8: Dune sand effect on railway track (RWDI, 2017) 13
Figure 2.1: PET aggregates (Hannawi et al., 2010) 24
Figure 2.2: Type of PET particles (Rahmani et al., 2013) 24
Figure 2.3: Coarse PUR foam waste (Fraj et al., 2010) 25
Figure 2.4: PVC waste; before crushing (left) and after crushing (right) (Kou et al., 2009) ... 25
Figure 2.5: Sample of waste plastic (Ismail and Al-Hashmi, 2008) 26
Figure 2.6: Expanded polystyrene beads (Xu et al., 2012) 26
Figure 2.7: Comparison of plastic waste aggregate (a) before heating and (b) after heating (Al Bakri et al., 2011) 28
Figure 2.8: LDPE before and after melt-densification (Reddy et al., 2012) 28
Figure 2.9: Shape of WPLA (Choi et al., 2005) 29
Figure 2.10: Shape of WPLA (Choi et al., 2009) 29
Figure 2.11: SLA (Kashi et al., 1999) 29
Figure 2.12: SLAs made using (a) 0:100, (b) 35:65 (b) and (c) 80:20 of fly ash to plastic (Jansen et al., 2001) 30
Figure 2.13: Variation in (a) dry density and (b) reduction in dry density (%) of concrete with replacement level of normal CA with shredded or virgin plastic 36
Figure 2.14: Variation in (a) dry density and (b) reduction in dry density (%) of concrete with replacement level of normal FA with shredded or virgin plastic 37
Figure 2.15: Variation in compressive strength of concrete with replacement level of CA with shredded or virgin plastic 39
Figure 2.16: Variation in compressive strength of concrete with replacement level of FA with shredded or virgin plastic 40

Figure 2.17: Variation in splitting tensile strength of concrete with replacement level of CA with shredded or virgin plastic 43
Figure 2.18: Variation in splitting tensile strength of concrete with replacement level of FA with shredded or virgin plastic 44
Figure 2.19: Variation in splitting tensile strength of concrete with plastic based aggregate incorporation 45
Figure 2.20: Variation in flexural strength of concrete with shredded or virgin plastic incorporation 46
Figure 2.21: Variation in modulus of elasticity of concrete with replacement level of CA with shredded or virgin plastic 47
Figure 2.22: Variation in modulus of elasticity of concrete with replacement level of FA with shredded or virgin plastic 48
Figure 2.23: Comparison between stress-strain response for concrete containing plastic particles and normal concrete 51
Figure 2.24: Stress versus axial and lateral strain for normal and plastic based aggregate concrete 52
Figure 2.25: SEM of mortar containing PET aggregate (a) 30% (enlargement: 43×), (b) 50% (enlargement: 35×) and (c) 100% (enlargement: 31×) (Marzouk et al., 2007) 54
Figure 2.26: Transition zone between cement paste and (a) WPLA; and (b) natural aggregate (28-day; magnified × 700) (Choi et al., 2005) 55
Figure 2.27: Variation in water absorption of concrete with plastic particles incorporation ... 57
Figure 3.1: Forms of plastics used in manufacturing of RPA 64
Figure 3.2: Fillers (RSF, FAF and QFF) used in manufacturing RPA 66
Figure 3.3: Particle size distribution of fillers (RSF, FAF and QFF) 67
Figure 3.4: Microstructure analysis of (a) RSF, magnification: 150 ×, (b) FAF, magnification: 2000 × and (C) QFF, magnification: 2500 × 68
Figure 3.5: Types of coarse aggregate used in this study: NA; LWA and LYA 69
Figure 3.6: Particle size distribution of normal weight (NA) and lightweight (LWA) coarse aggregates 70
Figure 3.7: Particle size distribution of red sand, crushed sand and combination of red and crushed sand 71
Figure 3.8: Flow chart of research phases 72

Figure 4.1: RPA made using 20:80 PET to QFF 84
Figure 4.2: Heating mixer machine 86
Figure 4.3: Manual hydraulic press 86
Figure 4.4: Cube of composite 87
Figure 4.5: RPA produced using heating mixer machine 87
Figure 4.6: Manufacturing process of RPA using extrusion machine 88
Figure 4.7: RPA produced using extrusion process 89
Figure 4.8: Manufacturing process of RPA using compression moulding press technique 90
Figure 4.9: Mould filled with mixture (recycled plastic and filler) 91
Figure 4.10: Mould filled with mixture and placed between two heated platens 91
Figure 4.11: Heated platens and control panel of 100 ton Wabash press machine 92
Figure 4.12: Sheets/slabs of RPA made from (a) LLDPE with RSF and (b) made from PET with QFF 92
Figure 4.13:12 mm grinding mesh 92
Figure 4.14: RPA produced using a crushing machine (Schorch) 93
Figure 4.15: RPAs produced using compression press technique i.e. (a) RP2F1A and (b) RP4F1A 93
Figure 4.16: RPA produced using shredded PET plastic with QFF 94
Figure 4.17: (a) Top view and (b) side view of RPA produced using pellet PET and QFF 94
Figure 4.18: Different types of RPAs (Group 1) made with LLDPE and fillers 96
Figure 4.19: Different types of RPAs (Group 2) made with PET and fillers 96
Figure 4.20: Particle size distribution curves for RPAs (Group 1) and LWA 102
Figure 4.21: Particle size distribution curves for RPAs (Group 2) and LWA 103
Figure 4.22: Particle size distribution curves for RPAs (Group 1) and NA 104
Figure 4.23: Particle size distribution curves for RPAs (Group 2) and NA 104
Figure 4.24: Fineness modulus of RPAs (Group 1) compared to NA and LWA 105
Figure 4.25: Fineness modulus of RPAs (Group 2) compared to NA and LWA 105
Figure 4.26: Bulk specific gravity of RPAs (Group 1) compared with NA, LWA and LYA 106
Figure 4.27: Bulk specific gravity of RPAs (Group 2) compared with NA, LWA and LYA 106
Figure 4.28: Water absorption of RPAs (Group 1) compared to NA, LWA and LYA 108
Figure 4.29: Water absorption of RPAs (Group 2) compared to NA, LWA and LYA 108
Figure 4.30: Dry unit weight of RPAs (Group 1) compared to NA, LWA and LYA 110

Figure 4.31: Dry unit weight of RPAs (Group 2) compared to NA, LWA and LYA 110
Figure 4.32: Void content of RPAs (Group 1) compared to NA, LWA and LYA..... 112
Figure 4.33: Void content of RPAs (Group 2) compared to NA, LWA and LYA..... 112
Figure 4.34: Aggregate crushing strength of (a) LWA and (b) RPAs (Group 1)..... 114
Figure 4.35: Impact value of RPAs (Group 2) compared to NA, LYA and LWA 114
Figure 4.36: SEM images of RPAs (Group 1) made with (a,b) RSF, (c) FAF and (d) QFF embedded in LLDPE matrix..... 116
Figure 4.37: SEM images of RPAs (Group 2) made with (a) RSF and (b) QFF at magnification: 100×..... 117
Figure 4.38: Optical microscopic images of (a) LWA, and RPAs (Group 2) made with (b) RSF, (c) FAF and (d) QFF 118
Figure 4.39: Ash percentages for three samples (S1, S2 and S3) of RP1F1A 119
Figure 5.1: Slump of RPAC-1, LWC and NC at W/C of 0.50 126
Figure 5.2: Slump of RPAC-2, LWC and NC at W/C of 0.50 127
Figure 5.3: Effect of W/C on slump of RPAC-1, LWA and NC..... 128
Figure 5.4: Fresh density of RPAC-1, LWC and NC at W/C of 0.50 129
Figure 5.5: Fresh density of RPAC-2, LWC and NC at W/C of 0.50 130
Figure 5.6: Effect of W/C on fresh density of RPAC-1, LWA and NC..... 130
Figure 5.7: 28-day dry density of RPAC-1, LWC and NC at W/C of 0.50..... 131
Figure 5.8: 28-day dry density of RPAC-2, LWC and NC at W/C of 0.50..... 132
Figure 5.9: Effect of W/C on 28-day dry density of RPAC-1, LWA and NC 133
Figure 5.10: Cube compressive strength of RPAC-1, LWC and NC at 7, 14 and 28 days and at W/C of 0.50 134
Figure 5.11: Cube compressive strength of RPAC-2, LWC and NC at 7, 14 and 28 days and at W/C of 0.50 136
Figure 5.12: Effect of W/C on 28-day cube compressive strength of RPAC-1, LWA and NC 137
Figure 5.13: Flexural strength of RPAC-1, NC and LWC at 7, 14 and 28 days and at W/C of 0.50 138
Figure 5.14: Flexural strength of RPAC-2, NC and LWC at 7, 14 and 28 days and at W/C of 0.50 139
Figure 5.15: Effect of W/C on 28-day flexural strength of RPAC-1, NA and LWC..... 141

Figure 5.16: SEM images of (a) LWC, (b) RP2F1C, (c) RP2F2C and (d) RP2F3C (28 days, magnified×2000) 143
Figure 5.17: Optical microscopic images of (a) LWC, (b) RP4F1C, (c) RP4F2C and (d) RP4F3C (28 days) 144
Figure 5.18: Flexural strength mode of failure for (a) LWC and (b, c, d) RPAC-1 145
Figure 5.19: Types of cracks for (a) LWC and (b) RPAC-1 146
Figure 5.20: 28-day chloride permeability of RPAC-1, NC and LWC at W/C of 0.50 147
Figure 5.21: 28-day chloride permeability of RPAC-2, NC and LWC at W/C of 0.50 148
Figure 5.22: Effect of W/C ratio on 28-day chloride permeability of RPAC-1, NC and LWC 149
Figure 6.1: Results of slump of RP2F1Cs, LWC and LAC 155
Figure 6.2: Results of slump of RP3F3Cs, NC and LAC 156
Figure 6.4: Results of fresh density of RP2F1Cs, LWC and LAC 158
Figure 6.5: Results of fresh density of RP3F3Cs, NC and LAC 159
Figure 6.6: Results of 28-day dry density of RP2F1Cs, LWC and LAC 160
Figure 6.7: Results of 28-day dry density of RP3F3Cs, NC and LAC 161
Figure 6.8: Results of 28-day cylinder compressive strength of RP2F1Cs, LWC and LAC . 162
Figure 6.9: Results of 28-day cylinder compressive strength of RP3F3Cs, NC and LAC 164
Figure 6.10: Results of 28-day flexural strength of RP2F1Cs, LWC and LAC 165
Figure 6.11: Results of 28-day flexural strength of RP3F3Cs, NC and LAC 166
Figure 6.12: Results of 28-day splitting tensile strength of RP2F1Cs, LWC and LAC 167
Figure 6.13: Results of 28-day splitting tensile strength of RP3F3Cs, NC and LAC 168
Figure 6.14: Results of 28-day elastic modulus of RP2F1Cs, LWC and LAC 169
Figure 6.15: Results of 28-day elastic modulus of RP3F3Cs, NC and LAC 170
Figure 6.16: Stress-strain curves of RP2F1Cs, LWC and LAC 171
Figure 6.17: Stress-strain curves of RP3F3Cs, NC and LAC 173
Figure 6.18: Results of 28-day Poisson's ratio of RP2F2Cs, LWC and LAC 174
Figure 6.19: Results of 28-day Poisson's ratio of RP3F3Cs, NC and LAC 175
Figure 6.20: Results of mass loss at 6 min of abrasion of RP2F1Cs and LWC at 28 day 176
Figure 6.21: Results of mass loss at 6 min of abrasion of RP3F3Cs and NC at 28 day 177
Figure 6.22: SEM images of (a) LAC, (b) LWC and (c) RP2F1C100 (28 days, enlargement: 2000×) 179

Figure 6.23: Optical microscopic images of (a) LAC, (b) LWC and (c) RP2F1C100 (28 days) 179
Figure 6.24: Correlation between splitting tensile strength and compressive strength 180
Figure 6.25: Comparison between the experimental results and the predictions of the analytical models relating splitting tensile strength to compressive strength of RP2F1C 181
Figure 6.26: Comparison between the experimental results and the predictions of the analytical models relating splitting tensile strength to compressive strength of RP3F3C 182
Figure 6.27: Correlation between flexural strength and compressive strength 183
Figure 6.28: Comparison between the experimental results and the predictions of the analytical models relating flexural strength to compressive strength of RP2F1C 185
Figure 6.29: Comparison between the experimental results and the predictions of the analytical models relating flexural strength to compressive strength of RP3F3C 185
Figure 6.30: Correlation between elastic modulus and compressive strength 187
Figure 6.31: Comparison between the experimental results and the predictions of the analytical models relating elastic modulus to compressive strength of RP2F1C..... 188
Figure 6.32: Comparison between the experimental results and the predictions of the analytical models relating elastic modulus to compressive strength of RP3F3C..... 188
Figure 7.1: Results of 28-day water absorption of RP2F1Cs, LWC and LAC 192
Figure 7.2: Results of 28-day water absorption of RP3F3Cs, NC and LAC..... 193
Figure 7.3: Results of 28-day chloride permeability of RP2F1Cs, LWC and LAC..... 194
Figure 7.4: Results of 28-day chloride permeability of RP3F3Cs, NC and LAC 195
Figure 7.5: Results of drying shrinkage of RP2F1Cs, LWC and LAC 197
Figure 7.6: Results of drying shrinkage of RP3F3Cs, NC and LAC 198
Figure 7.7: Results of time dependent strain for loaded specimens of RP3F3Cs and NC 201
Figure 7.8: Results of shrinkage strain for unloaded specimens of RP3F3Cs and NC 201
Figure 7.9: Results of creep strain of RP3F3Cs and NC 201
Figure 7.10: Results of 28-day thermal conductivity of RP2F1C100 and LWC in saturated and dry conditions 202
Figure 7.11: Results of 28-day compressive strength of RP2F1Cs, RP3F3Cs, LWC and NC at curing temperatures of 20, 30 and 40 °C 204
Figure 7.12: Correlation between 28-day chloride permeability and compressive strength .. 205

Figure 7.13: Comparison between the experimental results and the predictions of the analytical models relating creep coefficient of RP3F3C mixes 208
Figure 7.14: Regression and expermental curves for creep coefficients of RP3F3Cs' mixes210
Figure 7.15: Comparison between proposed model and the experimental results for creep coefficient of RP3F3C mixes 212

LIST OF TABLES

Table 1.1: Proportions for the main components in plastic production and waste stream 4
Table 1.2: Quantity of plastic waste produced, recycled and disposed in different regions 6
Table 2.1: Classification of lightweight concrete 19
Table 2.2: Types of plastic used in concrete 27
Table 2.3: Properties of existing plastic based aggregates 31
Table 2.4: Variation in slump of concrete with shredded or virgin plastic incorporation 32
Table 2.5: Variation in slump of concrete with plastic based aggregate incorporation 34
Table 2.6: Variation in fresh density of concrete with shredded or virgin plastic incorporation 35
Table 2.7: Variation in dry density of concrete with plastic based aggregate incorporation 38
Table 2.8: Variation in compressive strength of concrete with plastic based aggregate incorporation 42
Table 2.9: Variation in elastic modulus of concrete with plastic based aggregate incorporation 49
Table 3.1: Physical properties and basic components of the cement used 64
Table 3.2: Physical, mechanical and thermal properties of LLDPE and PET 65
Table 3.3: Physical properties of fillers (RSF, FAF and QFF) 66
Table 3.4: Elemental contents of filler particles determined by EDX 68
Table 3.5: Properties of coarse and fine aggregates used in this study 70
Table 3.6: Tests conducted and standards used in Phase-1 73
Table 3.7: Tests conducted and standards used in Phase-2 74
Table 3.8: Tests conducted and standards used in Phase-3 77
Table 3.9: Mix proportions per metre cubed for concrete mixes used in Phase-2 80
Table 3.10: Mix proportions per metre cubed for concrete mixes used in Phase-3 80
Table 4.1: Composition of manufactured RPA 95
Table 4.2: Properties of the RPAs manufactured in this study 98
Table 4.3: Comparison between the properties of RPAs and plastic based aggregates produced in previous studies 99
Table 5.1: Summary of RPAs concrete results in comparison with previous studies' findings 124
Table 6.1: Lightweight concrete properties according to ASTM C330/C330M-14 159

Table 6.2: Percentage difference in model predictions for the splitting tensile strength 183
Table 6.3: Percentage difference in model predictions for the flexural strength 186
Table 6.4: Percentage difference in model predictions for the elastic modulus.....189
Table 7.1: Percentage difference in model predictions for the chloride permeability 206
Table 7.2: Parameters of creep coefficient in different models.....207
Table 7.3: Regression analysis results of the RP3F3C mixes 209
Table 7.4: Calculations for calibrating the ACI models for RP3F3C mixes.....211
Table 7.5: Coefficient of correlation of the proposed model for the creep coefficient of RP3F3C mixes.....212

CHAPTER 1: INTRODUCTION

1.1 Background

Population growth, increasing urbanization, rapid technological growth and modern lifestyles have contributed to increase the quantities and types of wastes generated from various sources. In the last five decades, the growth of world's plastic industry has been massive, with an increase in production from around 15 to 322 million metric tons (PlasticsEurope, 2016; Trucost, 2016). Less than 30% of this amount is recycled, while the remaining (31-90%) is either burned or sent to landfill (El-Newehy, 2016; EPA, 2014; PlasticsEurope, 2016; Siddique et al., 2008). This occupies a large area of land and causes major environmental degradation and long-term health risks (Nizami et al., 2015; Ouda and Cekirge, 2014). Therefore, it is clear that despite extensive efforts (e.g. household recycling) the rate of recycling is still on the lower side and is not effective in reducing desired volume of the plastic waste; this is worsen by lack of the international environmental legislation and the prohibitive costs of recycling (Nizami et al., 2015).

Moreover, another major problem being faced by the environment is the accumulation of stockpiles of industrial or mineral wastes (i.e. fly ash and quarry fines), as well as the huge availability of natural granular materials (i.e. dune sand) in many parts of the world (i.e. Australia, China and North America) which has negative economic and environmental impacts.

Therefore, there is tremendous global scope for setting up secondary industries for recycling and using plastic and by-product waste to overcome these problems. The main potential market to utilize these materials successfully is in normal weight or lightweight concrete applications, such as the replacement of aggregates, which represents 60 to 75 percent of the

total volume of concrete. This is one of the effective methods to reduce the risk of these wastes as the quantity of concrete being used all over the world is huge, which allows large volumes of the waste to be utilized. Moreover, by using these wastes as a replacement for aggregates, the demand for natural aggregates will be reduced; as a result this will lower the environmental impact of concrete industry.

Another advantage of utilising these wastes in concrete is the necessity for new lightweight concrete that would address the problems associated with existing lightweight concrete made from either natural or manufactured lightweight aggregates. For example, concrete containing natural lightweight aggregate (i.e. pumice or scoria) lacks durability performance, has high mining and hauling costs, and suffers from high water absorption and excessive drying shrinkage (Choi et al., 2005). In the same context, incorporating one of the manufactured lightweight aggregates such as Lytag (LYA) in concrete adversely affects the durability performance due to its high permeability. In addition, LYA consumes ~~a~~ high energy input (i.e. 1100 °C) and addition of other chemical additives during its manufacturing process making it less sustainable (Chandra and Berntsson, 2002; Clarke, 2005; Dehdezi et al., 2015).

The effect of incorporating either plastic or industrial and mineral wastes as a replacement for aggregates on the performance of concrete has extensively been investigated. However, very few studies have been reported on the applicability of combining these wastes thermally to form a lightweight aggregate and then using in the concrete. Many studies have explored "direct replacement" of plastic as a percentage of natural aggregates in the concrete (Albano et al., 2009; Al-Manaseer and Dalal, 1997; Babu et al., 2006; Batayneh et al., 2007; Ferreira et al., 2012; Ismail and Al-Hashmi, 2008; Juki et al., 2013; Kou et al., 2009; Rahman et al., 2012; Rahmani et al., 2013; Rai et al., 2012; Sabaa and Ravindrarajah, 1997; Saikia and Brito,

2013; Saikia and de Brito, 2014; Tang et al., 2008). It was reported that, the workability and mechanical performance of concrete reduced by the use of plastic as a replacement of natural aggregate in the concrete.

Some studies have explored the effect of using plastic based aggregate on the fresh and hardened properties of the concrete (Choi et al., 2009; Choi et al., 2005; Jansen et al., 2001; Kashi et al., 1999; Slabaugh et al., 2007; Swan and Sacks, 2005). These investigations found that the compressive strength, splitting tensile strength and modulus of elasticity were reduced; whereas the slump showed both increasing and decreasing trends. However, these studies failed to develop a lightweight aggregate similar to those of natural aggregate in shape, size and stiffness. Moreover, the filler used in these studies was fly ash, which is not locally available in many parts of the world including Saudi Arabia. Additionally, an extrusion technique (a limited method for the production of aggregate) was employed in these works, which limited the scope of the aggregates produced. Finally, no large-scale tests were elaborated regarding the concrete containing plastic based aggregate, since the main focus was investigating specific properties (i.e. slump, dry density, compressive strength, splitting tensile strength and modulus of elasticity).

Therefore, this research presents the development of a new lightweight aggregate called recycled plastic aggregate (RPA). Various types of RPAs were manufactured using different recycled plastic and fillers and then were used in concrete as total or partial replacement of normal weight or lightweight coarse aggregate. Thus, a full spectrum of fresh, hardened and durability properties of RPA concrete is presented in comparison with reference mixes.

1.2 Overview of plastics

1.2.1 Plastic production, waste generation and recycling

The growth of plastic use has been exponential over recent decades in tandem with rising standards of living worldwide. Also there are inherent advantages of plastics in terms of being cheap, relatively strong and light, and allowing for simple design and production (Gu and Ozbakkaloglu, 2016). The total output of the world's plastic industry increased from 15 Mt in 1964 to approximately 322 Mt in 2015 (PlasticsEurope, 2016; Trucost, 2016).

Amongst different types of plastic, polyethylene components yield the highest percentages in the production phase and in the waste generation stream, as shown in Table 1.1. However, PET occupies second place in plastic production and third in plastic waste stream, due to its high durability and subsequent longer life period (Clark and Hardy, 2004; Hopewell et al., 2009; IEEP, 2011; PlasticsEurope, 2016; Siddique et al., 2008).

Table 1.1: Proportions for the main components in plastic production and waste stream

Type of plastic		**Global plastic production (%)** (IEEP, 2011)	**Plastic waste stream (%)**	
			USA (EPA, 2014)	**EU** (Siddique et al., 2008)
Polyethylene	Linear/Low density polyethylene (LLDPE/LDPE)	29	23.2	23
	High density polyethylene (HDPE)		17.4	17.3
Polyethylene terephthalate (PET)		20	14.2	8.5
Polypropylene (PP)		18	22.6	18.5
Other		33	22.5	32.7

Plastic has been recovered for reusing, recycling or energy production for a number of economic and environmental benefits: for instance, to decrease the consumption of raw materials and energy used in plastic production, and to reduce the costs of transporting and disposing of plastic waste responsibly, which could save around $18.41 billion each year

(Trucost, 2016). In addition, recycling 1 tonne of plastic yields a reduction of 1.45 tonnes of Carbon dioxide (CO_2) emissions (Hopewell et al., 2009).

There are mechanical, chemical and thermal methods of recycling plastic and using it for energy recovery (Mastellone, 1999; Siddique et al., 2008). Mechanical recycling includes size reduction, sorting, washing, drying, extrusion, water quenching and finally pelletizing (Aznar et al., 2006). Thermal reprocessing involves heating plastic until it melts/softens and then converting it into another shape. Various techniques such as extrusion or compression moulding can be used (Siddique et al., 2008). However, not all plastic can be recycled using these methods. For example, thermoplastic, which includes LLDPE, LDPE, HDPE, PET and PP is recyclable, but thermosetting plastic such as epoxy resin and unsaturated polyester is not mechanically recyclable due to its strong molecular bonds (Hopewell et al., 2009; Siddique et al., 2008).

For these and other reasons (see section 1.2.2), the recycling rate is still not encouraging relative to the quantity of plastic produced, leading to the disposal of large quantities of plastic each year. This is emphasised by the fact that plastic waste generation in Europe in 2014 was around 25.8 Mt, which accounts for more than half of the quantity of plastic produced (i.e. 58 Mt) (Gu and Ozbakkaloglu, 2016; PlasticsEurope, 2016). Similarly, as shown in Table 1.2, the recycling percentage is less than 30% compared with a high disposal rate (>30%). Plastic recycling began in earnest in the US in 1980, with a recycling rate of 0.3%, and despite growing public and policy awareness of the issue, the recycling rate had risen to only 8.8% by 2012 (Gu and Ozbakkaloglu, 2016).

Table 1.2: Quantity of plastic waste produced, recycled and disposed in different regions

Region	Plastic waste generated (Mt)	Plastic recycling (%)	Plastic disposal (%)	References
Saudi Arabia	2.7	10-15	85-90	(Alhumoud et al., 2004; El-Newehy, 2016; Hakami and Seif, 2015; Nizami et al., 2015)
USA	32	8.8	80	(EPA, 2014)
European countries	25.8	29.7	30.8	(Gu and Ozbakkaloglu, 2016; PlasticsEurope, 2016)
UK	3	28	41	(PlasticsEurope, 2015; Siddique et al., 2008)

1.2.2 Limitations of the recycling of plastic

There are several barriers to increase the plastic recycling. These inevitably lead to a high disposal rate and a reduction in the efficiency of plastic recycling. Firstly, the majority of plastic waste is found in the municipal solid waste (MSW) stream, even in countries where a parallel plastic recycling system is applied, which complicates the separation process. For example, plastic waste represents around 12.7% and 17.4% of the total quantity of MSW generated in the USA and Saudi Arabia respectively (EPA, 2014; Nizami et al., 2015). Secondly, plastic needs to be sorted into different categories based on type prior to its recycling due to the difference in the physical, thermal and microstructure properties; this decreases the efficiency of recycling (Hopewell et al., 2009; Rebeiz and Craft, 1995). Thirdly, the majority of plastic can only be recycled once due to the deterioration in its properties during reprocessing (Francis, 2016).

Most plastic cannot be recycled into its original purpose due to health and/or technical issues, and the recycling process generally leads to the degradation of its properties. This results in lower quality products, which subsequently cannot be recycled again (Hopewell et al., 2009). In most cases, plastic recycling is also cost ineffective as it is usually contaminated, effecting

a marginal reduction in price and quality relative to raw plastic (Alhumoud et al., 2004; Curlee, 1986). In addition to these technical and economical barriers to plastic recycling, a lack of stringent regulations and awareness regarding the disposal of plastic, and the low cost of landfill, particularly in countries with large areas of desert such as Saudi Arabia, entrench unreceptive behaviours (Ouda and Cekirge, 2014).

1.2.3 Disposal of plastic waste

Due to the limitations mentioned above on the recycling of plastic, a huge quantity of plastic (30 to 90%) is ultimately wasted in disposal (see Table 1.2), usually by incineration (Fig. 1.1) or dumping; the latter occupies a huge area of land (Fig. 1.2) and sea (Fig. 1.3). For example, approximately 2.8 million square metres are devoted to landfill each year in Saudi Arabia for disposal of waste (Alhumoud et al., 2004; El-Newehy, 2016; Hakami and Seif, 2015). Jambeck et al. (2015) also reported that 4.8 to 12.7 million metric tonnes of plastic waste are disposed of into the oceans. Furthermore, it is expected that by 2050, another 33 billion tonnes will be disposed of, which would cover the planet approximately 800 times (Rochman et al., 2013). Besides occupying large areas of land, dumping these wastes in landfill has a massive influence on the macro-environment and atmosphere. For instance, discarded plastic along with MSW generates about 3.4 to 3.9% of global harmful gas emissions such as carbon dioxide, nitrogen oxide and sulphur-dioxide, besides leaching hazardous elements such as methane (Al Ansari, 2012; Psomopoulos et al., 2009). Plastics degrade very slowly and remain in non-biological polymer forms that poison ecosystems for thousands of years (Andrady, 1994; Hopewell et al., 2009; Siddique et al., 2008; Sriningsih et al., 2014). Similarly, burning or incineration of the plastic waste is also not an effective solution, as it produces a large amount of air pollutants and the generation of toxic residues (Ouda et al., 2016; Psomopoulos et al., 2009; Sriningsih et al., 2014).



Figure 1.1: Burning of plastic waste (Deccan Chronicle, 2016)



Figure 1.2: Disposal Plastic waste into open land (Shutterstock, 2017)



Figure 1.3: Dumping plastic waste into seas and oceans (BBC, 2014)

1.3 Overview of industrial and mineral wastes or granular materials

Industrial and mineral wastes are by-product wastes generated during industrial activities or mining operations. For example, industrial wastes comprise ash, slag and metals; while, mining or quarry wastes include those produced from quarrying of different minerals such as rock, coal and stone. The accumulations of these wastes, as well as the availability of some naturally occurring materials (i.e. dune sand) have a serious impact on social, economic and environmental factors as described in the following sections. An overview was limited to fly ash, quarry fines and dune sand as given below, since these are the main filler candidates used in the present study.

1.3.1 Fly ash

Fly ash or pulverised fuel ash is a by-product of coal fired at power generation plants. It comprises the non-combustible particulates removed from flue gases (ASTM C618-15). Fly ash comprises very fine or powdered spherical (amorphous) particles with diameters ranging between 1 and 150μm (Kosmatka et al., 2002; Siddique and Khan, 2011; Yao et al., 2015). It has specific gravity ranging from 2.1 to 3 (Mattigod et al., 1990; Roy et al., 1981; Tolle et al., 1982). The chemical composition of fly ash is similar to that of cement, except it has a low content of calcium oxide (CaO) (Ahmaruzaman, 2010; Siddique and Khan, 2011).

It has been estimated that annual worldwide production of fly ash is between 750 to 780 Mt, with an average utilization rate ranging from 25 to 53.5% (Heidrich et al., 2013; Yao et al., 2015). Therefore, large heaps of fly ash (see Fig. 1.4) are disposed of in landfill (see Fig. 1.5), contaminating air, soils, plants and water (Ahmaruzaman, 2010; Siddique and Khan, 2011; Yao et al., 2015).



Figure 1.4: Heaps of fly ash (Irvin, 2010)



Figure 1.5: Landfill with fly ash (Rankin, 2017)

Due to the intrinsic problems of fly ash disposal, different applications have been identified to safely utilize it, such as in aggregate and concrete applications. Lightweight aggregate such as Lytag has been successfully produced by sintering fly ash at a high temperature of up to 1100 °C (Chandra and Berntsson, 2002; Clarke, 2005). Fly ash has been used along with plastic binder to form synthetic lightweight aggregate, as described in Chapter 2 (see section 2.3.2). Furthermore, fly ash has been widely used in concrete as an addition or replacement of either cement or fine aggregate. The inclusion of fly ash results in various advantages such as improving workability and ultimate strength, as well as reducing bleeding, segregation and

heat of hydration (Ahmaruzaman, 2010; Siddique and Khan, 2011). Also, it has been reported that implementing fly ash in concrete enhances durability due to a reduction in permeability (Siddique and Khan, 2011). The replacement ratio of fly ash in the concrete mixture varies from 5 to 65% of the total amount of the mixture, depending on the type of the fly ash and the concrete applications. However, using high volumes of fly ash as a replacement for cement (more than 40%) was found to reduce compressive strength at an early age (Siddique, 2004; Yao et al., 2015).

1.3.2 Quarry fines

Quarry fines or dust are generally produced during the crushing of rocks and other activities associated with milling or screening. The maximum size of quarry fines is about 0.063 to 5 mm (Manning, 2004; Mitchell, 2009). Quarry fines comprise silt and clay materials and are also a mixture of different fine particles. According to Manning (2004), the main mineral present in quarry fines resulting from crushing limestone rocks is calcite; while quartz is the main constituent of fines generated from crushing of other types of rocks (i.e. sandstone, igneous, sand and gravel).

The annual production of quarry fines in the USA was estimated at 175 Mt (Collins and Ciesielski, 1994) and in the UK at 53.9 Mt (Mitchell, 2009). These large quantities are accumulated in huge stockpiles (see Fig. 1.6), which have environmental impacts associated with air pollution and a disposal crisis (Galetakis and Soultana, 2016; Huffman, 2001; Safiuddin et al., 2007).



Figure 1.6: Quarry fines heaps at Gritstone quarry (Mitchell, 2016)

Quarry fines have been implemented as a replacement for fine aggregate in proportions ranging from 10-100% of concrete (Galetakis and Soultana, 2016). The inclusion of quarry fines at low levels (10-20%) yielded improvement in the mechanical and durability properties of concrete (Galetakis and Soultana, 2016; Manning, 2004; Topçu and Uğurlu, 2003). In addition, a few successful attempts have been made to incorporate quarry fines with clay or paper sludge to produce artificial lightweight aggregate (Frye, 1994; Wainwright et al., 2002; Weinecke and Faulkner, 2002).

1.3.3 Dune sand

Dune sand is abundantly available in desert regions around the world, including the Middle East and North Africa (MENA), parts of North America and Western Australia. Around 37% (i.e. 800,000 km^2) of the landmass of Saudi Arabia is covered with dune sand (Garzanti et al., 2013; Seif et al., 2016), making it the greatest "continuous body of aeolian sand on earth" (Garzanti et al., 2013). The maximum size of dune sand particles varies from one location to another; in general, 25% of particles are smaller than 0.15 mm (Luo et al., 2013). The main mineral present in dune sand is quartz (i.e. 83%), with small amounts of feldspar and rock fragments (Garzanti et al., 2013; Seif et al., 2016).

The movement of dune sand has environmental and economic impacts associated with sand storms (Al-Sanad et al., 1993; Barth, 1999; Seif et al., 2016). The migration of such sand damages infrastructure and utilities, such as power and communications lines, which impedes urban development and transportation systems in the country, as shown in Figures 1.7 and 1.8.



Figure 1.7: Road blocking due to the movement of dune sand (SoilSolutions, 2017)



Figure 1.8: Dune sand effect on railway track (RWDI, 2017)

Due to such problems, studies have investigated the possibility of using dune sand as a replacement of natural sand in mortar, concrete and pavements (Al-Harthy et al., 2007;

Guettala et al., 1997; Seif, 2013; Seif et al., 2016). These studies concluded that the dune sand does not satisfy the requirements of fine aggregate and exhibits a low strength performance at all levels; although workability was improved at lower replacement levels (<50%). On the other hand, Zhang et al. (2006) reported an improvement in both workability and strength by using China desert sand as replacement for fine aggregate. Further application for dune sand was investigated by Alhozaimy et al. (2012), who explored the possibility of using ground dune sand as a cement replacement, which resulted in a reduction in the compressive strength of concrete.

1.4 Statement of the problem

Sustainable use of natural resources is a key issue in the 21st century, together with unprecedented increase in global population and urbanization. Recycling is considered as one of the effective methods to reduce the volume of waste as well as the consumption rate of the raw materials; which addresses the concern regarding the depletion of natural resources and the availability of landfill sites.

In terms of concrete, global consumption of aggregates was around 48.3 billion metric tonnes in 2015 and this figure is expected to increase to 51.7 billion metric tonnes by 2019 (Fredonia, 2012; Fredonia, 2017). Besides the depletion of non-sustainable resources of aggregate (i.e. rock), the excess depletion of natural rock causes geological disturbances in the equilibrium of the environment; which may result in various hazards including subsidence, flooding and landslides (Aigbedion and Iyayi, 2007).

Another serious issue for the environment is that the worldwide quantity of plastic production increases every year, whereas the recycling percentage is still very low; this results in a huge volume of plastic waste, as described in section 1.2.1. This waste ultimately ends in landfill

and oceans or is burnt for total elimination, releasing toxins into the water, air and soil and thus poisoning the ecosystem and human food chain, posing grave environmental, health and economic threats (see section 1.2.3). Other types of waste (i.e. industrial, mining) have also a significant impact on the environment and occupy large areas of land, i.e. fly ash and quarry fines (see section 1.3). Granular material such as dune sand can also affect the environment and urban development, as mentioned earlier in section 1.3.3.

Therefore, keeping above facts in view, the current research was planned to investigate the use of the above materials (plastic, fly ash, quarry fines and dune sand) to form a new aggregate that can be used in the concrete as a replacement for natural aggregate. This would achieve the double goal of conserving the natural resources from the quarrying and reducing the risks arising from the accumulation of plastic and filler wastes.

1.5 Aim and objectives

The aim of this study was to manufacture the recycled plastic aggregate (RPA) and replace conventional normal weight or lightweight coarse aggregate either fully or partially for lightweight concrete production. In order to achieve this aim, the following objectives were set:

- Develop appropriate mix proportions for polymer and fillers to produce the aggregates.
- Manufacture of recycled plastic aggregate (RPA).
- Evaluate the physical, mechanical and microstructural properties of the RPA.
- Investigate the effect of fillers and binders on the properties of RPA.
- Produce lightweight concrete using RPA.
- Optimize the RPA concrete in terms of fresh, hardened and durability properties.

- Examine the effect of different replacement ratios of optimized RPA with that of normal weight or lightweight aggregate in the concrete.

1.6 Research hypotheses and innovative features of the research

Aggregate is one of the main components of concrete, forming 60-75% of the total volume; thus concrete is directly influenced by the characteristics of the aggregate. Accordingly, lightweight concrete can be produced using lightweight aggregate, which can be developed using very light materials such as plastic or plastic based aggregate.

This research will provide a better understanding of the behaviour of lightweight concrete in terms of strength, durability and deformation due to the effect of replacing natural/conventional lightweight aggregate with manufactured RPA made from different kinds of plastic and by-product wastes or granular materials. Moreover, using plastic and filler in RPA manufacturing would result in various advantages, including.

1. The area occupied by waste could be saved together with environmental pollution reduction.
2. Minimizing the accumulation problems associated with local materials (i.e. dune red sand and quarry fines waste).
3. Decreasing the energy and costs associated with transporting and disposing of plastic and by-product wastes.
4. Reducing the consumption of natural resources of aggregate.
5. Developing new aggregates comparable to natural aggregate in terms of shape, size and texture but being lighter in weight.
6. Solving the problems associated with the existing lightweight concrete and producing concrete with unique features (i.e. high deformation or ductility).

1.7 Thesis Outline

- Chapter 1 provides an overview of plastic and by-product waste or granular materials and presents the aim, objectives and importance of this research.
- Chapter 2 describes the types of existing lightweight aggregates, particularly synthetic aggregates, and presents a critical review of previous studies concerning the production of concrete using plastic particles or plastic based aggregates.
- Chapter 3 describes the experimental approach conducted to obtain the required data, including the materials used, research design programme, concrete mix design and test procedures implemented for both aggregate and concrete.
- Chapter 4 provides full details of the techniques used for manufacturing the RPA, and covers the characteristics of RPAs produced in this research.
- Chapter 5 consists of the results and discussion for RPA concrete optimization assessment (made at 100% of RPA).
- Chapter 6 describes the results and discussion on the fresh and hardened properties of optimized concrete mixes at different replacement levels of either LWA or NA, with optimized RPA. Analytical correlations between different mechanical properties are also developed in this chapter.
- Chapter 7 shows the results and discussion on durability properties and some other characteristics of optimized concrete mixes at different replacements levels of either LWA or NA, with optimized RPA. Additionally, analytical relationships amongst durability properties are obtained.
- Chapter 8 gives conclusions drawn from this study and making recommendations for further work.

CHAPTER 2: LITERATURE REVIEW

2.1 General

Concrete is the most broadly used construction material in the world with annual demand reaching 11.5 billion tonnes in 2014 (Joshua et al., 2015). It is obvious that in concrete construction there are important advantages in reducing its weight. One of the most successful approaches is by using lightweight construction materials. Therefore, these lightweight materials (i.e. lightweight aggregates) can be used to produce lightweight concrete of satisfactory strength with the additional features of thermal and noise insulation. Thus, lightweight aggregates are beneficial in reducing the total weight of the structure. In addition, the use of lightweight aggregate in concrete can help reduce element size and consequently reduce the cost of materials, handling, transporting, and ultimately the overall cost.

Since the aim of this research was to develop a novel lightweight aggregate (made from plastic and fillers) and investigate its utilization in concrete; this literature review is focused on concrete made using lightweight aggregates. A general background is given regarding concrete made from various types of conventional, natural, or manufactured lightweight aggregates. This is followed by a detailed review of the previous studies in which shredded or plastic particles were used directly as aggregate, or combined with other materials to develop a plastic based aggregate; where both were used as full or partial replacements for aggregates in concrete.

2.2 Lightweight concrete

Lightweight concrete can be defined as any type of concrete having an oven dry density less than 2000 kg/m^3 (Clarke, 2005). It has several advantages, such as a high strength/weight ratio as well as good thermal and noise insulation. It yields a significant reduction in the amount of

material used, element sizes, construction time, handling and transporting costs and energy used (Chandra and Berntsson, 2002; Clarke, 2005; Kayali, 2008; Neville, 2011; Shannag, 2011; Tanyildizi and Coskun, 2008). For these reasons, its demand for structural, non-structural and special applications has increased. These applications include, but are not limited to, *in situ* buildings, precast units and bridges, along with other special structures such as ships, floating docks and underwater storage tanks (Clarke, 2005). Lightweight concrete is classified into three broad types based on the following criteria as seen in Table 2.1:

- Production method
- Properties of produced concrete
- Aggregate used

To fulfil the scope of the study, consideration has been given to lightweight concrete made using different lightweight aggregates, which have been classified according to their type of aggregate used.

Table 2.1: Classification of lightweight concrete

Classifications	**Type**			**References**
	I	**II**	**III**	
Based on production method	Lightweight concrete produced from pours aggregates	Cellular, aerated or foamed lightweight concrete produced by introducing large voids in concrete	No fines lightweight concrete produced without fine aggregates	Neville (2011)
Based on the properties of produced concrete (i.e. dry density, compressive strength)	Structural lightweight concrete used in structural applications (has dry density ranging from 1350 to 1900 kg/m^3; minimum compressive strength of 17 MPa)	Moderate strength lightweight concrete used in structural fill (has dry density varies between 800 and 1350 kg/m^3; compressive strength 7-17 MPa)	Non-structural lightweight concrete used for non-structural applications such as insulating purposes (has very low dry density ranging between 300 and 800 kg/m^3; compressive strength less than 7 MPa)	(ACI 213R-03; Clarke, 2005; Neville, 2011)
Based on type of aggregate used	Lightweight concrete developed using natural lightweight aggregate such as pumice, scoria and palm oil shells aggregates	Lightweight concrete made using synthetic aggregate developed from natural materials (i.e. clay, slate). These types include perlite and vermiculite aggregates	Lightweight concrete obtained from synthetic by-product materials (i.e. fly ash, blast furnace slag, plastic waste). These aggregates may comprise Lytag or plastic based aggregates	(Chandra and Berntsson, 2002; Clarke, 2005; Neville, 2011)

2.2.1 Lightweight concrete using natural lightweight aggregates

Lightweight aggregate concrete can be produced from naturally available aggregates, for instance volcanic or organic aggregates. These aggregates are quarried or collected from their natural resources and have been used directly as an aggregate in concrete (Chandra and Berntsson, 2002).

The volcanic aggregates, for instance pumice and scoria, were used in their natural form. Pumice is highly amorphous and has a glassy and hard structure, having an oven-dry loose bulk density and water absorption range from 500 to 880 kg/m^3 and from 30 to 40% respectively (Clarke, 2005). It has been reported that pumice aggregate concrete yields compressive strength reaching 25 MPa and has low thermal conductivity, due to air entrapped in its voids (Demirboğa et al., 2001; Haktanir and Altun, 2002; Hossain and Lachemi, 2007; Hossain, 2004; XIAOPENG, 2005). However, this concrete is associated with problems such as a lack of durability, high mining and hauling costs, excessive drying shrinkage, high water absorption and lack of local capacity (Choi et al., 2009; Choi et al., 2005; Dhir et al., 1985).

Similarly, organic aggregates (i.e. agriculture or seashell wastes) have been used totally or partially as low-cost construction materials. These wastes may include palm oil shells, coconut shell, date seed, rubber seed, corncob, cockle shells and periwinkle shells (Ettu et al., 2013; Gunasekaran et al., 2012; Muthusamy et al., 2014; Pinto et al., 2012; Reddy et al., 2014; Shafigh et al., 2012). It has been reported that the specific gravity, bulk density and water absorption of the above mentioned aggregates varied from 0.694 to 2.33, 462 to 600 kg/m^3 and 8 to 33%, respectively (Prusty and Patro, 2015). Additionally, the workability and hardened properties decrease with the increase of the quantity of these aggregates. The compressive strength of concrete made with agro-wastes vary between 2 and 19 MPa

(Chandra and Berntsson, 2002; Prusty and Patro, 2015); while periwinkle shell yields compressive strength higher than 20 MPa (Prusty and Patro, 2015).

2.2.2 Lightweight concrete using synthetic aggregates

The majority of synthetic aggregates are formed either from natural materials such as clay, shale and slate, or from by-product such as fly ash, slag and sludge, using a thermal process (Chandra and Berntsson, 2002; Clarke, 2005; Neville, 2011). In addition, the physical properties of these aggregates are influenced by both the type of materials and process used (Chandra and Berntsson, 2002). The synthetic aggregates developed from natural materials include perlite, vermiculite, expanded clay (Leca), expanded shale (Liapor) and expanded slate (Granulex) aggregates. The manufacturing processes of these aggregates are similar; where the raw material is subjected to high temperature, expansion followed by cooling and finally crushing or grinding. However, the temperature degree and processing time varies from one type to another, depending upon the inert materials used and the manufacturing techniques.

It has been reported that the unit weight and water absorption of these aggregates varies from 190 to 931 kg/m^3 and 6 to 26% (Chandra and Berntsson, 2002; Clarke, 2005; Koksal et al., 2015; Mladenovič et al., 2004). In addition, the lightweight concrete made with perlite and vermiculate achieves very low dry density (500-700 kg/m^3) and compressive strength ($\leq$ 3MPa) (Neville, 2011). While, Leca and Granulex aggregate concrete yields a higher density and strength, ranging from 1300 to 1750 kg/m^3 and from 20 to 35 MPa, respectively (Neville, 2011). Moreover, the inclusion of these aggregates enhances thermal conductivity and fire resistance; while durability properties are affected due to the high degree of water absorption

of these aggregates (Abidi et al., 2015; Chandra and Berntsson, 2002; Clarke, 2005; Formosa et al., 2008; Melo et al., 2012; Schackow et al., 2014).

On the other hand, various types of synthetic lightweight aggregates such as sintered PFA/fly ash aggregate (Lytag), expanded pelletized slag (Litex), sludge ash and plastic aggregates have been produced using different kinds of industrial or by-product. These include pulverized fuel ash (PFA), blast furnace slag (bfs) and sludge ash (Chandra and Berntsson, 2002; Clarke, 2005; Neville, 2011). The main steps of manufacturing these aggregates are sintering the wastes at different high temperatures ranging from 1050 to 1400 °C, cooling, drying, crushing or pelletizing and finally grading or screening (Chandra and Berntsson, 2002; Clarke, 2005).

The majority of the particles of these aggregates are similar in shape and texture, such as Lytag aggregate which has uniform spherical particles with a smooth porous cellular structure (Chandra and Berntsson, 2002; Clarke, 2005). Moreover, it has been reported that the bulk density of Lytag and Litex aggregates range from 750 to 850 and from 650 to 950 kg/m^3, respectively (Clarke, 2005; Neville, 2011). In addition, Lytag aggregate has very high water absorption (9-15%); while, Litex aggregate achieves low water absorption (3-5%) (Clarke, 2005).

The addition of these aggregates in concrete alters the mechanical and durability performance depending on the properties of the aggregate itself and its cohesion with cement paste. For example, the incorporating of Lytag aggregate in concrete yields lightweight concrete having a dry density of 1800 Kg/m^3 and high compressive strength (>30 MPa) (Ahmad et al., 2013; Bai et al., 2004; Bethanis, 2007; Neville, 2011; Wainwright and Robery, 1997; Zhang, 2011). Similarly, Neville (2011) reported that the Litex aggregate concrete achieved high strength

(above 40 MPa) and a relatively higher density (2100 kg/m^3) compared to Lytag. On the other hand, the durability of concrete containing Lytag is adversely affected due to its high permeability. Nonetheless, the resistance of concrete containing Lytag and Litex aggregates towards freezing-thawing and heat transfer increases due to a large amount of entrapped air in their voids (Chandra and Berntsson, 2002; Clarke, 2005; Dehdezi et al., 2015).

2.3 Synthetic plastic

Plastic has been extensively used as synthetic aggregate in concrete in which either virgin or waste plastic has been implemented as a replacement for natural aggregate. However, there have only been a few studies on the indirect use of plastic as a synthetic aggregate in which the plastic has been converted to aggregate using any modification. These types of aggregate and their developing procedures are explained below.

2.3.1 Shredded or virgin plastic particles as aggregate

Different types of plastic have been used directly in concrete as a replacement for either coarse or fine aggregate (CA or FA); since they have a low density in comparison with that of natural aggregate and this makes them more suitable for the production of lightweight concrete. These types include, but are not limited to: polyethylene terterphalate (PET), low density polyethylene (LDPE), high density polyethylene (HDPE), expanded polystyrene (EPS), polypropylene (PP) and polyvinyl chloride (PVC). These types have been used as they are in a virgin form or in a shredded form of waste plastic. Therefore, the treatment process for plastic waste comprises sorting, washing, drying and finally shredding or grinding. For instance, different authors have used shredded PET bottles (see Fig. 2.1 and Fig. 2.2) as an FA replacement at various levels (from 5 to 75%) (Albano et al., 2009; Frigione, 2010; Hannawi et al., 2010; Juki et al., 2013; Rahmani et al., 2013). However, other studies reported that

shredded PET plastic was used as a replacement for CA and FA from 5 to 15% (Ferreira et al., 2012; Saikia and Brito, 2013; Saikia and de Brito, 2014; Silva et al., 2013).



Figure 2.1: PET aggregates (Hannawi et al., 2010)



Figure 2.2: Type of PET particles (Rahmani et al., 2013)

Similarly, LDPE and HDPE have been used as a replacement for fine aggregate at different substitution levels varying between 0.4 to 7.5% (Chaudhary et al., 2014; Galvão et al., 2011; Naik et al., 1996). However, these plastics have been implemented as a replacement for total aggregate at different levels (from 10 to 40%). Moreover, several kinds of plastic such as polyurethane foam wastes (PUR foam-Fig. 2.3), ethylene vinyl acetate (EVA), PVC (Fig. 2.4) and scrap car bumpers were shredded and used as replacements for CA or FA in concrete at different percentages ranging from 5 to 100% (Al-Manaseer and Dalal, 1997; Fraj et al., 2010; Kou et al., 2009; Lima et al., 2010).



Figure 2.3: Coarse PUR foam waste (Fraj et al., 2010)



Figure 2.4: PVC waste; before crushing (left) and after crushing (right) (Kou et al., 2009)

In addition, mixed plastic collected from a waste stream was treated (Fig. 2.5) and incorporated as a replacement for either CA or FA at various levels from 10 to 20% (Batayneh et al., 2007; Elzafraney et al., 2005; Ismail and Al-Hashmi, 2008; Rai et al., 2012). Waste or virgin EPS (Fig. 2.6) has also been incorporated as a replacement for CA at various levels (from 10 to 80%) (Babu and Babu, 2003; Babu and Babu, 2004; Herki et al., 2013; Ravindrarajah, 1999; Sabaa and Ravindrarajah, 1997; Tang et al., 2008). It was also used as a replacement for total aggregate from 5 to 95% (Babu et al., 2006; Babu et al., 2005; Chen and Liu, 2004; Madandoust et al., 2011; Ravindrarajah and Tuck, 1994; Xu et al., 2012).



Figure 2.5: Sample of waste plastic (Ismail and Al-Hashmi, 2008)



Figure 2.6: Expanded polystyrene beads (Xu et al., 2012)

The physical properties and type of plastic used by different researchers is shown in Table 2.2 (Gu and Ozbakkaloglu, 2016); where the properties of plastic vary depending on their type and processing method. For example, the highest unit weight was attained by shredded PET (660 kg/m^3); while the lowest belongs to virgin EPS (8 kg/m^3). In addition, the maximum water absorption is reported for EVA (44%) followed by PUR foam (14%); whereas, the water absorption for other types ranges from 0 to 13%.

Table 2.2: Types of plastic used in concrete

Type of plastic	Particle size (mm)	Bulk density (kg/m^3)	Specific gravity	Water absorption (%)	Study
PET bottles (Pc)	≤ 11.2	351	1.34	0.18	Saikia and Brito (2013) and Saikia and de Brito (2014)
PET bottles (Pf)	≤ 4	555		0.25	
PET bottles	≤ 5	-	-	-	Juki et al. (2013)
PET bottles (Pc)	≤ 11.2	261	1.3	0.75	Silva et al. (2013)
PET bottles (Pf)	≤ 4	438	1.28	0.11	
PET bottles (Pc)	-	261	1.31	0.73	Ferreira et al. (2012)
PET bottles (Pf)	-	438	1.28	0.09	
PET bottles	≤ 2.36	660	1.32	-	Frigione (2010)
PET bottles	≤ 4	327	-	0	Remadnia et al. (2009)
PET bottles		220	-	-	Yesilata et al. (2009)
PET bottles	0.26-1.14	-	-	-	Albano et al. (2009)
Mixed plastic (80% PET and 20% PS)	Length 0.15-12, width (0.15-4)	386.7	-	0.02	Ismail and Al-Hashmi (2008)
PET bottles	≤ 12.5	-	1.32	7.4	Galvão et al. (2011)
LDPE bags	≤ 4.8	-	0.86	3.9	
LDPE bags	≤ 2.36	-	0.93	-	Chaudhary et al. (2014)
Waste HDPE			-	-	Naik et al. (1996)
Waste HDPE	≤ 10	534	1	-	Elzafraney et al. (2005)
Waste PVC	-	684	1	-	
Waste PP	-	460	1	-	
PVC pipes	≤ 5	546	1.4	0	Kou et al. (2009)
Waste EPS	≤ 8	457	0.8	13	Herki et al. (2013)
Waste EPS (coarse)	4–16	-	0.22–0.24	4.1	Kan and Demirboğa (2009)
Waste EPS (fine)	0–4	-	0.31–0.34		
Waste EPS	≈ 4	24	-	-	Tang et al. (2008)
Waste EPS	≤ 3.7	26.8	-	-	Sabaa and Ravindrarajah (1997)
Virgin EPS	≈ 3	30	-	-	Xu et al. (2012)
Virgin EPS	≈ 4.75-9.5	10.4-13.6	0.018-0.025	0	Madandoust et al. (2011)
Virgin EPS	≤ 8	9-66.5	0.014-1.02	-	Babu et al. (2006)
Virgin EPS	3-8	12-20	0.01-0.029	-	Haghi et al. (2006)
Virgin EPS	4.75-6.3	9.5-20	0.014-0.029	-	Babu et al. (2005)
Virgin EPS	3-8	8.5-20	-	-	Chen and Liu (2004)
Virgin EPS	4.75-6.3	9.5-20	0.014-0.029	-	Babu and Babu (2003)
Virgin EPS	≈ 3	-	0.67	-	Ravindrarajah (1999)
Rigid PUR foam waste	≤ 20	21	0.045	13.9	Fraj et al. (2010)
EVA	≤ 9.5	100	0.24	44.3	Lima et al. (2010)
Waste plastic	-	-	0.91	-	Rai et al. (2012)
Waste plastic	≤ 9.5	-	-	-	Batayneh et al. (2007)

On the other hand, another technique for developing synthetic aggregate using shredded plastic is by reducing the size of the plastic into plastic particles using thermal processing prior to utilising it in concrete. For instance, the size of plastic waste can be reduced using extrusion and then a shredding process (Ferreira et al., 2012; Koide et al., 2002; Mathew et al., 2013; Saikia and Brito, 2013; Saikia and de Brito, 2014; Sawyers, 1995; Silva et al., 2013). However, other studies (Al Bakri et al., 2011; Reddy et al., 2012) showed that the size of plastic waste (i.e. LDPE,HDPE) can be reduced by shaping plastic into the required shape and then ultimately exposing it to heat, as shown in Figure 2.7 and Figure 2.8. These studies revealed that the density of those plastics modified thermally was much higher than those prepared by shredding only. For example, the bulk density for PET plastic obtained by shredding and thermal recycling (melting) was 438 and 739 kg/m^3 respectively (Ferreira et al., 2012; Saikia and Brito, 2013; Saikia and de Brito, 2014; Silva et al., 2013).



(a)



(b)

Figure 2.7: Comparison of plastic waste aggregate (a) before heating and (b) after heating (Al Bakri et al., 2011)



Figure 2.8: LDPE before and after melt-densification (Reddy et al., 2012)

2.3.2 Plastic based aggregates

In the available literature, many studies have been conducted to investigate the effect of using shredded or virgin plastic directly in concrete as synthetic aggregate. However, to the author's best knowledge, very few attempts have been conducted to study the effect of the indirect use of plastic, in which it was used in developing plastic-based aggregate prior to its use in

concrete. A synthetic aggregate has been developed using thermal processes for a mixture of plastic and additives (Choi et al., 2009; Choi et al., 2005; Jansen et al., 2001; Kashi et al., 1999; Malloy et al., 2001; Phillips and Richards, 2004; Slabaugh et al., 2007; Swan and Sacks, 2005).

For instance, Choi et al. (2009) and Choi et al. (2005) developed waste plastic lightweight aggregate (WPLA) from waste PET bottles and coated it with granulated blast furnace slag (GBFS) or river sand powder, as shown in Figures 2.9 and 2.10. The production process of WPLA comprises collection, cleaning, shredding of plastic (5-15 mm), heating, coating with additives, extruding, air cooling and finally sieving.

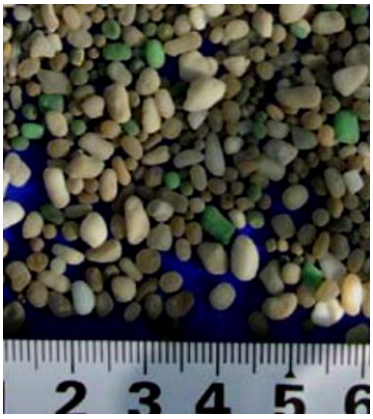


Figure 2.9: Shape of WPLA (Choi et al., 2005)



Figure 2.10: Shape of WPLA (Choi et al., 2009)

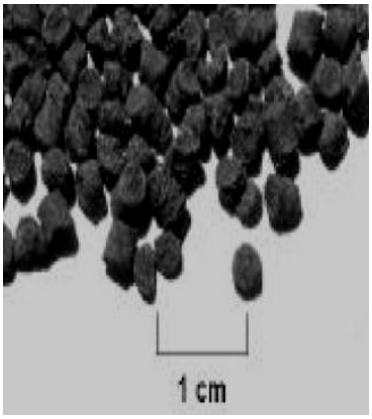


Figure 2.11: SLA (Kashi et al., 1999)

On the other hand, different researchers (Jansen et al., 2001; Kashi et al., 1999; Malloy et al., 2003; Slabaugh et al., 2007; Swan and Sacks, 2005) developed synthetic lightweight aggregate (SLA) from fly ash and plastic using an extrusion technique, as shown in Figure 2.11 and Figure 2.12. In these studies, the plastic was in a single form such as polystyrene (PS), LDPE, HDPE or in a mixed form of PET, HDPE, LDPE, PP, PS and HIPS. In addition, the proportions of fly ash to plastic were between 0:100 and 80:20. The manufacturing

process of the SLA comprised the mixing of fly ash and plastic, followed by heating, then extrusion of the blends through a specified die into a water bath for cooling, solidifying and finally crushing. In the same context, Phillips and Richards (2004), produced a synthetic aggregate called Plasmatex by mixing and heating fine materials (i.e. china clay, foundry sand and quarry fines) with mixed polymer waste plastic (MPWP) in a pugmill. Then, the mixture was cast in oval briquettes (50 mm), cooled and finally crushed. The proportion of fine materials to MPWP was 30:70, 60:40, and 70:30.



a b c

Figure 2.12: SLAs made using (a) 0:100, (b) 35:65 (b) and (c) 80:20 of fly ash to plastic (Jansen et al., 2001)

Table 2.3 represents the properties of plastic based aggregate available in the literature. As can be seen in this table, the increase in fly ash content in the SLA matrix leads to a higher unit weight and water absorption (Jansen et al., 2001; Kashi et al., 1999). This increase in unit weight is due to the lower bulk density of the plastic as compared to the fly ash. However, the high porosity or entrapped air which are associated with high fly ash content in the SLA matrix are the main cause of the increase in the water absorption. Moreover, the findings of these studies revealed that the amount of fly ash had a significant effect on the shape and texture of the SLA. A higher fly ash content (i.e. 80%) in the SLA tends to produce rounded edge particles with a rougher surface texture, in contrast to the angular and smooth surface

particles obtained with a low content of fly ash (up to 35%). This can be explained by the fact that the SLA made with a higher plastic content tends to shred rather than break.

In summary, plastic based aggregates have been used as a lightweight aggregate either partially or totally as a replacement for either CA or FA in concrete. Moreover, a large amount of additives or fillers (i.e. 60 and 70%) is very desirable from a perspective of concrete performance because the shape and texture of the SLA particle enhances with a higher quantity of filler (Malloy et al., 2001; Phillips and Richards, 2004).

Table 2.3: Properties of existing plastic based aggregates

Type of Aggregate	**Properties of Aggregate**					**Study**
	Maximum Particles size (mm)	Particles shape and texture	Unit weight (kg/m3)	Specific Gravity	Absorption (%)	
WPLA	-	Spherical/ smooth	1390	-	-	Choi et al. (2005)
WPLA	-	Spherical/ smooth	1390	-	0	Choi et al. (2009)
SLA (80:20 fly ash: HDPE)	-	-	-	1.9	-	Kashi et al. (1999)
SLA (0:100 fly ash: HDPE)	9.5	Angular/ smooth	-	0.91	0.3	Jansen et al. (2001)
SLA (35:65 fly ash: HDPE)			-	1.09	1.2	
SLA (80:20 fly ash: HDPE)		Rounded edges/rough	-	1.60	19.3	
SLA (80:20 fly ash: PS)	2.36	Firm to noticeably deformable	-	1.68	3.48	Swan and Sacks (2005)
SLA (80:20 fly ash: LDPE)			-	1.53	8.14	
SLA (80:20 fly ash: HDPE)			-	1.56	3.46	
SLA (80:20 fly ash: MP)			-	1.60	7.49	
SLA (0:100 fly ash: MP)	> 4.56	Firm to noticeably deformable	-	0.92	1.39	Slabaugh et al. (2007)
SLA (10:90 fly ash: MP)			-	0.87	2.28	
SLA (30:70 fly ash: MP)			-	0.88	2.28	
SLA (50:50 fly ash: MP)			-	0.77	5.60	
SLA (70:30 fly ash: MP)			-	0.96	2.15	
Plasmatex	14	Irregular/ honeycombed	-	1.52-1.6	2.1-4.2	Phillips and Richards (2004)

WPLA: Waste plastic lightweight aggregate
SLA: Synthetic lightweight aggregate

2.4 Fresh properties of concrete

2.4.1 Slump

2.4.1.1 Effect of shredded or virgin plastic on slump

The slump of the concrete made with the shredded or virgin plastic aggregates depends on W/C, type, and proportion of plastic particles used. Table 2.4, summarizes the findings given by previous studies for the natural aggregates being replaced directly with plastic (Al Bakri et al., 2011; Albano et al., 2009; Batayneh et al., 2007; Ismail and Al-Hashmi, 2008; Kou et al., 2009; Rahmani et al., 2013; Rai et al., 2012; Tang et al., 2008).

Table 2.4: Variation in slump of concrete with shredded or virgin plastic incorporation

Study	Form of plastic	Replacement level (%)	Replacement type	W/C ratio	Slump (mm)	Maximum percentage deviation WRT control
Rahmani et al. (2013)	PET	0, 5, 10, 15	FA	0.42	70-40	-43
				0.54	80-35	-56
Albano et al. (2009)	PET	0,10, 20	FA	0.5	87-50	-42
				0.6	79-21	-73
Ismail and Al-Hashmi (2008)	Waste plastic	0,10,15,20	FA	0.53	76-50	-25
Batayneh et al. (2007)	Waste plastic	0,5,10,15,20	FA	0.56	78-57	-95
Rai et al. (2012)	plastic pallet	0,5,10,15	FA	0.44	71-32	-57
Tang et al. (2008)	EPS	0,20,40	CA	0.5	55-65	18
	EPS	60,80	CA	0.5	60-55	-16
Kou et al. (2009)	PVC	0,5,15,30,45	FA	0.32	175-170	-3
Al Bakri et al. (2011)	Waste plastic balls	0,100	CA	0.5	55-13	-76

The data given in Table 2.4 indicates that the most dominant factor affecting slump was the type and form of the plastic, followed by replacement percentage, replacement type and finally, W/C ratio. For instance, replacing 20% of FA with waste plastic resulted in a 95%

reduction (Batayneh et al., 2007); while, the reduction varied between 42 and 73% due to incorporating PET at same replacement type and proportion (Albano et al., 2009).

The reduction in slump was attributed to the increase in friction between the plastic particles which leads to less fluidity. This friction is due to the large contact surface area of the plastic particles as well as the lack of uniformity in the particles' shape (Batayneh et al., 2007; Ismail and Al-Hashmi, 2008; Rahmani et al., 2013; Rai et al., 2012). On the other hand, Tang et al. (2008) found an increasing trend by using EPS as a replacement for CA (up to 40%). This increase is accounted for by the lower water absorption of the EPS due to its closed cell structure, which leads to more free water existing after the mix. Other researchers (Albano et al., 2009; Babu and Babu, 2004) claimed that the great absorption capacity of lightweight aggregate reduces its workability due to its high porosity; since the real water absorption of lightweight aggregate is not precisely measured because of its closed cellular structure.

In addition, slump was examined visually in different studies (Ravindrarajah, 1999; Ravindrarajah and Tuck, 1994). It was observed that the EPS concrete was stiff and rubbery and caused difficulties during mixing, placing and finishing.

2.4.1.2 Effect of plastic based aggregate on slump

The slump of concrete containing plastic based aggregates (Table 2.5) is also influenced by the same parameters observed in the case of shredded or virgin plastic incorporation.

Table 2.5: Variation in slump of concrete with plastic based aggregate incorporation

Study	Type of aggregate	Replacement level (%)	Replacement type	W/C ratio	Slump (mm)	Maximum percentage deviation WRT control
Choi et al. (2005)	WPLA	0, 25, 50, 75	FA	0.45	135-205	52
				0.49	105-214	104
				0.53	100-223	123
Jansen et al. (2001)	SLA (Fly ash :HDPE) (0:100)	0, 100	CA	NA	76-89	17
	SLA (Fly ash: HDPE) (35:65)				76-76	0
	SLA (Fly ash: HDPE) (80:20)				76-64	-16
Slabaugh et al. (2007)	SLA (Fly ash :MP) (0:100)	0, 100	CA	NA	95.3-82.6	-13
	SLA (Fly ash: MP) (10:90)				95.3-88.9	-7
	SLA (Fly ash: MP (30:70)				95.3-101.6	7
	SLA (Fly ash :MP) (50:50)				95.3-76.2	-20
	SLA (Fly ash: MP) (70:30)				95.3-88.9	-8

Table 2.5 shows that replacing FA with WPLA substantially increased concrete workability due to the spherical shape, smooth texture and lower water absorption of WPLA, as presented earlier in Table 2.3 (Choi et al., 2009; Choi et al., 2005). Furthermore, Jansen et al. (2001) and Slabaugh et al. (2007) noticed that concrete made totally with SLAs as a replacement for CA had a different effect on slump depending on the proportion of fly ash and plastic in the SLAs' matrix. For instance, SLAs having fly ash to plastic proportions of 0:100 and 80:20 resulted in a 17% (increase) and a 16% (decrease) in slump respectively (Jansen et al., 2001).

2.4.2 Fresh density

2.4.2.1 Effect of shredded or virgin plastic on fresh density

The density of concrete made with synthetic plastic was less than that of normal concrete due to its aggregate weighing less. Table 2.6 presents the fresh density of lightweight concrete made with shredded or virgin plastic particles obtained from different studies.

Table 2.6: Variation in fresh density of concrete with shredded or virgin plastic incorporation

Study	Form of plastic	Replacement level (%)	Replacement type	W/C ratio	Fresh density (kg/m^3)	Maximum percentage deviation WRT control
Rahmani et al. (2013)	PET	0, 5, 10, 15	FA	0.42	2453-2385	-3
				0.54	2414-2337	-3
Saikia and de Brito (2014)	PET	0,5,10, 15	FA	NA	2387- 2254	-6
			CA		2387-2233	-6
Ferreira et al. (2012) and Silva et al. (2013)	PET	0, 7.5	CA	NA	2362-2215	-6
			FA		2362-2236	-5
			FA		2362-2301	-3
Ismail and Al-Hashmi (2008)	Waste plastic	0,10,15,20	FA	0.53	2478-2264	-9
Batayneh et al. (2007)	Waste plastic	0,5,10,15,20	FA	0.56	2320-2495	8
Kou et al. (2009)	PVC	0,5,15,30,45	FA	0.32	1795-1530	-15
Sabaa and Ravindrarajah (1997)	EPS	0,30,50,70	CA	0.42	2375-1640	-30
				0.54	2340-1605	-31
Ravindrarajah (1999)	EPS	0,10,20,30	CA	0.35	2455-2080	-15
Chen and Liu (2004)	EPS	0,25,40,55	FA and CA	0.37	2435-876	-64
Tang et al. (2008)	EPS	0,20,40,60,80	CA	NA	2330-1396	-40
Kan and Demirboğa (2009)	MEPS	0,25,50,75, 100	FA and CA	NA	1956-876	-55
Fraj et al. (2010)	PUR foam	0,34,35,45	CA	NA	2472-1656	-33
Rai et al. (2012)	Plastic Pellet	0,5,10,15	FA	0.44	2600-2320	-11

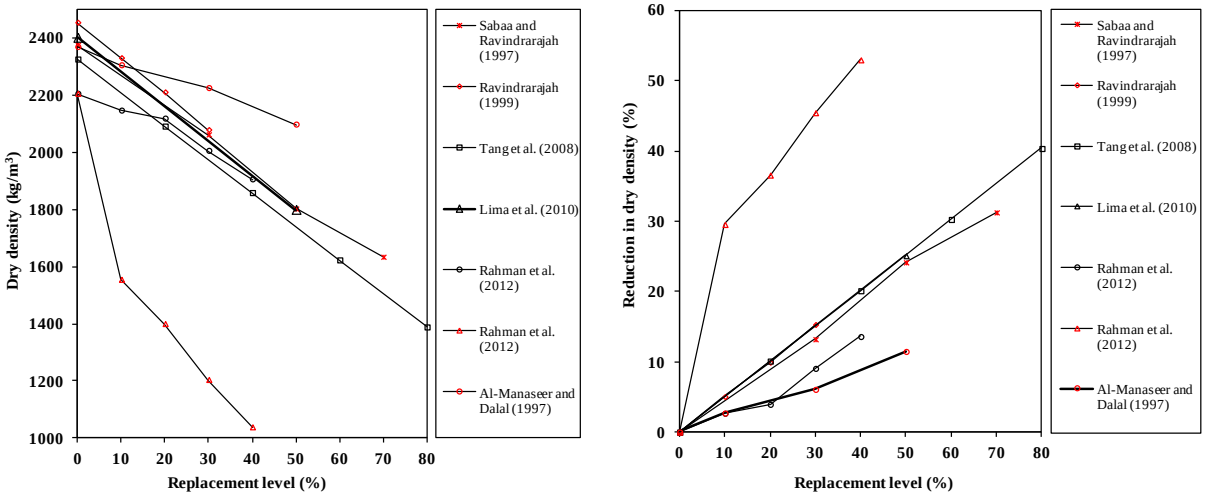
The fresh density was significantly affected by the plastic proportion and the replacement type, along with the type of plastic used (Table 2.6). For example, a 40 and 64% decrease in fresh density was noticed at 80 and 55% replacement levels of CA and total aggregate respectively with EPS (Chen and Liu, 2004; Tang et al., 2008). However, 20% replacement of FA with waste plastic yields a 9% reduction (Ismail and Al-Hashmi, 2008). This reduction in fresh density was mainly due to the lower density of plastic as compared with natural aggregate (Ferreira et al., 2012; Fraj et al., 2010; Ismail and Al-Hashmi, 2008; Rahmani et al., 2013; Rai et al., 2012; Saikia and de Brito, 2014; Silva et al., 2013). Another explanation for this reduction is attributed to the increase in the voids' content, which resulted from the entrapped air that is associated with the increase of the plastic particles' content in the mix (Tang et al., 2008). On the other hand, Batayneh et al. (2007) observed a marginal increase (8%) in fresh density due to replacing 20% of FA with waste plastic, as shown in Table 2.6.

2.5 Hardened properties of concrete

2.5.1 Dry density

2.5.1.1 Effect of shredded or virgin plastic on dry density

The dry density of concrete made with plastic particles is directly influenced by the same factors that affected the fresh density. Figures 2.13 and 2.14 depict the effect of the substitution of either CA or FA with plastic particles on the dry density of concrete.

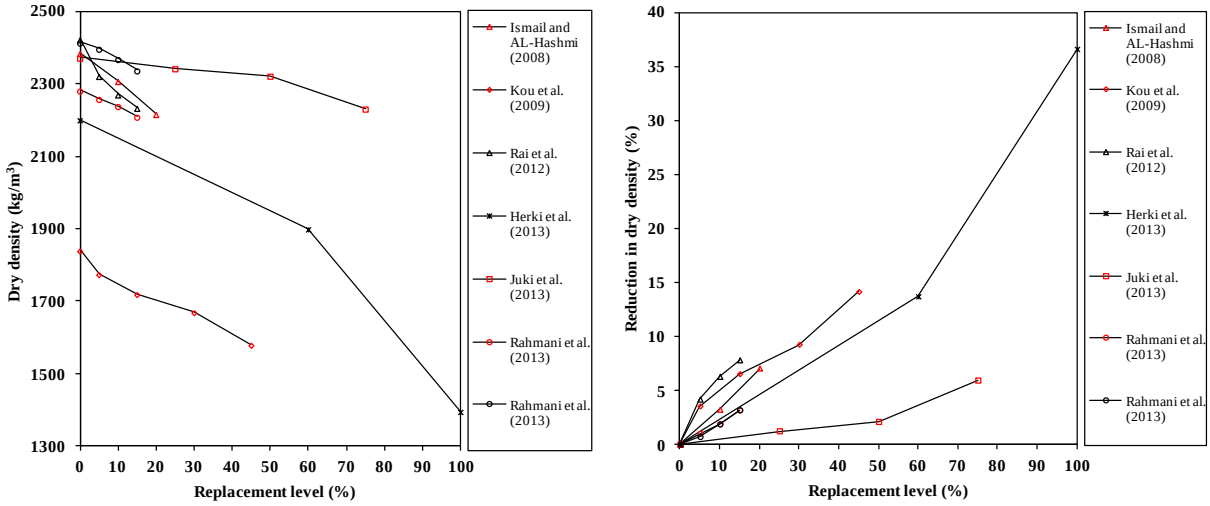


(a) (b)

Figure 2.13: Variation in (a) dry density and (b) reduction in dry density (%) of concrete with replacement level of normal CA with shredded or virgin plastic

The findings of previous studies (Fig. 2.13 and Fig. 2.14) revealed that the most effective parameter for density reduction is the quantity of plastic particles, followed by the type of replacement and finally the type of plastic used. The maximum reductions in dry density of concrete varied from 11 to 53% at different replacement levels (from 40 to 80%) of CA with plastic (Al-Manaseer and Dalal, 1997; Haghi et al., 2006; Lima et al., 2010; Rahman et al., 2012; Ravindrarajah, 1999; Sabaa and Ravindrarajah, 1997; Tang et al., 2008). However, replacing FA with plastic by 15 to 100% resulted in less reduction, ranging from 3 to 36% (Herki et al., 2013; Ismail and Al-Hashmi, 2008; Juki et al., 2013; Kou et al., 2009; Rahmani et al., 2013; Rai et al., 2012). In addition, the plastic type has a significant effect on dry

density, as mentioned above; since the maximum reduction in dry density was 13 and 52% due to replacing CA with HDPE and EPS plastic particles respectively, at a level of 40% (Rahman et al., 2012). Nonetheless, some researchers (Fraj et al., 2010; Juki et al., 2013) found a marginal decrease (less than 10%) with a large replacement level of normal aggregate with plastic (from 75 to 100%).



(a) (b)

Figure 2.14: Variation in (a) dry density and (b) reduction in dry density (%) of concrete with replacement level of normal FA with shredded or virgin plastic

Overall, these studies (Al-Manaseer and Dalal, 1997; Fraj et al., 2010; Ismail and Al-Hashmi, 2008; Kou et al., 2009; Rahman et al., 2012; Rahmani et al., 2013; Rai et al., 2012) indicate that this reduction is associated with a lower unit weight of plastic particles in comparison with normal weight aggregate. However, Rahmani et al. (2013) linked this reduction to the increase in pores or channels in the hardened mix. These pores are created due to the difference in the shape and size of the plastic particles and additionally, because of the free water that occupies space in the hardened mix as a result of the low water absorption of the plastic particles.

2.5.1.2 Effect of plastic based aggregate on dry density

The effect of plastic based aggregate (i.e. having less weight than the replacement aggregate) on the dry density of concrete was investigated in limited studies (Choi et al., 2009; Choi et al., 2005; Jansen et al., 2001; Kashi et al., 1999; Slabaugh et al., 2007). The general trend showed that the dry density reduced with the increase in the plastic based aggregate content.

Table 2.7: Variation in dry density of concrete with plastic based aggregate incorporation

Study	Type of aggregate	Replacement level (%)	Replacement type	W/C ratio	Dry density (kg/m^3)	Maximum percentage deviation WRT control
Choi et al. (2005)	WPLA	0, 25, 50, 75	FA	0.45	2300-1940	-16
				0.49	2300-2000	-13
				0.53	2300-2010	-13
Kashi et al. (1999)	SLA (Fly ash: HDPE) (25:75)	100	CA	0.50	1480	NA
	SLA (Fly ash: HDPE) (35:65)				1490	NA
	SLA (Fly ash: HDPE) (50:50)				1520	NA
	SLA (Fly ash: HDPE) (65:35)				1630	NA
	SLA (Fly ash: HDPE) (80:20)				1700	NA
Jansen et al. (2001)	SLA (Fly ash: HDPE) (0:100)	0, 100	CA	NA	2323-1792	-23
	SLA (Fly ash: HDPE) (35:65)				2323-1858	-20
	SLA (Fly ash: HDPE) (80:20)				2323-1969	-15
Slabaugh et al. (2007)	SLA (Fly ash: MP) (0:100)	0, 100	CA	NA	2417-1856	-23
	SLA (Fly ash: MP) (10:90)				2417-1866	-23
	SLA (Fly ash: MP) (30:70)				2417-1846	-24
	SLA (Fly ash: MP) (50:50)				2417-1917	-21
	SLA (Fly ash: MP) (70:30)				2417-1886	-22

In some studies, (Choi et al., 2009; Choi et al., 2005), it was found that replacing 75% of FA with WPLA reduced the dry density by 16, 13 and 13% at a W/C of 0.45, 0.49 and 0.53 respectively. Similarly, a significant reduction ranging from 15 to 24% had also been observed due to replacing CA totally with SLA (Jansen et al., 2001; Slabaugh et al., 2007). Additionally, these studies concluded that the density of SLA concrete is proportionally increased with the increases in fly ash content in the aggregate (i.e. SLA) matrix as given in Table 2.7.

2.5.2 Compressive strength

2.5.2.1 Effect of shredded or virgin plastic on compressive strength

The compressive strength of concrete made with either shredded or virgin plastic particles is found sensitive to many factors; including the type, shape and proportion of plastic substituted and the W/C ratio (Gu and Ozbakkaloglu, 2016). Results of previous studies concerning the effect of replacing CA and/or FA with plastic on compressive strength of concrete are presented in Figures 2.15 and 2.16 respectively.

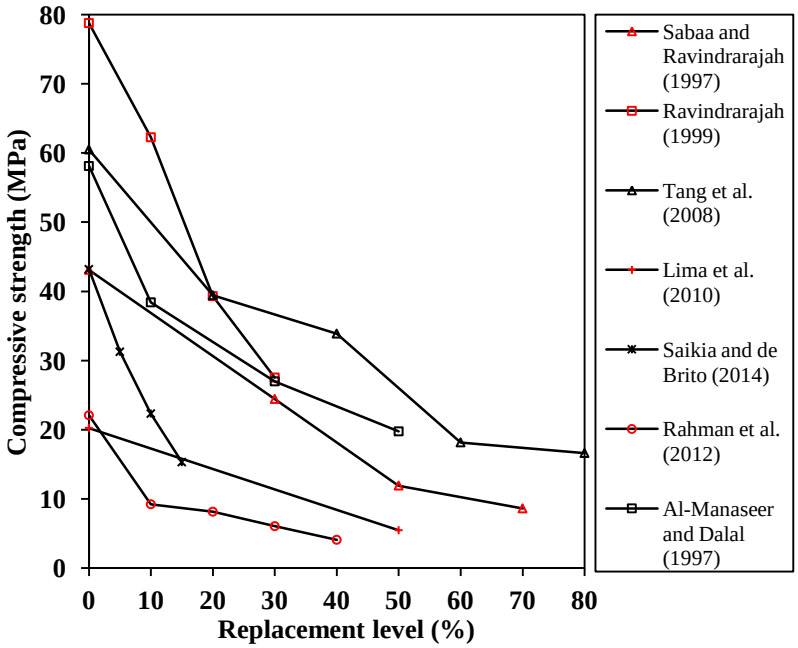


Figure 2.15: Variation in compressive strength of concrete with replacement level of CA with shredded or virgin plastic

Figures 2.15 and 2.16 suggest that the most dominant factors influencing the reduction in compressive strength were the replacement type and the type of plastic, similar to dry density. This is confirmed by the fact that the maximum reduction in compressive strength varied between 62 and 82% due to replacing normal CA with plastic particles (i.e. EPS, HDPE, PET, PUR foam and EVA) at different levels (15-80%) (Al-Manaseer and Dalal, 1997; Fraj et al., 2010; Lima et al., 2010; Rahman et al., 2012; Ravindrarajah, 1999; Sabaa and Ravindrarajah, 1997; Saikia and de Brito, 2014; Tang et al., 2008). While, in the case of replacing FA with

plastic particles, a significant reduction ranging from 15 to 72% was found at various replacement levels between 15 and 100% (Albano et al., 2009; Batayneh et al., 2007; Herki et al., 2013; Ismail and Al-Hashmi, 2008; Juki et al., 2013; Kou et al., 2009; Rahmani et al., 2013; Rai et al., 2012; Saikia and de Brito, 2014). Moreover, it has been reported that the compressive strength was reduced in the range from 33 to 97% due to replacing both CA and FA with plastic at different replacement levels (25 to 100%) (Babu et al., 2005; Babu and Babu, 2003; Chen and Liu, 2004; Kan and Demirboğa, 2009; Ravindrarajah and Tuck, 1994; Wong, 2010).

The type of plastic substituted has also a prominent effect on the magnitude of strength; since the concrete made with LDPE or HDPE plastic particles had a large strength reduction (i.e. 12-49%) even at very low substitution levels (1 to 7.5%), as reported by (Chaudhary et al., 2014; Galvão et al., 2011; Naik et al., 1996).

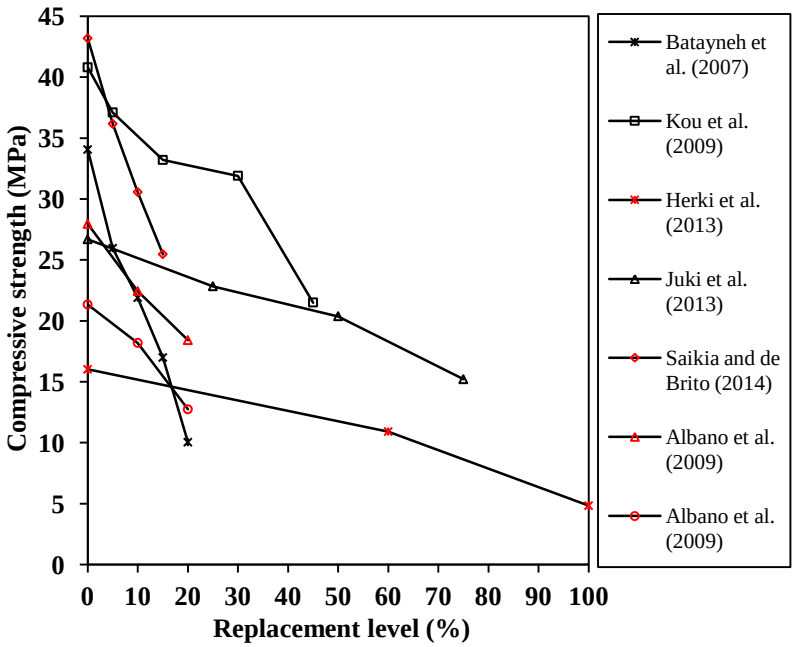


Figure 2.16: Variation in compressive strength of concrete with replacement level of FA with shredded or virgin plastic

The majority of the studies attributed this reduction in strength to the weak interfacial transition zone (ITZ) because of poor bonding between the cement paste and the plastic particles (Al-Manaseer and Dalal, 1997; Ismail and Al-Hashmi, 2008; Juki et al., 2013; Kou et al., 2009; Rahman et al., 2012; Rahmani et al., 2013; Rai et al., 2012; Saikia and Brito, 2013; Saikia and de Brito, 2014). According to, Ismail and Al-Hashmi (2008) and Kou et al. (2009), this reduction or weak bonding is related to the hydrophobic nature of plastic towards water, which restricts or decreases the cement hydration around the plastic particles.

Other studies, (Kou et al., 2009; Rai et al., 2012) had accredited the reduction in compressive strength to the lower packing level of the concrete matrix, which resulted from the difference in the shape of the plastic particles. Additionally, the lower strength of the plastic particles as compared to normal aggregate is another explanation for the strength reduction (Al-Manaseer and Dalal, 1997; Batayneh et al., 2007; Fraj et al., 2010; Juki et al., 2013; Rahman et al., 2012). Finally, the reduction in compressive strength can be linked with the high porosity of plastic particles which leads to a high voids' content and thereby less strength (Fraj et al., 2010; Ravindrarajah, 1999; Tang et al., 2008).

2.5.2.2 Effect of plastic based aggregate on compressive strength

The previous findings reported in the literature concerning the compressive strength of concrete made with plastic based aggregates are given in Table 2.8. The general observation was that there was a reduction in the compressive strength with the incorporation of plastic based aggregate as a replacement for either CA or FA. As shown in Table 2.8, the compressive strength reduced significantly by 33, 33 and 31% at a 75% replacement level of FA with WPLA at different W/Cs of 0.45, 0.49 and 0.53, respectively (Choi et al., 2009; Choi et al., 2005). Similarly, replacing CA totally with SLA resulted in a reduction ranging from

43-72% (Jansen et al., 2001; Malloy et al., 2001; Slabaugh et al., 2007). On the other hand, Jansen et al. (2001) and Kashi et al. (1999), observed an increase in compressive strength varying between 20 and 46%, with an increase in the fly ash content in the SLA matrix from 35 to 80%.

Table 2.8: Variation in compressive strength of concrete with plastic based aggregate incorporation

Study	Type of aggregate	Replacement level (%)	Replacement type	W/C ratio	Compressive strength (MPa)	Maximum percentage deviation WRT control
Choi et al. (2005)	WPLA	0, 25, 50, 75	FA	0.45	37.2-24.9	-33
				0.49	34.6-23.2	-33
				0.53	31.5-21.8	-31
Kashi et al. (1999)	SLA (Fly ash: HDPE) (25:75)	100	CA	0.50	15.1	NA
	SLA (Fly ash: HDPE) (35:65)				14.3	NA
	SLA (Fly ash: HDPE) (50:50)				15.2	NA
	SLA (Fly ash: HDPE) (65:35)				19.3	NA
	SLA (Fly ash: HDPE) (80:20)				20.9	NA
Jansen et al. (2001)	SLA (Fly ash: HDPE) (0:100)	0, 100	CA	NA	35.5-14.2	-60
	SLA (Fly ash: HDPE) (35:65)				35.5-16.7	-53
	SLA (Fly ash: HDPE) (80:20)				35.5-20.1	-43
Malloy et al. (2001)	SLA (fly ash/ HDPE) (80:20)	0, 100	CA	0.50	42-20	-52
	SLA (fly ash/ MP) (80:20)				42-22	-48
Slabaugh et al. (2007)	SLA (Fly ash: MP) (0:100)	0, 100	CA	NA	39.9-11.1	-72
	SLA (Fly ash: MP) (10:90)				39.9-11.4	-71
	SLA (Fly ash: MP) (30:70)				39.9-11.2	-72
	SLA (Fly ash: MP) (50:50)				39.9-12.6	-68
	SLA (Fly ash: MP) (70:30)				39.9-13.6	-66

2.5.3 Splitting tensile strength

2.5.3.1 Effect of shredded or virgin plastic on splitting tensile strength

Splitting tensile strength is also influenced by the same factors that affect compressive strength, such as the replacement level of the plastic, the W/C ratio and the form and type of plastic used. The previous findings for the splitting tensile strength of concrete containing

plastic particles as replacement for either CA or FA are plotted in Figures 2.17 and 2.18, respectively.

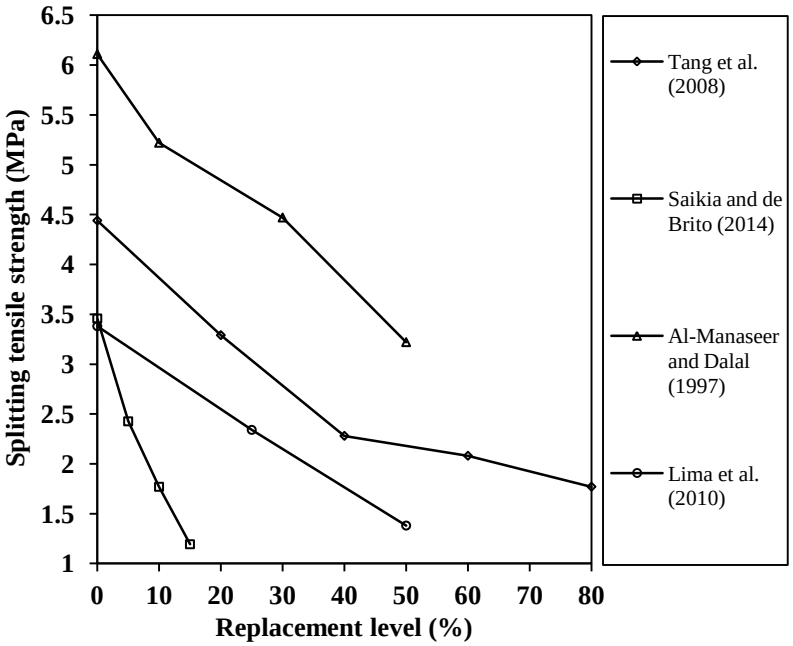


Figure 2.17: Variation in splitting tensile strength of concrete with replacement level of CA with shredded or virgin plastic

The general trend of these studies showed that the splitting tensile strength of concrete made with plastic particles has an inverse relationship with the proportion of shredded or virgin plastic. However, the type of replacement has the most prominent effect, since replacing CA with plastic particles resulted in a larger reduction as compared with those studies in which FA was replaced with plastic particles. For instance, replacing CA with different plastic particles at various levels from 15 to 80% yields a substantial reduction ranging from 47 to 72% (Al-Manaseer and Dalal, 1997; Lima et al., 2010; Saikia and de Brito, 2014; Tang et al., 2008). However, a reduction varying between 16 and 64% was observed due to replacing FA with plastic at different replacement levels (15-75%), as reported by (Albano et al., 2009; Batayneh et al., 2007; Juki et al., 2013; Kou et al., 2009; Rahmani et al., 2013; Saikia and de Brito, 2014). Additionally, replacing 20% of FA with PET and mixed waste plastic particles showed a reduction of 22 and 64% respectively; which suggests that the type of plastic used

also had a significant effect on the reduction of the splitting tensile strength (Albano et al., 2009; Batayneh et al., 2007).

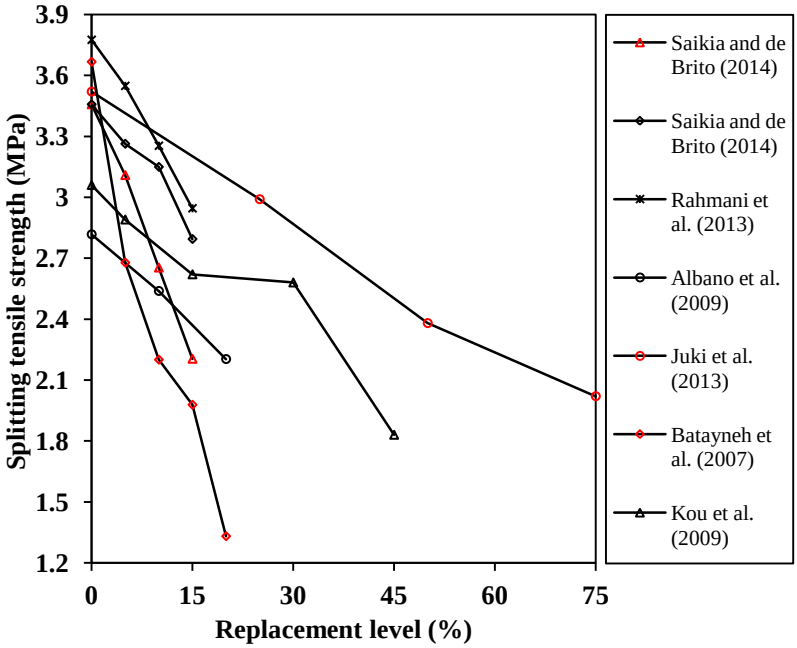


Figure 2.18: Variation in splitting tensile strength of concrete with replacement level of FA with shredded or virgin plastic

The reduction in splitting tensile strength can be explained by the dissimilarity in the shape, texture and hardness between plastic particles and conventional aggregates (Kou et al., 2009; Rahmani et al., 2013; Saikia and de Brito, 2014; Sakr and El-Hakim, 2005). Another possible reason for this reduction is due to the reduction in the modulus of elasticity of plastic particles, as reported by Gu and Ozbakkaloglu (2016). However, other researchers, (Kou et al., 2009; Saikia and Brito, 2013), claimed that this reduction resulted from less bonding between plastic particles and the cement paste due to accumulated water around the surface of the plastic particles.

2.5.3.2 Effect of plastic based aggregate on splitting tensile strength

A limited amount of studies can be found regarding the effect of incorporating recycled plastic based aggregate as a CA or FA replacement on the splitting tensile strength of

concrete, as shown in Figure 2.19. Previous studies (Choi et al., 2005; Jansen et al., 2001) observed a reduction ranging from 26 to 38% and from 37 to 40% due to replacing CA at 100% and FA at 75% respectively, with plastic based aggregate (i.e. SLA or WPLA). According to Jansen et al. (2001), this could be due to the weaker bond strength and the lower modulus of elasticity of SLAs. Nonetheless, the splitting tensile strengths of SLA concrete increased by 19% as the fly ash proportions in the SLA matrix increased from 0 to 80%.

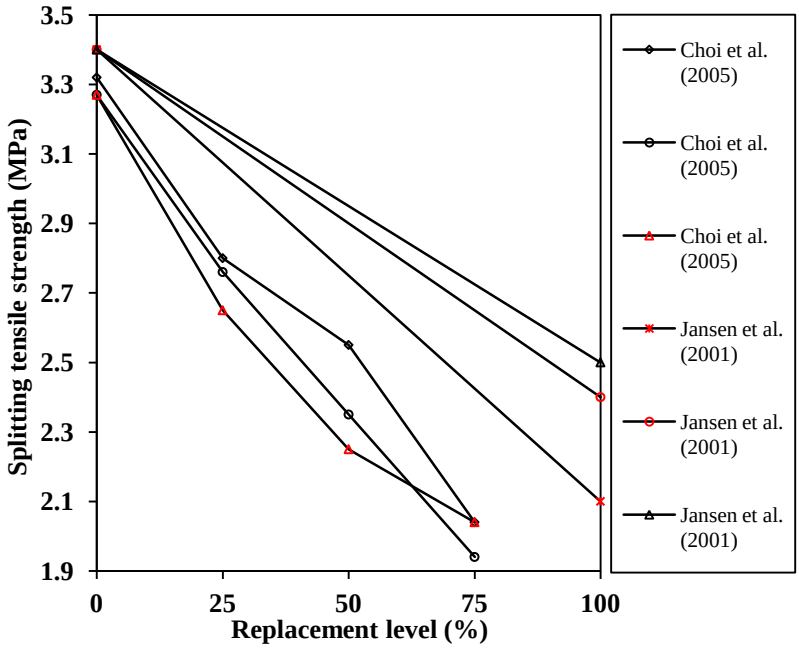


Figure 2.19: Variation in splitting tensile strength of concrete with plastic based aggregate incorporation

2.5.4 Flexural strength

2.5.4.1 Effect of shredded or virgin plastic on flexural strength

Flexural strength is controlled by the same parameter influencing both compressive and splitting tensile strength, as mentioned previously. In order to study this effect, the findings concerning flexural strength of previous studies have been gathered (Fig. 2.20), when either CA or FA has been replaced with shredded or virgin plastic. These studies reported reduction of 50-59% in the flexural strength, due to replacing CA with various plastic particles from 15 to 50% (Lima et al., 2010; Saikia and de Brito, 2014). However, replacing FA with plastic

particles at levels varying from 15 to 75% resulted in a reduction ranging between 13 to 60%; which is lower as compared to those reductions observed in the case of the CA replacement (Batayneh et al., 2007; Ismail and Al-Hashmi, 2008; Juki et al., 2013; Rahmani et al., 2013; Rai et al., 2012; Saikia and de Brito, 2014). Similarly, as reported for compressive and splitting tensile strength, changing the type of plastic used also had a dominating impact on the reduction percentage. For example, the flexural strength was decreased by 13 and 43% at same replacement level (15%) of FA with PET and waste plastic pellet, respectively (Rahmani et al., 2013; Rai et al., 2012).

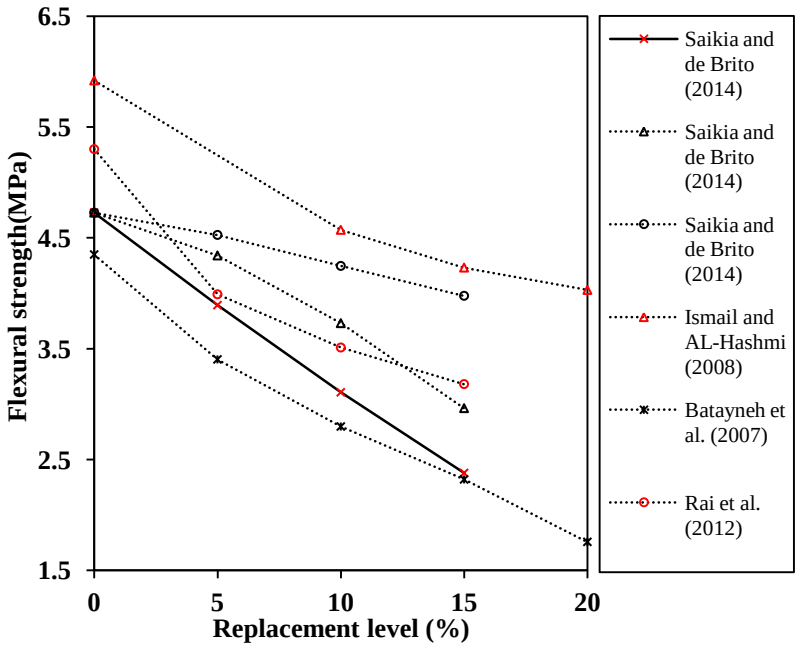


Figure 2.20: Variation in flexural strength of concrete with shredded or virgin plastic incorporation (Solid lines represent CA replacement; dotted lines represent FA replacement)

The reduction in flexural strength can be attributed to the same factors that would affect compressive and splitting tensile strength. Therefore, it has been reported that this reduction might be related to the reduction in adhesive or bonding between the paste and the surface of the plastic aggregate. This resulted from the hydrophobic nature of plastic which may hinder cement hydration (Ismail and Al-Hashmi, 2008; Rai et al., 2012).

2.5.5 Modulus of elasticity

2.5.5.1 Effect of shredded or virgin plastic on modulus of elasticity

In the case of concrete containing shredded or virgin plastic, the modulus of elasticity is influenced by a range of variables, including proportion level of plastic particles, W/C ratio, plastic type, ITZ, and the modulus of elasticity of plastic itself.

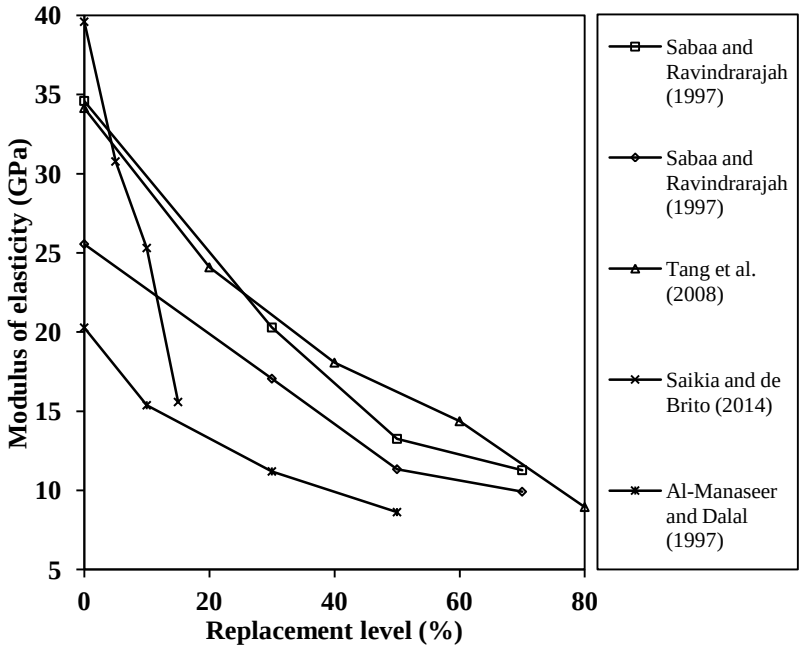


Figure 2.21: Variation in modulus of elasticity of concrete with replacement level of CA with shredded or virgin plastic

The findings of previous studies concerning the influence on the modulus of elasticity due to using different types of plastic particles as a replacement of CA or FA are respectively presented in Figures 2.21 and 2.22. The general tendency of the results of these studies indicated a decreasing trend in the modulus of elasticity of concrete, varying according to the type of replacement, followed by the substitution level and finally, the type of plastic used. Therefore, the incorporating of different types of plastic such as PET, EPS, PVC and shredded car bumpers as CA replacement at various contents (15-80%), yields substantial reductions ranging between 57 and 73% (Al-Manaseer and Dalal, 1997; Sabaa and Ravindrarajah, 1997; Saikia and de Brito, 2014; Tang et al., 2008). Whereas, other studies, (Albano et al., 2009;

Juki et al., 2013; Kou et al., 2009; Rahmani et al., 2013; Saikia and de Brito, 2014) observed less reduction (from 20 to 70%) in the case of replacing FA with plastic particles at different substitutions (from 15 to 75%).

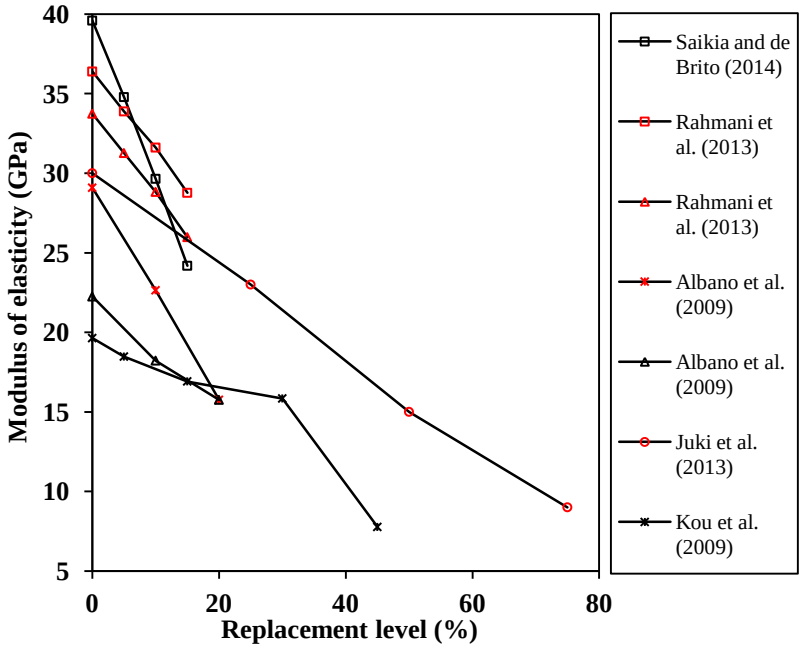


Figure 2.22: Variation in modulus of elasticity of concrete with replacement level of FA with shredded or virgin plastic

The majority of the previous studies attributed this reduction to the low modulus of elasticity of the plastic particles themselves (Rahmani et al., 2013; Saikia and de Brito, 2014). In addition, it accounts for the poor bonding between the plastic particles and the cement paste which reduces the compressive strength and consequently the modulus of elasticity, as reported in several works (Babu et al., 2005; Kou et al., 2009; Rahmani et al., 2013; Ravindrarajah and Tuck, 1994). Moreover, Kou et al. (2009) and Tang et al. (2008) claimed that this reduction was related to the increasing incompatibility between the low and high modulus of elasticity of plastic aggregate and the cement matrix respectively. Therefore, the concentration of stress at the interfaces between the aggregates and the cement paste would increase, due to this incompatibility; ultimately, the modulus of elasticity is reduced (Bremner and Holm, 1986).

2.5.5.2 Effect of plastic based aggregate on modulus of elasticity

The previous findings for the modulus of elasticity for concrete made with plastic based aggregate as a replacement for CA or FA are given in Table 2.9. The findings of these studies showed a significant reduction in the 28-day modulus of elasticity varying from 21 to 39% and from 34 to 42% at 75 and 100% replacement levels of FA and CA respectively with plastic based aggregate. According to Malloy et al. (2001), changing the type of plastic in the developed plastic based aggregate matrix had no effect on the modulus of elasticity of concrete (Table 2.9). However, Jansen et al. (2001) found that the elastic modulus increased by 14% as the fly ash content in the plastic aggregate (i.e. SLA) increases from 0 to 80%.

Table 2.9: Variation in elastic modulus of concrete with plastic based aggregate incorporation

Study	Type of aggregate	Replacement level (%)	Replacement type	W/C ratio	Modulus of elasticity (GPa)	Maximum percentage deviation WRT control
Choi et al. (2005)	WPLA	0, 25, 50, 75	FA	0.45	25.5-15.6	-39
Choi et al. (2005)				0.49	23.3-16.7	-28
Choi et al. (2005)				0.53	23.5-18.5	-21
Jansen et al. (2001)	SLA (Fly ash: HDPE) (0:100)	0, 100	CA	NA	21.8-12.6	-42
	SLA (Fly ash: HDPE) (35:65)				21.8-13	-40
	SLA (Fly ash: HDPE) (80:20)				21.8-14.4	-34
Malloy et al. (2001)	SLA (Fly ash: HDPE) (80:20)	0,100	CA	0.5	23.5-14.5	-38
	SLA (Fly ash: MP) (80:20)				23.5-14.5	-38

2.5.6 Poisson's ratio

Poisson's ratio of concrete is the ratio between lateral and axial strain, and it can be used to identify the ductile or deformable behaviour of concrete. Thus, a high value of Poisson's ratio is a strong identification of ductility response and vice versa. Previous studies (Jansen et al., 2001; Kou et al., 2009) reported that Poisson's ratio of concrete containing plastic particles or plastic based aggregates (i.e. 0.24 to 0.29) is higher than those of conventional concrete (i.e.

0.19 to 0.2). For instance, Kou et al. (2009) reported that Poisson's ratio was increased by 57% at a 45% replacement level of FA with shredded PVC plastic. Similar findings were also reported by Jansen et al. (2001), who observed an increase in the Poisson's ratio ranging from 20 to 30% at 100% replacement level of CA with different types of plastic based aggregate (i.e. SLAs). However, the Poisson's ratio was deceased by 10% as the fly ash content in the SLA matrix increased from 0 to 80% (Jansen et al., 2001).

The increase in Poisson's ratio is related to the elastic and high deformation of plastic particles (Hannawi et al., 2010; Kou et al., 2009). On the other hand, Jansen et al. (2001) linked this improvement to the weak bonding between plastic based aggregate and the cement matrix. Subsequently, the failure pattern is formed in the same direction (i.e. parallel) of the load which would increase the later strain and thus, leads to a high Poisson's ratio.

2.5.7 Stress-strain response and failure mechanism

The response of concrete subjected to compression loading (stress-strain relationship) is significantly influenced by the properties of the aggregate used. Figure 2.23 depicts the effect of using shredded plastic as an aggregate replacement on the stress-strain response performed in different studies. The findings of these studies (Fig. 2.23) show that the axial strain to failure increased in a range varying from 100 to 200% at a 50% replacement level of CA with shredded plastic, as compared to that of normal concrete at the same stress level (Al-Manaseer and Dalal, 1997). A similar trend showing an increase ranging from 14 to 27% was also observed at a 5% replacement level only of FA with PET (Frigione, 2010). Moreover, Babu et al. (2005) also reported that the steepness of the stress-strain curve decreased and failure occurred at higher strain with respect to the increase of the plastic particle content.

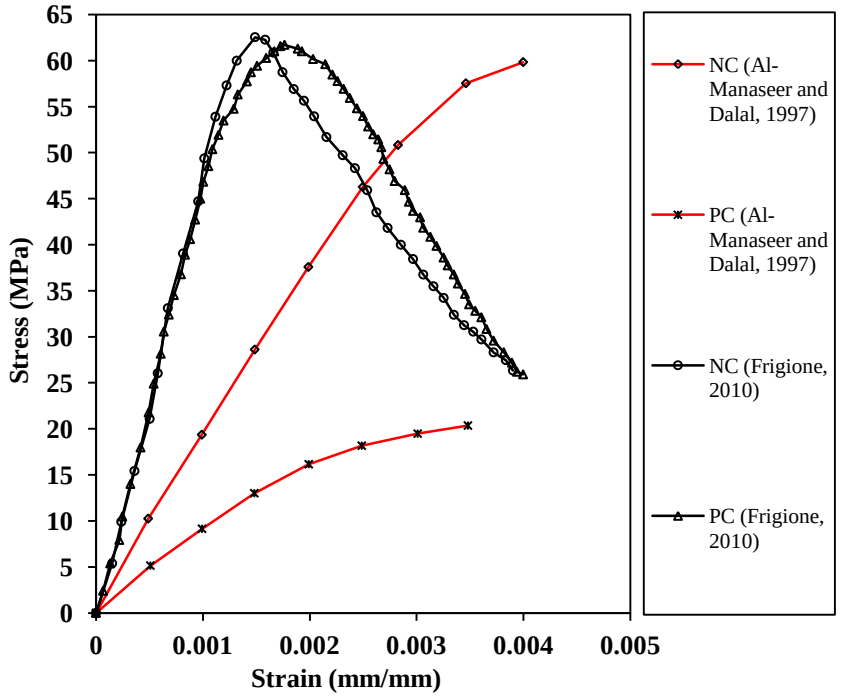


Figure 2.23: Comparison between stress-strain response for concrete containing plastic particles and normal concrete

Similarly, concrete made with plastic based aggregate (Fig. 2.24) follows the same behaviour as concrete containing shredded plastic particles (Jansen et al., 2001; Kashi et al., 1999; Malloy et al., 2001). These studies showed a prominent increase in the strain ranging between 78 and 184% for concrete made with 100% replacement of CA with SLA, in comparison with normal concrete at the same stress. In spite of that, Jansen et al. (2001) revealed that the axial and lateral strain is reduced by about 50 and 87% respectively at the same stress, with respect to the increase in fly ash content in the aggregate (SLA) matrix from 0 to 80%.

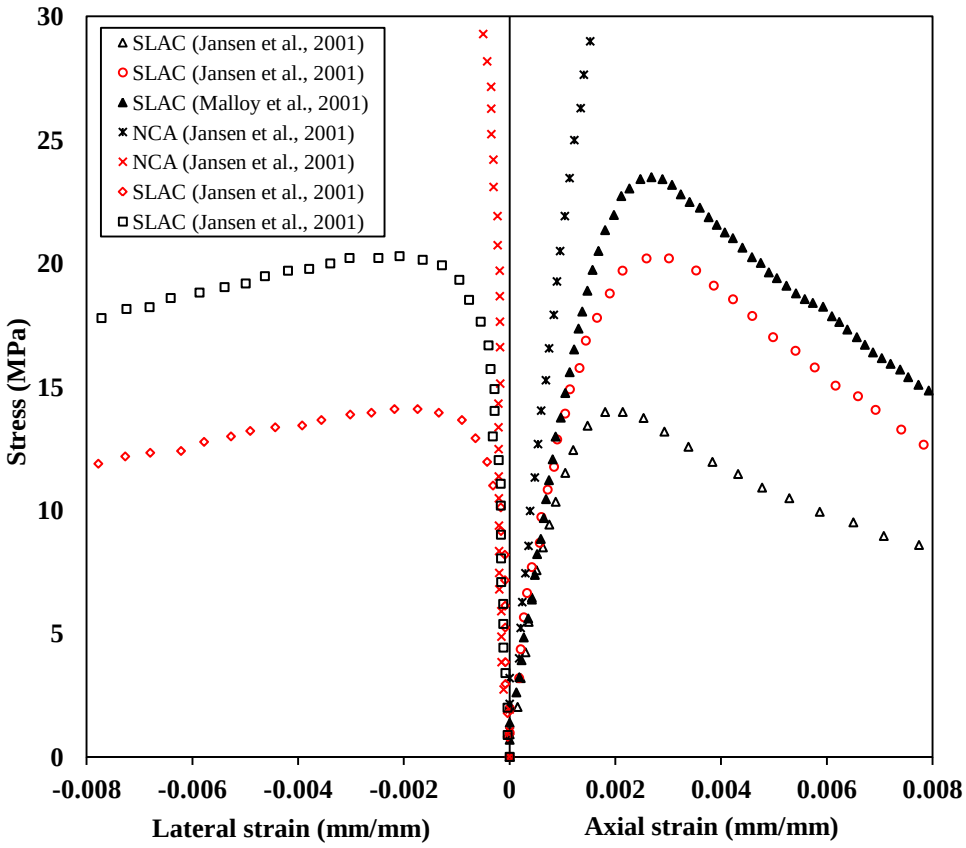


Figure 2.24: Stress versus axial and lateral strain for normal and plastic based aggregate concrete

Moreover, concrete made with shredded or plastic based aggregate exhibits a different mode of failure as compared with normal concrete, in which the stress gradually decreases after reaching the ultimate load; while the sample continued straining or deforming (i.e. ductile response) (Al-Manaseer and Dalal, 1997; Babu et al., 2006; Babu et al., 2005; Babu and Babu, 2003; Chen and Liu, 2004; Kashi et al., 1999; Ravindrarajah, 1999; Slabaugh et al., 2007; Xu et al., 2012). Similarly, other studies have observed that the concrete specimens containing shredded plastic or plastic based aggregate can maintain the load for a period of time while the strain is increasing (deforming), even after failure and with no separation or full disintegration (Babu et al., 2005; Kashi et al., 1999; Rahmani et al., 2013; Saikia and de Brito, 2014). On the other hand, Al-Manaseer and Dalal (1997) and Kou et al. (2009) reported that the plastic aggregates were ‘‘de-bonded’’ from the cement matrix instead of splitting, due to poor bonding with the cement paste.

This ductility phenomenon is attributed to the presence of plastic which deforms under load (Chen and Liu, 2004; Jansen et al., 2001; Kashi et al., 1999; Malloy et al., 2001; Ravindrarajah, 1999; Slabaugh et al., 2007). However, Rahmani et al. (2013) and Saikia and de Brito (2014) linked this behaviour with the elasticity and flexibility of plastic, which can bridge the crack propagation.

2.5.8 Abrasion resistance

Although several works have been carried out on the effect of using plastic particles on the fresh and hardened properties of concrete, only a few studies (Ferreira et al., 2012; Saikia and de Brito, 2014) have focused on the effect of incorporating this plastic into the abrasion resistance of concrete. For instance, Ferreira et al. (2012) reported that the abrasion resistance improved from 28 to 37% for concrete made with different types of PET plastic (i.e. PC, PF and PP) at only a 7.5 % replacement level of CA and FA. Similarly, Saikia and de Brito (2014) found a high resistance (33-42%) towards abrasion or weight loss due to substituting CA and FA with shredded PET plastic at 15%.

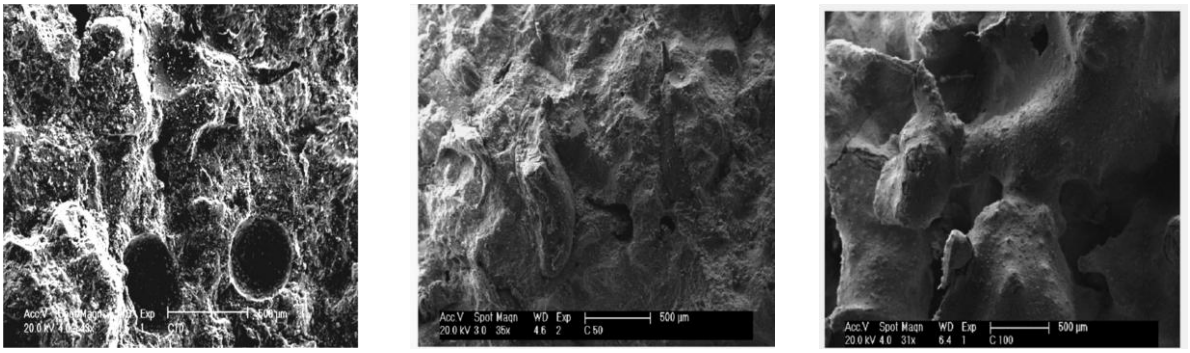
According to Ferreira et al. (2012), this improvement is associated with the increase of resistance to abrasion given by plastic particles due to their plasticity nature. However, Saikia and de Brito (2014) proposed that this property stemmed from the concrete's compressive strength and form and the size together with roughness of the plastic particles.

2.5.9 Microstructure analysis

Concrete made using shredded plastic or plastic based aggregate is influenced morphologically by a range of variables, including the type and size of the plastic particles used (Gu and Ozbakkaloglu, 2016). Different studies (Fraj et al., 2010; Laukaitis et al., 2005) indicated that the cement matrix adhered well to the plastic particles (i.e. PUR foam,

polystyrene granule) with no fractures or micro cracks. According to Fraj et al. (2010), this observation is related to the absence of the wall effect in the interfaces between PUR foam plastic and cement mortar. However, Laukaitis et al. (2005) attributed this to the crumbled shape and large size of the plastic particles which resulted in better bonding with the cement paste.

On the other hand, Marzouk et al. (2007) presented different observations for mixes made with 30, 50 and 100% replacement of FA with PET, as shown in Figure 2.25. The finding of this study (Fig. 2.25) indicated that the composites are strongly compacted at up to 50% replacement; while more pores appeared at higher substitution rates (i.e. 100%). According to Marzouk et al. (2007), these morphological variations (i.e. increased pores) offer a reason for the lower mechanical characteristics (i.e. compressive strength) and bulk density of the mix.

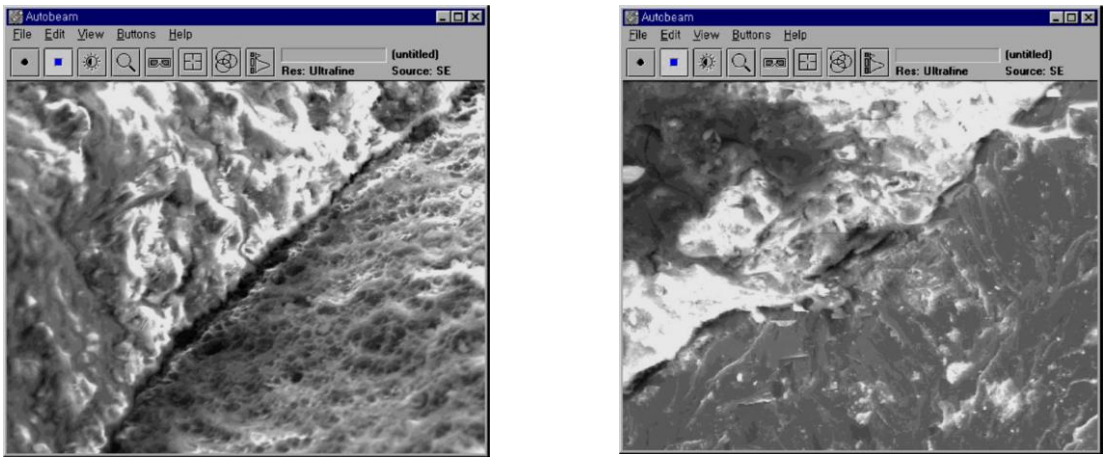


a b c

Figure 2.25: SEM of mortar containing PET aggregate (a) 30% (enlargement: 43×), (b) 50% (enlargement: 35×) and (c) 100% (enlargement: 31×) (Marzouk et al., 2007)

A similar finding was also obtained when the FA was replaced with plastic based aggregate in concrete in which the ITZ of the concrete made with the plastic based aggregate (i.e. WPLA) was broader than that of conventional concrete, as seen in Figure 2.26 (Choi et al., 2005). According to the authors, this observation can be attributed to the smooth texture and rounded shape of WPLA which leads to fewer joint angles or anchors with the cement matrix. The

hydrophobic nature of plastic which limits water migration and consequently cement hydration also endorses this observation (Choi et al., 2005). Furthermore, it was found that the presence of GBFS adhered on the surface of aggregate (i.e. WPLA) strengthen the aggregate surface due to the consumption of calcium hydroxide.



(a) (b)

Figure 2.26: Transition zone between cement paste and (a) WPLA; and (b) natural aggregate (28-day; magnified × 700) (Choi et al., 2005)

2.5.10 Drying shrinkage

The effect of incorporating shredded or virgin plastic as a replacement for CA and/or FA on drying shrinkage has been investigated in extant literature (Chen and Liu, 2004; Kou et al., 2009; Sabaa and Ravindrarajah, 1997; Tang et al., 2008).

Bulk of these studies reported an increase in drying shrinkage ranging from 39 to 149% at replacement levels ranging from 45 to 80% of CA with plastic particles after different drying periods (28-240 day) (Fraj et al., 2010; Sabaa and Ravindrarajah, 1997; Tang et al., 2008). Similarly, Chen and Liu (2004) found an increase in drying shrinkage by 78% at a 55% replacement level of both CA and FA with EPS at 90 days. This increase can be related to the low resistance of plastic particles to the shrinkage induced by the cement paste; since plastic

particles have high compressibility and low stiffness simultaneously (Chen and Liu, 2004; Ravindrarajah and Tuck, 1994; Sabaa and Ravindrarajah, 1997; Tang et al., 2008).

On the other hand, Kou et al. (2009) reported a contrary trend in which the drying shrinkage was reduced by 72% at a 45% replacement level of FA with PVC plastic at 112 days. The author linked the decrease in shrinkage with low capillary tensile force resulting from low water loss from the concrete matrix. According to Kou et al. (2009), concrete made with plastic particles has less shrinkage, since plastic has an impervious nature which yields low water loss and thereby less capillary tensile stress is produced (Chandra and Berntsson, 2002; Kou et al., 2009).

2.5.11 Creep

Increase in strain measured over a long time period of sustained constant load can be defined as creep. Creep is influenced by a number of factors including compressive strength, modulus of elasticity and type of aggregate. Thus, concrete made with shredded or virgin plastic is expected to exhibit higher creep and shrinkage strain, due to its low compressive strength and the modulus of elasticity of the plastic particles. This was confirmed by Sabaa and Ravindrarajah (1997), who reported that the 150-day creep coefficient (i.e. ratio between creep strain and instantaneous strain) of EPS concrete ranged from 2.37 to 3.04, compared to 1.59 to 1.84 recorded for normal concrete. Thus, the increase in the 150-day creep coefficient of EPS mixes compared with that of normal concrete ranged from 28 to 91% as the replacement level of CA with EPS plastic was increased from 0 to 70%. Furthermore, the rate of initial creep was also increased where a larger proportion of EPS particles were used.

According to Sabaa and Ravindrarajah (1997), the reason for the greater creep rate in the EPS concrete is accounted for by the changes of volume over time, due to the high compressibility

of plastic particles (i.e. EPS); in addition to the low modulus of EPS particles, which cannot restrict the cement matrix creep tendency.

2.6 Durability related properties

2.6.1 Water absorption

Water absorption is usually used to measure the quality of concrete; since it has a direct influence on the ingress of chemicals or hazards soluble within it. The findings of previous works concerning the water absorption of concrete containing shredded plastic particles at various replacement levels are given in Figure 2.27.

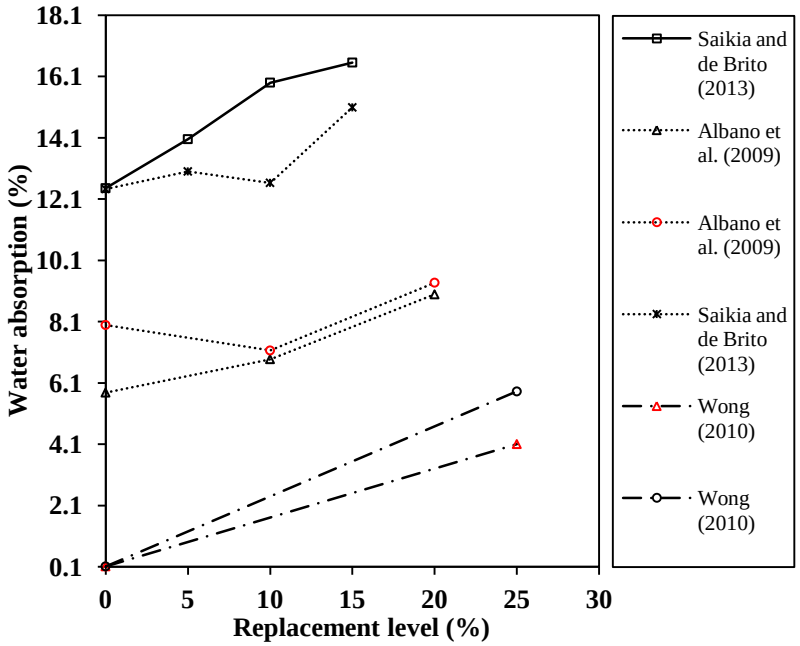


Figure 2.27: Variation in water absorption of concrete with plastic particles incorporation (Solid lines represent CA replacement; dotted lines represent FA replacement; semi-dotted lines represent both)

Water absorption values reported in previous studies increased from 17 to 55% at different substitutions varying from 15 to 20% of FA with PET plastic (Albano et al., 2009; Saikia and Brito, 2013). However, replacing CA with PET plastic at 15% resulted in a higher increase in water absorption (33%) as compared to those observed with the FA replacement (Saikia and

Brito, 2013). Furthermore, Babu et al. (2006) and Wong (2010) reported prominent increase ranging between 55 and 98% due to substituting both CA and FA with different plastics (i.e. EPS, LDPE and HDPE) from 25 to 50%.

The increases in water absorption are a result of the increases in porosity and the interconnected pores of concrete (Kearsley and Wainwright, 2001). Several authors have attributed this increase to the difference in shape and size of plastic and natural aggregates, which resulted in a less dense mix with a high number of voids (Albano et al., 2009; Babu and Babu, 2003; Saikia and Brito, 2013). However, few studies (Babu et al., 2006; Babu and Babu, 2004) linked this increase with the micro-cracking created due to the high drying shrinkage of concrete containing plastic particles.

2.6.2 Chloride ion penetration

The extent to which chloride ions penetrate into concrete depends upon the permeability of the concrete (Gu and Ozbakkaloglu, 2016). The permeability increases as the porosity and the amount of interconnected pores increase (Kearsley and Wainwright, 2001). However, concrete made with plastic particles has high porosity and less chloride permeability simultaneously. The explanation for this behaviour is related to the impervious nature of plastic towards water, which hinders the path of chloride ion (Kou et al., 2009). According to Babu and Babu (2003) and Kou et al. (2009), chloride permeability decreased by 36 and 43% at 45 and 37% replacement levels of FA and all aggregates (i.e. both CA and FA) with PVC and EPS respectively.

2.7 Physical properties

2.7.1 Fire resistance

The main disadvantage of using plastic as an aggregate in concrete is its low resistance to fire and its rapid rate of catching fire. Therefore, Albano et al. (2009) examined the effect of high temperature (i.e. 200, 400 and 600 °C) on the flexural strength of concrete containing recycled PET as FA replacement at 0, 10 and 20% levels. The study results showed that the reduction in flexural strength due to the increases in temperature from 25 to 600 °C varied from 4 to 27% and from 3 to 42% for normal concrete (i.e. has 0% PET) and PET concrete (i.e. has 20% PET), respectively. Similarly, Koide et al. (2002) found that the compressive and tensile strength of concrete containing plastic waste was reduced by almost 10% for each 20 °C increase in temperature up to 120 °C.

Additionally, it was reported that the samples of PET concrete (made with a 20% replacement level of bigger particles) disintegrated at 600 °C. According to Albano et al. (2009), PET degraded at higher temperatures leaving holes or voids which ultimately weaken the bonding and accelerate failure occurrence.

2.7.2 Thermal conductivity

Thermal conductivity is one of the most commonly used indicators to identify the ability of material to resist heat flow. Concrete made with shredded or virgin plastic is thermally non-conductive, since plastic has low conductivity (Elzafraney et al., 2005; Laukaitis et al., 2005; Mounanga et al., 2008; Yesilata et al., 2009). For instance, Yesilata et al. (2009) observed a reduction in thermal conductivity ranging from 10 to 17% at a 100% replacement level of CA and FA with different types of PET particles. Similarly, Laukaitis et al. (2005) indicated that

the thermal conductivity coefficient of composite made with different polystyrene granules varied from 0.06 to 0.064 W/m.K.

According to Laukaitis et al. (2005), the increase of resistance to heat transfer is accredited to the low conductivity of plastic towards heat. However, Mounanga et al. (2008) suggests that this increase is due to the presence of entrapped air in plastic particles (i.e. PUR foam) due to their porous texture.

2.8 Summary of existing developments

There is a corroborated consensus from different researchers with respect to reduction in density, compressive strength, flexural strength, splitting tensile strength, modulus of elasticity and abrasion of concrete with the increases in the content of plastic particles or plastic based aggregates in the mix. However, there were contrary reports concerning the effect of plastic particles or plastic based aggregates on the workability of concrete.

Although few research studies were conducted on the impact of using plastic particles as aggregate on the durability of concrete, these studies reported low chloride permeability together with high water absorption, drying shrinkage and creep strain with the inclusion of plastic particles. While, just a few researchers were of the opinion that drying shrinkage reduces as plastic particles increase in a concrete mix.

Finally, a general consensus was reported regarding the reduction of thermal conductivity as well as concrete's strength under fire, due to increasing the proportions of plastic particles as a replacement for aggregates in concrete. In summary, the differences in opinions could be attributed to the difference in the source of materials used and the methods employed, including any experimental errors.

2.9 Gap of knowledge

From several works' findings reviewed in this chapter, the majority of the research (42 studies) investigated the effect of using shredded or virgin plastic directly as a replacement for either CA or FA, on the fresh and hardened properties of concrete. On the other hand, four studies developed a plastic based aggregate from plastic and fly ash and then used it as a CA replacement in concrete. While, only two research studies investigated the effect of incorporating plastic based aggregate produced from PET and coated with GBFS or river sand as an FA replacement in concrete.

The plastic based aggregates developed in these studies had the same shape and size. For making better concrete, it is essential that the aggregates have well-graded particle sizes. Additionally, in most of these studies, plastic was used in a mixed form; except by some researchers who used PET, LDPE, PS and HDPE as their main plastic candidate. Furthermore, in these studies, the fillers used were mainly limited to fly ash and the local granular materials available in those areas. Moreover, the previous studies had limited techniques for aggregate production (i.e., extrusion), which restricted the scope of its practical utilization.

In considering the development of a plastic based aggregate, it was realised that a defined type of plastic and the low cost fillers needs to be utilized in the manufacturing of well-graded aggregates for the production of concrete. The latter needed be widely and locally available, granular and stable at temperature of about 500 °C. These fillers could include red dune sand and quarry fines. For a practical applicability and maximum utilization of a plastic based aggregate, it is essential to explore using different techniques, prior to its incorporation in concrete.

Finally, to the best of the author's knowledge, the engineering and durability properties of concrete containing plastic based aggregates have not been investigated. Therefore, a full spectrum of fresh, hardened and durability properties of concrete needs to be examined at various replacement of CA with plastic-based aggregate. This provides an opportunity to reduce both the disposal of plastic and the consumption of natural aggregates; occupying around 60-75% of the total volume of concrete.

CHAPTER 3: MATERIALS AND EXPERIMENTAL DESIGN

3.1 General

Properties of materials used for both the manufacture of aggregate and concrete production are presented in this chapter. The overall experimental programme, including the techniques used and tests conducted on both aggregate and concrete, are also given. This is followed by a description of the concrete mix design and its subsequent mixture proportions. Finally, the casting and curing procedure used are also described.

3.2 Materials used

A wide range of materials were used in this research for both aggregate and concrete investigations. Recycled plastic and fillers were used in the manufacturing of recycled plastic aggregate (RPA), as described in sections 3.2.1 and 3.2.2 respectively. However, cement, water, coarse aggregate and fine aggregate were used in the concrete investigation.

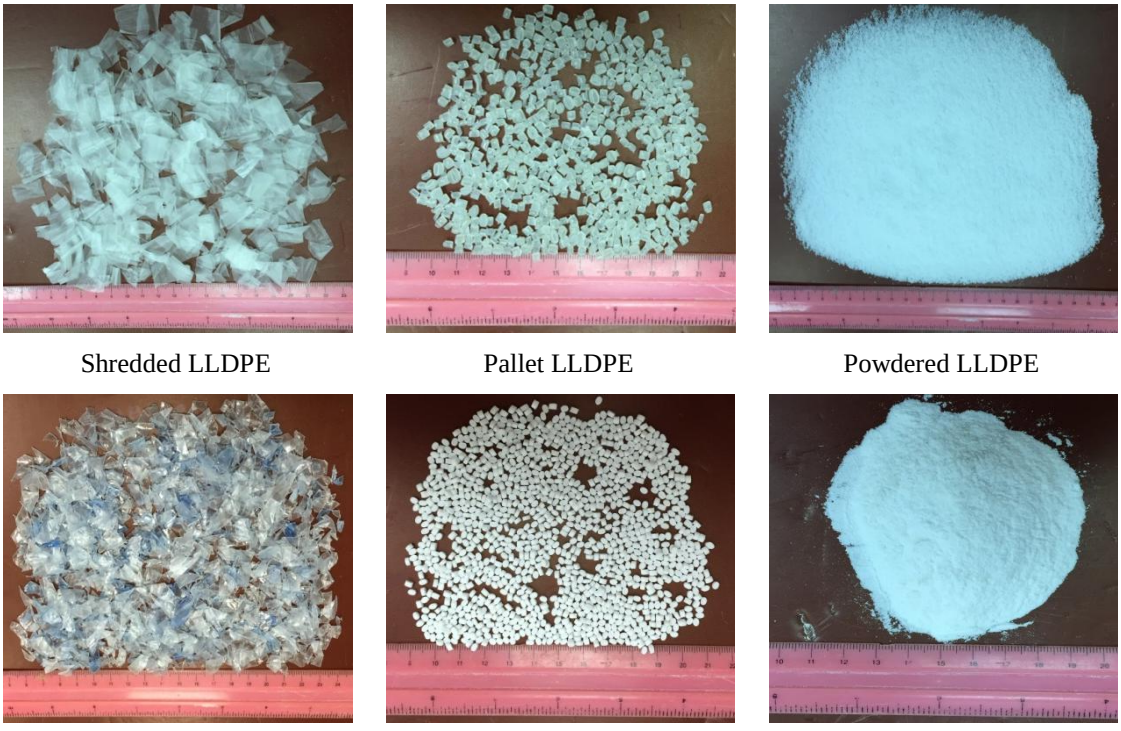
Normal tap water, free from impurities, was used in this study. In addition, ordinary Portland cement which is manufactured locally (in Saudi Arabia) and complied with the requirements of ASTM C150/C150M-16 (i.e. fineness, specific gravity, consistency, time of setting) was also used. The physical properties and basic constituents of the cement used in this investigation are shown in Table 3.1. Additionally in this study, the type of fine aggregates used were fixed throughout the study, while coarse aggregate was the only changing parameter, as explained later in section 3.2.3. Details of each material used in the present study are given below.

Table 3.1: Physical properties and basic components of the cement used

Properties	Measured Values
Fineness (cm^2/gm)	3500
Specific Gravity	3.15
Consistency (%)	23.5
Initial setting time (min)	45
Final setting time (min)	135
C_3S (%)	67.36
C_2S (%)	7.07
C_3A (%)	7.62
C_4AF (%)	11

3.2.1 Recycled plastic waste

Recycled plastic was one of the prime materials used in this research, as a binder in RPA manufacturing. Recycled plastic (LLDPE and PET) was used in three different forms: shredded, pallet and powdered, as shown in Figure 3.1.



Shredded LLDPE | Pallet LLDPE | Powdered LLDPE

Shredded PET | Pallet PET | Powdered PET

Figure 3.1: Forms of plastics used in manufacturing of RPA

These types of plastic were supplied by a local supplier (in Riyadh, Saudi Arabia) who collects all types of waste plastic from the local vicinity and treats them as follows. The treatment process starts by collecting the plastic, followed by purifying, shredding, melting and pelletizing, before it is powdered into its final form. The source of PET was from waste bottles used for drinking water, available in very large quantities in daily plastic waste generation. The LLDPE was collected from the waste formed by plastic bags used, for example, in ice and frozen food packaging and carrier bags. The physical, mechanical and thermal properties of LLDPE and PET given in the datasheet are presented in Table 3.2 (MDB, 2003; Sabic, 2009; Sabic, 2013; SpecialChem, 2015).

Table 3.2: Physical, mechanical and thermal properties of LLDPE and PET

Property	**Plastic type**	
	LLDPE	**PET**
Density (kg/m^3)	918	838
Specific Gravity	0.93-0.96	1.29-1.4
Water absorption (%)	0.005-0.010	0.10-0.20
Melt temperature (°C)	190-215	285
Ultimate tensile strength (MPa)	20.7-44.8	48.3-72.4
Young's modulus of elasticity (GPa)	0.621-0.896	2.76-4.14

Table 3.2 shows that plastic has trace amount of water absorption. Additionally, there is no significant difference between the densities of the two plastic types; however, the LLDPE melts at a relatively lower temperature compared to that of the PET. This data also indicates that plastic (i.e. LLDPE, PET) has high tensile strength capacity compared with low elastic modulus.

3.2.2 Filler materials

The fillers used in this research were either by-product wastes or natural granular materials. These fillers represent the second component in the matrix of RPA. Fillers used include red

dune sand filler (RSF), fly ash filler (FAF) and quarry fines filler (QFF), as shown in Figure 3.2. The RSF and QFF were locally available; while the FAF (Class F) was supplied by an international supplier (SIKADUR).



Figure 3.2: Fillers (RSF, FAF and QFF) used in manufacturing RPA

Physical properties of these fillers (RSF, FAF, QFF) are presented in Table 3.3. The specific gravity and absorption of RSF and QFF were made according to ASTM C128-15. Similarly, the unit weight of RSF and QFF was measured by following ASTM C29/C29M-16. However, the physical properties of the FAF were performed in accordance with ASTM C618-15.

Table 3.3: Physical properties of fillers (RSF, FAF and QFF)

Properties	**Fillers**		
	FAF	**QFF**	**RSF**
Density (kg/m^3)	-	1531	1649
Specific gravity	2.3	2.71	2.62
Absorption (%)	-	1.52	0.38
Median size (µm)	9.55	19.27	215
Colour	Dark Grey	Cream	Red
Shape	Spherical	Angular	Irregular

The particle size distribution of fillers (see Fig. 3.3) was conducted using a laser particle size analyser. From the gradation curve, the median size distribution (D50) of all fillers (i.e. RSF,

FAF, QFF) was observed (see Table 3.3). The particle size analysis test results showed that FAF was the finest among the three types of fillers and RSF was the most coarse.

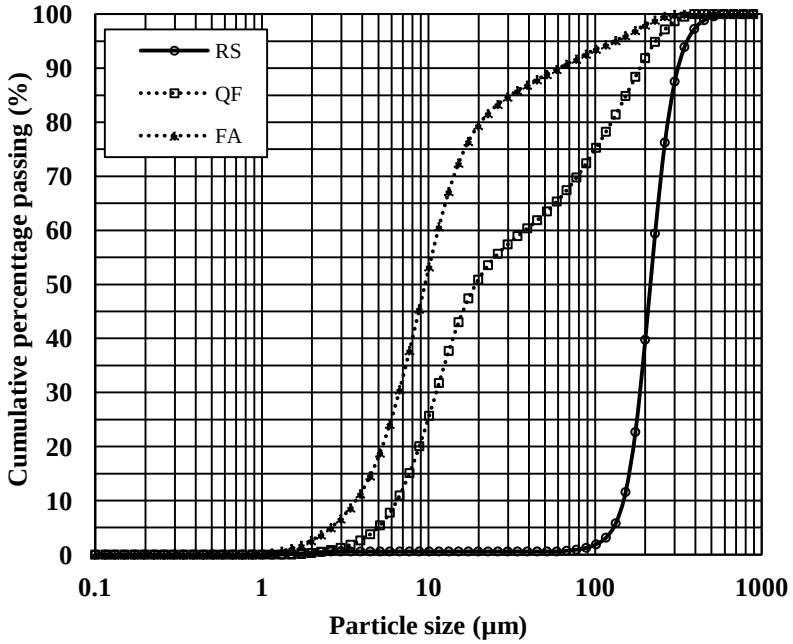
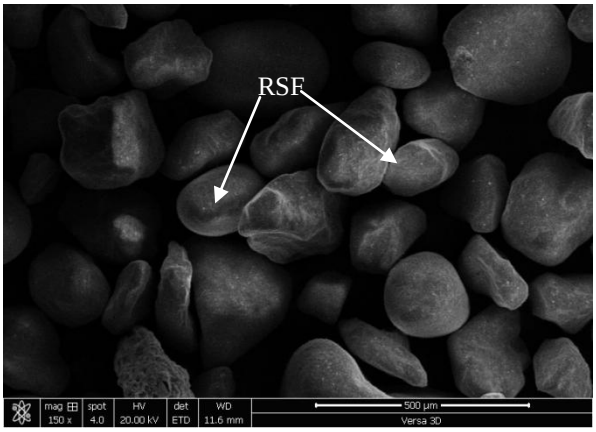


Figure 3.3: Particle size distribution of fillers (RSF, FAF and QFF)

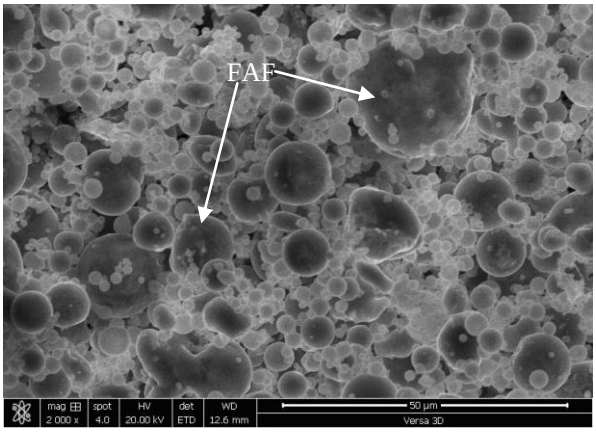
Scanning electronic microscopy (SEM) imaging and element analysis of FAF, QFF and RSF were also performed using SEM and energy dispersive X-ray (EDX). Table 3.4 illustrates the EDX element analysis of these fillers, while the SEM images are shown in Figure 3.4. As it can be seen in Table 3.4, the EDX analysis of RSF indicates a prominent presence of oxygen, carbon, calcium and silicon, with a low content of other elements such as aluminium while, silicon and aluminium were of the major elements found in FAF. Additionally, the main elements in QFF were calcium and oxygen. The SEM images indicated that the majority of RSF particles have an irregular shape, having a size of $\leq$ 250 µm. The SEM also confirmed that the FAF and QFF have smaller particles in which the FAF comprised irregular spherical particles (10-20 µm) compared with the angular particles (>20µm) observed in the QFF.

Table 3.4: Elemental contents of filler particles determined by EDX

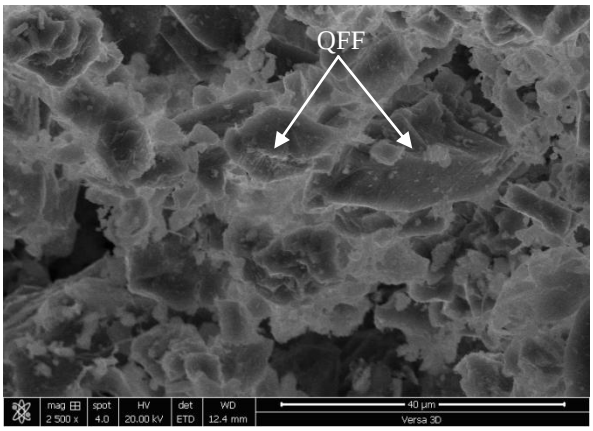
Element	Element content (%) in each filler		
	RSF	FAF	QFF
C	35.9	-	-
O	33.4	57.73	56.29
Na	0.04	-	-
Mg	0.06	-	-
Al	1.04	21.40	6.97
Si	14.54	20.21	7.15
K	0.7	0.66	0.2
Ca	13.7	-	28.77
Ti	0.01	-	-
Fe	0.5	-	0.6



a



b

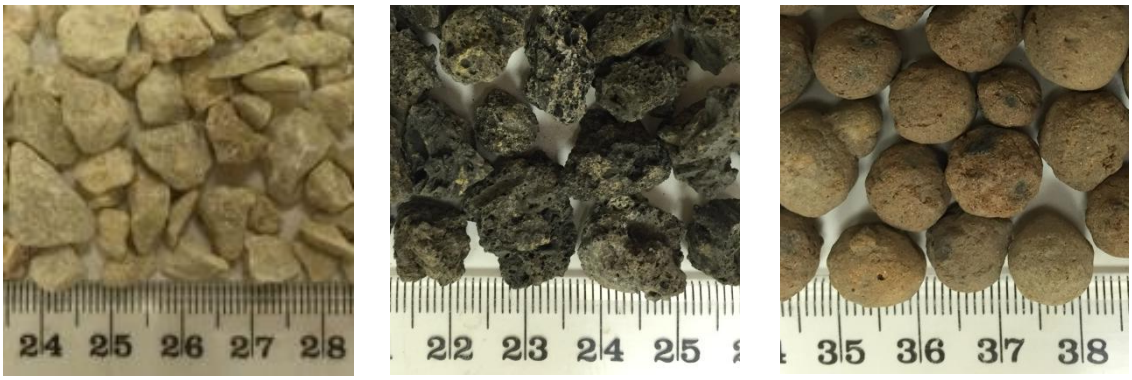


c

Figure 3.4: Microstructure analysis of (a) RSF, magnification: 150 ×, (b) FAF, magnification: 2000 × and (C) QFF, magnification: 2500 ×

3.2.3 Coarse and fine aggregates

In this study, four different types of coarse aggregates were used which include natural aggregate (NA), local volcanic lightweight aggregate (LWA), Lytag aggregate (LYA) and recycled plastic aggregate (RPA). The NA, LWA and LYA (see Fig.3.5) were used for the preparation of different types of control concrete for comparison purposes with concrete made with RPA, which is the key material in this research. Thus, a normal weight concrete mix (NC) was prepared using NA, while the conventional lightweight concrete (LWC) and Lytag lightweight concrete (LAC) were used as reference mixes for concrete containing natural and manufactured lightweight aggregates respectively.



NA LWA LYA

Figure 3.5: Types of coarse aggregate used in this study: NA; LWA and LYA

The NA was collected locally from rock quarry. Similarly, the LWA was collected from the western region of Saudi Arabia, whilst the LYA was supplied by Lytag International Ltd. in the UK. The properties of NA, LWA and LYA are shown below in Table 3.5. Properties of RPA, together with its manufacturing process, are described in Chapter 4.

The sieve analysis was conducted for NA and LWA, and the particle size distribution curve for these aggregates, together with the standard limits specified in ASTM C33/C33M-16 and ASTM C330/C330M-14 for normal weight and lightweight aggregates, are presented in

Figure 3.6. However, the grading of LYA was prepared in the lab in accordance with LWA grading because it was supplied in a single grade by the manufacturer.

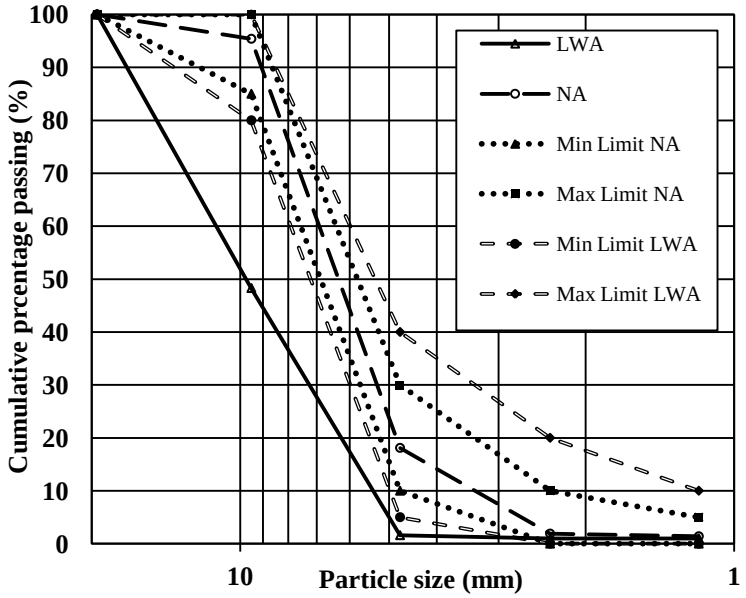


Figure 3.6: Particle size distribution of normal weight (NA) and lightweight (LWA) coarse aggregates

On the other hand, the fine aggregate used in this investigation was only normal weight fine aggregate comprising 65% red sand and 35% crushed sand. It satisfied the ASTM C33/C33M-16 and ASTM C136/C136M-14 grading requirements, as shown in Figure 3.7. The properties of both of these aggregates (coarse, fine) are also presented in Table 3.5.

Table 3.5: Properties of coarse and fine aggregates used in this study

Test	**Coarse Aggregate**			**Fine Aggregate**	
	NA	**LWA**	**LYA**	**Crushed sand**	**Red sand**
Bulk Specific Gravity (OD Basis)	2.59	1.41	1.44	2.59	2.62
Bulk Specific Gravity (SSD Basis)	2.63	1.67	1.69	2.69	2.63
Apparent Specific Gravity	2.69	1.41	1.91	2.77	2.64
Dry Unit weight (kg/m^3)	1554	697	889	1599	1589
Void Content (%)	37.79	50	39.02	38.14	39.20
Absorption (%)	1.48	18.6	16.82	1.67	0.28
Fineness Modulus	5.83	6.5	-	3.89	1.54
Type	Crushed	Uncrushed	Pelletising	Crushed	Uncrushed
Nominal Maximum Size (mm)	10	10	10	4.75	1.18

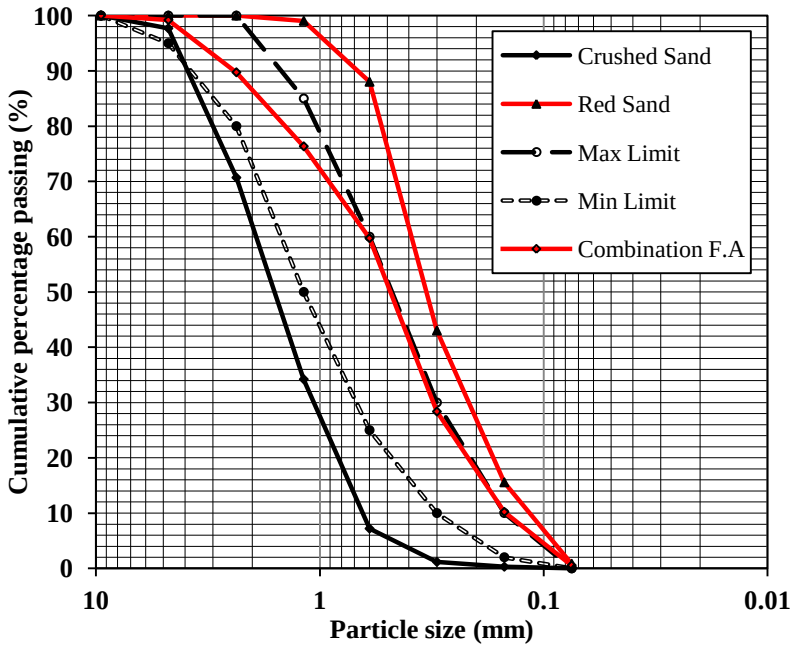


Figure 3.7: Particle size distribution of red sand, crushed sand and combination of red and crushed sand

3.3 Research methodology and techniques used

The laboratory testing work is divided into three major phases:

- ***Phase-1***: Production of recycled plastic aggregate (RPA) and its investigation;
- ***Phase-2***: Preliminary results for RPA optimization of concrete mixes using RPA at full replacement with NA or LWA coarse aggregate at a water to cement ratio of 0.50 and 0.60. The two best aggregates and water to cement ratios were selected from this phase based on strength and durability findings.
- ***Phase-3*:** Detailed concrete investigation using the above RPA selected aggregates at 25, 50, 75 and 100% replacement of either NA or LWA at W/C ratio of 0.50. Also, for comparison purposes, concrete mixes made at 100% of NA, LWA and LYA were prepared at the same W/C ratio.

A flow chart showing the three phases of research is shown in Figure 3.8. Detailed description of each phase is presented in separate section following the flow chart.

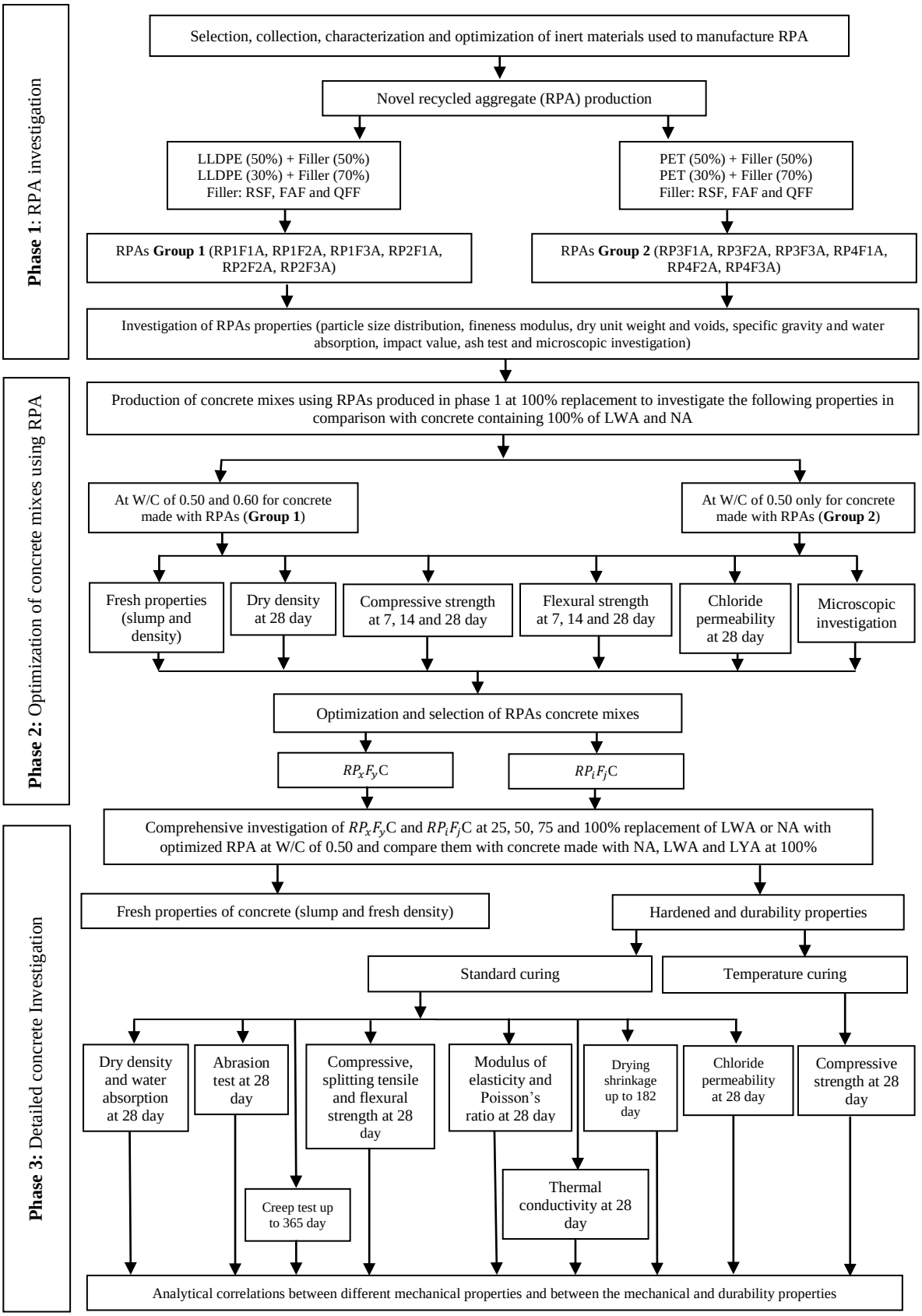


Figure 3.8: Flow chart of research phases

3.3.1 Research programme in Phase-1

Phase 1 of the study involved the selection, characterization and optimization of the inert materials used to manufacture RPAs. This phase also included the production of RPAs (Group1 and Group 2) and the investigation of their individual properties (see flow chart, Fig. 3.8). Therefore, twelve different kinds of RPAs were manufactured and about 15-20 kilograms of each type of aggregate was produced. One hundred and forty seven RPA samples were investigated and compared with thirty six aggregate samples produced from the reference aggregates (NA, LWA and LYA). Tests conducted on the aggregates comprised those for particle size distribution, fineness modulus, dry unit weight and voids, specific gravity and absorption, and impact value. SEM investigations and ash test for RPAs were also made in this phase to study the microstructure and bonding between the composite of RPA. The summary of standards used in the aggregate tests is presented in Table 3.6. However, more details about these tests are given in Appendix A1. This phase is described in detail in Chapter 4 of this study.

Table 3.6: Tests conducted and standards used in Phase-1

Test	**Standard used**	
	Normal weight aggregate	**Lightweight aggregate**
Particle size distribution and fineness modulus	ASTM C136/C136M-14	ASTM C136
Unit weight and voids	ASTM C29/C29M-16	ASTM C29/C29M-16
Specific gravity	ASTM C127-15	ASTM C127-15
Water absorption	ASTM C127-15	ASTM C127-15
Impact value test	BS 812-112:1990	BS 812-112:1990
Ash test	-	ASTM D2584-11

3.3.2 Research programme in Phase-2

As it can be seen in Figure 3.8, Phase 2 of the research included the production of nine concrete mixes using 100% of RPAs (Group 1) at W/C ratios of 0.50 and 0.60. Four control

mixes made with LWA and NA were also developed at the same W/C ratios. Similarly, six concrete mixes containing 100% of RPAs (Group 2) at W/C ratio of 0.50, and two reference mixes made with LWA and NA, were also produced.

Accordingly, in this phase a total of four hundred and forty four concrete samples were produced and evaluated from twenty one different mixes. These samples were examined in terms of slump, fresh density, hardened density, compressive strength, flexural strength and chloride permeability, to study the effect of incorporating RPAs in concrete at 100% replacement of either NA or LWA.

In addition, after compression and flexural tests, the concrete specimens were assessed visually to identify their mode of failure. Then, SEM and optical microscopic analysis of these samples was conducted to study the interfacial transition zone (ITZ) and interlocking between aggregate and cement paste. Table 3.7 presents the summary of the tests conducted in this phase, together with curing period and standard used, as described in detail in Appendix A2. Finally in this phase, the two best aggregate and water to cement ratio were selected based on the fresh, hardened and durability results. This phase is described in detail in Chapter 5.

Table 3.7: Tests conducted and standards used in Phase-2

Test	**Curing period (day)**	**Standard used**
Slump	-	ASTM C143/C143M-15
Fresh density	-	ASTM C138/C138M-16
Dry density	28	BS EN 12390-7:2009
Compressive strength	7, 14, 28	ASTM C579-02
Flexural strength	7, 14, 28	ASTM C580-02
Chloride permeability	28	ASTM C1202-12

3.3.3 Research programme in Phase-3

In this phase, the optimized aggregate of RPA (RP2F1A, RP3F3A) chosen from the previous phase was used in concrete at different replacement from 25 to 100% (on volumetric basis) of reference aggregates (NA, LWA, LYA). Therefore, the mixes of RP2F1C were produced at 25, 50, 75 and 100% of LWA with RP2F1A at the optimized W/C (i.e. 0.50). Similarly, RP3F3C samples were developed at the same replacement levels of NA with RP3F3A and at the same W/C ratio. However, the mixes of LAC were made at 100% of LYA as a reference mix of concrete containing manufactured lightweight aggregate, as mentioned earlier in section 3.2.3.

The effects of increasing the replacement levels of reference aggregates with the optimized RPA (RP2F1A or RP3F3A) on fresh, hardened, morphology, durability and some other properties were then investigated. Fresh properties comprise slump and fresh density, while hardened properties include dry density, compressive strength, splitting tensile strength, flexural strength, modulus of elasticity, Poisson's ratio and abrasion resistance. Durability properties were evaluated by water absorption, chloride permeability, drying shrinkage and creep tests. Additionally, thermal conductivity and the effect of temperature curing were also studied. These tests were conducted in accordance with the test methods described in Appendix A2. However, a summary of these tests, together with the curing period, standards used and investigated replacement level, are shown in Table 3.8. In addition, correlations were developed either between different mechanical properties or between mechanical and durability properties.

Overall in this phase, an extra quantity of about 29 and 53 kg of the optimized aggregates (RP2F1A and RP3F3A) were prepared to perform the concrete tests as described above.

Subsequently, a total of three hundred sixty two concrete samples were produced and evaluated from twelve different mixes. The findings of this phase are divided into two chapters; the fresh and hardened properties are presented in Chapter 6 and the durability and other properties are presented in Chapter 7.

Table 3.8: Tests conducted and standards used in Phase-3

Test type	Type of concrete					Curing period (day)	Replacement % of LWA/NA with RPA	Standard used	Further information
	RP2F1C	RP3F3C	NC	LWC	LAC				
Slump	✓	✓	✓	✓	✓	-	25,50,75,100	ASTM C143/C143M-15	-
Fresh density	✓	✓	✓	✓	✓	-	25,50,75,100	ASTM C138/C138M-16	-
Dry density	✓	✓	✓	✓	✓	-	25,50,75,100	BS EN 12390-7:2009	-
Cylinder compressive strength	✓	✓	✓	✓	✓	28	25,50,75,100	ASTM C39/C39M-16	
Flexural strength	✓	✓	✓	✓	✓	28	25,50,75,100	ASTM C580-02	-
Splitting tensile strength	✓	✓	✓	✓	✓	28	25,50,75,100	ASTM C496/C496M-11	-
Modulus of elasticity, Poisson's ratio and stress strain behaviour	✓	✓	✓	✓	✓	28	25,50,75,100	ASTM C469/C469M-14	-
Abrasion resistance	✓	✓	✓	✓	-	28	25,50,75,100	ASTM C944/C944M-12	-
Water absorption	✓	✓	✓	✓	✓	28	25,50,75,100	BS 1881-122:2011	-
Drying shrinkage	✓	✓	✓	✓	✓	Up to 182	50,100	ASTM C157/C157M-14	-
Chloride permeability	✓	✓	✓	✓	✓	28	25,50,75,100	ASTM C1202-12	-
Creep test	-	✓	✓	-	-	Up to 365	25,50,75,100	ASTM C512/C512M-15	-
Thermal conductivity	✓	-	-	✓	-	28	100	ASTM C177-13	-
Temperature curing (30, 40°C)	✓	✓	✓	✓	-	28	25,50,75,100	-	Using compressive strength

3.4 Concrete mix design

A proper mix design is important for the proper mixing, placing in fresh state and achieving the desired properties of hard concrete. The materials used to make concrete are not uniform and a range of factors in determining mixes have an impact on its characteristics, both when fresh and after hardening. Therefore, it is necessary to create large numbers of experimental mixes and concrete specimens to allow ideal mix designs to be identified (ACI 211.2-98; Mehta and Aïtcin, 1990). Previously, concretes made with shredded or plastic based aggregates were generally designed via volume replacement, with substitution of plastic based fine or coarse aggregate by volume in place of natural aggregate in which the ACI 211.2 was used as a standard guide for their mix proportions (Babu et al., 2006; Babu et al., 2005; Babu and Babu, 2003; Gu and Ozbakkaloglu, 2016).

In this research, the fresh and hardened properties of the reference mixtures (LWC and NC) were defined in a way that yielded slump of 100 mm and minimum compressive strength of 25-30 MPa at 28 days for non-air entrained concrete. Therefore, initially LWC (as a natural lightweight control mix) and NC (as a normal weight control mix) were proportioned in accordance with ACI 211.2-98 and ACI 211.1-91 for lightweight and normal weight concretes respectively. For comparison purposes, a third control mix (LAC) was designed using LYA as a manufactured lightweight control mix.

The concrete mixes containing LYA and RPA were designed relative to reference mix (i.e. LWC or NC) by keeping the amount of cement and free water constant to eliminate any effect, except that resulting from changing the type and replacement level of the coarse aggregate. For a given mix, the quantities of coarse aggregate of LWA, NA, LYA and RPA were calculated, as explained below, using the replacement level (i.e. on volumetric basis);

unit weights; and the quantity of reference aggregate (i.e. LWA or NA) used in the reference mix (i.e. LWC or NC).

- Amount of RPA or LYA (kg/m^3) = (replacement level/100) × [(unit weight of RPA or LYA/unit weight of reference aggregate) × (quantity of reference aggregate)]
- Amount of reference aggregate (kg/m^3) = [1- (replacement level/100)] × (quantity of reference aggregate)

The volume (and subsequently weight) of the normal-weight fine aggregate was calculated by subtracting the total volume of the aforementioned ingredients from 1 m^3. Finally, the total water amount was adjusted according to the absorption and moisture content of the aggregates. An example of mix design calculations for different mixes is given in Appendix A3.

In total, thirty three concrete mixes were designed and proportioned based on the above procedures, and their subsequent mix proportions per 1 m^3 are presented in Table 3.9 and Table 3.10. Table 3.9 represents the mix proportions for the concrete used in phase 2, while mix quantities for those used in phase 3 are shown in Table 3.10. In these tables, NC, LWC and LAC refer to the concrete mixes including 100% NA, LWA and LYA, respectively. However, the sample designation "RPxFyC0.5" refers to a concrete mix made using RPA, that contains recycled plastic type x and filler type y at W/C ratio of 0.50. However, the designation "RPxFyCX" refers to a concrete mix containing aggregate type namely RPxFyA at a replacement level of X% on a volumetric basis.

Table 3.9: Mix proportions per metre cubed for concrete mixes used in Phase-2

Concrete type	Group	W/C	Total water	Free water	Cement	Fine Aggregates	Coarse aggregate		
							NA	LWA	RPA
			kg/m^3						
NC0.5	Group 1	0.50	243.9	228	456	770	784	-	-
LWC0.5			299	228	456	909	-	352	-
RP1F1C0.5			241.9	228	456	902	-	-	303
RP1F2C0.5			248.8	228	456	686	-	-	271
RP1F3C0.5			249.3	228	456	937	-	-	257
RP2F1C0.5			244.0	228	456	893	-	-	378
RP2F2C0.5			259	228	456	952	-	-	272
RP2F3C0.5			260.4	228	456	975	-	-	267
NC0.6		0.60	244	228	380	833	784	-	-
LWC0.6			299.5	228	380	972	-	352	-
RP1F1C0.6			242.3	228	380	964	-	-	303
RP1F2C0.6			249.2	228	380	749	-	-	271
RP1F3C0.6			249.7	228	380	1001	-	-	257
NC0.5	Group 2	0.50	243.9	228	456	770	784	-	-
LWC0.5			299	228	456	909	-	352	-
RP3F1C0.5			237.4	228	456	735	-	-	572
RP3F2C0.5			235.3	228	456	729	-	-	535
RP3F3C0.5			237.7	228	456	737	-	-	565
RP4F1C0.5			240.8	228	456	708	-	-	637
RP4F2C0.5			239.2	228	456	729	-	-	570
RP4F3C0.5			242.6	228	456	729	-	-	618

Table 3.10: Mix proportions per metre cubed for concrete mixes used in Phase-3

Concrete type	W/C	Total water	Free water	Cement	Fine Aggregate	Coarse aggregate			
						NA	LWA	RPA	LYA
		kg/m^3							
LAC	0.50	302.4	225	450	759	-	-	-	452
LWC		296.2			922	-	352	-	-
RP2F1C25		282.4			918	-	264	95	-
RP2F1C50		269.6			913	-	176	189	-
RP2F1C75		255.6			909	-	88	284	-
RP2F1C100		241.1			906	-	-	378	-
LAC	0.50	302.4	225	450	759	-	-	-	452
NC		240.3			880	688	-	-	-
RP3F3C25		239			847	516	-	141	-
RP3F3C50		237.6			815	344	-	282	-
RP3F3C75		236.2			782	172	-	423	-
RP3F3C100		234.8			750	-	-	565	-

3.5 Mixing, casting and curing

Preparation, mixing, casting and curing for concrete made with shredded plastic or plastic based aggregates are similar to those used for standard concrete (Gu and Ozbakkaloglu, 2016). Therefore, concretes were mixed, cast and cured until the day of testing, according to ASTM C192/C192M-16 guidance, in the following manner. The casting of concrete samples was done in two layers and compaction was performed by using a vibrating table for approximately 3 sec. Once a specimen had been cast, it was left under polyethylene sheets for 24 hrs. Each sample was then demoulded, before being subject to one of the curing conditions described below:

Standard curing: Once demoulded, specimens were cured in water at room temperature at 20±2 ^{o}C until the day of testing. This curing method was followed for all specimens except those samples used to measure the effect of temperature curing.

Temperature curing: Once demoulded, specimens were cured in water at 30±2 ^{o}C, and 40±2% ^{o}C until testing at 28 days. Compressive strength was then tested to investigate the effect of temperatures of curing water on the strength of concrete.

CHAPTER 4: MANUFACTURE AND CHARACTERISATION OF RECYCLED PLASTIC AGGREGATE

4.1 General

This chapter presents the selection and analysis of the inert materials used to manufacture recycled plastic aggregate (RPA), along with the selection of their mix proportions. In addition, it includes the manufacturing techniques used for a range of RPAs and the evaluation of their individual properties. The main steps included in this chapter are listed below:

a) selection, characterization and preparation of materials used (recycled plastic and fillers);

b) optimization of manufacturing techniques used to manufacture RPA; and

c) the production and investigation of RPA manufactured via optimized method.

4.2 Selection, characterization, optimization and preparation of materials used

The quality of RPA is influenced directly by the inert material used in its production. Therefore, it is crucial to choose these materials precisely by taking into consideration their local availability, quantity and their performance in an aggregate matrix. In this study, the materials used in the manufacturing of RPA were selected, characterized, optimized and then prepared for the production process as described in the following subsections.

4.2.1 Selection and characterization of recycled plastic and filler types

In the case of the optimization of recycled plastic, a certain kind of recycled plastic, mentioned latter in the same section, was used rather than using it as a mixture. This is due to the fact that not all plastic can be recycled, along with the differences in the physical, thermal and microstructure properties of plastic such as melting temperature, which varies from one type to another (see section 1.2) (Hopewell et al., 2009; Rebeiz and Craft, 1995). Therefore,

linear low density polyethylene (LLDPE) and polyethylene terephthalate (PET) were chosen amongst various recycled plastics, based on their bulk availability in the plastic production and waste stream, as explained in section 1.2.1.

Similarly, three types of fillers, namely red dune sand filler (RSF), fly ash filler (FAF) and quarry fines filler (QFF) were selected according to their local availability and based on their similarity with the major components in concrete. Thus, initially, RSF was selected due to its abundant local availability and negative impact, as mentioned earlier (see section 1.3.3); it also represents one of the major components of concrete (i.e. fine aggregate). The QFF was chosen since it has calcitic limestone (i.e. major component in coarse aggregate); while FAF was selected as it acts as mineral admixture in concrete. In addition, these two secondary fillers (FAF and QFF) were chosen due to their huge accumulation as industrial and mineral wastes, as reported in section 1.3.1 and 1.3.2. These materials (recycled plastic and fillers) were characterized, as previously illustrated in Chapter 3 (see sections 3.2.1 and 3.2.2).

4.2.2 Optimizing the mixing proportions

After optimizing the types of recycled plastic and filler, their mixing proportion was selected; keeping in view the prime objective of the research to use the least plastic proportion, along with the highest possible content of filler. Moreover, the selection was made taking into consideration the proportions that yielded the better performance in aggregate and concrete. This can be achieved by maximizing as much as possible the amount of fillers, as concluded in previous studies in section 2.3.2. Accordingly, this can be found at proportions of 50:50 recycled plastic to filler weight ratio or lower. Therefore, the initial mix design was made at 20:80 (recycled plastic: filler), but the composite produced was inhomogeneous because of the least amount of binder, as shown in Figure 4.1. Consequently, the amount of binder was

increased at the expense of the filler's proportions to 30%, which then resulted in an adequate mix.

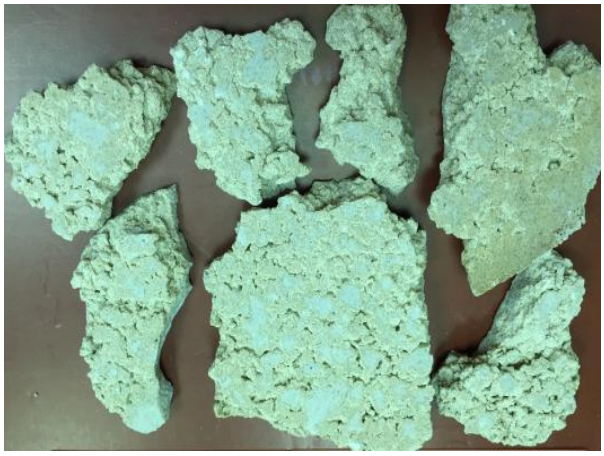


Figure 4.1: RPA made using 20:80 PET to QFF

Therefore, the appropriate proportion of recycled plastic to filler selected for the manufacturing of RPA was 30:70. This was in agreement with the average of plastic to additives proportions used previously in the literature (section 2.3.2). However, for the sake of a detailed investigation; 50:50 was also implemented to determine the effect of the filler proportion on the properties of produced aggregates and thereby concrete.

4.2.3 Preparation of composite mix

Once the type and proportions of recycled plastic and fillers were defined, the recycled plastic and fillers were then prepared for manufacturing of RPA. Recycled plastic was sorted into different polymer groups and then treated as described in section 3.2.1. Initially it was prepared in a shredded form with a maximum size of 10 mm, while other forms (pallet or powder forms) (see Fig. 3.1) were also implemented based on their performance with the filler in the RPA matrix, as described later, in section 4.3.4. Fillers (i.e. RSF, FAF and QFF) were also prepared by sieving using sieve number 60 (250 μm). Both recycled plastic and fillers were stored and kept at room temperature.

Ultimately, the RPA was produced from the optimized type of recycled plastic (LLDPE and PET) prepared in shredded, pallet and powder form with three fillers (i.e. RSF, FAF and QFF) at 50:50 and 30:70 plastic to filler ratios. This was done by using different techniques, as explained in detail in the following section.

4.3 Techniques used for manufacturing of recycled plastic aggregate

4.3.1 General

After selecting the recycled plastic and filler types along with their proportions, it is necessary to optimize the manufacturing technique used. Initially, attempts were made to produce the RPA thermally by using the "asphalt/heating mixer", but difficulty was found in melting the plastic and also in the crushing process. Therefore, it was decided to use another thermal technique, which is the "extrusion process". This technique was successful compared to the first technique. However, it was difficult to produce RPA with different particle shapes and sizes since the RPA produced, was in the form of rods. Thus, a new technique was required in order to achieve the aim of the current study. The RPA was finally produced by mixing recycled plastic together with filler through the "compression moulding press" process. A detailed description of each technique's process is illustrated below.

4.3.2 Using a heating mixer technique

The first attempt in the manufacturing of RPA was made with an asphalt mixer machine as it provides heating during mixing. This allows plastic to soften and easily bond with filler particles, producing a homogeneous mixture. In addition, this technique was selected since it was used to develop plastic-asphalt composite as reported by Partanen et al. (2010). The procedures of developing the RPA using this method include heating, mixing, casting, pressing, cooling and finally crushing, as given in the following steps:

1- Firstly, the recycled plastic and filler was prepared, as mentioned in section 4.2.3.

2- Then, filler such as RSF was loaded into the heating mixer (asphalt mixer) (see Fig. 4.2) as soon as the temperature reached the required level (i.e. 170 ^{o}C). The filler was heated for a few minutes (i.e. 10-15 min) before adding the shredded plastic in the next step.

3- Afterwards, the shredded plastic of LLDPE was fed into the heating mixer and kept for 5-10 min for softening and bonding with the filler.

4- The mixture was then poured into 50 mm^3 cubes and manually pressed at 15 tons using a hydraulic press (Fig. 4.3).



Figure 4.2: Heating mixer machine



Figure 4.3: Manual hydraulic press

5- Samples were kept at room temperature for one hour and then demoulded from the cubes (see Fig. 4.4).

6- Finally, cube samples were immersed in liquid nitrogen and then immediately crushed using a compression machine to obtain different particle sizes of RPA, as shown in Figure 4.5.



Figure 4.4: Cube of composite



Figure 4.5: RPA produced using heating mixer machine

Although the manufacturing of RPA was possible using this method, it was very difficult, for the following reasons. First, this was due to seepage of heat from the boundary of the mixer; this hinders the mix reaching the required temperature. Secondly, the crushing of the cubes was impossible unless they were immersed in liquid nitrogen to change their state to a glass state. Therefore, it was concluded that the manufacturing of RPA using this method is practically impossible, and another method such as an extrusion machine would have to be implemented, as shown in the next subsection.

4.3.3 Using an extrusion technique

After an unsuccessful attempt to manufacture RPA using the heating mixer machine as stated above, another technique had to be adopted. Therefore, the extrusion process was selected because it had been used in different studies to manufacture similar plastic based aggregates, as mentioned in section 2.3.2. Therefore, RPA produced by this method was manufactured using a single screw extruder equipped with a 10 mm die. The manufacturing process of the RPA consisted of heating, extruding, followed by water cooling and finally grinding, as shown in Figure 4.6.

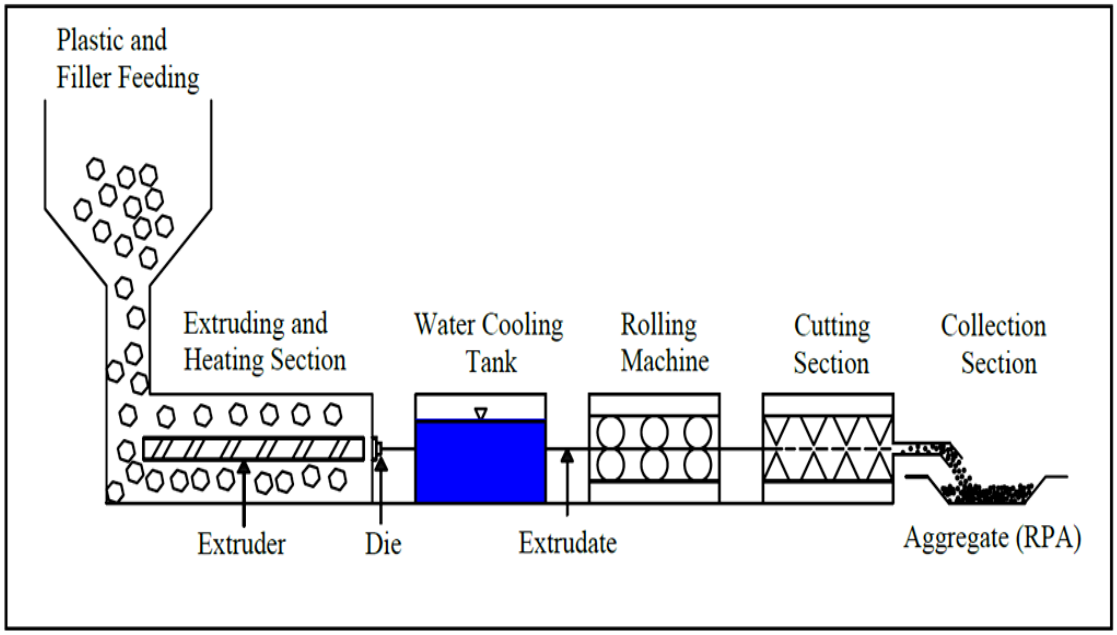


Figure 4.6: Manufacturing process of RPA using extrusion machine

The detailed explanation of these phases is as follows:

1- The shredded plastic (i.e. LLDPE) and fillers (i.e. RSF) were prepared in the same way, as described previously in section 4.2.3.

2- Then, LLDPE and RSF were loaded into the extruder through the feeding zone at the same time, once the extruder reached the required temperature (i.e. 170 ^{o}C).

3- Afterwards, the plastic materials began to melt while extruder started to mix the molten plastic with filler and press it towards the die.

4- Subsequently, the molten mixture was extruded in the form of a molten straight rod through the 10 mm die towards the water cooling tank.

5- The molten rod converted to solid state as soon as it touched the water due to the sudden drop in its temperature. This rod was pulled towards the cutter machine via a water tank using a roller machine.

6- Finally, the solid rod was cut into the final shape (pellet form), as shown in Figure 4.7 using a cutter machine.



Figure 4.7: RPA produced using extrusion process

In summary, the aggregate produced using this method had relatively identical sizes, due to the fixed size of the die. Also, the particle shapes were identical because the rod (extrudate) was identically cut rather than granulated or crushed. For these reasons, a different technique (i.e. compression moulding press) was employed in order to overcome these issues.

4.3.4 Compression moulding press technique

Evidence from the first method (heated mixer machine) suggests that temperature is the most important factor; while the second technique (extrusion process), shows that pressure is among the most significant aspects for the production of RPA. Therefore, a method that combines both key parameters together without any constraint on the shape of the final product was required. Consequently, a compression moulding press was selected for the reason that it has the dual function of performing heating and pressing simultaneously (ASTM D4703-15).

The novel technique of making RPA using the compression moulding press (Fig. 4.8), involves mixing plastic with filler to form a homogenized mixture, melting the plastic in the homogenized mixture, pressing the mixture to form a composite sheet or slab and finally crushing this composite to form the aggregates.

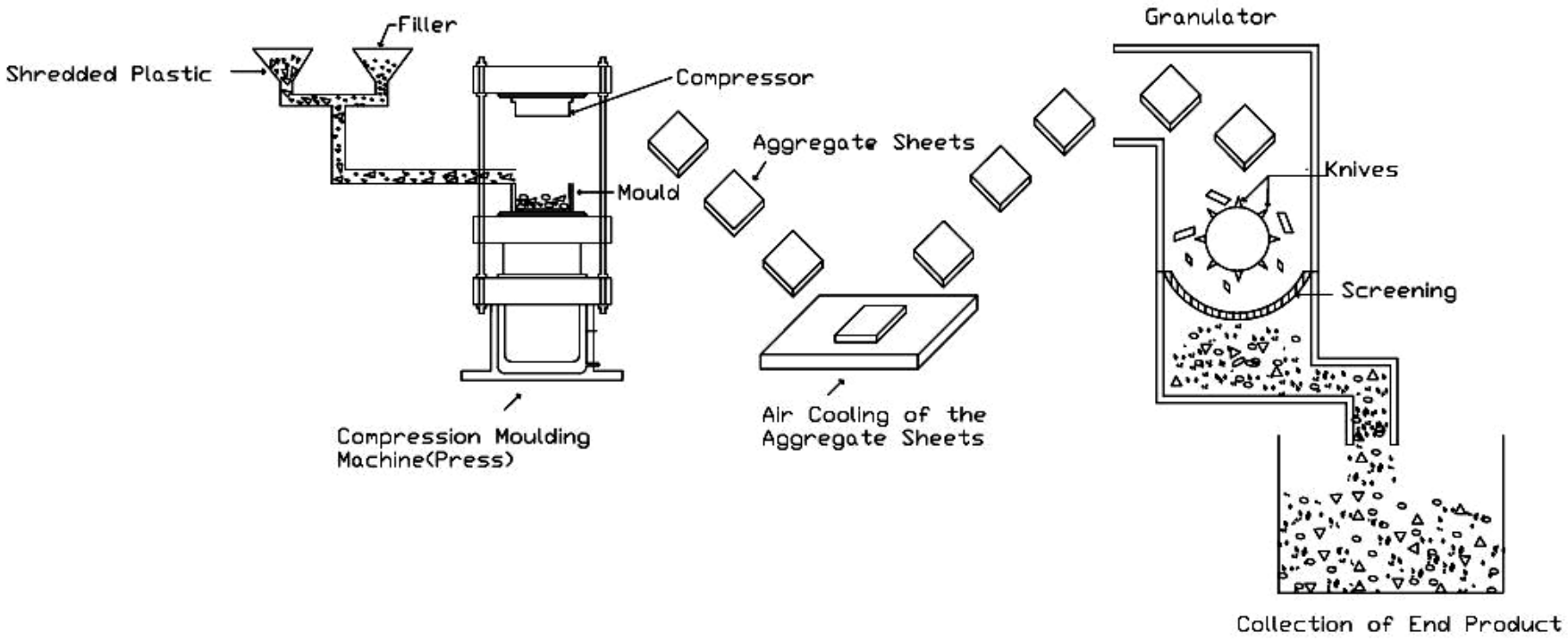


Figure 4.8: Manufacturing process of RPA using compression moulding press technique

The developed technique for RPA manufacturing has been patented in Alqahtani et al. (2014); where the novel RPAs were successfully manufactured using a 100-ton Wabash compression press (see Fig. 4.8) in accordance with the following procedures:

1- Recycled plastic (i.e. LLDPE or PET) and fillers (i.e. RSF, FAF, QFF) were prepared, as explained in section 4.2.
2- These materials were preliminarily mixed to produce a homogenised mixture. This mixture was then pre-dried at 110±5 °C for 1hr.
3- Afterwards, the mixture was poured into a flat mould having dimensions of 400 by 400 by 12 mm, as shown in Figure 4.9.
4- Then, a mould containing the plastic filler mixture was placed between the two heated platens of the press machine, as shown in Figures 4.10 and 4.11.
5- The mixtures containing LLDPE and PET were then heated at 175 and 300 °C respectively, under a pressure force of 25 tons for 15 minutes.



Figure 4.9: Mould filled with mixture (recycled plastic and filler)

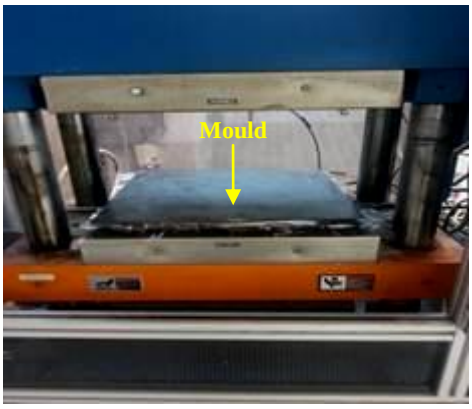


Figure 4.10: Mould filled with mixture and placed between two heated platens

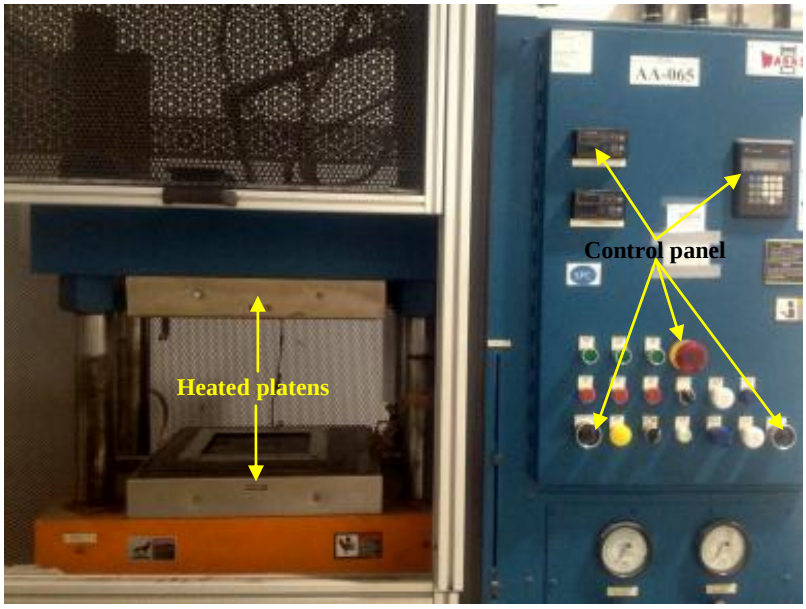
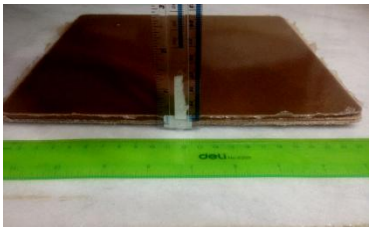


Figure 4.11: Heated platens and control panel of 100 ton Wabash press machine

6- After full melting of the recycled plastic and subsequent encapsulation of the filler, the obtained sheet/slab (see Fig. 4.12) was slowly removed from the machine and air cooled in the mould at room temperature for 1hr.

7- The required mesh, with a hole size of 12 mm (see Fig. 4.13) was prepared and fixed into the grinding machine in order to control the maximum size of the produced aggregate.





a **b**

Figure 4.12: Sheets/slabs of RPA made from (a) LLDPE with RSF and (b) made from PET with QFF



Figure 4.13:12 mm grinding mesh

8- Finally, the sheet/slab produced in the previous step was crushed using a Schorch crushing machine (see Fig. 4.14) to produce the novel RPA (Fig. 4.15).



Figure 4.14: RPA produced using a crushing machine (Schorch)



a



B

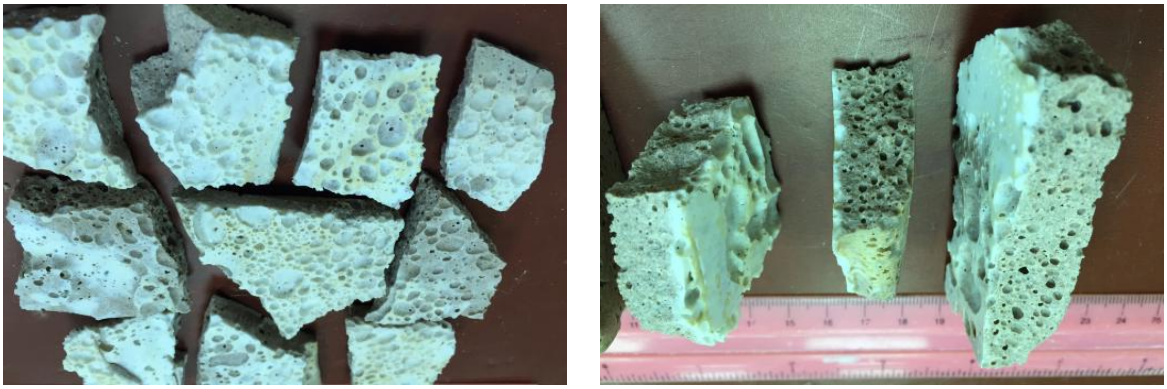
Figure 4.15: RPAs produced using compression press technique i.e. (a) RP2F1A and (b) RP4F1A

It is worth mentioning that the recycled plastic used in this method was initially in a shredded form. However, the RPA produced using shredded plastic showed separate layers of filler and plastic, as shown in Figure 4.16, which indicates a poor homogeneity in the mixture. The reason behind this might be due to the difference in the size of the constituents which were mixed together. Thus the plastic layers appeared at the top, due to the light weight of the shredded plastic compared to the filler.



Figure 4.16: RPA produced using shredded PET plastic with QFF

To resolve this problem, the recycled plastic was used in a pelleted form (see Fig. 3.1) in order to achieve a homogeneous mix of filler and recycled plastic. The RPA produced however, also showed incompatibility of proper mixing between the plastic pellets and the filler. Furthermore, a honeycombed surface of aggregate with internal voids was seen, as shown in Figure 4.17. Therefore, in order to manage these issues and for maximum homogeneity of the composite, the particle size of the recycled plastic and filler should match to the maximum possible extent. For that reason, the recycled plastic was ground to a powder form, having a maximum size of 0.250 mm and thus homogeneity was achieved, due to the large contact surface area between both ingredients.



a **B**

Figure 4.17: (a) Top view and (b) side view of RPA produced using pellet PET and QFF

In summary, using this method, two types of plastic, LLDPE or PET, were mixed at 30% and 50% (by weight) with RSF or with different types of fillers such as FAF or QFF, to make the RPA. Overall, twelve different types of RPA were manufactured based on the above mixing proportions, as presented in Table 4.1. These samples were identified by a sample name in the format RPxFyA: where RPx defines the recycled plastic type and proportions of plastic to filler; Fy identifies the filler type; and A symbolizes the aggregate. For example, RP1F1A can be explained as follows: RP1 means 50% LLDPE to 50% filler; F1 stands for red dune sand filler; and A represents the aggregate.

Table 4.1: Composition of manufactured RPA

Sr.	Group	Designation	Plastic Type	Plastic Percentage	Filler Type	Filler Percentage
1	Group 1	RP1F1A	LLDPE	50	RSF	50
2		RP1F2A	LLDPE	50	FAF	50
3		RP1F3A	LLDPE	50	QFF	50
4		RP2F1A	LLDPE	30	RSF	70
5		RP2F2A	LLDPE	30	FAF	70
6		RP2F3A	LLDPE	30	QFF	70
7	Group 2	RP3F1A	PET	50	RSF	50
8		RP3F2A	PET	50	FAF	50
9		RP3F3A	PET	50	QFF	50
10		RP4F1A	PET	30	RSF	70
11		RP4F2A	PET	30	FAF	70
12		RP4F3A	PET	30	QFF	70

4.4 Characterization of manufactured recycled plastic aggregate

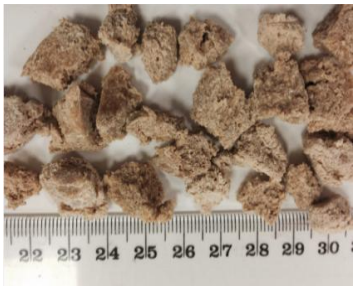
The novel RPAs were manufactured in two different groups as explained in the previous section. Therefore, the RPAs produced in Group 1 and Group 2 had different colours, sizes, shapes and textures are shown in Figures 4.18 and 4.19, respectively. The colour of the RPAs was mainly affected by the colour of the filler used in its matrix. For instance, the RPA containing RSF was red compared with the grey colour achieved by the RPA made with FAF.



RP1F1A



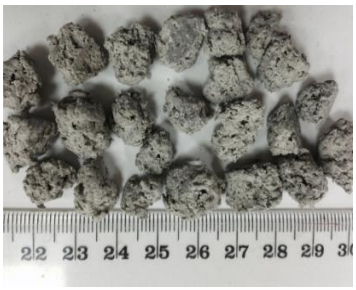
RP1F2A



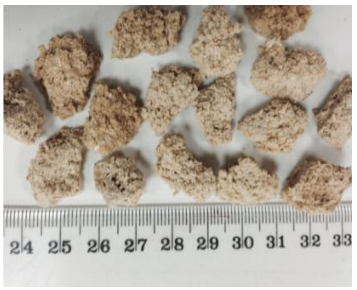
RP1F3A



RP2F1A



RP2F2A



RP2F3A

Figure 4.18: Different types of RPAs (Group 1) made with LLDPE and fillers



RP3F1A



RP3F2A



RP3F3A



RP4F1A



RP4F2A



RP4F3A

Figure 4.19: Different types of RPAs (Group 2) made with PET and fillers

In the following subsections, the developed RPAs were investigated in terms of their physical, mechanical and morphological properties, in accordance with the relevant test procedures explained in section 3.3.1. The summary of the findings of these tests are presented in Table

4.2. In addition, these results were compared with NA, LWA and LYA (see section 3.3.1) as well as with findings of similar plastic based aggregates reported in the literature, as illustrated in Table 4.3. Moreover, the effect of the filler proportions, together with the type of binder, on the performance of the aggregate was also discussed.

It should be noted that the results of RPA (Group 1) described in this section have been published in Alqahtani et al. (2016).

Table 4.2: Properties of the RPAs manufactured in this study

Property	RPAs (Group 1)						RPAs (Group 2)					
	RP1FIA	**RP1F2A**	**RP1F3A**	**RP2F1A**	**RP2F2A**	**RP2F3A**	**RP3FIA**	**RP3F2A**	**RP3F3A**	**RP4F1A**	**RP4F2A**	**RP4F3A**
Bulk Specific Gravity (OD basis)	1.2	0.81	1.08	1.48	1.17	1.19	1.81	1.68	1.79	1.95	1.79	1.94
Bulk Specific Gravity (SSD basis)	1.23	0.86	1.15	1.52	1.28	1.31	1.83	1.69	1.81	1.98	1.81	1.97
Apparent Specific Gravity	1.24	0.86	1.16	1.54	1.32	1.35	1.84	1.7	1.83	2.01	1.83	2.00
Absorption (%)	2.71	6.11	5.95	2.75	9.17	9.81	0.89	0.56	0.95	1.38	1.21	1.68
Dry Unit Weight (kg/m^3)	600	537	510	750	540	529	1132	1058	1119	1260	1128	1222
Voids (%)	50	51.43	52.63	51.8	53.74	55.44	37.44	37.02	33.35	24.97	32.82	27.22
Fineness Modulus	6.4	5.87	5.96	6.32	5.86	5.84	5.79	5.57	5.67	5.87	5.65	5.74
Impact Value (%)	-	-	-	-	-	-	17.11	15.76	15.40	21.33	22.64	19.84
Particles Shape and Texture	Sub angular and partially rough	Sub rounded and smooth	Sub angular and rough	Sub angular and partially rough	Sub rounded and smooth	Sub angular and rough	Sub-angular and partially rough	Sub-angular and partially smooth	Angular and rough	Sub-angular and partially rough	Sub-angular and partially smooth	Angular and rough
Colour	Red	Grey	Yellow	Red	Grey	Yellow	Red	Grey	Yellow	Red	Grey	Yellow
Type	Crushed											
Nominal Maximum Size (mm)	10											

Table 4.3: Comparison between the properties of RPAs and plastic based aggregates produced in previous studies

Type of Aggregate	Properties of Aggregate					Reference
	Maximum Particles size (mm)	Particles shape and texture	Unit weight (kg/m^3)	Specific Gravity	Absorption (%)	
RPA (Group 1)	10	See Table 4.2	510-750	0.81-1.48	2.71-9.81	Current study
RPA (Group 2)	10	See Table 4.2	1058-1260	1.68-1.95	0.56-1.68	Current study
WPLA	-	Spherical /smooth	1390	-	-	Choi et al. (2005)
WPLA	-	Spherical/ smooth	1390	-	0	Choi et al. (2009)
SLA (80:20 fly ash: HDPE)	-	-	-	1.9	-	Kashi et al. (1999)
SLA (0:100 fly ash: HDPE)	9.5	Angular/ smooth	-	0.91	0.3	Jansen et al. (2001)
SLA (35:65 fly ash: HDPE)			-	1.09	1.2	
SLA (80:20 fly ash: HDPE)		Rounded edges/rough	-	1.60	19.3	
SLA (80:20 fly ash: PS)	2.36	Firm to noticeably deformable	-	1.68	3.48	Swan and Sacks (2005)
SLA (80:20 fly ash: LDPE)			-	1.53	8.14	
SLA (80:20 fly ash: HDPE)			-	1.56	3.46	
SLA (80:20 fly ash: MP)			-	1.60	7.49	
SLA (0:100 fly ash: MP)	> 4.56	Firm to noticeably deformable	-	0.92	1.39	Slabaugh et al. (2007)
FSLA (0:100 fly ash: MP)			-	0.30	13.22	
SLA (10:90 fly ash: MP)			-	0.87	2.28	
FSLA (10:90 fly ash: MP)			-	0.32	8.50	
SLA (30:70 fly ash: MP)			-	0.88	2.28	
FSLA (30:70 fly ash: MP)			-	0.38	8.57	
SLA (50:50 fly ash: MP)			-	0.77	5.60	
FSLA (50:50 fly ash: MP)			-	0.82	2.76	
SLA (70:30 fly ash: MP)			-	0.96	2.15	
FSLA (70:30 fly ash: MP)			-	1.04	2.13	
Plasmatex	14	Irregular/ honeycombed	-	1.52 -1.6	2.1-4.2	Phillips and Richards (2004)
Plastic waste	> 5	Angular shape and smooth	1200	-	0	Koide et al. (2002)

4.4.1 Shape and texture

The shape and texture of an aggregate has an influence on paste demand, voids' content, workability and strength. For example, a spherical shape and smooth surface of aggregate particles would enhance workability, but at the same time it weakens the interlocking between the aggregate and cement matrix (O'Flynn, 2000; Rached et al., 2009).

The shape and surface textures of aggregate particles (see Table 4.2) were evaluated based on descriptive (qualitative) examination using optical microscopic investigation. The RPA (Group 1) (Fig 4.18) produced using RSF, FAF and QFF was sub-angular, sub-rounded and sub-angular respectively, despite the proportion of plastic to filler in the RPA matrix. However, the shape of the RPA (Group 2) developed with RSF, FAF and QFF was more angular with sharp edges, compared with that of RPA (Group1), as shown in Figure 4.19. This can be explained by the high degree of stiffness of RPA (Group 2), since it breaks in the crushing phase of aggregate production, rather than shredding, as found in Group 1. The reason for this contradictory behaviour relates to the type of plastic; since the manufacturing process, type and proportions of filler were the same.

In addition, the surface textures for RPA (Group 1) were partially rough, smooth and rough for RPA made with RSF, FAF and QFF respectively, regardless of the amount of polymer and filler in the RPA matrix (see Fig 4.18). Similarly, the texture of the RPA (Group 2) (Fig. 4.19) varied from partially smooth to rough depending on the type of filler used. In general, the textures of RPA (Group 1) were rougher (*more fibrous*) than those of RPA (Group 2). This observation can be linked to the behaviour of the RPA during the crushing, since RPA (Group 1) was shredded instead of crushed, as mentioned above.

Therefore, it can be concluded that the RPA (Group 2) is comparable to that of NA in terms of particle shape and texture. However, the RPA in both Groups 1 and 2 were entirely different to LWA and LYA. Moreover, the shape of the aggregates manufactured in this study (RPAs) are different from the manufactured aggregates (see Table 4.3) reported in the literature (Choi et al., 2009; Choi et al., 2005; Jansen et al., 2001). Similarly, the texture of RPAs is also different from those aggregates produced by (Slabaugh et al., 2007; Swan and Sacks, 2005).

These differences are valid and they can be related to the difference in the manufacturing method, type and amount of both plastic and filler used.

Overall, it is expected that concrete made with RPA containing QFF would obtain better interlocking with the cement matrix and ultimately this would improve its strength; since its aggregate particles have better angularity and roughness amongst the RPAs. On the other hand, it can be assumed that the workability of concrete made with RPAs (Group 1) that contain FAF might be improved, due to the semi-roundness and smoothness of its particle shape and texture.

4.4.2 Particle size distribution

Aggregate particle size has a vital effect on both fresh and hardened concrete properties. For example, well graded aggregate provides better workability and strength in contrast to poorly graded aggregate. Additionally, the amount of cement paste needed for bonding is less in the case of well graded aggregate, compared with that needed in the case of poorly graded aggregate (Quiroga and Fowler, 2004; Rached et al., 2009).

Accordingly, in this study, sieve analysis was conducted for RPA (Group 1) and RPA (Group 2) to develop the particle size distribution curves plotted in Figures 4.20 and 4.21, respectively. The particle size distribution curves for LWA and the *lightweight* standard limits are included for comparison purposes. The particle size distribution curves of the RPA were also compared with those of NA and the *normal weight* standard limits, as shown in Figures 4.22 and 4.23. As it can be seen in these figures, the nominal maximum size of the RPAs, LWA and NA is 10 mm.

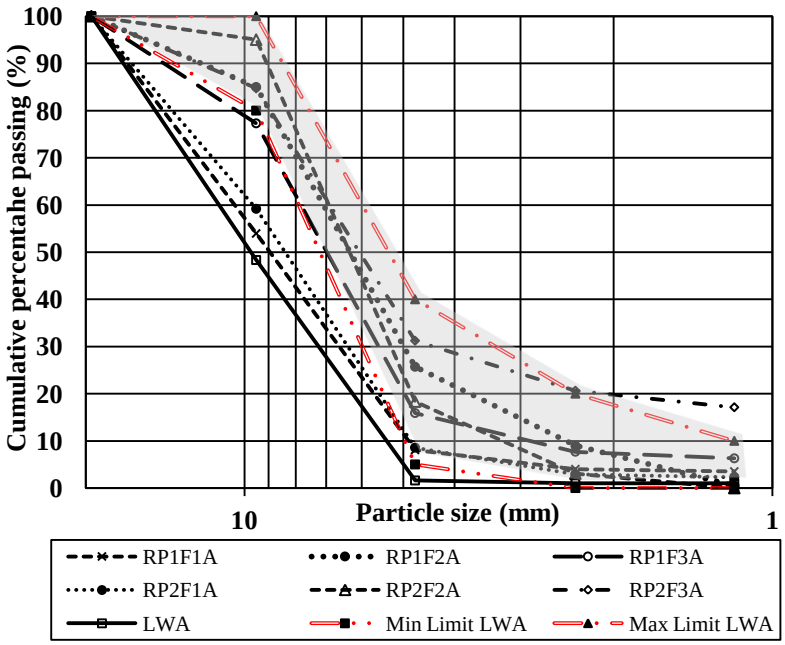


Figure 4.20: Particle size distribution curves for RPAs (Group 1) and LWA

The tested aggregates were classified into different sets as per the findings of the sieve analysis. For instance, RPA (Group 1) and LWA shown in Figure 4.20 can be classified into three sets, as follows:

- Set 1, which completely satisfied the ASTM C330/C330M-14 requirements (i.e. within standard limits) such as RP1F2A, RP1F3A and RP2F2A;
- Set 2, which deviated by 41% from the maximum permissible limits of the lower sieve size, such as RP2F3A. This is due to the fineness of the QFF compared to RSF;
- Set 3, which deviated from the minimum permissible limits of the upper sieve size by 32 and 26% for RP1F1A and RP2F1A respectively. This is because the particle size of the RSF was coarser when compared to other types of fillers. Similarly, LWA deviated by 39% from the minimum limits of the upper sieve size.

Similarly, the RPA (Group 2) (Fig. 4.21) was classified in the same way into the following categories:

- Set 1, comprised aggregates that totally satisfied the ASTM C330/C330M-14 requirements such as RP3F1A;
- Set 2, contains aggregates that deviated from the maximum limits of the lower sieve size (#4) as seen in RP3F2A, RP3F3A, RP4F2A and RP4F3A. These aggregates diverged by 23, 16, 19 and 8%, respectively;
- Set 3, which deviated from the minimum limits of the upper sieve (#3/8). For example, RP4F1A marginally deviated by 3.5%, while LWA significantly diverged by 39%.

These findings indicated that the RPAs made with RSF were the coarsest, followed by those RPAs made with QFF and finally, the finest were the RPAs made with FAF. This is attributed to the sizes of the filler particles themselves since the median size of RSF was the largest; while FAF had the smallest size amongst all the fillers, as shown previously in Figure 3.3.

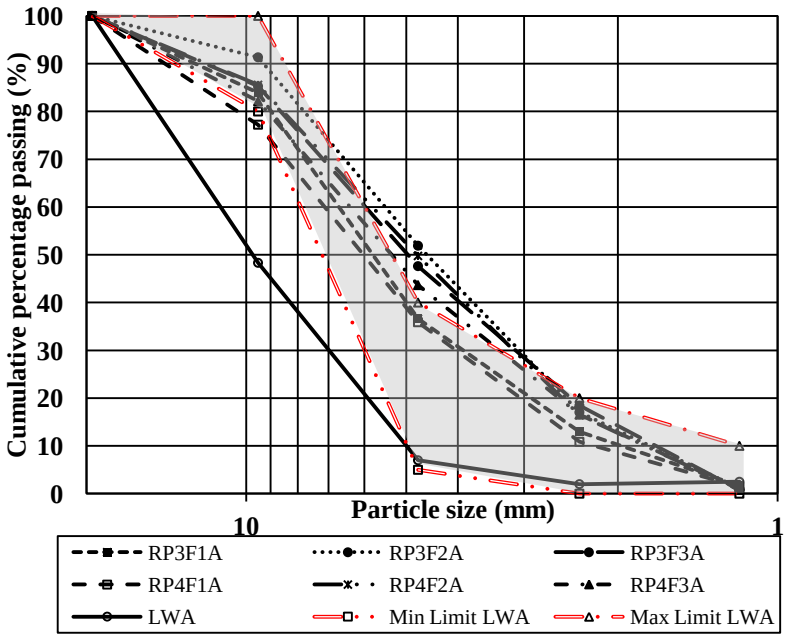


Figure 4.21: Particle size distribution curves for RPAs (Group 2) and LWA

In the case of the comparison of RPA with NA, the RPAs of Group 1 did not satisfy the normal weight aggregate particle size distribution requirements, except for those aggregates

made with FAF, as illustrated in Figure 4.22. Further, Figure 4.23 demonstrates that the particle size distribution of RPAs (Group 2) is poor compared with that of NA and it does not comply with the minimum or maximum particle size distribution requirements for the normal weight coarse aggregate.

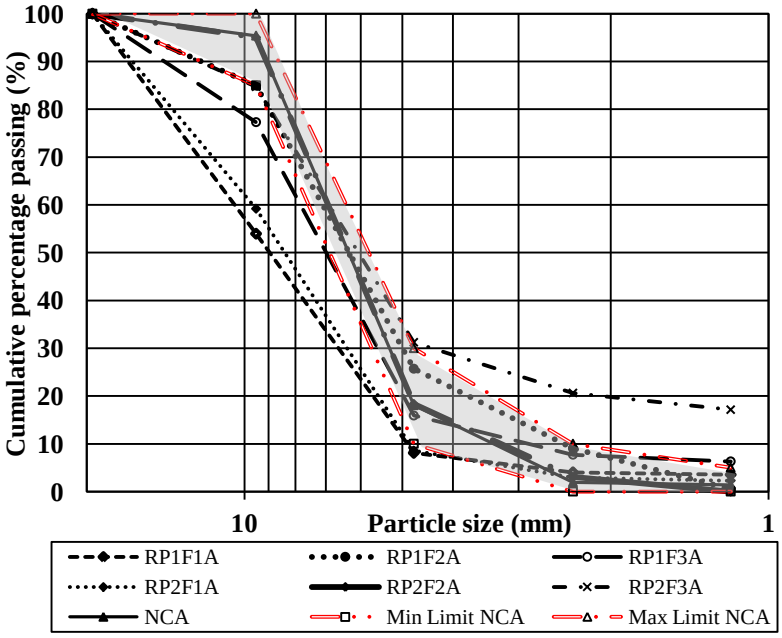


Figure 4.22: Particle size distribution curves for RPAs (Group 1) and NA

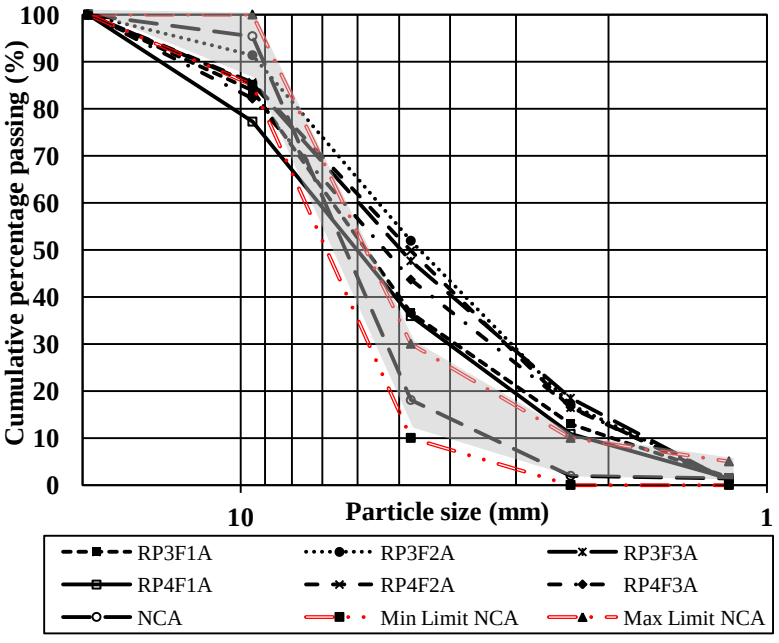


Figure 4.23: Particle size distribution curves for RPAs (Group 2) and NA

4.4.3 Fineness modulus

The fineness modulus (FM) of aggregate is usually used to identify the degree of the fineness of the aggregate which would ultimately affect the workability of the concrete (Maier and Durham, 2012; Russell and Freyne, 1998). A large value of FM is a strong identification for the coarse material and vice versa (Domone and Illston, 2010). The results of FM for RPAs (Groups 1 and 2) are shown in Figures 4.24 and 4.25 respectively, as compared with NA and LWA.

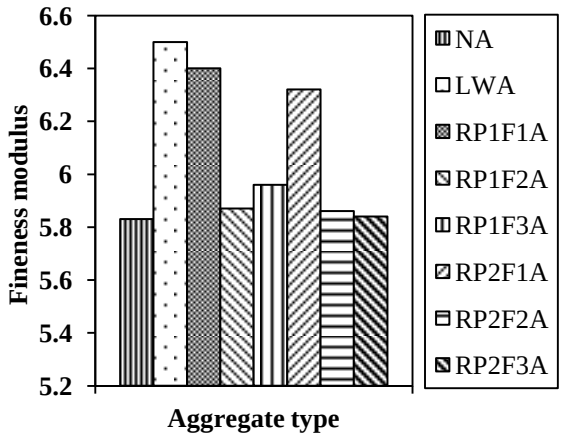


Figure 4.24: Fineness modulus of RPAs (Group 1) compared to NA and LWA

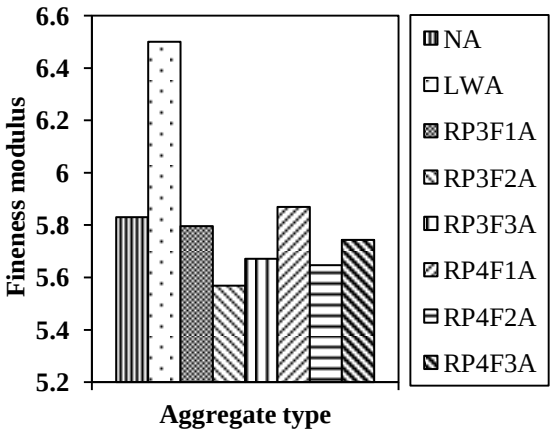


Figure 4.25: Fineness modulus of RPAs (Group 2) compared to NA and LWA

The FM of RPAs (Group 1), made with 70% RSF, FAF or QFF, was 2.7, 9.8 and 10.1% respectively, less than that of LWA; while it was 8, 0.5 and 0.2% respectively, higher than that of NA for the same type of aggregates. However, the general trend of the FM of the RPAs (Group 2) showed a marginal reduction varying from 0.6 to 4.5%, as compared to NA; with exception of RP4F1A, which was slightly higher by 0.7%. Similarly, a comparison with LWA revealed a decreasing trend ranging from 10 to 14%.

These results indicate that the RPAs containing RSF (i.e. RP1F1A and RP4F1A) were the coarsest, since they had the largest FM (i.e. 6.4, 5.87) amongst the RPAs in both groups. This

can be linked with the large size of the RSF particles compared with the sizes of other types of fillers (see section 3.2.2). In contrast, RP2F3A and RP3F2A were the finest among the RPAs (Group 1) and RPAs (Group 2) respectively, since they had the smallest values of FM (i.e. 5.84, 5.57). In addition, these results show that the FM of the RPAs (Group 1) were marginally decreased (< 3%) with the increase in filler percentage (i.e. from 50 to 70%). However, the FM was slightly increased (< 2%), in the case of the RPAs in Group 2 for the same type of filler. Thus, the increase in filler percentage in the RPA matrix had no significant effect on the FM of the RPAs.

4.4.4 Bulk specific gravity

The specific gravity of an aggregate is the ratio between the weight of the aggregate to the weight of water that occupies the same volume (Klieger, 1994). The bulk specific gravity is a significant property since it is used to calculate the volume of an aggregate in a concrete mix. Due to this significance, the bulk specific gravity of RPA (Group 1) and RPA (Group 2) was measured in saturated surface dry (SSD) and oven dry (OD) states, as presented in Table 4.2. Moreover, the comparison between the specific gravity (OD) of RPA (Group 1) and (Group 2) and that of reference aggregates (NA, LYA and LWA) is shown in Figures 4.26 and 4.27.

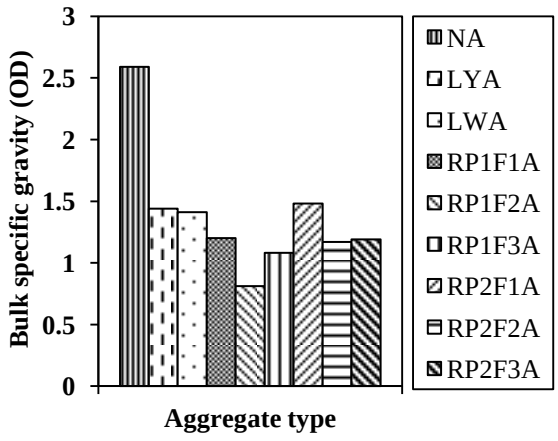


Figure 4.26: Bulk specific gravity of RPAs (Group 1) compared with NA, LWA and LYA

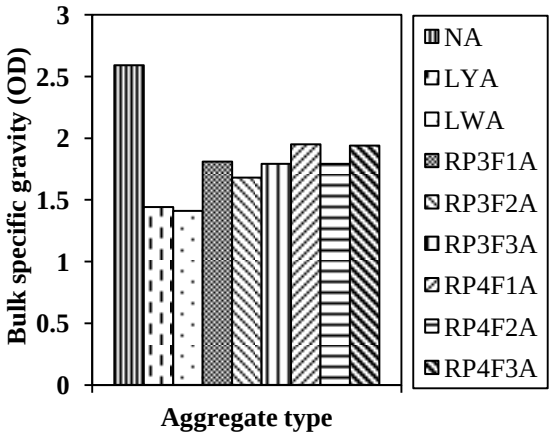


Figure 4.27: Bulk specific gravity of RPAs (Group 2) compared with NA, LWA and LYA

As can be seen in Figure 4.26, the specific gravities of RPA (Group 1) were less than those of NA, LWA and LYA; except for RP2F1A which yielded marginal increases (i.e. 5%) as compared to LYA and LWA. The percentage decreases in the bulk specific gravity of RPA (Group 1) varied from 15 to 43%, from 16 to 44% and from 43 to 69% as compared to those of LWA, LYA and NA, respectively. In the case of RPA (Group 2) (Fig. 4.27), the specific gravity increased in a range from 19 to 38% and from 16 to 35% with respect to those of LWA and LYA. However, the specific gravity of RPAs (Group 2) was 25 to 35% less than that of NA.

The decrease in the specific gravity of RPA (Group 1) was due to the low specific gravity of the LLDPE plastic (i.e. 0.9) in the RPA matrix. Additionally, the maximum and minimum specific gravity was achieved by RP2F1A (i.e. containing RSF) and RP1F2A (i.e. containing FAF), respectively, since the RSF had higher specific gravity than FAF. On the other hand, the observed increase in specific gravity of RPA (Group 2) as compared to that of RPA (Group 1) is because the specific gravity of PET (i.e. 1.3-1.4) is relatively higher than that of LLDPE (i.e. 0.93-0.96) (see Table 3.2). Additionally, this can be attributed to the least number of voids between aggregates in Group 2 as compared to that in Group 1 (see Table 4.2), since the type, proportions of filler and manufacturing process was constant in both cases.

The results also indicate that the increase in RSF, FAF and QFF portions from 50 to 70% in RPA (Group 1) increased the specific gravity by 23, 44 and 10%, respectively. However, the increasing effect was less prominent in RPA (Group 2), which varied from 6 to 8% for the same type and proportions of filler. This relates to the fact that the differences between the specific gravity of LLDPE and the fillers are relatively higher, compared with those between

PET and the fillers (see Table 3.2 and Table 3.3.). Finally, the present study's results show that RPA (Group 1) is lighter, while RPA (Group 2) is heavier, than those plastic based aggregates developed in previous studies (Jansen et al., 2001; Kashi et al., 1999; Phillips and Richards, 2004; Swan and Sacks, 2005). In those studies, the specific gravity ranged from 0.9 to 1.9 for different plastic based aggregates, as presented in Table 4.3.

4.4.5 Water absorption

The water absorption of an aggregate plays a significant role on the quality of concrete as well as the total amount of water needed in the mix. The accurate estimation of water absorption is essential since excess water increases the porosity; while a shortage of water yields an incomplete reaction between the cement and the water along with a reduction in slump (Rodrigues et al., 2013). The water absorption results for RPA (Group 1) and RPA (Group 2) are presented in Figures 4.28 and 4.29 respectively.

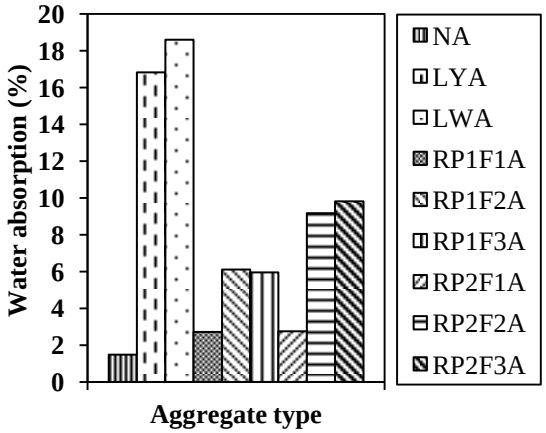


Figure 4.28: Water absorption of RPAs (Group 1) compared to NA, LWA and LYA

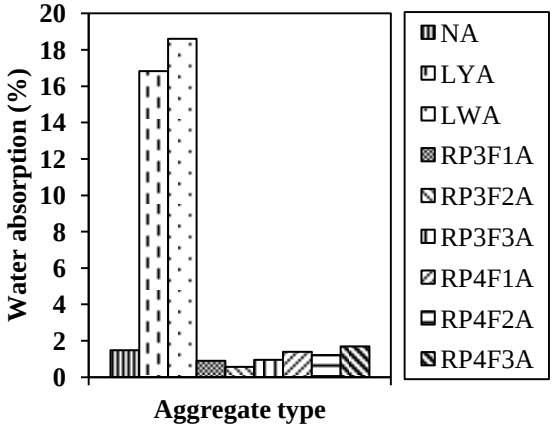


Figure 4.29: Water absorption of RPAs (Group 2) compared to NA, LWA and LYA

The results shown in Figure 4.28 reveal that the water absorption of RPA (Group 1) is less by 47 to 85% and by 42 to 84% than that of LWA and LYA, respectively; whereas the water absorption of the same aggregates is higher by 83 to 563% than that of NA. On the other hand, the RPAs (Group 2) had less water absorption as compared to LYA, LWA and NA;

with the exception of RP4F3A, which had a 13% increase compared to NA. The observed reductions varied from 91 to 97%, from 90 to 96.7% and from 7 to 62% as compared to LWA, LYA and NA, respectively. This significant reduction in the water absorption of the RPAs as compared to LWA and LYA is accounted for by the non-absorbent nature of plastic in the RPA matrix (see Table 3.2).

The comparison between the results of the two groups indicates that the water absorption of the RPAs from Group 2 is lower compared to that of the first group. A possible explanation is likely due to the presence of more internal voids in the RPAs (Group 1) (see section 4.4.9), which can preserve some water. This is a valid justification since all parameters are fixed apart from the type of plastic, which has a negligible effect on absorption (see Table 3.2). Results also showed that the RPA containing RSF had the least water absorption amongst the RPAs from Group 1; while for Group 2 it was the RPA made with FAF which had the least water absorption. The reason for this is not clear, but it may be related to the porosity of the new composite (plastic and filler), since plastic itself only absorbs a very small amount of water.

The increase in the RSF, FAF and QFF percentage from 50 to 70% increased the water absorption by 1.5, 33.4 and 39.3% respectively, for RPA (Group 1); whereas it increased by 55, 116 and 77% respectively, for RPA (Group 2) for the same type of fillers. This increase is accredited to the high porosity of composite due to less binder, as well as the high degree of water absorption of fillers, compared with the limited absorbent capacity of plastic. Similarly, different studies (Jansen et al., 2001; Kashi et al., 1999) attributed this increase to the increase in the porosity of synthetic aggregate due to the increases in the fly ash content.

The water absorption of the RPAs (Group 1) is in agreement with those reported in previous works (Jansen et al., 2001; Phillips and Richards, 2004; Slabaugh et al., 2007; Swan and Sacks, 2005). However, the RPAs (Group 2) had less water absorption compared with the same authors' studies. In those works, the maximum water absorption of aggregates varied between 4.2 and 19.3%, as illustrated in Table 4.3. Overall, using RPAs in concrete would resolve the high degree of water absorption associated with existing natural or manufactured lightweight aggregates.

4.4.6 Unit weight

The density of concrete is controlled by the density of the aggregate, since it represents the largest quantity of the concrete's components. The density of aggregate is influenced by the size and shape of the aggregate's particles; where a poorly graded aggregate yields higher voids between the aggregate, which ultimately leads to less density (ACI 301-05). Due to this significant factor, the dry density of the RPAs (Group 1) and (Group 2) was measured, as shown in Figure 4.30 and Figure 4.31, in comparison with NA, LWA and LYA.

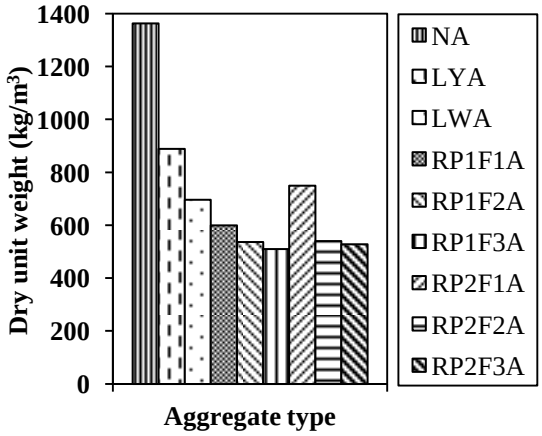


Figure 4.30: Dry unit weight of RPAs (Group 1) compared to NA, LWA and LYA

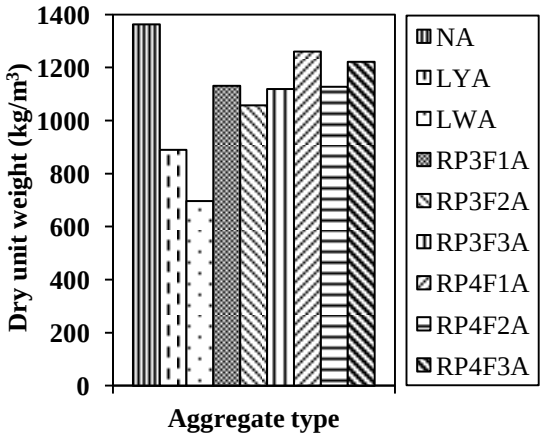


Figure 4.31: Dry unit weight of RPAs (Group 2) compared to NA, LWA and LYA

Figure 4.30 shows a reduction in the dry density of RPAs (Group 1) ranging from 14 to 27%, from 16 to 43% and from 45 to 63% as compared to LWA, LYA and NA respectively; except

for RP2F1A which had a marginal increase (i.e.7%) as compared to LWA. This reduction is due to the lighter weight of the inert materials such as plastic. Another reason is related to the increase in void percentages either between the aggregate particles (see Table 4.2) or within the aggregate particles, as confirmed by the SEM images (see section 4.4.9).

On the other hand, RPA (Group 2) had higher dry density varying from 52 to 81% and from 19 to 42% as compared to LWA and LYA, as shown in Figure 4.31; whereas the dry density of the same aggregates was 8 to 22% less than that of NA. This increase in Group 2 dry density compared with that of Group 1 is likely due to the lower percentage of voids between the aggregates' particles (see Table 4.2). This reason seems valid since all parameters remained the same, except the plastic type, which had less effect on the unit weight, as already explained in the specific gravity section.

The increase in the RSF, FAF and QFF ratio from 50 to 70% in the RPA (Group 1) yielded an increase in dry density of 20, 0.5 and 3.5% respectively. Similarly, the dry density of the RPAs (Group 2) was increased by 11, 7 and 9% respectively, for the same type of filler. This increase is due to the fact that the density of the fillers is almost double that of plastic, as presented in Tables 3.2 and 3.3. Similarly Jansen et al. (2001) and Kashi et al. (1999) found that the density of synthetic aggregate was increased with the increase in the fly ash ratio due to the lower weight of plastic compared to filler. Additionally, the results revealed that the maximum dry density was achieved by the RPA made with 70% RSF in both groups (i.e. RP2F1A and RP4F1A); since the RSF had the peak density among all the fillers.

In addition, the current study's results indicate that the density of the RPAs (Group 1) was lower, in a range varying between 37.5 and 63%, as compared with aggregates developed in different works (Choi et al., 2009; Choi et al., 2005; Koide et al., 2002), as given in Table 4.3.

However, the density of the RPAs (Group 2) is comparable to the densities of aggregates developed in the same studies. Overall, the dry densities of the RPAs (Group 1) satisfied the maximum requirements (i.e. 880 kg/m^3) of ASTM C330/C330M-14 for structural lightweight aggregate; while, RPAs (Group 2) have exceeded this limit by 20-43%. Therefore, these results suggest that utilizing RPAs (Group 1) in concrete would reduce the overall weight of the structure, which can result in significant cost savings.

4.4.7 Aggregate void content

The voids between aggregates' particles are generally controlled by the shape and size of the particles where poorly graded aggregate yields a higher percentage of voids (Gambhir, 2013). Subsequently, the amount of voids influences the cement paste demand since more voids need more paste to fill them (Rached et al., 2009). Therefore, the comparisons between the voids' percentages in the RPAs for both groups and the reference aggregates (NA, LWA and LYA) are presented in Figures 4.32 and 4.33.

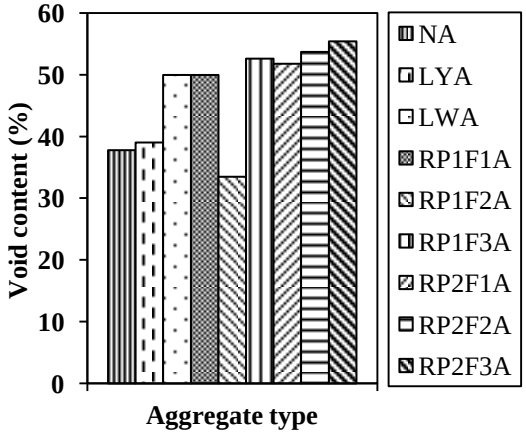


Figure 4.32: Void content of RPAs (Group 1) compared to NA, LWA and LYA

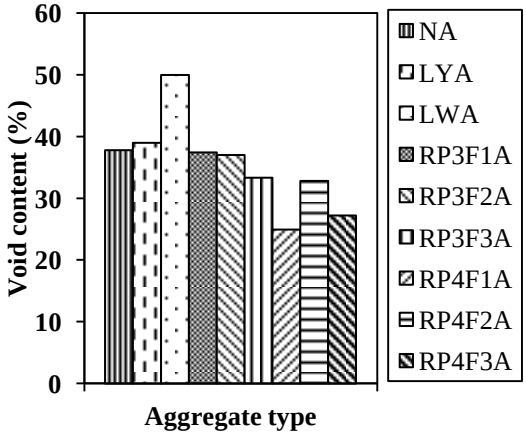


Figure 4.33: Void content of RPAs (Group 2) compared to NA, LWA and LYA

Figure 4.32 shows that the void percentage of RPAs (Group 1) is higher than that of LWA, LYA and NA with the exception of RP1F2A. On average, the increase in voids' percentage in the RPAs (Group 1) was 5, 35 and 39% as compared to LWA, LYA and NA respectively.

However, the void content of the RPAs (Group 2) (Fig 4.33) was 25 to 45.5%, 4 to 36% and 1 to 34%, lower than that of LWA, LYA and NA respectively.

These results indicate that the percentage of voids in the aggregates of Group 2 is lower as compared to Group 1; which reveals that the aggregates' particles in Group 2 have a better angularity compared to those in Group 1, as shown in Figure 4.18 and 4.19. In addition, the present study's results showed an increasing trend varying from 4 to 60% and from 11 to 18% in the RPAs (Group 1) and RPAs (Group 2) respectively, due to increasing the ratios of RSF, FAF and QFF from 50 to 70%.

4.4.8 Strength

The mechanical properties of aggregates such as their strength have a direct effect on the strength of concrete (Kozul and Darwin, 1997). The impact value test was carried out on the RPAs (Group 2) and the results were compared with those of reference aggregates (NA, LWA and LYA). The test findings showed that the impact values of NA, LWA and LYA were 9.65, 39 and 21.55% respectively; while the strength of the RPAs (Group 1) could not be measured using this test, as they were not crushable due to the plastic nature of their matrix, as confirmed in Figure 4.34.



Figure 4.34: Aggregate crushing strength of (a) LWA and (b) RPAs (Group 1)

The RPAs (Group 2) (see Fig. 4.35) were crushable and yielded a significant reduction in their impact value, varying from 43 to 61% as compared to LWA. Similarly, in comparison with LYA, a reduction ranging from 1.1 to 28.5% was observed; except for RP4F2A, which had a marginal increase (i.e. 5%). The lower impact value for the RPAs (Group 2) is likely to be due to good bonding in the composite matrix with fewer voids, as shown in the SEM and optical microscopic images (see section 4.4.9). However, in comparison with NA, substantial increases in the aggregate impact value, varying from 60 to 135%, were also observed.

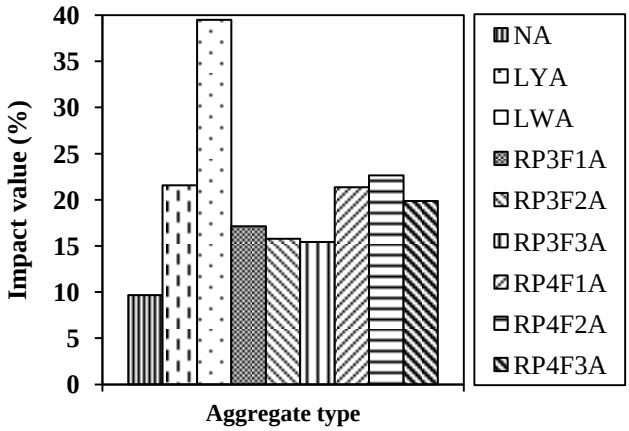


Figure 4.35: Impact value of RPAs (Group 2) compared to NA, LYA and LWA

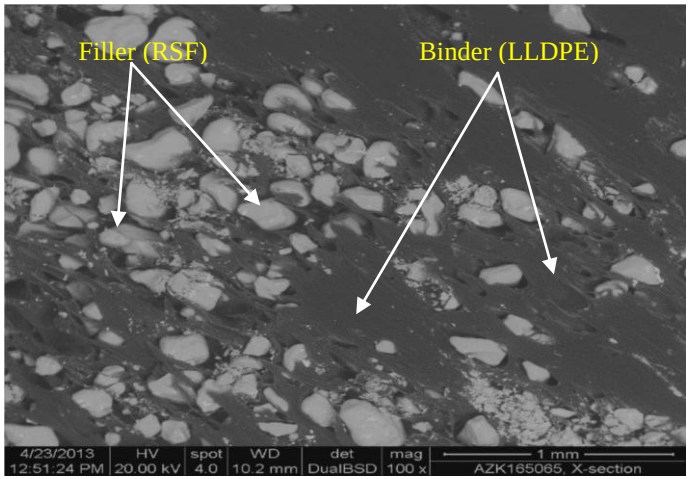
Therefore, the present study results showed that the aggregate strength of the RPAs (Group 2) was higher than that of LWA and LYA, but less strong as compared to that of NA. In addition, the polymer type had a significant effect on the crushability of RPA; since RPA

(Group 1) is not crushable compared with the crushable aggregate of RPA (Group 2). Finally, the increase in the percentage of RSF, FAF and QFF from 50 to 70% in the RPAs (Group 2) matrix decreased the aggregate strength by 24.7, 43.6 and 29% respectively, because less binder yielded less bonding between the filler particles.

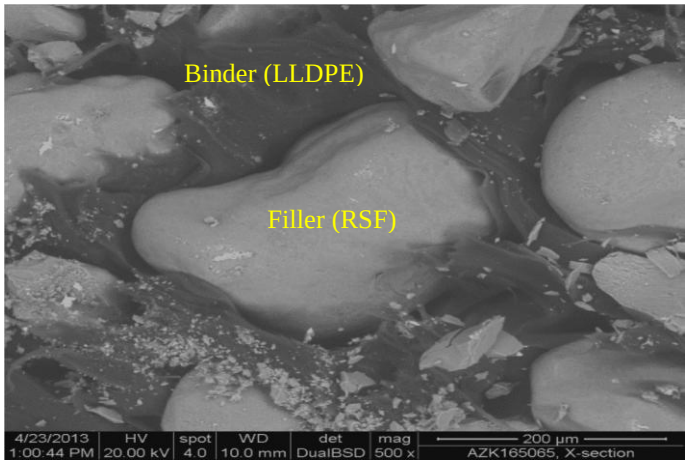
In summary, the impact value observed for the RPAs (Group 2) was less than the maximum allowable limit (i.e. 30%) given by BS 812-112:1990. Therefore, these results suggest that the strength of concrete containing RPAs (Group 2) would be higher than that made with LWA.

4.4.9 Microscopic investigation

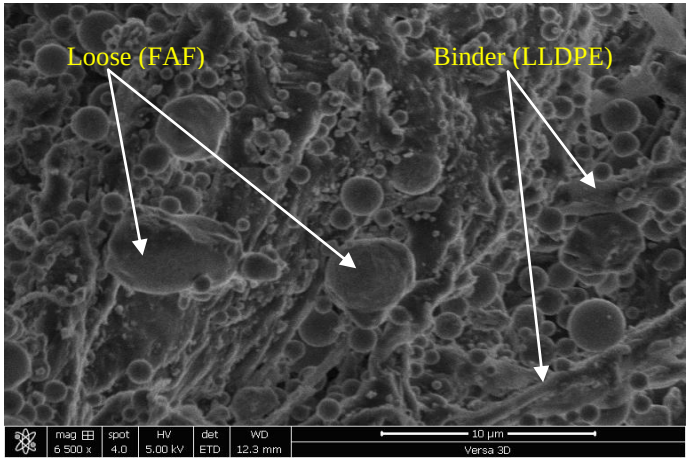
The uniformity between the binder (plastic) and filler (i.e. RSF, FAF and QFF) in the RPA matrix was assessed by using scanning electron microscopy (SEM) and an optical microscope. The surface examination of the RPAs (Group 1) containing RSF (Fig. 4.36a) demonstrated an uneven distribution of filler particles, with concentrated regions of finer particles, and a few coarser particles. Additionally, these images confirmed that the filler particles are embedded in the binder (i.e. plastic) in a random distribution, as shown in Figure 4.36 (a, b), with a few disconnected voids around these fillers. This was expected behaviour, as two dissimilar constituents were mixed together. However, the SEM images of the RPAs (Group 1) containing FAF (Fig. 4.36c) showed that the FAF particles are loose at the surface, which might prevent or weaken the bond between the RPA particles and the cementitious matrix. The image of the RPAs (Group 1) made with QFF (Fig. 4.36d) indicate that the QFF has an angular particle shape which would result in better interlocking with the plastic matrix to form hard aggregates.



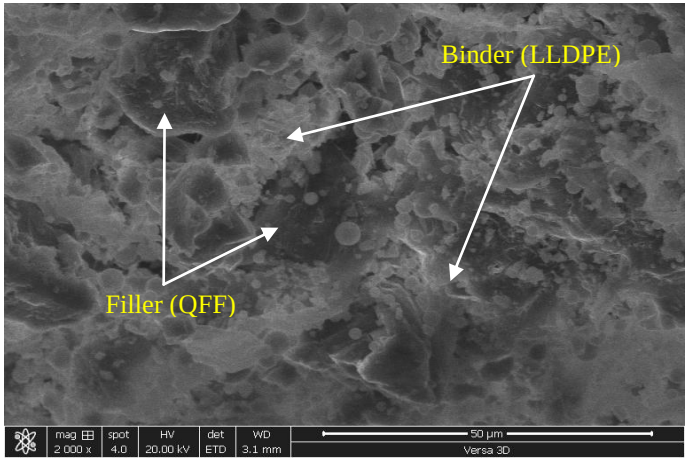
a



b



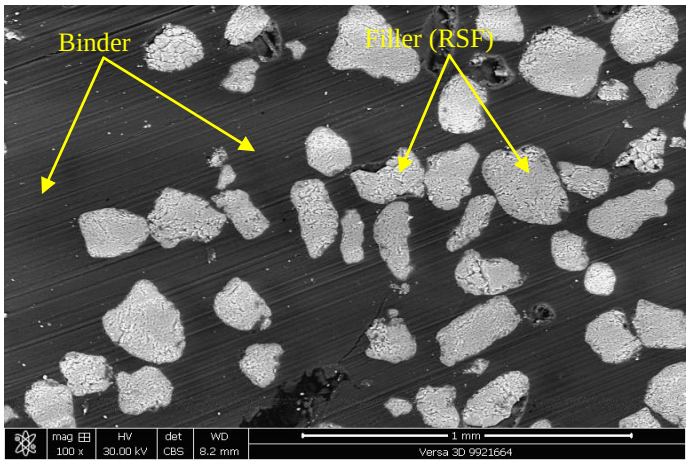
c



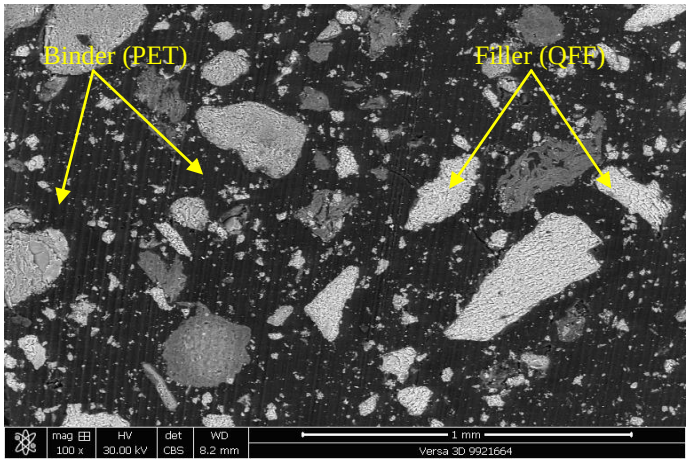
d

Figure 4.36: SEM images of RPAs (Group 1) made with (a,b) RSF, (c) FAF and (d) QFF embedded in LLDPE matrix

Similarly, the SEM images of the RPAs (Group 2) indicate a non-uniform distribution between the plastic (PET) and fillers, as given in Figure 4.37. Moreover, these images show better interlocking between the binder and filler, with fewer voids as compared to the RPAs (Group 1). This better bonding was also proved by optical microscope images, as seen in Figure 4.38. However, these images showed the presence of voids in the RPA containing FAF (Fig. 4.38c) compared with entrapped air bubbles formed in the LWA, as shown in Figure 4.38a. Accordingly, it is expected that the RPA (Group 2) concretes would possess higher strength in comparison with that made from LWA.



a



b

Figure 4.37: SEM images of RPAs (Group 2) made with (a) RSF and (b) QFF at magnification: 100×

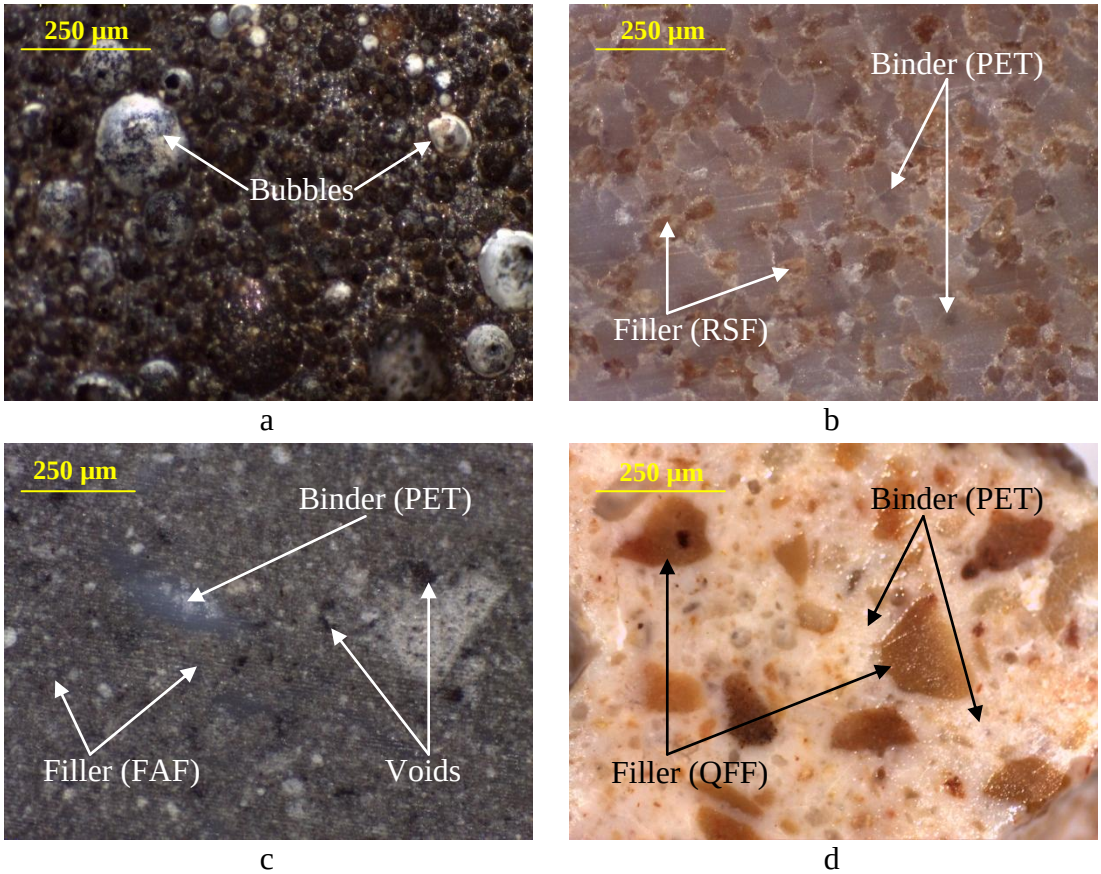


Figure 4.38: Optical microscopic images of (a) LWA, and RPAs (Group 2) made with (b) RSF, (c) FAF and (d) QFF

4.4.10 Ash test

The ash content test was conducted to assess the efficiency of the mixing and manufacturing process for the production of RPA. This was evaluated by determining the amount or percentage of filler existing after firing the plastic during the test, as shown in Figure 4.39, in accordance with test procedures explained in ASTM D2584-11. Representative samples were taken from the corners and the middle of three different aggregate sheets of RP1F1A. The findings of each sheet showed an error estimate of less than ±5%. Thus, these results prove that the mixing and manufacturing method used for the RPA production yields adequate mix proportions between plastic and filler with respect to the planned proportions.

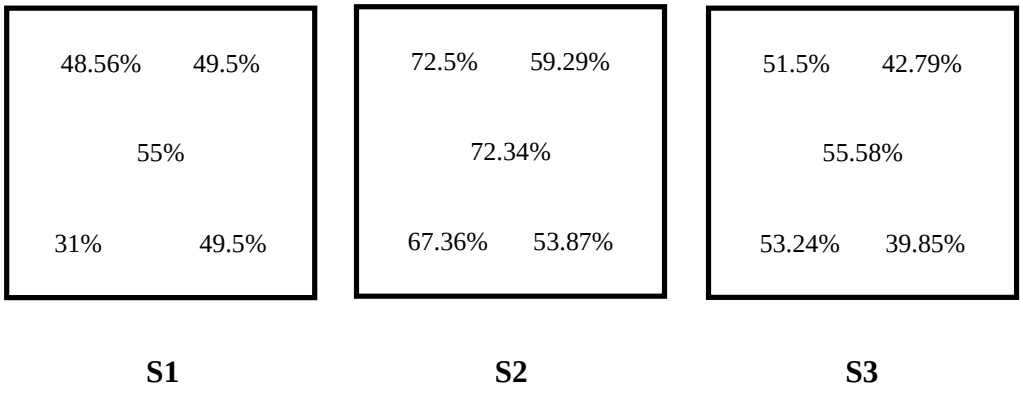


Figure 4.39: Ash percentages for three samples (S1, S2 and S3) of RP1F1A

4.5 Cost analysis of recycled plastic aggregate

The cost of manufacturing synthetic aggregate is associated principally with the cost of both the manufacturing process and raw materials. The manufacturing processes of RPAs and LYA aggregates or other manufactured lightweight aggregates are similar, as both require heating and cooling mechanisms. The heating process for manufacturing RPAs requires a lower temperature but additional compression, as compared to lightweight aggregates such as LYA, which requires a high heating temperature of 1100 °C (LYTAG, 2016). Therefore, the additional compression needed in the case of the RPAs compensates for the high temperature needed for production of LYA or other types of manufactured lightweight aggregate. Subsequently, it is assumed that the cost evaluation depends on the cost of materials required for the production of RPA and LYA aggregates only.

The raw material used for manufacturing LYA or other types of manufactured lightweight aggregate; for instance, slag, clay and shale; costs $12 to $13 per ton (Kashi et al., 1999) and fly ash $12-15 per ton (Ahmaruzaman, 2010; Bedick, 1995). On the other hand, the local cost of raw materials used for manufacturing RPA such as LLDPE, red dune sand (RSF) and fly ash (FAF) are $853/ton, $0-5/ton and $160-170/ton respectively. Further, the international

cost for the same materials is $1322/ton, $7.70/ton and $12-15/ton respectively (Ahmaruzaman, 2010; Block, 2016; USGS, 2015).

In the current study, the cost calculation was made based on the prices of the locally collected materials. Using Eq. 4.1., the cost for RPA produced using local LLDPE and RSF is $427.75/ton and $257.65/ton at 50:50 and 30:70 ratios of LLDPE to RSF respectively (Kashi et al., 1999). In the same way, the cost of RPA produced using LLDPE and FAF is $509/ton and $371.4/ton respectively at the same proportions.

Material Costs ($/ton) = % of plastic × (LLDPE cost) + % of filler × (filler cost) (Eq.4.1)

In addition, the calculated cost of RPA would also be compensated by taking into consideration the cost of the landfill required for dumping LLDPE and FAF. The landfill cost of LLDPE is $49 per ton (EPA, 2015) and $50/ton for FAF (Bedick, 1995; Birckhead, 1995). Therefore, the expression below (Eq. 4.2) was used to calculate the material cost after taking landfill cost into consideration (Kashi et al., 1999).

Material Costs ($/ton) = % of plastic × (LLDPE cost-x_1) + % of filler × (filler cost-x_2) (Eq.4.2)

Where:

x_1= disposal cost of LLDPE in ($/ton)

x_2 = disposal cost of filler in ($/ton)

As a result, the cost of RPA produced using LLDPE and RSF, using Eq. 4.2, was reduced to $403.25/ton and $242.95/ton respectively at 50:50 and 30:70 ratios of LLDPE to filler. Similarly, the cost of RPA produced using LLDPE and FAF was also reduced to $459.5/ton and $321.7/ton respectively, at the same proportions.

Although, the RPA produced at a 30:70 ratio of LLDPE to RSF is the most economic amongst that produced, the cost of materials used to produce RPA is still not cost-effective, due to the low cost of the dumping of plastic and fillers, together with the high price of recycled plastic. However, the cost will be reduced if stricter regulations are implemented which will ultimately increase the disposal cost and taxes on natural aggregate mining. Also, the material cost of RPA production will be more cost-effective if the price of recycled plastic is reduced by taking plastic waste directly from the household or using it directly without any further treatment.

Ultimately, the production cost of RPA does not consider the energy recovered and the environmental benefits associated with the reduction in plastic and filler waste. For example, recovering 3 million tons of plastic waste would reduce CO_2 emissions by 3.8 million tons (EPA, 2015). Furthermore, the cost-effectiveness study does not consider the fact that this type of aggregate (RPA) would have some unique properties, including ductility due to the presence of the plastic in its matrix, which will enhance the market demand in particular sectors. Finally, due to the reduction in the weight of RPA, there will be potential cost savings because of reductions in the construction and transporting costs.

4.6 Summary

This chapter presents the possibility of developing recycled plastic aggregate (RPA) using plastic acting as a binder and by-product waste or granular materials acting as filler. Therefore, two types of plastic (i.e. LLDPE, PET) and three types of filler (i.e. RSF, FAF, QFF) were selected as main components of RPA at two optimised proportion levels (i.e. 30:70, 50:50 plastic: filler ratios). The choice of these materials was selected based on the availability and performance. Different trials were performed to produce this aggregate until a

novel technique was achieved using a compression moulding press machine. Accordingly, twelve different types of RPAs were successfully manufactured in two groups using the optimized technology. The physical, mechanical and microstructure properties of the RPAs were tested and compared to conventional normal weight (i.e. NA) or lightweight aggregates (i.e. LWA, LYA), where significant differences were observed and discussed. Additionally, the cost of producing RPA was calculated based on the material cost, to assess its economic feasibility.

These manufactured plastic aggregates will be used in the next chapter (Chapter 5) to produce lightweight concrete and study the effect of RPA on the performance of the produced concrete.

CHAPTER 5: INVESTIGATION FOR RECYCLED PLASTIC AGGREGATE OPTIMIZATION

5.1 General

This chapter presents the second phase (phase-2) of this research, in which recycled plastic aggregate concrete (RPAC) was produced using the RPAs Group 1 and 2 at 100% replacement level. RPAs Group 1 and 2 were manufactured using compression moulding press technique, in which two types of plastic (i.e. LLDPE, PET) were mixed with three types of fillers (i.e. RSF, FAF, QFF) at two optimized proportions (i.e. 50:50 and 30:70 plastic to filler ratio), as reported earlier in Chapter 4. The fresh, hardened, durability and microscopic properties of RPAC were then investigated and compared with control concrete made with LWA and NA, as previously mentioned in section 3.3.2. The findings were also compared with findings of previous studies in which concrete was made from plastic based aggregate, as shown in Table 5.1.

Based on the results of this chapter, the best two aggregates of the RPAs and one W/C ratio will be selected for more detailed investigation based on the performance of the RPA concrete in the above tests. The tasks set for this chapter are given below:

a) Investigation of the effect of recycled plastic aggregate (RPAs) on the fresh, hardened, durability and morphological properties of concrete;

b) Optimization of W/C ratio; and

c) Selection of RPA optimized concrete mixes for further or detailed investigation.

It should be noted that the results of RPAC-1 described in this chapter were published in Alqahtani et al. (2016).

Table 5.1: Summary of RPAs concrete results in comparison with previous studies' findings

Study	Type of aggregate	Replacement type	Replacement level (%)	W/C	Slump (mm)	28-day Dry density (kg/m^3)	28-day Compressive strength (MPa)
Current study	RPAs (**Group 1**)	CA	100	0.50	40-220	1795-2014	14-18
				0.60	145-240	1827-1961.5	12-15
	RPAs (**Group 2**)	CA	100	0.50	100-250	1872-2002	25-39
Choi et al. (2005) and Choi et al. (2009)	WPLA	FA	0, 25, 50, 75	0.45	135-205	2300-1940	37.2-24.9
				0.49	105-214	2300-2000	34.6-23.2
				0.53	100-223	2300-2010	31.5-21.8
Kashi et al. (1999)	SLA (Fly ash: HDPE) (25:75)	CA	100	0.50	-	1480	15.1
	SLA (Fly ash: HDPE) (35:65)				-	1490	14.3
	SLA (Fly ash: HDPE) (50:50)				-	1520	15.2
	SLA (Fly ash: HDPE) (65:35)				-	1630	19.3
	SLA (Fly ash: HDPE) (80:20)				-	1700	20.9
Jansen et al. (2001)	SLA (Fly ash: HDPE) (0:100)	CA	0, 100	NA	76-89	2323-1792	35.5-14.2
	SLA (Fly ash: HDPE) (35:65)				76	2323-1858	35.5-16.7
	SLA (Fly ash: HDPE) (80:20)				76-64	2323-1969	35.5-20.1
Malloy et al. (2001)	SLA (fly ash/ HDPE) (80/20)	CA	0, 100	0.50	-	-	42-20
	SLA (fly ash/ MP) (80/20)				-	-	42-22
Slabaugh et al. (2007)	SLA (Fly ash: MP) (0:100)	CA	0, 100	NA	95.3-82.6	2417-1856	39.9-11.1
	FSLA (Fly ash: MP) (0:100)				95.3	2417-1795	39.9-10.1
	SLA (Fly ash: MP) (10:90)				95.3-88.9	2417-1866	39.9-11.4
	FSLA (Fly ash: MP) (10:90)				95.3-76.2	2417-1795	39.9-10.3
	SLA (Fly ash: MP) (30:70)				95.3-101.6	2417-1846	39.9-11.2
	FSLA (Fly ash: MP) (30:70)				95.3-88.9	2417-1835	39.9-11.1
	SLA (Fly ash: MP) (50:50)				95.3-76.2	2417-1917	39.9-12.6
	FSLA (Fly ash: MP) (50:50)				95.3-88.9	2417-1866	39.9-12.1
	SLA (Fly ash: MP) (70:30)				95.3-88.9	2417-1886	39.9-13.6
	FSLA (Fly ash: MP) (70:30)				95.3-177.8	2417-1866	39.9-12.3

5.2 Fresh properties of recycled plastic aggregates concrete

5.2.1 Slump

The workability of RPAC-1 (containing RPA from Group 1) and RPAC-2 (concrete containing RPA from Group 2) was measured using the slump test, as given in Figures 5.1 and 5.2 respectively. The results presented in Figure 5.1 show that the slump of RP1F2C0.5 was 100 and 9% higher; whereas that of RP2F3C0.5 was about 64 and 80% lower, as compared with NC and LWC respectively. The increase in slump for RP1F2C0.5 was attributed to the sub-rounded particles' shape and smooth surface texture of the aggregate (i.e. RP1F2A) (see section 4.4.1). Thus, this leads to fewer interfaces between the aggregate particles (i.e. a lower packing level) leaving more free cement paste that yielded a higher flow. In addition, loose filler particles (i.e. FAF) in RP1F2A (see Fig. 4.36) would enhance the workability of the mix. A similar increasing trend was observed by Choi et al. (2005) and (2009), who reported that the slump of concrete made with plastic based aggregate at 75% replacement level was significantly increased between 51 and 123%, as seen in Table 5.1. However, the low slump observed in RP2F3C0.5 is ascribed to the increase in the surface area, which leads to harsh concrete, since RP2F3A achieved the least FM (i.e. less coarser particles) among RPA (Group 1) (see section 4.4.2 and 4.4.3).

RP1F1C0.5 and RP2F1C0.5 achieved slump levels within the limits (75-125 mm) specified by ACI 213R-03 since the aggregates (i.e. RP1F1A and RP2F1A) were the coarsest amongst RPA (Group 1) (i.e. have the highest FM) (see section 4.4.2 and 4.4.3). This yields lower packing level which leads to a high flow. However, this was neutralized by the low slump resulting from the increase in the packing level due to the angularity of aggregate particles. Therefore, it can be concluded that the reduction in slump for RPAC-1 ranged from 52.5 to

80% and from 14 to 64% in comparison with LWC and NC, respectively. However, Jansen et al. (2001) and Slabaugh et al. (2007), observed a slighter decreasing trend ranging between 7 and 20% at 100% replacement of CA with plastic based aggregate.

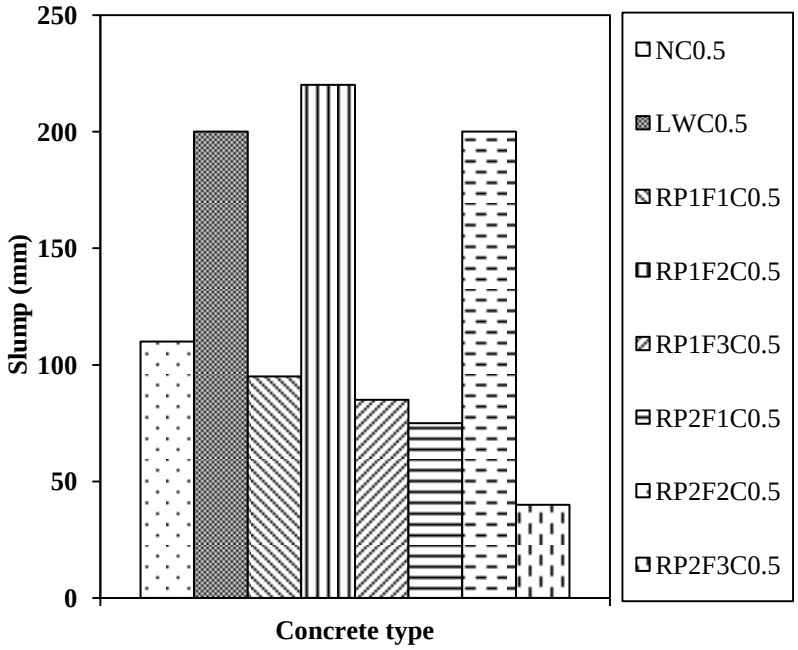


Figure 5.1: Slump of RPAC-1, LWC and NC at W/C of 0.50

On the other hand, there was a significant increase in the slump of RPAC-2 in comparison with NC; whereas fluctuating results were seen as compared with LWC, as shown in Figure 5.2. The increase in slump of RPAC-2 varied between 25 and 150% as compared to NC. This increase is in good agreement with the results of the previous studies of Choi et al. (2005) and (2009); which observed a similar increasing trend ranging from 51 to 123% at 75% replacement of NA with plastic based aggregate. However, with respect to LWC, the slump of RP3F1C0.5 and RP4F1C0.5 increased by 10 and 19%; while that of RP3F2C0.5, RP3F3C0.5 and RP4F2C0.5 decreased by 52, 10 and 40% respectively. These results revealed that the maximum slump amongst RPAC-2 was achieved by concretes made with RP3F1A and RP4F1A, since these aggregates were the coarsest amongst RPA (Group 2). However, the minimum slump was attained by those made with RP3F2A and RP4F2A, since these

aggregates were less coarse amongst RPA (Group 2), as reported earlier in section 4.4.3. Accordingly, the packing level reduces with the coarser aggregates, which leads to high workability and vice versa, as explained previously.

Furthermore, comparison of the two group results indicates that the slump of RPAC-2 was much higher than that of RPAC-1. This increase is because the RPAs (Group 2) grading is poorer compared to that of the first group. This would reduce the packing level and thus decrease the demand for cement paste, which ultimately increases the workability of the mix. In addition, the textures of RPA (Group 1) are rougher (more fibrous) than RPA (Group 2); which generates more friction between aggregate particles and thus reduces the flow of the mix.

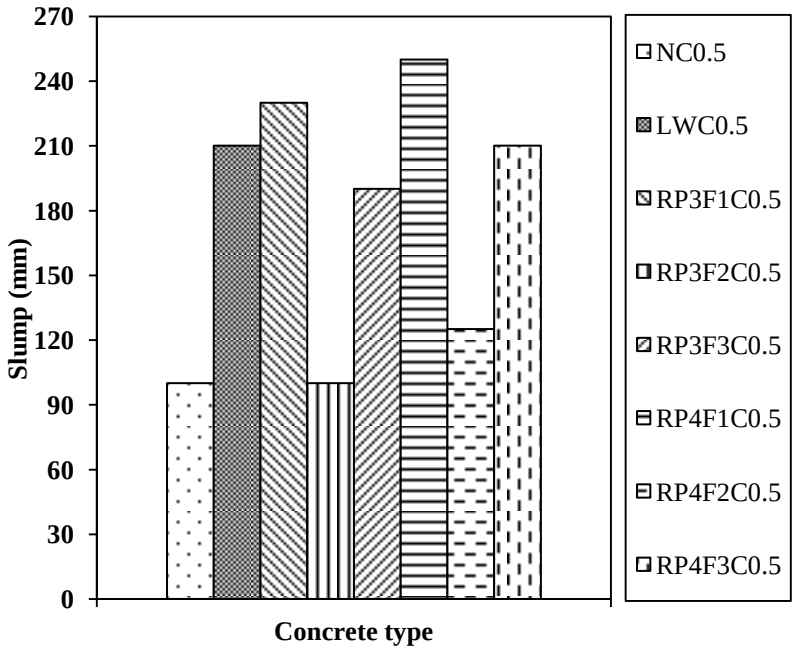


Figure 5.2: Slump of RPAC-2, LWC and NC at W/C of 0.50

Additionally, the increase of W/C ratio from 0.50 to 0.60 (see Figure 5.3) increased slump by 46, 8 and 41%, for RPAC-1 containing RP1F1A, RP1F2A and RP1F3A, respectively; compared to the 2 and 73% increase attained by LWC and NC. This increase can be linked

with the reduction in the amount of cement which requires less water for interaction, leaving more free water, as similarly observed by Rahmani et al. (2013). Also, it is inferred from the results that the effect of an increase in the W/C ratio by 0.1 is more prominent in RPAC-1 as compared to LWC.

Overall, RP1F1C0.5, RP1F3C0.5 and RP2F1C0.5 from RPAC-1 satisfied the workability requirements of structural lightweight concrete (i.e. 75-125mm) specified in ACI 213R-03; while only two mixes from the second group (i.e. RP3F2C0.5 and RP4F2C0.5) satisfied this limit.

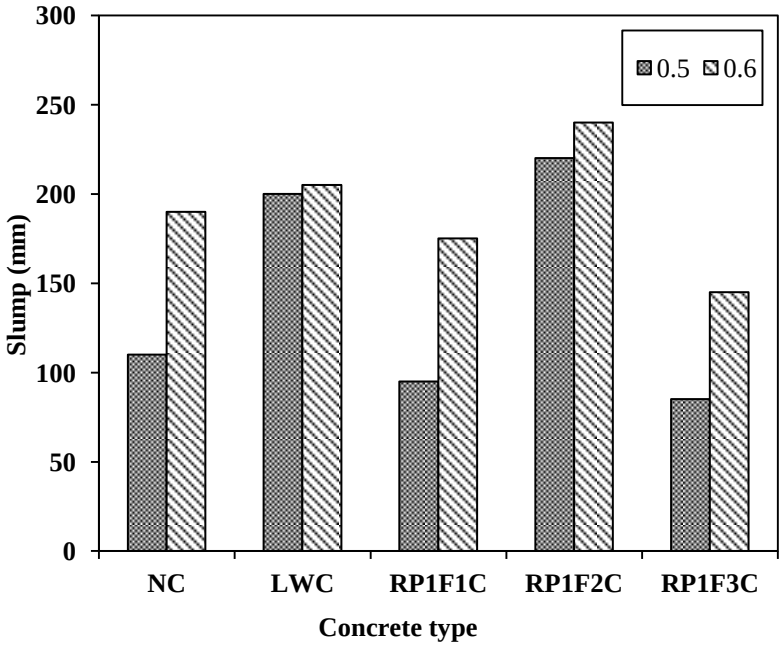


Figure 5.3: Effect of W/C on slump of RPAC-1, LWA and NC

5.2.2 Fresh density

The density of fresh concrete containing RPAs (Groups 1) and (Group 2) is given in Figures 5.4 and 5.5, respectively. The results given in Figure 5.4 show that the fresh density of RPAC-1 was reduced (the highest reduction was 10% for RP1F2C0.5) except for RP2F1C0.5, which had a marginal increase of 1.3% compared to LWC. However, in comparison with NC, a significant reduction varying from 11 to 21% was observed. The lightweight nature of the

RPA concrete was expected, due to the fact that a large volume of the concrete, around 60 to 70%, comprised lightweight material (i.e. 100% of RPAs). The highest reduction in fresh density was found in RP1F2C0.5 because the RP1F2A has the least specific gravity amongst the RPA (Group 1).The maximum fresh density was achieved by RP2F1C0.5 which can be linked with the highest specific gravity/density of RP2F1A amongst the RPAs (Group 1), as discussed previously in sections 4.4.4 and 4.4.6.

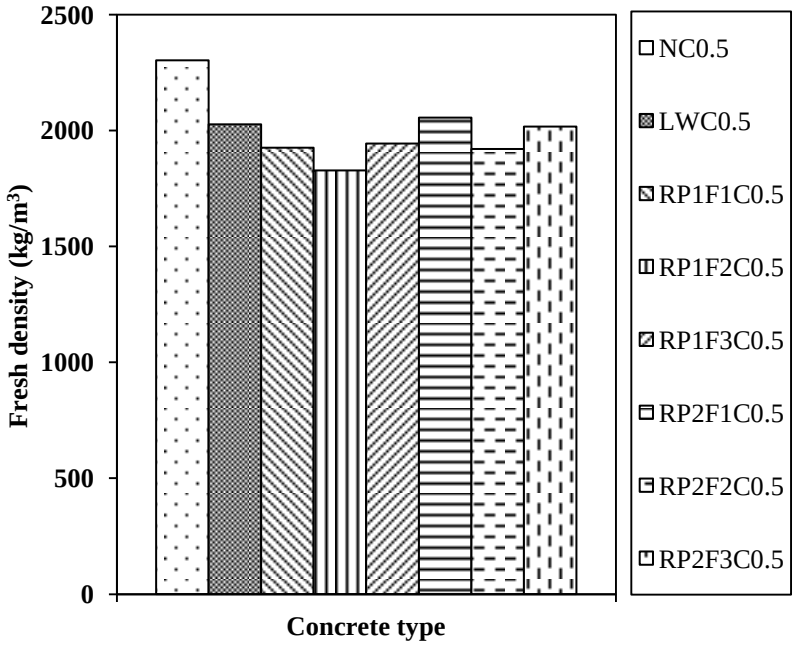


Figure 5.4: Fresh density of RPAC-1, LWC and NC at W/C of 0.50

Similarly, the fresh densities of RPAC-2 had an average reduction of 15% as compared to NC, while a marginal variation of ±3% was found with respect to LWC, as seen in Figure 5.5. Amongst RPAC-2, the maximum and minimum fresh density was attained by RP4F1C0.5 and RP3F2C0.5 respectively; since the largest and smallest density amongst RPA (Group 2) was attained by the aggregates used in these mixes (i.e. RP4F1A and RP3F2A) (see section 4.4.6).

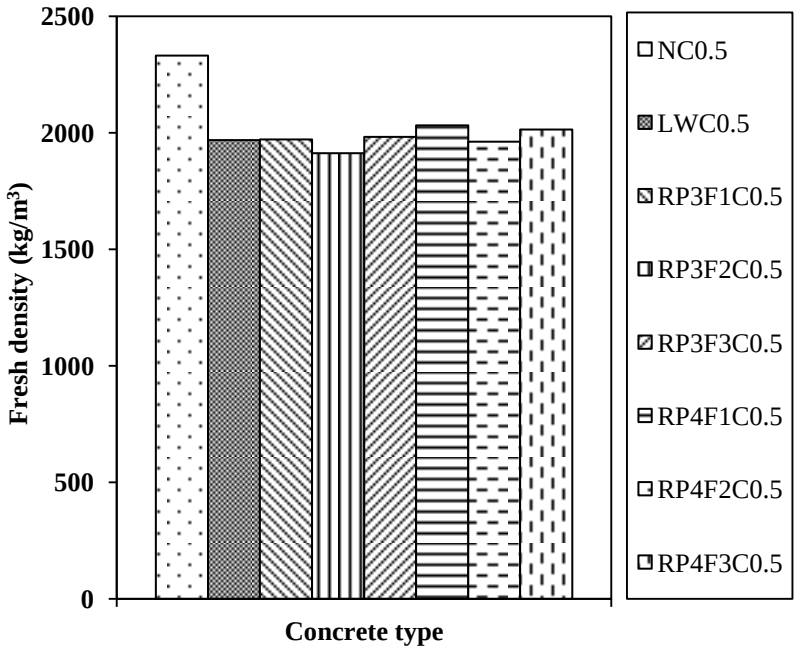


Figure 5.5: Fresh density of RPAC-2, LWC and NC at W/C of 0.50

Furthermore, the increase in the W/C ratio from 0.50 to 0.60 (see Figure 5.6) resulted in a marginal decrease (i.e. 3%) in the fresh density of RPAC-1, LWC and NC. It seems that the nominal decrease in fresh density of both RPA's, LWA and NA concretes' was due to the least reduction in the quantity of the cement (i.e. 15%); which affected the overall density of the concrete, as the density of cement is greater than that of aggregates.

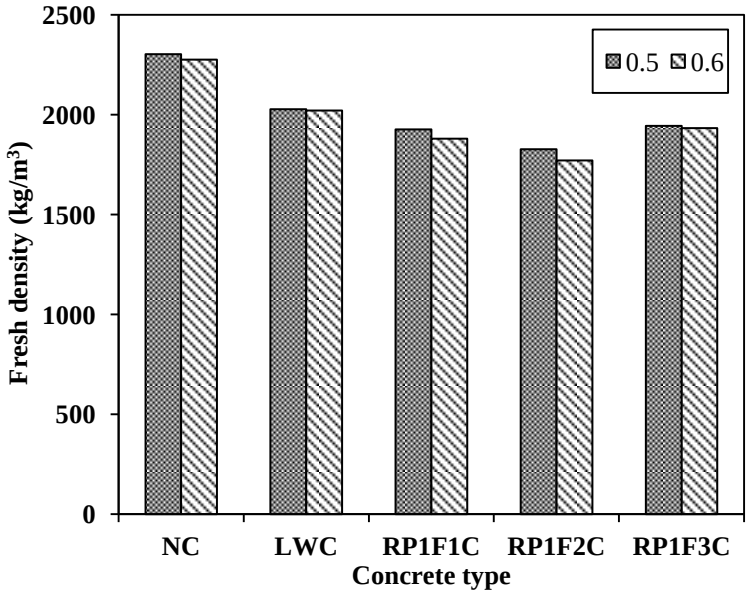


Figure 5.6: Effect of W/C on fresh density of RPAC-1, LWA and NC

5.3 Hardened properties of recycled plastic aggregates concrete

5.3.1 Dry density

Tests were carried out on RPA concrete to evaluate its fulfilment of density requirements specified for lightweight concrete. Figures 5.7 and 5.8 depict the dry density results for the RPAC-1 and RPAC-2 respectively, in comparison with NC and LWC. The results presented in Figure 5.7 show that the 28-day dry density of RPAC-1 was insignificantly less (i.e. maximum reduction 9%), except for RP2F3C0.5 which had a marginal increase (1.8%) compared to that of LWC.

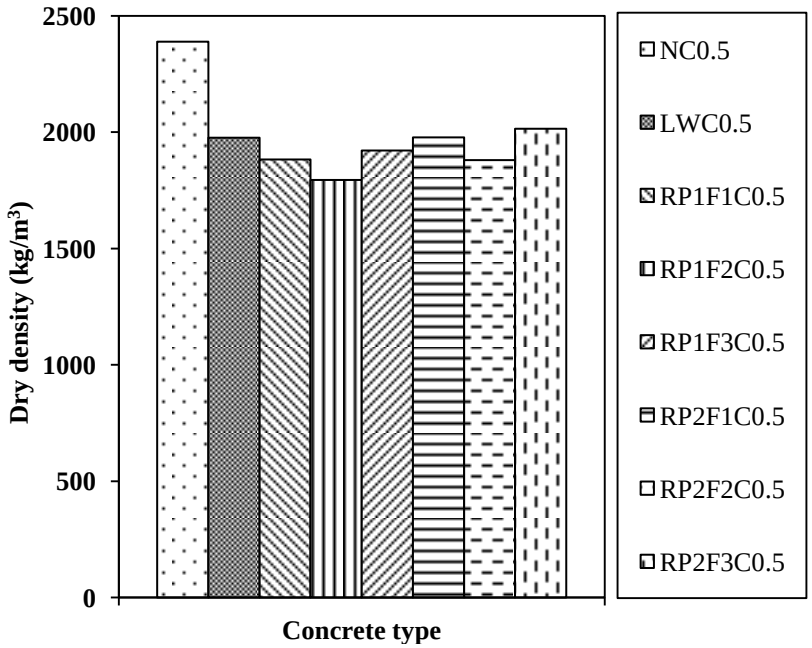


Figure 5.7: 28-day dry density of RPAC-1, LWC and NC at W/C of 0.50

However, with respect to the NC, the reduction in dry density of RPAC-1 ranged from 16 to 25%. The light weight of the plastic and filler particles which formed the RPA was indeed the major cause of the reduction in dry density of the aggregates (see section 4.4.6) and subsequently the RPA concrete. This reduction is in strong agreement with some studies (Choi et al., 2009; Choi et al., 2005; Jansen et al., 2001; Kashi et al., 1999; Slabaugh et al., 2007); where different replacement levels (i.e. 75-100%) of normal CA or FA with plastic

based aggregates resulted in a significant reduction (15-31%) in dry density (see Table 5.1). As observed with fresh density, these results indicate that the least dry density amongst RPAC-1 is attained by RP1F2C0.5 due to the lowest specific gravity of its aggregate (i.e.RP1F2A) among all the RPA (Group 1).

On the other hand, the findings in Figure 5.8 revealed that there was a marginal variation (i.e. from -2 to 5%) between the dry density of RPAC-2 and LWC. However, in comparison with NC, the dry density of RPAC-2 was significantly lower (i.e. 14-20%). In addition, these results showed that the minimum dry density of RPAC-2 was achieved by RP3F2C0.5, since RP3F2A has the lowest specific gravity/density amongst RPA (Group 2), as observed previously with fresh density.

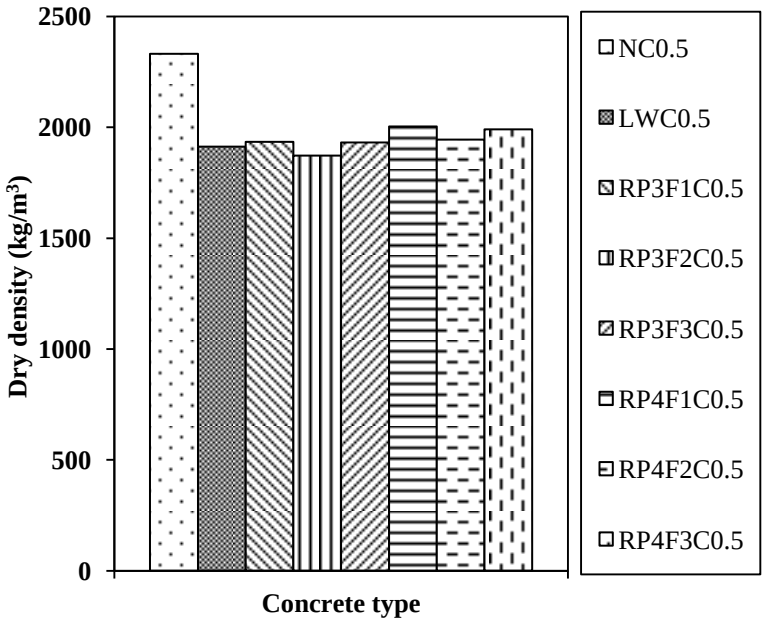


Figure 5.8: 28-day dry density of RPAC-2, LWC and NC at W/C of 0.50

Normally dry density decreases with an increase in the W/C ratio. However, this was not the case in this study since the increase in W/C ratio from 0.50 to 0.60 did not have a significant effect on the dry density of NC, LWC or RPAC-1 containing RP1F1A, RP1F2A and RP1F3A, as shown in Figure 5.9, as observed with fresh density.

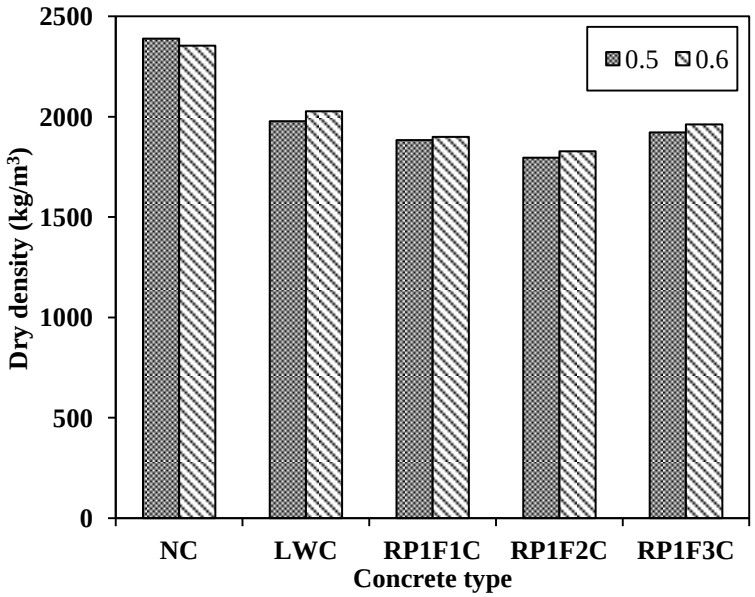


Figure 5.9: Effect of W/C on 28-day dry density of RPAC-1, LWA and NC

In summary, the present study results suggest that the dry density of RPAC-1 and RPAC-2 are within the limits (i.e. 1400-1900 kg/m^3) specified in ACI 213R-03 with a marginal increase (6%).

5.3.2 Compressive strength

The cube compressive strength results for RPAC-1 and RPAC-2 are shown in Figures 5.10 and 5.11 respectively, as compared to NC and LWC at different ages (7, 14 and 28 days), for a W/C of 0.50. The general observation from these two figures indicates that the compressive strength of all mixes increased with age (from 7 to 14 and from 14 to 28 days) as expected. Moreover, the compressive strength of RPAC-1 and RPAC-2 was less than that of NC. However, with respect to LWC, RPAC-1 had lower while RPAC-2 had higher compressive strength.

Figure 5.10 shows that, the percentage increase in compressive strength from 7 to 14 days varied from 11.5 to 31% for RPAC-1, compared to 18 and 19% attained by NC and LWC, respectively. Similarly, the increase in the curing period from 14 to 28 days yielded an

increase ranging from 4 to 20% for RPAC-1, in comparison with 15 and 17% observed for NC and LWC, respectively.

At 28 days, the lowest reduction in compressive strength amongst RPAC-1 was observed in RP2F3C0.5, which was 40 and 59% less strong than conventional LWC and NC, respectively. By contrast, the maximum reduction in RPAC-1 was seen in RP1F2C0.5, and was 53 and 68% as compared to conventional LWC and NC respectively. These results are in agreement with those reductions ranging from 31 to 66% (see Table 5.1), where 75 to 100% of CA or FA was replaced with plastic based aggregates (Choi et al., 2009; Choi et al., 2005; Jansen et al., 2001; Malloy et al., 2001; Slabaugh et al., 2007).

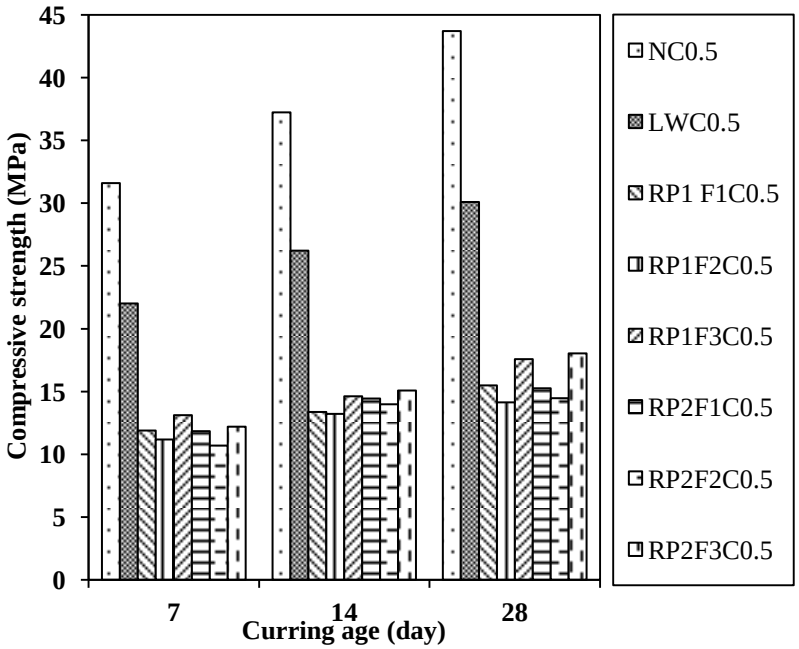


Figure 5.10: Cube compressive strength of RPAC-1, LWC and NC at 7, 14 and 28 days and at W/C of 0.50

Based on all of the above discussion, RP2F3C0.5 had the least reduction in compressive strength among RPAC-1, because the aggregate used (i.e. RP2F3A) had the least FM (i.e. less coarse), better angularity and roughness texture amongst RPA (Group 1) (see section 4.4.1 and 4.4.3). Consequently, the packing level increases which leads to better interlocking

between this type of aggregate and the cement matrix, as confirmed by the SEM image (see Fig. 5.16d). However, generally, the reduction in the compressive strength of RPAC-1 with respect to LWC and NC was due to a decrease in the amount of rigid aggregate, which was replaced by lightweight aggregate (RPA Group 1). Additionally, it is attributed to the weak resistance of the ITZ against stress (see section 5.3.4). This resulted from the poor bonding between the RPA and the cement paste. The poor bonding is most likely due to the hydrophobic nature of plastic existing in the RPA that might hinder the cement hydration in the ITZ, as reported elsewhere (Ismail and Al-Hashmi, 2008; Kou et al., 2009).

In the case of RPAC-2 (Fig. 5.11), the percentage increase in compressive strength with respect to the increase in the curing period (7-14 days) varied from 3 to 19%, as compared to 16 and 18% found in NC and LWC respectively. Similarly, the improvement percentage due to increasing the curing period from 14 to 28 days ranged between 7 and 34% for RPAC-2; in contrast with 13 and 19% attained by NC and LWC respectively. Interestingly, at 28 days, the RPAC-2 observed a significant increase ranging between 13 and 39.7%, as compared to LWC, except for RP4F1C and RP4F2C, which demonstrated a marginal decrease (8%). This is attributed to the high strength of the aggregate (RPA Group 2) as compared to LWA, as reported earlier in section 4.4.8.

However, with respect to NC, the 28-day compressive strength of RPAC-2 was reduced by 7 to 39%. This reduction is less compared to reductions reported in various studies (Choi et al., 2009; Choi et al., 2005; Jansen et al., 2001; Malloy et al., 2001; Slabaugh et al., 2007). In past studies, the reduction in compressive strength ranged from 31 to 66% at different replacement levels (from 75 to 100%) of normal CA or FA with plastic based aggregates. Besides the low strength of the aggregates (RPA Group 2) as compared to NA, the explanation for this

reduction is consistent with those reported by Kou et al. (2009) and Rai et al. (2012); it is attributed to the decrease in the packing level of the mix since RPA (Group 2) has a relatively poorer grading (see section 4.4.2). These results showed that the highest compressive strength amongst RPAC-2 was achieved by RP3F3C0.5 since its aggregate (i.e. RP3F3A) attained the highest strength among all the RPAs (Group 2) (see section 4.4.8).

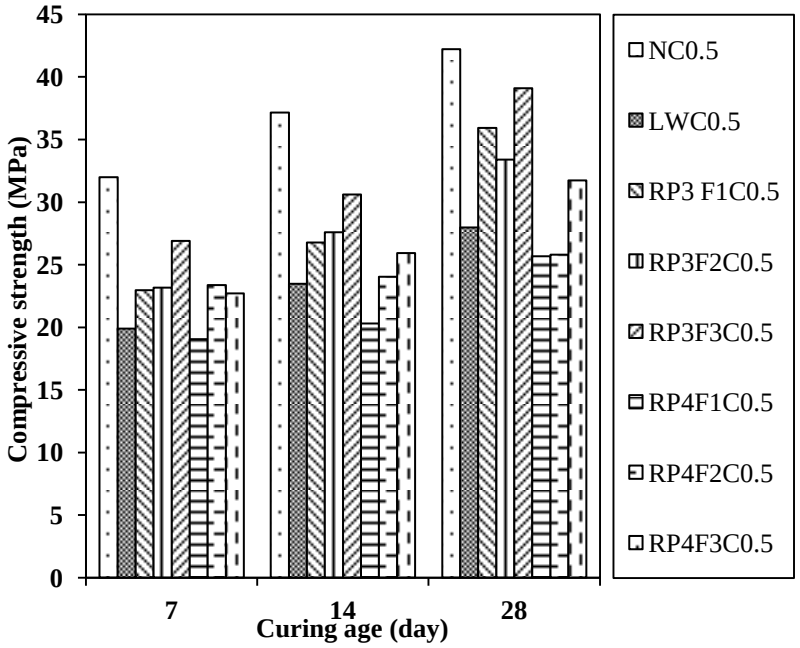


Figure 5.11: Cube compressive strength of RPAC-2, LWC and NC at 7, 14 and 28 days and at W/C of 0.50

In addition, the present study's results indicate that the variations in 28-day compressive strength with respect to the increase in filler percentage from 50 to 70% in the RPA matrix were ±2.5% for RPAC-1. However, the variations in 28-day compressive strength of RPAC-2 were more prominent (from -19 to -28.5%). This variation is related to the decrease in the strength of the aggregate (RPA Group 2) with the increase in the filler percentage in its matrix (see section 4.4.8).

The influence of increasing the W/C ratio from 0.50 to 0.60 on the 28-day cube compression strength of RPAC-1 as compared to LWC and NC is depicted in Figure 5.12. A general trend

indicated that the compressive strength was inversely proportional to the W/C as expected. The compressive strength of concrete containing RP1F1A, RP1F2A and RP1F3A was decreased by 17, 6 and 16% respectively, due to the increase in W/C from 0.50 to 0.60. This is in comparison with decreases of 28 and 21% associated with NC and LWC, respectively.

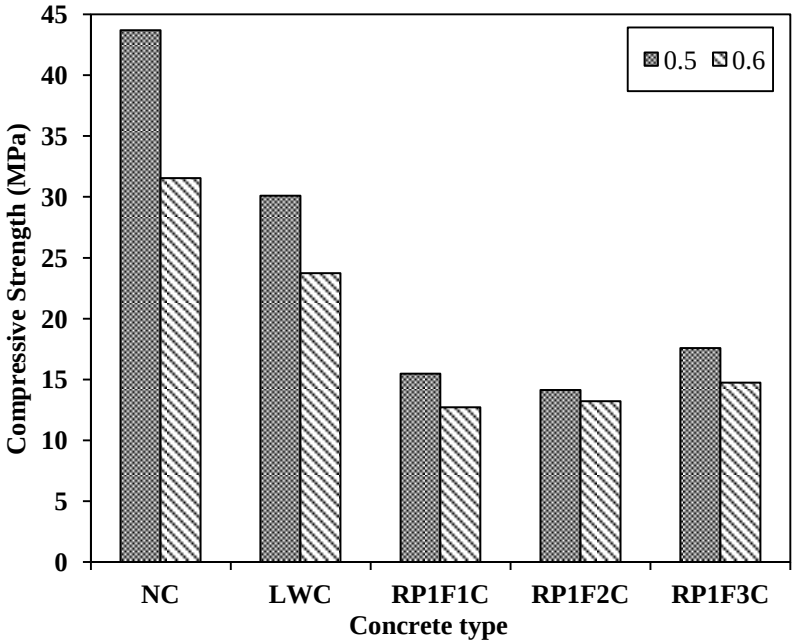


Figure 5.12: Effect of W/C on 28-day cube compressive strength of RPAC-1, LWA and NC

In summary, by considering that the ratio between cylinder to cube compressive strength is equal to 0.8 (Hamad, 2015; Neville, 1995), the 28-day cylinder compressive strength of RPACs-1 deviated by 15-33% from the minimum requirement of the ASTM C330/C330M-14 (i.e. 17 MPa). However, for the RPACs-2 it was 17 to 82% higher than the minimum requirement for the same standard. Thus, these results suggest that the RPACs-2 could potentially be used in structural lightweight applications; while the RPACs-1 could still be used in non-structural applications such as backfill for trenches, where low strength (i.e. between 7 and 17 MPa) is required, as given in the ACI 213R-03.

5.3.3 Flexural strength

The flexural strength results of RPAC-1 and RPAC-2 are presented in Figures 5.13 and 5.14 respectively, as compared to NC and LWC at different ages (7, 14 and 28 days) and at a W/C ratio of 0.50. In these figures, there was an increasing trend in the flexural strength with respect to the increase in the curing period (i.e. from 7 to 14 and from 14 to 28 days). Furthermore, the flexural strength of RPAC-1 and RPAC-2 was lower compared to the NC and LWC, except for that of RPAC-2, which showed a higher flexural strength compared to LWC at an early age (7 days), as seen in Figure 5.14.

It is clear from Figure 5.13 that the increase of curing time from 7 to 14 days yielded an increase in the flexural strength ranging from 6 to 23% for RPAC-1, as compared to 30 and 19% achieved by NA and LWC, respectively. However, the increase from 14 to 28 days resulted in a less prominent increase ranging from 8 to 16% of RPAC-1, compared with 1 and 11% found in NC and LWC, respectively. This is due to the high strength gained at early ages (i.e. 7 days) of the ultimate strength observed at 28 days.

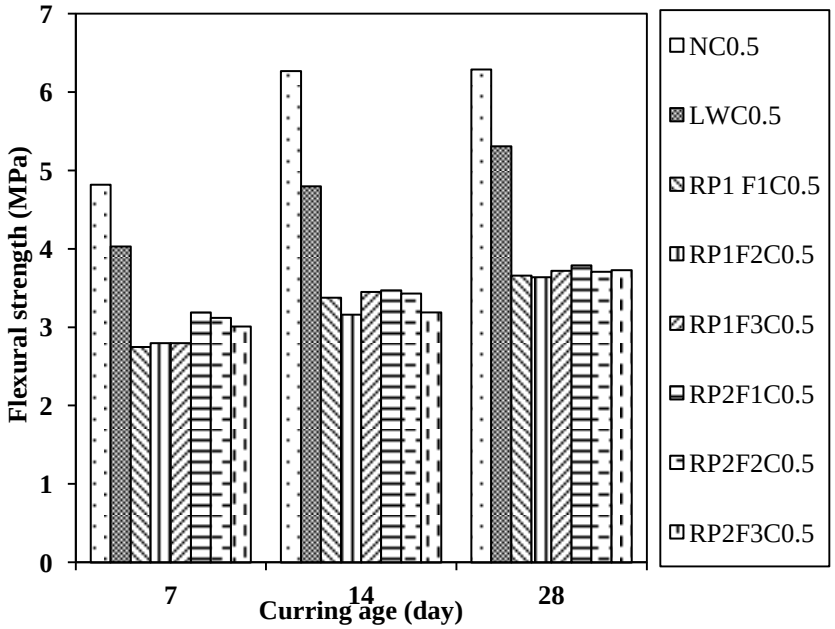


Figure 5.13: Flexural strength of RPAC-1, NC and LWC at 7, 14 and 28 days and at W/C of 0.50

At 28 days, the minimum reduction in flexural strength of RPAC-1 was observed in RP2F1C0.5, being 27 and 39% weaker compared to LWC and NC; whereas, the maximum reduction was seen in RP1F2C0.5, at about 31 and 42%, as compared to LWC and NC. Although, the variation in the 28-day flexural strength reduction amongst RPAC-1 was less prominent compared with that for compressive strength, it can also be controlled by the same factors influencing the compressive strength reduction (see section 5.3.2) and is associated with a lower amount of rigid aggregates, together with the poor bonding in the ITZ. This is supported by the SEM images depicted in section 5.3.4.

Similarly, in the case of RPAC-2 (see Fig. 5.14), the rate of flexural strength increase varied from 5 to 18% in comparison with 6 and 53% achieved by NC and LWC respectively, due to the increases in the curing period from 7 to 14 days. In the same context, the increasing of the curing time from 14 to 28 days yielded an increase in flexural strength ranging from 3 to 27% for RPAC-2, compared to 13 and 25% attained by NC and LWC.

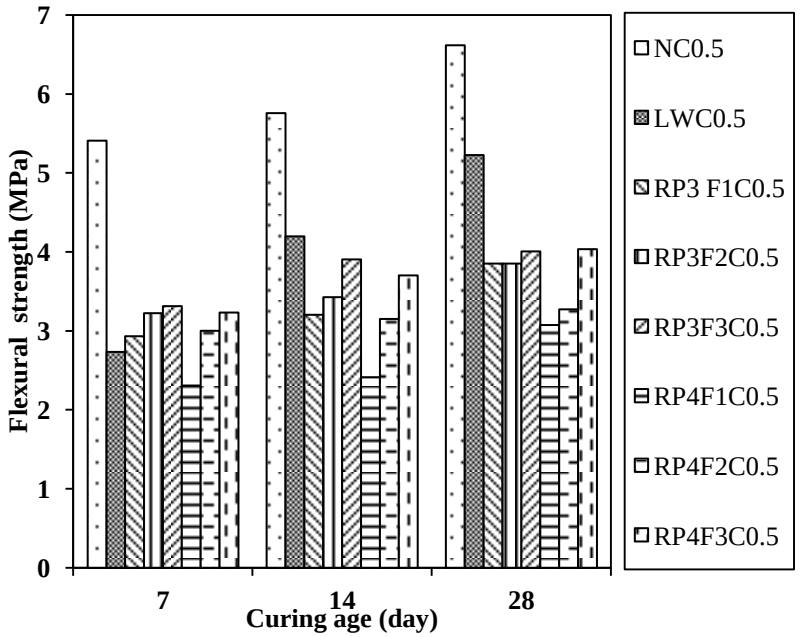


Figure 5.14: Flexural strength of RPAC-2, NC and LWC at 7, 14 and 28 days and at W/C of 0.50

Interestingly, Figure 5.14 indicates that the RPAC-2 achieved a higher flexural strength (i.e. 7-21%) at 7 days; except for RP4F1C0.5, which had 15% lower strength compared to LWC. However, this trend changed at 14 and 28 days, where the RPAC-2 obtained a lower flexural strength compared to both NC and LWC. These results revealed that the lowest reduction in 28-day flexural strength amongst RPAC-2 was 39 and 23%, as compared to NC and LWC respectively, which was given by RP3F3C0.5 and RP4F3C0.5. While, the highest reduction was observed in RP4F1C0.5, which was 53 and 41% lower with respect to NC and LWC. This is accredited to the variation in the strength of the aggregate amongst RPA (Group 2), since RP3F3A and RP4F3A have higher aggregate strength than RP4F1A (see section 4.4.8). However, the explanation for the reduction in 28-day flexural strength of RPAC-2 could be accredited by the less dense packing level of the mix due to the poor grading of the aggregate (RPA Group 2) (see section 4.4.2).

Furthermore, the results given in Figure 5.13 and Figure 5.14 indicate that the increase in filler percentage from 50 to 70% in the RPA matrix yielded a marginal reduction (less than 4%) in the 28-day flexural strength of RPAC-1; in contrast to a higher reduction varying from 15 to 20% found in RPAC-2, as observed with compressive strength. A possible explanation can be linked to the reduction in the strength of the aggregate with respect to the increase in filler proportions (see section 4.4.8).

The effect of increasing the W/C from 0.50 to 0.60 on the 28-day flexural strength of RPAC-1, LWC and NC was also investigated, as shown in Figure 5.15. This figure shows that the flexural strength was inversely proportional to the W/C ratio. This increase yielded a reduction in the 28-day flexural strength of concrete containing RP1F1A, RP1F2A and

RP1F3A by 18, 17 and 15%, respectively, as compared to 8 and 11% for LWC and NC, respectively.

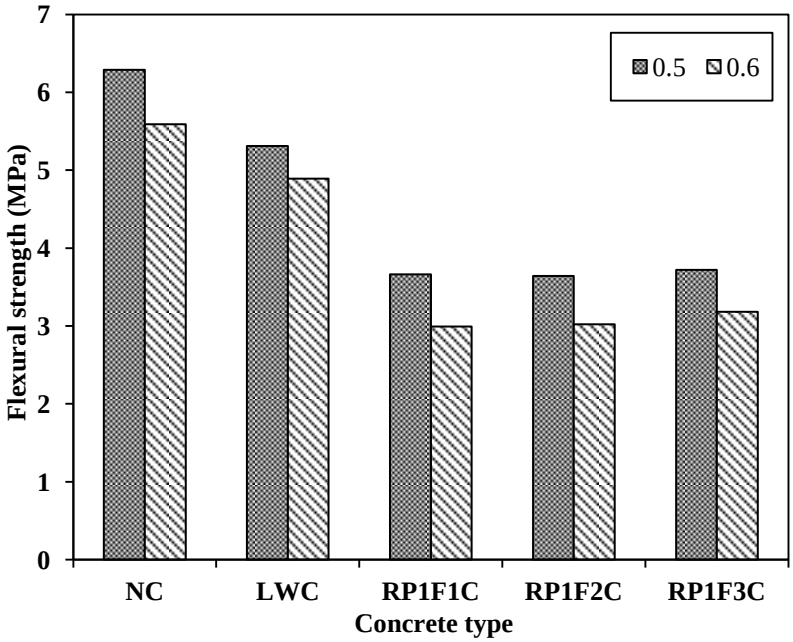


Figure 5.15: Effect of W/C on 28-day flexural strength of RPAC-1, NA and LWC

Overall, the present study's results reveal that the 28-day flexural strength of RPAC-1 and RPAC-2 was less strong than conventional concrete (LWC and NC). Nonetheless, these reductions are less compared to those reported in other studies (Lima et al., 2010; Saikia and de Brito, 2014). In those studies, the variation in flexural strength reduction varied between 50 to 59% by replacing CA with plastic particles at different levels (15-50%).

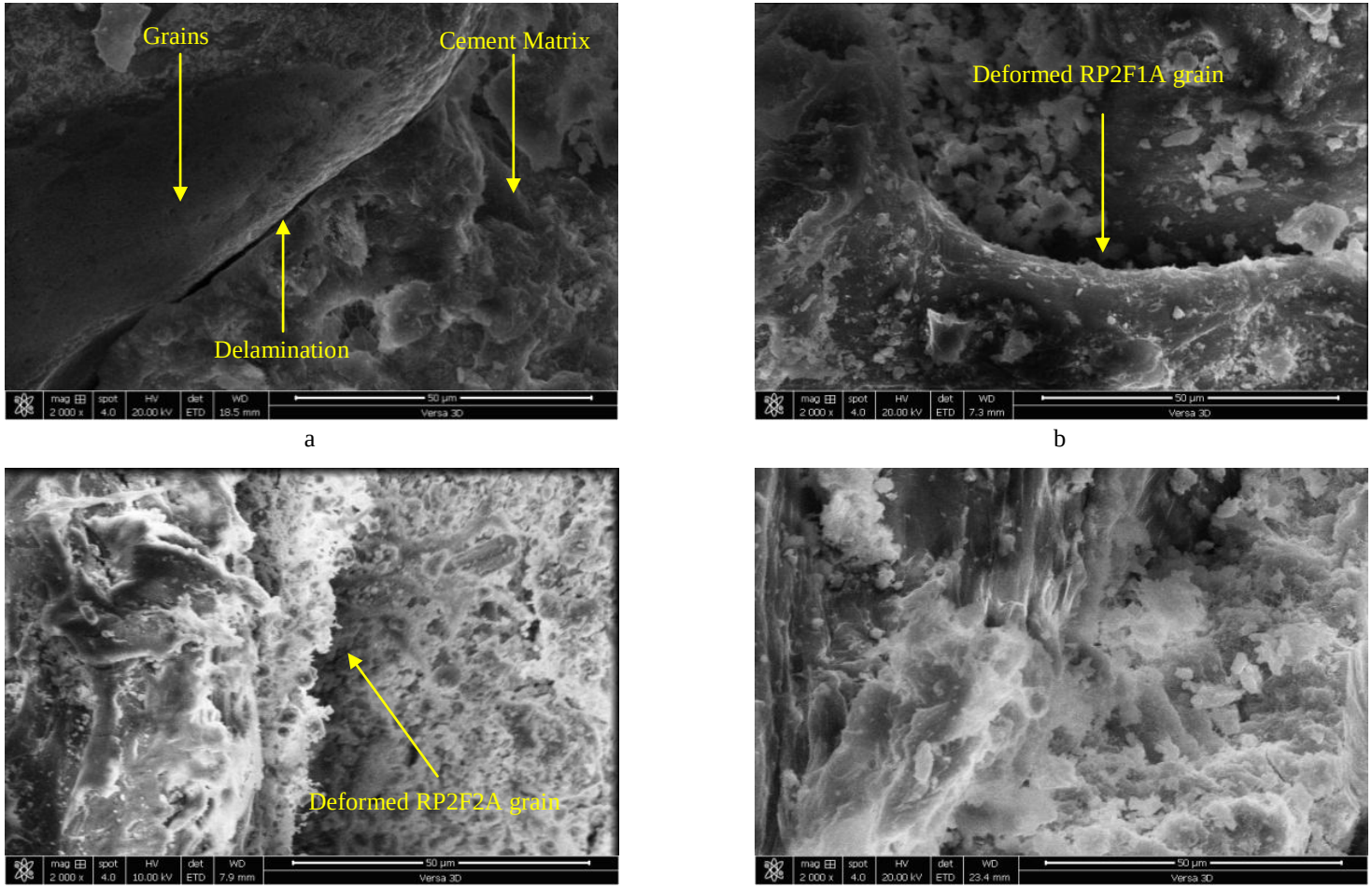
For the sake of comparison with ASTM C330/C330M-14, the 28-day splitting tensile strength was estimated using the 28-day flexural strength of RPAC-1 and RPAC-2; since the ratio between splitting tensile strength and flexural strength is equal to 0.75 (Neville, 1995; Raphael, 1984). Thus, the estimated 28-day splitting tensile strength for RPAC-1 and RPAC-2 ranged from 2.7 to 2.8 MPa and from 2.3 to 3.03 MPa, respectively. Therefore, it is evident that RPACs-1 and RPACs-2 have potential use in structural lightweight applications, since

they satisfy the minimum requirements of the 28-day splitting tensile strength (i.e. 2.1 MPa) described in ASTM C330/C330M-14.

5.3.4 Microscopic investigations

A detailed analysis of the microstructure of concrete samples made with RPA (Group 1) and LWA was performed using SEM imaging at 28 days, as shown in Figure 5.16. However, the morphology of RPAC-2 was assessed using an optical microscope at the same age, as shown in Figure 5.17. In the case of RPAC-1, it is clear from the SEM image that the RP2F3A (Fig. 5.16d) is strongly bonded to the concrete cementitous matrix; followed with RP2F1A as the next most bonded (Fig. 5.16b). However, the RP2F2A (Fig. 5.16c) obtained the least bonding to the cement paste amongst the RPAC-1, since it yielded wider space in the ITZ than that exhibited between the cement matrix and other RPAs (i.e.RP2F1A and RP2F3A). This was attributed to the greater extent of the roughness of the aggregate made with QFF (i.e. RP2F3A) and RSF (i.e. RP2F1A); as well as due to its high degree of angularity in contrast to RP2F2A (i.e. containing FAF), which has a smoothness of surface texture and a spherical particle shape. In addition, the loose filler particles of the FAF in the RP2F2A matrix prevent good bonding, as shown previously in Figure 4.36.

These observations explain the increase in the compressive strength of RPAC-1 containing RP2F3A (i.e. has QFF) compared to the lower strength achieved by RPAC-1 having RP2F2A (i.e. has FAF). However generally, the concrete made with LWA (Fig. 5.16a) shows a tight mode of failure as compared to those in RPAC-1; which reveals that the LWA is more strongly bonded to the cement matrix than the RPA (Group 1). A similar observation was found by Marzouk et al. (2007), who linked the improvement in the mechanical performance of concrete with its ITZ bonding.



a b c d

Figure 5.16: SEM images of (a) LWC, (b) RP2F1C, (c) RP2F2C and (d) RP2F3C (28 days, magnified×2000)

In the case of RPAC-2, the general observation of the microscopic images given in Figure 5.17 show that the interfaces between the cement matrix and the aggregate are defined and clear in the case of RPAC-2, in contrast with that for LWC. Additionally, Figure 5.17a exhibits that the LWA particles have a porous structure with internal air voids. This is compared with the solid structure found in RPAC-2, as shown in Figure 5.17b, c, d. This observation can be taken as one of reasons for the increase in compressive strength of RPAC-2 as compared to LWC. This explanation is supported by Marzouk et al. (2007), who reported that the presence of pores in the concrete matrix negatively affects its mechanical properties.

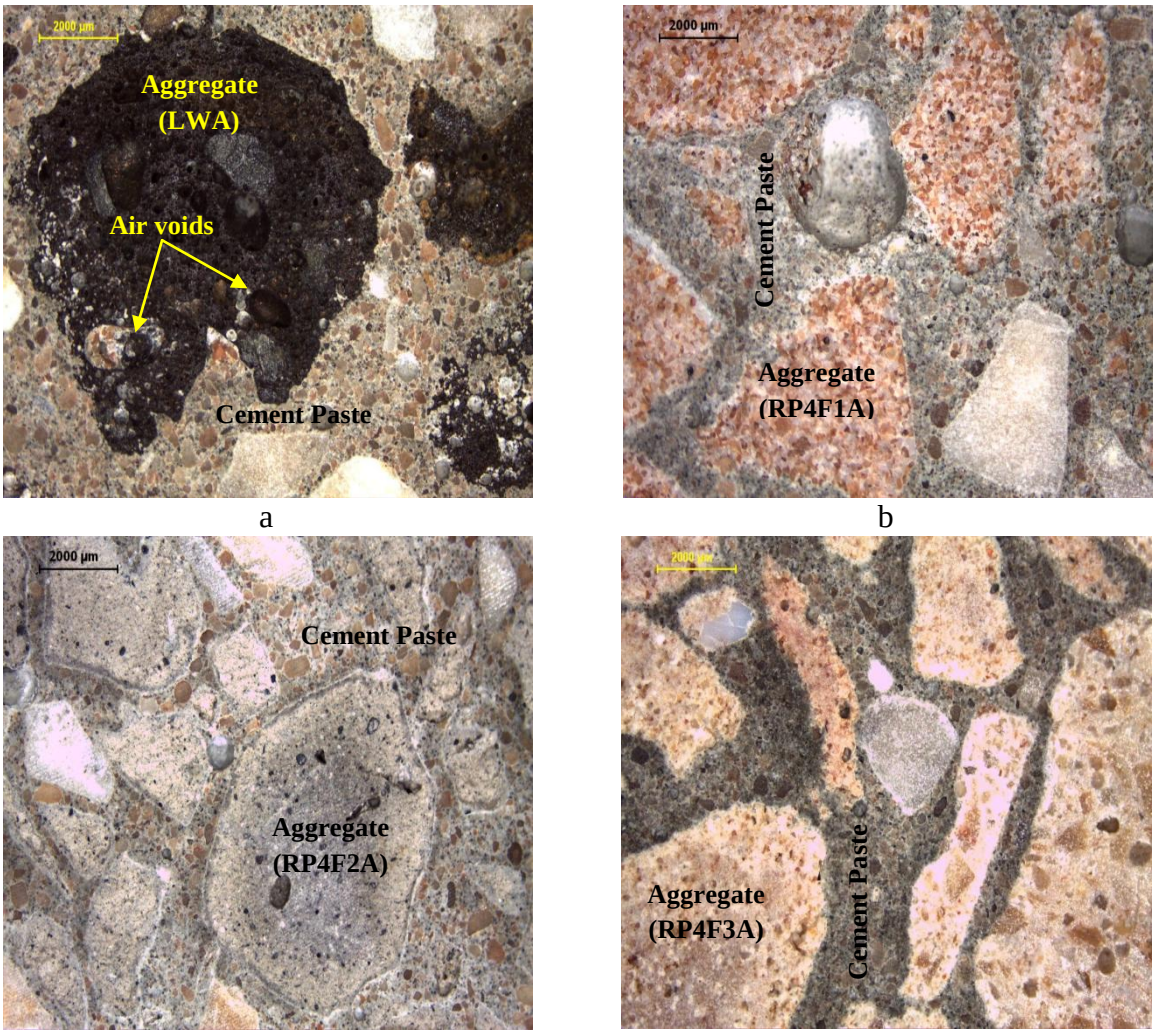


Figure 5.17: Optical microscopic images of (a) LWC, (b) RP4F1C, (c) RP4F2C and (d) RP4F3C (28 days)

5.3.5 Mechanism of failure

At failure, the concrete made using LWA, NA and RPA (Group 2) behaved as expected under flexural loading. However, the use of RPA (Group 1) in concrete resulted in a more complex response, as there was a greater difference in the stiffness between the aggregate and the cement matrix, compared to LWA and NA. Figure 5.18a shows the brittle failure for LWC; while RPAC-1 being more ductile and energy absorbent, thus, under loading, stress transfer from the aggregate to the matrix. Since no significant boundary failure was observed between the aggregate and the matrix, RPAC-1 deforms in a ductile manner with no through-sample cracking until significant deformation has taken place, which ultimately leads to collapse for the entire composite. This behaviour can be seen in Figure 5.18 (b, c, d), which is similar to that observed by other researchers (Al-Manaseer and Dalal, 1997; Babu et al., 2005; Kashi et al., 1999; Rahmani et al., 2013; Ravindrarajah, 1999; Saikia and de Brito, 2014). In these studies, it has been reported that the mode of failure for concrete containing shredded or plastic based aggregate is more gradual with no full disintegration observed due to the high deformation of plastic with loads.

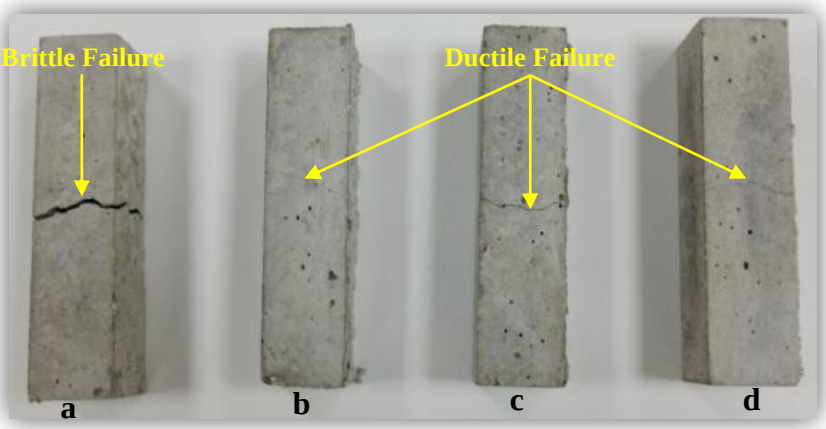
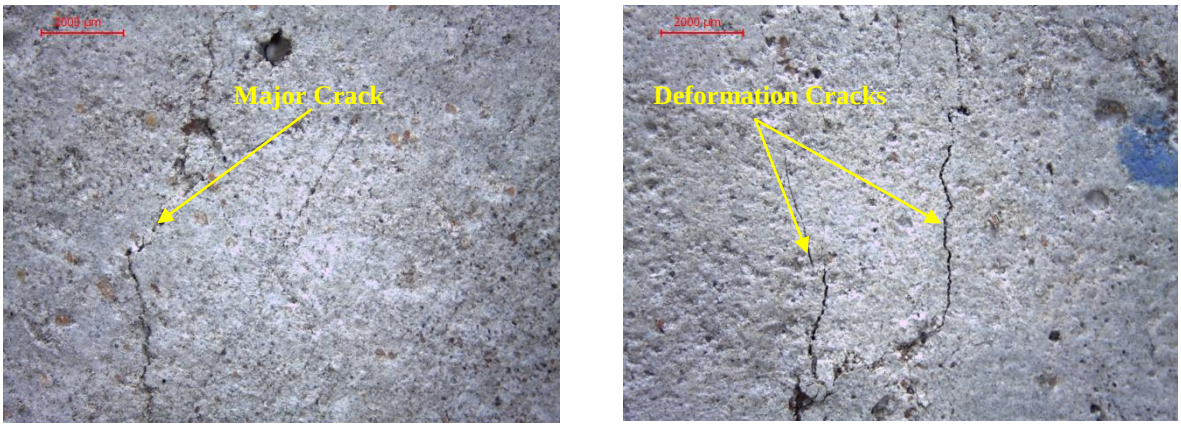


Figure 5.18: Flexural strength mode of failure for (a) LWC and (b, c, d) RPAC-1

Furthermore, under compression loading, two mechanisms of failure were observed using an optical microscope, as follows:

1-The mode of failure in NC, LWC and RPAC-2 is characterised by crack propagation through the aggregate itself, leading to major cracks, as shown in Figure 5.19a.

2- On the other hand, due to the plastic nature within the matrix of RPA (Group 1), the mode of failure becomes different. It is found that stress transfer leads to deformation in the aggregate, instead of crushing or cracks through the aggregate, as shown in Figure 5.19b. This is in agreement with Saikia and de Brito (2014) and Rahmani et al. (2013), who found that the ‘‘crack propagation interval’’ was prolonged due to the presence of plastic particles.



a b

Figure 5.19: Types of cracks for (a) LWC and (b) RPAC-1

5.4 Durability related properties of recycled plastic aggregates concrete

The resistance of concrete containing RPAs towards ingressive soluble (i.e. chloride) was evaluated using a chloride ion penetration test. The results for RPAC-1 and RPAC-2 are presented in Figures 5.20 and 5.21 respectively, in comparison with NC and LWC.

In general, as seen in Figure 5.20, the variation in the 28-day chloride permeability of RPAC-1 varied from -10 to 15% and from -8 to 18% with respect to LWC and NC, respectively. These results revealed that the highest and lowest chloride permeability was achieved by

RP1F2C0.5 and RP2F1C0.5 respectively amongst RPAC-1. The possible explanation for this variation is similar to that observed by Gu and Ozbakkaloglu (2016), which is linked to the water absorption of the aggregates (see section 4.4.5), since RP1F2A had 122% higher water absorption than RP2F1A. Additionally, the existence of the internal voids in RPA (Group 1) (see section 4.4.9) has a great influence on the amount of chloride ions transported into the sample, as similarly observed by Verbeck and Helmuth (1968).

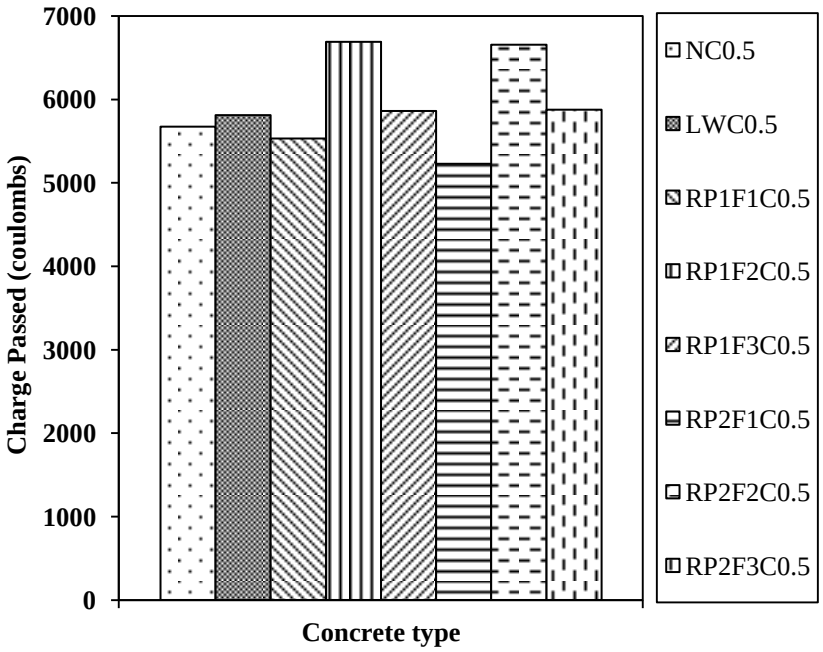


Figure 5.20: 28-day chloride permeability of RPAC-1, NC and LWC at W/C of 0.50

On the other hand, the general trend from Figure 5.21 shows that the chloride penetration of RPAC-2 was reduced in a range varying from 32 to 70% and from 38 to 73%, as compared to NC and LWC respectively. The impermeable property of RPA particles (i.e. less water absorption) was indeed the main reason for this reduction, which therefore distracts the transfer of chloride ions. A similar observation was also reported by Kou et al. (2009), who found that chloride permeability reduced by 36% at 45% replacement of FA with PVC aggregate.

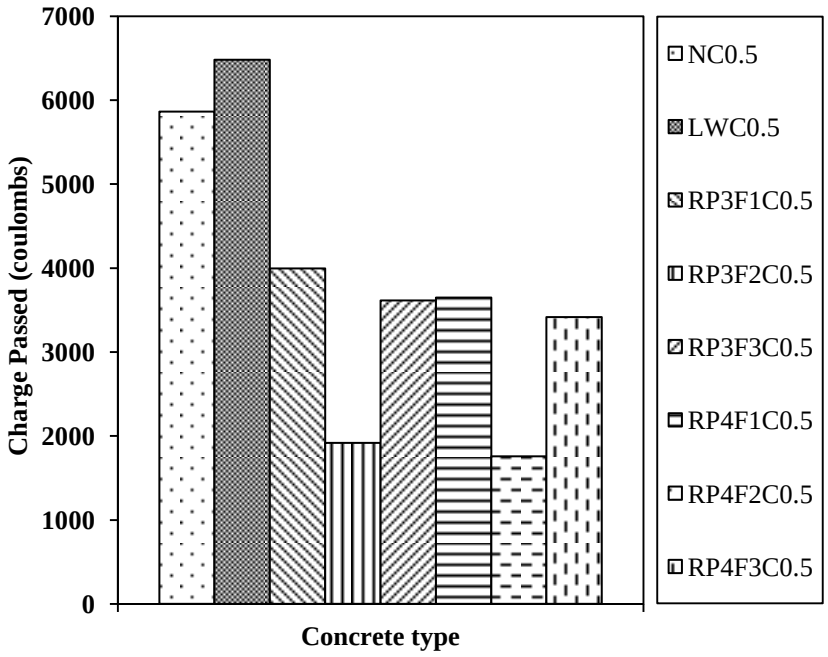


Figure 5.21: 28-day chloride permeability of RPAC-2, NC and LWC at W/C of 0.50

In addition, Figure 5.21 indicates that the least permeability amongst RPAC-2 was attained by RP3F2C0.5 and RP4F2C0.5; which yielded a significant reduction varying from 67 to 70% and from 70 to 73%, in comparison with NC and LWC respectively. However, the highest permeability was found in RP3F1C0.5 and RP4F1C0.5 which had less reduction ranging from 32 to 38% and from 38 to 44%, as compared to NC and LWC respectively. This variation in the permeability of RPAC-2 is related to the level of packing in the mix (Verbeck and Helmuth, 1968), since there were no significant differences in the water absorption amongst the RPA (Group 2). Accordingly, the aggregates with the least FM (i.e. less coarser aggregate) such as RP3F2A and RP4F2A (see section 4.4.3) achieve a dense level of packing which ultimately decreases the permeability of the mix. While the coarser aggregates (i.e. with high FM), such as the RP3F1A and RP4F1A yield a less dense packing level, which leads to high permeability.

A comparison of the two concrete groups reveals that RPAC-2 is more resistant to chloride penetration compared to the RPAC-1. This is due to the closed microstructure (i.e. fewer

voids) of RPA (Group 2) compared with the relatively high voids accumulated in RPA (Group 1), as observed previously in section 4.4.9. Additionally, these figures showed a marginal reduction (varying from 5 to 8%) in the 28-day chloride permeability of RPAC-1 and RPAC-2 due to the increase in the proportions of RSF, FAF and QFF in the RPA matrix from 50 to 70%. This indicates that the increase in the filler percentage in the RPA matrix had no significant effect on the chloride permeability.

Moreover, this study considered the effect of increasing the W/C from 0.50 to 0.60 on the 28-day chloride permeability of RPAC-1 in comparison with that for NC and LWC, as shown in Figure 5.22. This figure exhibits the lesser sensitivity of RPAC-1 to the increase in the W/C ratios, in which the difference in the 28-day chloride permeability insignificantly varied between -10% and 7%. Similarly, the chloride permeability of LWC was slightly increased by about 7%; while the NC was not affected by the increase in the W/C ratio.

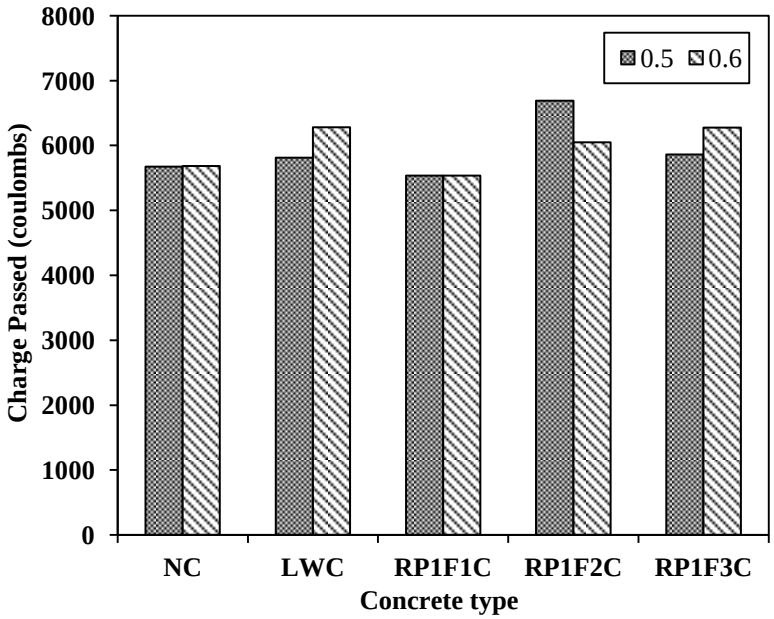


Figure 5.22: Effect of W/C ratio on 28-day chloride permeability of RPAC-1, NC and LWC

In summary, the present study's results indicate that the resistance of concrete to chloride ion penetrability increases with the incorporation of RPAs. In spite of that, RPAC-1 still classified

as highly penetrable concrete according to the requirements described in the ASTM C1202-12. However, these results suggest a potential use for RPAC-2 in structural and non-structural lightweight applications that are exposed to the risk of chloride attack, since it is classified as having low to moderate chloride penetrability according to ASTM C1202-12.

5.5 Optimization of water to cement ratios

Regarding the optimization of the water to cement ratio used, the study results show that the difference in W/C ratio (i.e. 0.50 to 0.60) does not have a significant impact on the properties of concrete; apart from the fact that the strength properties have a reverse relationship with the W/C ratio and vice versa for the workability properties. Moreover, RPAC made with a W/C of 0.60 neither satisfied the maximum requirements of slump specified in ACI 213R-03 nor the minimum requirements of compressive strength described in ASTM C330/C330M-14. Therefore, it was decided to use the W/C of 0.50 for further investigation.

5.6 Selection of RPA concrete optimized mixes

Finally, two optimized concrete mixes were selected: one mix from RPAC-1 and the second mix from RPAC-2, based on their performance in the fresh, hardened and durability properties as compared to LWC and NC, as discussed in the following sections:

5.6.1 Optimized mix selected from RPAC-1

The findings for RPAC-1 indicate that the percentage variation between the maximum and minimum results in fresh density, dry density and, 28-day compressive and flexural strength insignificantly varied from 4 to 13% and from 3 to 10%, as compared to LWC and NC respectively. However, the slump showed a significant difference between the highest and lowest results of 89% and 164%, as compared to LWC and NC respectively. Similarly, 28-

day chloride permeability had maximum and minimum results that differed by 26 and 25% with respect to NC and LWC.

As stated above, the criteria for selection was based on the difference in performance of the concrete mixes in terms of fresh, hardened and durability properties, which was found insignificant except for the slump and chloride permeability observation. Therefore, the controlling factors for selection are limited to slump and chloride permeability in this case.

The slump results showed that only three mixes namely, RP1F1C0.5, RP2F1C0.5, RP1F3C0.5 had achieved the requirements of ACI 213R-03. However, amongst these three mixes, the least chloride permeability was achieved by RP2F1C0.5 (i.e. containing RP2F1A). Subsequently, the concrete made with RP2F1A (i.e. RP2F1C) achieved the selection criteria amongst the RPAC-1.

Moreover, the aggregate used in this mix is RP2F1A, which has 70% dune red sand filler (RSF). This material (i.e. RSF) is abundantly available in the KSA and free of charge, and therefore it is the ideal material to be used as filler in this regard. Additionally, by using RSF, the environmental and economic problems associated with the sand storms would also be resolved to some extent, as reported in section 1.3.3.

Ultimately, concrete made with RPA containing RSF at 70% qualified under the selection criteria and was chosen for further detailed investigation. Therefore, the optimized mix selected from RPAC-1 was RP2FIC along with LWC, which was designated as a reference mix for any further investigations because it is more comparable to RPAC-1 than NC.

5.6.2 Optimized mix selected from RPAC-2

For RPAC-2, the results revealed that the difference in percentages between the highest and lowest outcomes obtained in slump, 28-day compressive and flexural strength, and 28-day chloride permeability were 125, 32, 14 and 38% respectively, as compared to NC. Similarly, the variation percentages observed for each property were 71, 48, 18 and 35% respectively, as compared to LWC. In contrast, the fresh and dry density demonstrated marginal deviation percentages (less than 10%) between the minimum and maximum observations in comparison with NC and LWC. Therefore, the selection criteria for optimized concrete from this group were in line with the performance in slump, strength and durability properties, since the difference in the fresh and dry density was insignificant.

In the case of compressive strength, the highest strength at 28 days was seen in RP3F3C; which was 39.8% higher than LWC, while it was only 7% lower than NC. Similarly, in flexural strength, the maximum was observed in RP3F3C and RP4F3C; which showed similar reductions of 23 and 39% as compared to LWC and NC, respectively. However, in the slump and chloride permeability tests, the RP3F2C and RP4F2C showed the best performance.

Nonetheless, by referring to the results of chloride permeability, it was clear that RP3F3C still had a moderate penetrability according to the ASTM C1202-12, even if it has higher permeability than those obtained by RP3F2C and RP4F2C. Therefore, selection criteria were limited to slump and strength performance between RP3F3C and either RP3F2C or RP4F2C. These mixes obtained a contrary performance in these two properties, as explained above. Consequently, priority has been given to strength performance at the expense of slump.

Therefore, RP3F3C (i.e. made with RP3F3A) was selected as the optimized mix from RPAC-2 for further investigations. This was chosen together with NC, which was elected as the

reference mix, with concrete chosen from this group since RPAC-2 yielded higher compressive strength than LWC, as elaborated earlier in section 5.3.2.

5.7 Summary

This chapter presents the possibility of producing lightweight concrete made totally with manufactured recycled plastic aggregates (RPAs). Therefore, fifteen different mixes of recycled plastic aggregate concrete (RPAC) were successfully produced in two groups (i.e. RPAC-1, RPAC-2) at two water to cement ratios (i.e. 0.50, 0.60).

The effect of the RPAs on the fresh, hardened and durability properties of the RPAC was examined and compared with that of either normal weight concrete (NC) or lightweight concrete (LWC), where significant differences were observed and discussed.

The results of this chapter show that the RPAC-2 is the most promising, as it meets the dry density, compressive strength and splitting tensile strength requirements of the ASTM C330/C330M-14, together with the chloride permeability requirements of the ASTM C1202-12. However, RPAC-1 satisfies the dry density, compressive strength and splitting tensile strength requirements of ACI 213R-03 for non-structural lightweight concrete. The RPAC-1 had a deformable mode of failure, compared to those conventional types of failure observed for RPAC-2, NC and LWC.

In this chapter, two optimized mixes (i.e. RP2F1C, RP3F3C), together with an optimized water to cement ratio (i.e. 0.50), were selected based on their performance in the fresh, hardened and durability tests. Consequently, these two mixes will be used in the next chapters (Chapters 6 and 7) to study the effect of the optimized aggregate (i.e. RP2F1A, RP3F3A) on the fresh, hardened and durability properties at different replacement levels (i.e. from 25 to 100%).

CHAPTER 6: INVESTIGATION OF FRESH AND HARDENED PROPERTIES OF OPTIMIZED CONCRETE MIXES

6.1 General

The third phase of this research included the production of the optimized concrete mixes (RP2F1C, RP3F3C) chosen from the previous phase described in Chapter 5. Thus, RP2F1C and RP3F3C mixes were produced at different levels varying from 25 to 100% (on volumetric basis) of reference aggregates (i.e. LWA or NA) with the optimized aggregate (RP2F1A, RP3F3A) at a fixed W/C of 0.50. Additionally, another reference mix (i.e. LAC) was also made with 100% LYA.

The effect of the replacement level (from 25 to 100 %) on the fresh and hardened properties (see section 3.3.3) of the RP2F1C and RP3F3C mixes were evaluated and compared to their corresponding control mixes (either NC or LWC). Moreover, the RP2F1C and RP3F3C mixes containing the 100% replacement level were compared with the LAC for the same properties. The investigated fresh properties of concrete include slump and fresh density. Hardened properties comprised dry density, compressive, flexural, splitting tensile strength, modulus of elasticity, stress-strain relationship, Poisson's ratio and abrasion resistance.

In addition, the results of the RP2F1C and RP3F3C were further compared with previously published data concerning the impact of incorporating shredded plastic or plastic based aggregate as a replacement of aggregate in concrete. The peak replacement level that satisfied the requirements of ASTMC330/C330M-14 and yielded an adequate performance simultaneously was also identified. Finally, correlations were developed between compressive strength and other mechanical properties. It should be noted that the results of RP2F1C described in this chapter have been published in Alqahtani et al. (2017).

6.2 Fresh properties of RP2F1C and RP3F3C mixes

6.2.1 Slump

Workability and flow characteristics of fresh concrete are normally measured using slump. The effect of replacing LWA and NA with RP2F1A and RP3F3A respectively at different substitution levels (25-100%) on slump is shown in Figures 6.1 and 6.2, as compared to LAC and either LWC or NC.

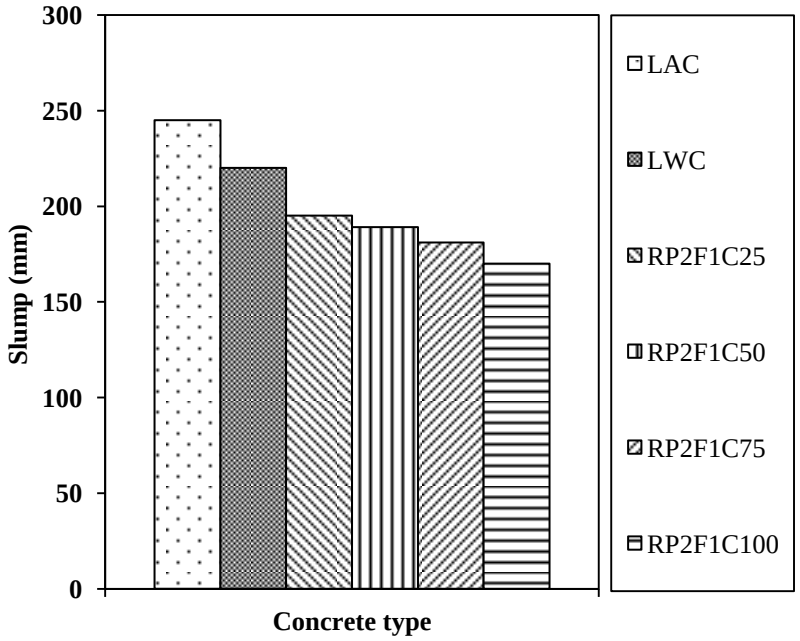


Figure 6.1: Results of slump of RP2F1Cs, LWC and LAC

The decrease in the slump of the RP2F1C mixes (see Fig. 6.1) compared with that of LWC ranged from 11 to 23% (25 to 50 mm) as the replacement level was increased from 25 to 100%. This result is comparable to those of Jansen et al. (2001) and Slabaugh et al. (2007) who reported slump reductions of 7 to 20% due to replacing CA totally with plastic based aggregate (i.e. SLA). However, the slump reduction observed in RP2F1C was less prominent than those reported in previous works (Al Bakri et al., 2011; Tang et al., 2008); where substituting 80 to 100% of CA directly with plastic particles decreased the slump by 16 to 76%. The decrease in the slump of the RP2F1C mixes is considered to be due to the

angularity and fibrous surface texture of the RP2F1A particles (see section 4.4.1). This increases the packing level in the mix in which more surface area of the aggregate particles needs to be covered by the cement paste and thereby reduces the flow ability of the mix, as observed by Rahmani et al. (2013).

On the other hand, the slump of RP3F3C (see Fig. 6.2) observed a significant increase ranging from 47 to 100% (45 to 95 mm) with respect to NC, as the replacement level increased from 25 to 100%. This observed increase is in agreement with those reported elsewhere (Choi et al., 2005; Jansen et al., 2001), in which replacing 75 to 100% of CA with plastic based aggregate (i.e. WPLA, SLA) increased slump by 17 to 123%. The increase in slump of the RP3F3C could be attributed to the poor grading of RP3F3A, as compared to natural coarse aggregate (see Fig. 4.23), which decreased the packing level and ultimately increased the flow of the mix.

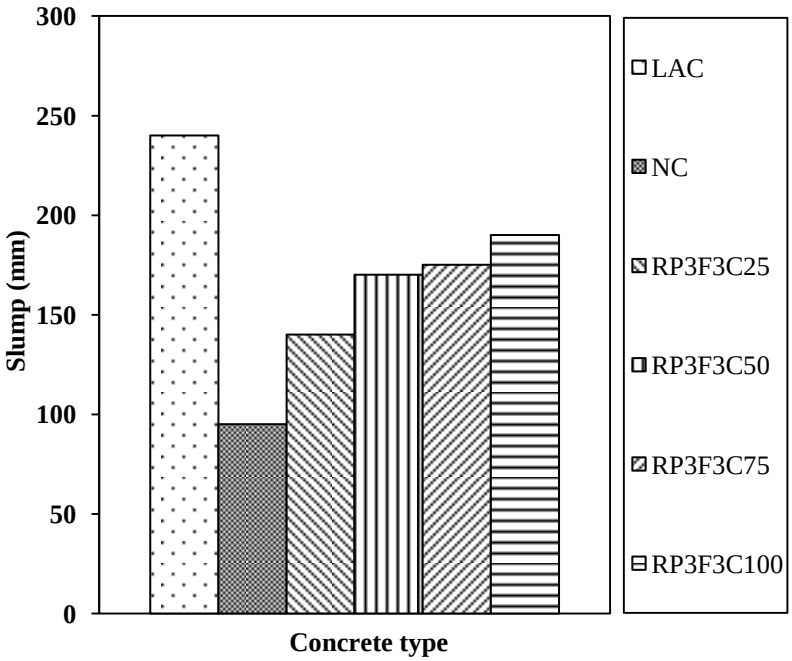


Figure 6.2: Results of slump of RP3F3Cs, NC and LAC

Another important finding was that the reduction in the slump of RP2F1C100 and RP3F3C100 compared with that of LAC was 31 and 21% respectively, as shown in Figures

6.1 and 6.2. The higher slump of LAC is not only due to the relatively high-water absorption of LYA (see Table 3.5), that might not be absorbed totally during the mix, but also can be ascribed to its spherical particle shape and smooth surface texture. To verify the stability or homogeneity of the mix, a sample of LAC was cut 24 hours after casting and, as can be seen in Figure 6.3, no segregation could be detected.



Figure 6.3: Section of a LAC sample

Although the RP2F1C and RP3F3C mixes had relatively higher slump values compared to those specified in ACI 213R-03, this could still be beneficial in the casting and pumping of this type of concrete over a long distance.

6.2.2 Fresh density

Figures 6.4 and 6.5 present the fresh density of concrete made at different replacement levels (from 25 to 100%) of LWA and NA with RP2F1A and RP3F3A respectively, together with that of LAC and either LWC or NC.

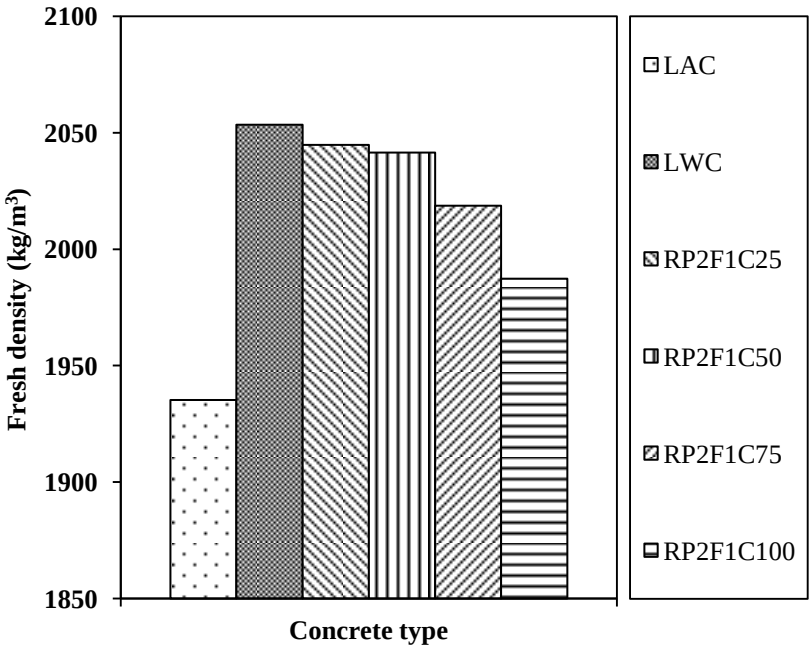


Figure 6.4: Results of fresh density of RP2F1Cs, LWC and LAC

As shown in Figure 6.4, RP2F1C mixes had a marginally (i.e. less than 4%) lower fresh density than the LWC mix, which is attributed to the similarity in the unit weights of their aggregates (RP2F1A, LWA) (see section 4.4.6). Similarly, RP3F3C mixes (see Fig. 6.5) yielded a reduction in fresh density ranging from 5 to 17% as the replacement levels of NA with RP3F3A increased from 25 to 100% as compared to NC. This reduction is because the unit weight of NA is 22% higher than that of RP3F3A (see section 4.4.6). These results are consistent with other studies (Ismail and Al-Hashmi, 2008; Kou et al., 2009; Rai et al., 2012; Ravindrarajah, 1999; Saikia and de Brito, 2014), where replacing FA or CA with shredded or plastic particles at replacement levels ranging from 15 to 45% resulted in a decrease in the fresh density by 6 to 15%. Additionally, there was a marginal difference (i.e. 3%) between the fresh density of LAC and that of both RP2F1C and RP3F3C, which included 100% manufactured lightweight aggregate as CA (Fig. 6.4 and Fig. 6.5).

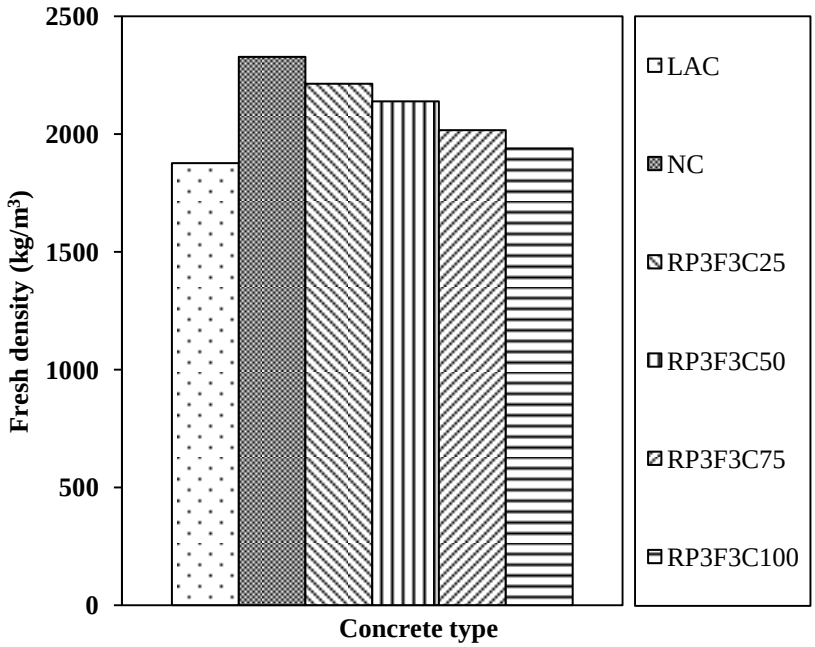


Figure 6.5: Results of fresh density of RP3F3Cs, NC and LAC

Overall, the present study's results confirm that RP2F1A and RP3F3A can be used totally to replace LWA and NA respectively, as well as LYA, without significant effect on the fresh density.

6.3 Hardened properties of RP2F1C and RP3F3C mixes

The following sections present the properties of the hardened concrete mixes considered in this chapter and compare their mechanical properties with the requirements of ASTMC330/C330M-14 (see Table 6.1).

Table 6.1: Lightweight concrete properties according to ASTM C330/C330M-14

Average 28-day density, max (kg/m^3)	Average 28-day splitting tensile strength, min (MPa)	Average 28-day compressive strength, min (MPa)
1840	2.3	28
1760	2.1	21
1680	2.1	17

6.3.1 Dry density

The results of the dry density of concrete containing RP2F1A and RP3F3A as replacement for LWA and NA at different levels (from 25 to 100%), are respectively presented in Figures 6.6 and 6.7, compared to LAC together with either LWC or NC.

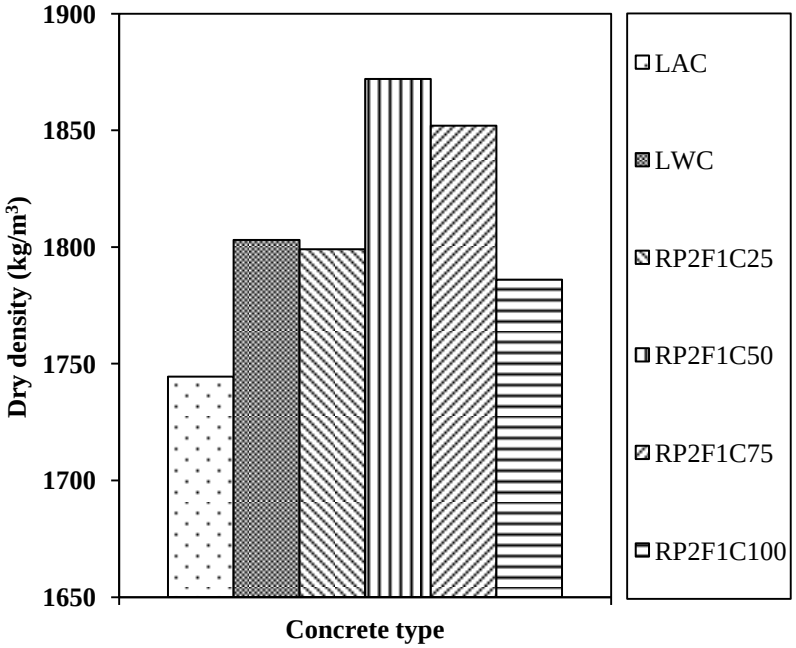


Figure 6.6: Results of 28-day dry density of RP2F1Cs, LWC and LAC

Similar to the case of fresh density, there was a marginal difference (about 3%) in dry density between any of the RP2F1C mixes and LWC. This is attributable to the comparable unit weights of RP2F1A and LWA (see section 4.4.6). However, the results obtained in Figure 6.7 indicate that the dry density of RP3F3C decreased by 4-19% due to replacing 25-100% of NA with RP3F3A, as compared to that of NC. This reduction is accounted for by the difference between the densities of the aggregate (RP3F3A, NA), as observed in the fresh density section.

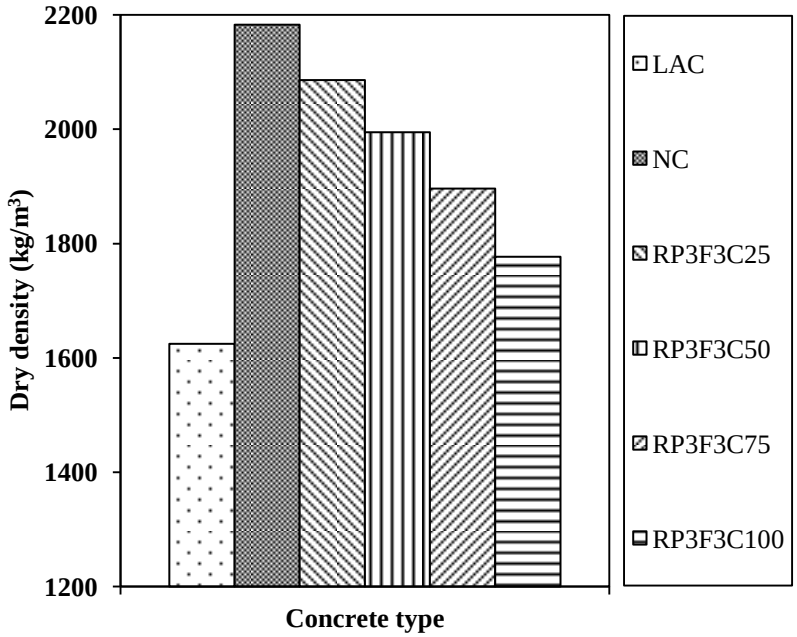


Figure 6.7: Results of 28-day dry density of RP3F3Cs, NC and LAC

The results of the RP2F1C mixes are in good agreement with some studies (Fraj et al., 2010; Juki et al., 2013), where high replacement levels (i.e. 75 to 100%) of CA or FA with plastic particles resulted in a marginal decrease (6-10%) in dry density. However, the RP2F1C mixes were less sensitive to the reduction in dry density compared to those reported elsewhere (Choi et al., 2005; Jansen et al., 2001; Slabaugh et al., 2007), where replacing 75 to 100% of CA or FA with plastic based aggregate (i.e. SLA, WPLA) yielded a reduction varying between 13 and 24%. In addition, the results of the RP3F3C mixes are comparable to the above studies in both cases, when either CA or FA was replaced by plastic particles or plastic based aggregates.

Moreover, RP2F1C100 and LAC (see Fig. 6.6), containing 100% manufactured lightweight aggregate as CA, had dry density results that differed slightly by less than 3%. Similarly, there was a marginal difference (9%) between the dry density of RP3F3C100 and LAC, where both were made with 100% manufactured lightweight CA, as shown in Figure 6.7.

In summary, the dry density results of the PR2F1C mixes were either within or slightly (i.e. less than 2%) higher than the uppermost limit (1840 kg/m^3) specified by ASTMC330/C330M-14 (see Table 6.1). Also, the dry density of the RP3F3C mixes were marginally (3-13%) higher than the uppermost limit mentioned above, except for RP3F3C100. This suggests that the produced lightweight concrete mixes, with up to 100% replacement levels, has potential for use in structural applications where low density is required. This finding is important as the use of lightweight concrete can help reduce element size and consequently reduce the cost of materials, handling, transporting, and ultimately the overall cost of the structure.

6.3.2 Compressive strength

Figures 6.8 and 6.9 show the results of the 28-day cylinder compressive strength of RP2F1C and RP3F3C mixes respectively, together with those of LAC and LWC or NC.

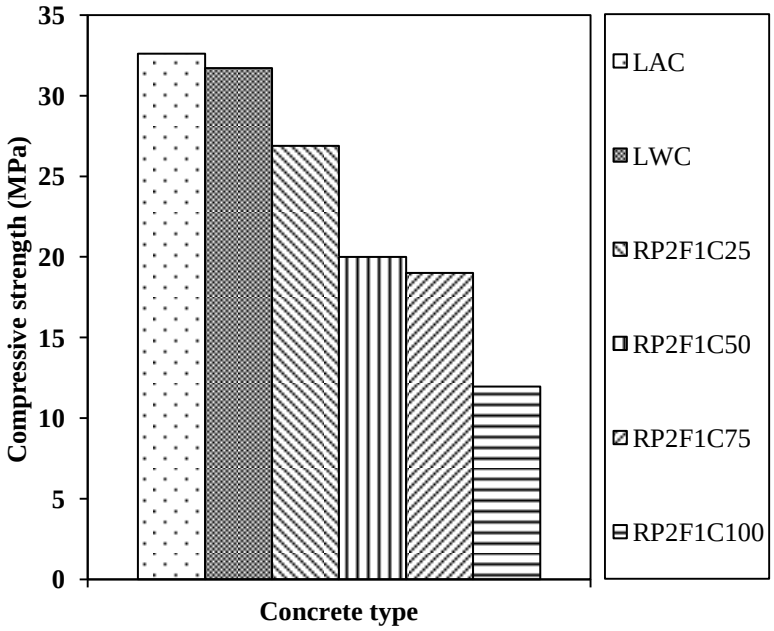


Figure 6.8: Results of 28-day cylinder compressive strength of RP2F1Cs, LWC and LAC

As can be seen in Figure 6.8, the decrease in the compressive strength of the RP2F1C mixes compared with that of LWC varied from 15 to 62% (4.8 to 19.7 MPa), as the replacement level of LWA with RP2F1A was increased from 25 to 100%. Similarly, RP2F1C100 had a

28-day compressive strength that was 63% (20.6 MPa) less than that of LAC, where both had a 100% manufactured lightweight aggregate as CA (i.e. R2F1A, LYA).

The reduction in the compressive strength of the RP2F1C mixes is related to the weak resistance of the interfacial transition zone (ITZ) against loads. This weak resistance results from the weak bonding between RP2F1A and the cement matrix, as proved by SEM imaging (see section 6.3.9). The deterioration in the compressive strength of RP2F1C can also be related to the hydrophobic nature of the plastic existing in the RP2F1A matrix, which prevents good bonding and generates a thin layer around the RP2F1A particles, as depicted in Figure 6.23 (section 6.3.9). This observation is consistent with those reported elsewhere (Ismail and Al-Hashmi, 2008; Kou et al., 2009).

On the other hand, Figure 6.9 shows a relatively moderate decrease varying from 15 to 28% (6.5 to 11.6 MPa) in the 28-day cylinder compressive strength of the RP3F3C mixes, compared to that of NC as the replacement level of NA with RP3F3A was increased from 25 to 100%. This reduction might be explained by the lower strength of the aggregate (i.e. RP3F3A) compared to that of NA, as well as the decrease in the packing level in the mix, since RP3F3A has a poorer grading compared to that of NA (see sections 4.4.2 and 4.4.8), as similarly explained by Kou et al. (2009) and Rai et al. (2012). In contrast, the compressive strength of RP3F3C100 (100% RP3F3A) was 11% (2.9 MPa), higher than that of LAC, (100% LYA) which could be linked to the high strength of the RP3F3A compared with that of LYA (sections 4.4.8).

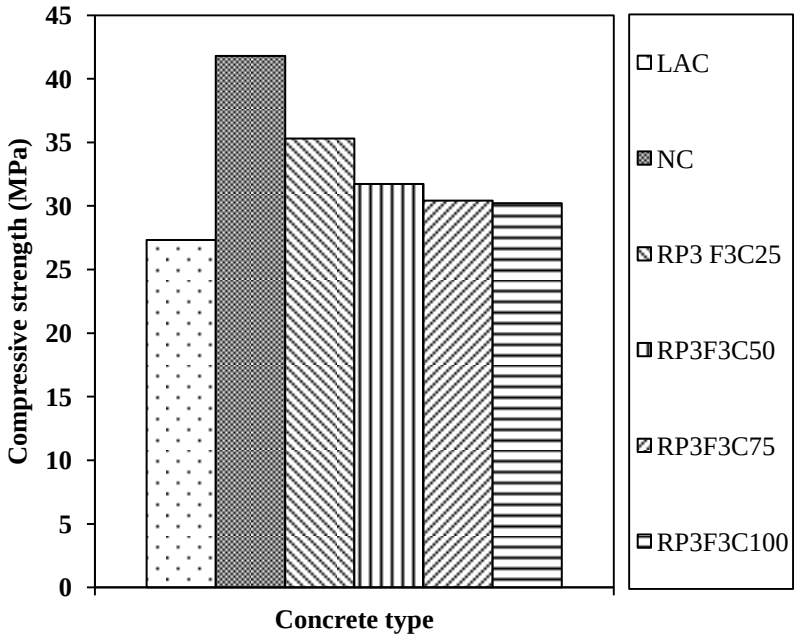


Figure 6.9: Results of 28-day cylinder compressive strength of RP3F3Cs, NC and LAC

Moreover, the results of the RP2F1Cs' mixes are in agreement with those reductions (ranging from 31 to 72%) reported in the literature (Choi et al., 2005; Jansen et al., 2001; Kashi et al., 1999; Malloy et al., 2001; Slabaugh et al., 2007); where 75 to 100% of CA or FA was replaced with plastic based aggregates (i.e. SLA or WPLA). Additionally, RP2F1Cs achieved less reduction than those reported in other studies (Al-Manaseer and Dalal, 1997; Fraj et al., 2010; Lima et al., 2010; Rahman et al., 2012; Ravindrarajah, 1999; Sabaa and Ravindrarajah, 1997; Saikia and de Brito, 2014; Tang et al., 2008); where replacing 15-80% of CA with plastic particles decreased the strength by 62 to 82%. On the other hand, RP3F3Cs are much stronger in relation to all the previous studies mentioned above, in which either normal CA or FA was replaced totally or partially with either plastic particles or plastic based-aggregates.

Overall, the RP2F1C mixes with 25, 50 and 75% replacement levels, as well as the RP3F3C mixes at all replacement levels, had compressive strength results higher than 17 MPa as required by ASTMC330/C330M-14 (see Table 6.1). However, of these mixes, only RP2F1C25 and RP3F3C100 meet both the density and the compressive strength requirements

listed in Table 6.1. Thus, the results suggest that RP2F1C25 (25% RP2F1A) and RP3F3C100 (100% RP3F3A) could potentially be used in structural lightweight applications where low density and moderate strength are required.

6.3.3 Flexural strength

The effect of replacing LWA and NA with RP2F1A and RP3F3A at different replacement levels from 25 to 100% on the 28-day flexural strength is respectively shown in Figures 6.10 and 6.11, as compared to LAC together with either LWC or NC.

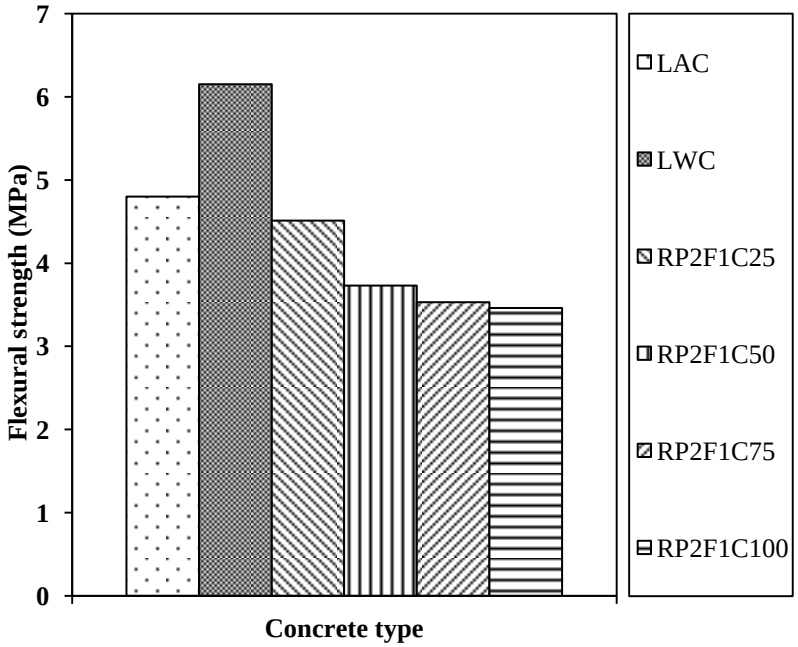


Figure 6.10: Results of 28-day flexural strength of RP2F1Cs, LWC and LAC

Figure 6.10 depicts a significant reduction in the flexural strength of the RP2F1C mixes ranging from 27 to 44% (1.7 to 2.7 MPa) compared with that of LWC, as the replacement level was increased from 25 to 100%. Additionally, RP2F1C100 had a flexural strength that was 27% (1.3 MPa) less than that of LAC. As in the case of compressive strength, this decrease in flexural strength of RP2F1C may be explained by the weak adhesion in the ITZ

between the RP2F1A and the cement paste due to the hydrophobic nature of plastic (Ismail and Al-Hashmi, 2008; Rai et al., 2012) (see section 6.3.9).

Similarly, the 28-day flexural strength of the RP3F3Cs' mixes (see Fig. 6.11) decreased by 3-26% (0.2-1.4 MPa) due to the increase in the replacement level of NA with RP3F3A from 25 to 100%. This reduction is attributed to the decrease in the packing level together with the reduction in strength of the aggregate itself, as previously explained in the case of compressive strength. In the same context, RP3F3C100 was insignificantly lower (15%) (0.7 MPa) compared to that of LAC, where both were made with manufactured lightweight aggregate as CA.

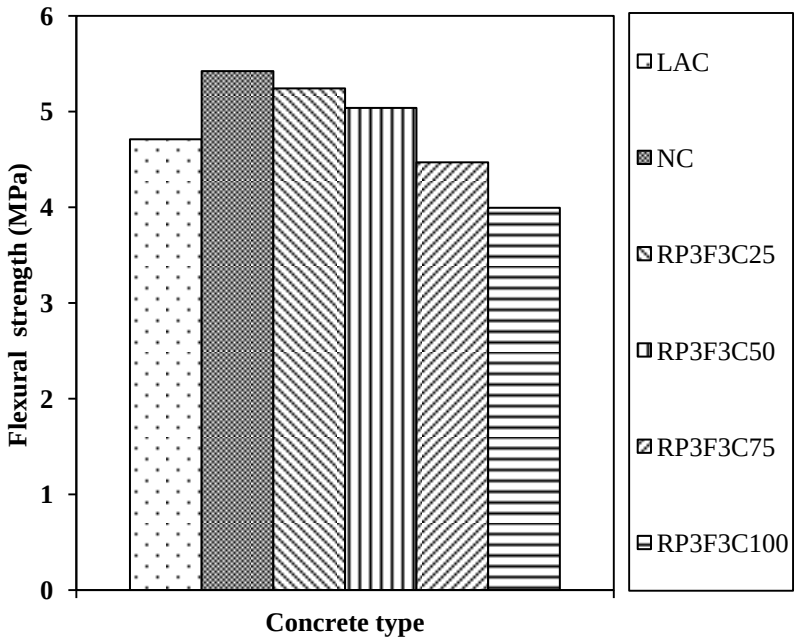


Figure 6.11: Results of 28-day flexural strength of RP3F3Cs, NC and LAC

In summary, RP2F1Cs and RP3F3Cs exhibited less reduction in 28-day flexural strength compared to those reductions observed by Lima et al. (2010) and Saikia and de Brito (2014); who observed a reduction of 50 to 59% due to replacing 15 to 50% of CA with plastic particles. In addition, the RP2F1Cs and RP3F3Cs showed a lesser variation between the

higher and lower reduction of 28-day flexural strength compared to those of compressive strength.

6.3.4 Splitting tensile strength

The results of the 28-day splitting tensile strength of RP2F1C and RP3F3C mixes made at different replacement levels (25-100%) of LWA and NA with RP2F1A and RP3F3A respectively, are presented in Figures 6.12 and 6.13 in comparison to those of LAC together with either LWC or NC.

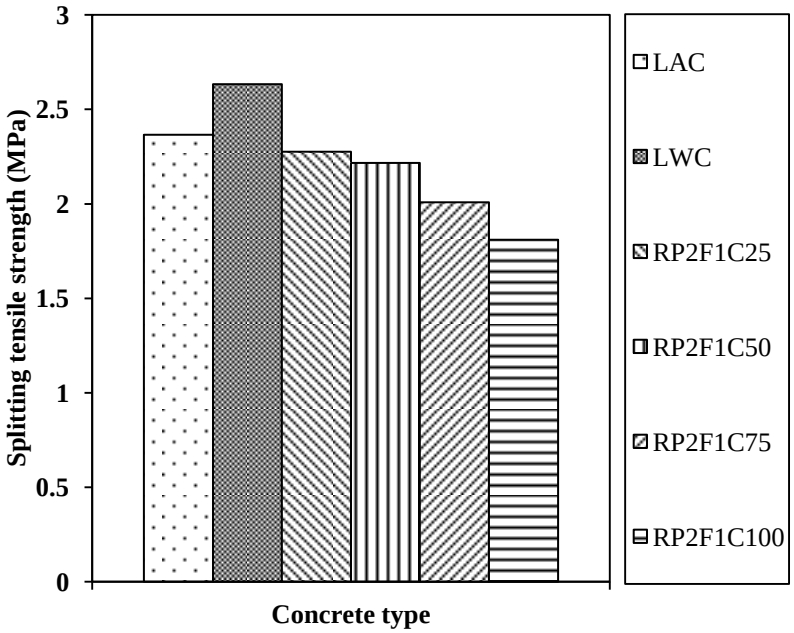


Figure 6.12: Results of 28-day splitting tensile strength of RP2F1Cs, LWC and LAC

The reduction in the splitting tensile strength of the RP2F1C mixes (see Fig. 6.12) compared with that of LWC varied from 12 to 31% (0.3 to 0.8 MPa) as the replacement level was increased from 25 to 100%. Moreover, replacing LYA totally with RP2F1A yielded a 25% (0.6 MPa) lower splitting tensile strength for RP2F1C100 than that of LAC. Similar to the explanation given for the reduction in compressive and flexural strengths, the splitting tensile strength of the RP2F1C mixes decreases due to the weak bond between the RP2F1A and the

cement paste. This is supported by the SEM and optical images shown in Figures 6.22 and 6.23, respectively (see section 6.3.9).

Similarly, the 28-day splitting tensile strength of RP3F3C reduced by 7-37% (0.3-1.4 MPa) compared to that of NC; this was due to increasing the replacement levels of NA with RP3F3A from 25 to 100%, as shown in Figure 6.13. Additionally, there was a marginal difference (4%) between the splitting tensile strength of RP3F3C100 and LAC. This reduction in RP3F3C as compared to NC is likely related to a decrease in its aggregate strength besides the decrease in the packing level of the mix, as previously reported in the case of compressive and flexural strength.

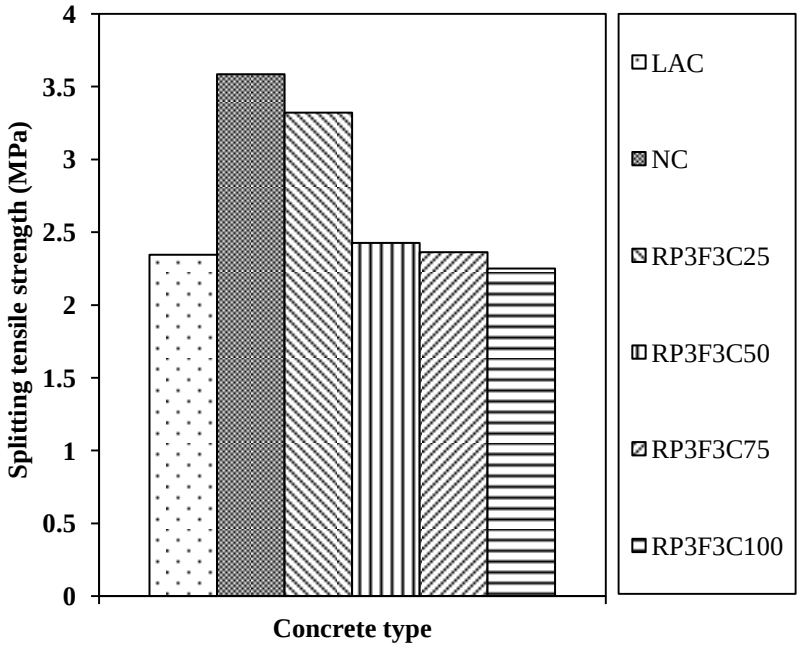


Figure 6.13: Results of 28-day splitting tensile strength of RP3F3Cs, NC and LAC

The results of RP2F1C and RP3F3C are in agreement with the findings of Jansen et al. (2001), who reported splitting tensile strength reductions of 26-38% as a result of substituting 100% of CA with plastic based aggregates (i.e. SLA). Moreover, the percentage reduction in the splitting tensile strength of the RP2F1C and RP3F3C mixes is less than those reported in the extant literature (Al-Manaseer and Dalal, 1997; Lima et al., 2010; Saikia and de Brito,

2014; Tang et al., 2008); where replacing 15-80% of CA directly with plastic particles decreased the 28-day splitting tensile strength by 47-72%.

Overall, the splitting tensile strength of the RP2F1C mixes with 25 and 50% replacement levels, as well as RP3F3C mixes at all levels, was higher than 2.1 MPa as required by ASTMC330/C330M-14. However, similar to the case of compressive strength, only RP2F1C25 and RP3F3C100 meet both the density and the splitting tensile strength requirements listed in Table 6.1. These results further confirm the potential of RP2F1C25 and RP3F3C100 as a sustainable lightweight structural concrete mix.

6.3.5 Modulus of elasticity

Figures 6.14 and 6.15 compare the results of the 28-day elastic modulus of RP2F1C and RP3F3C mixes with those of LAC and LWC or NC respectively.

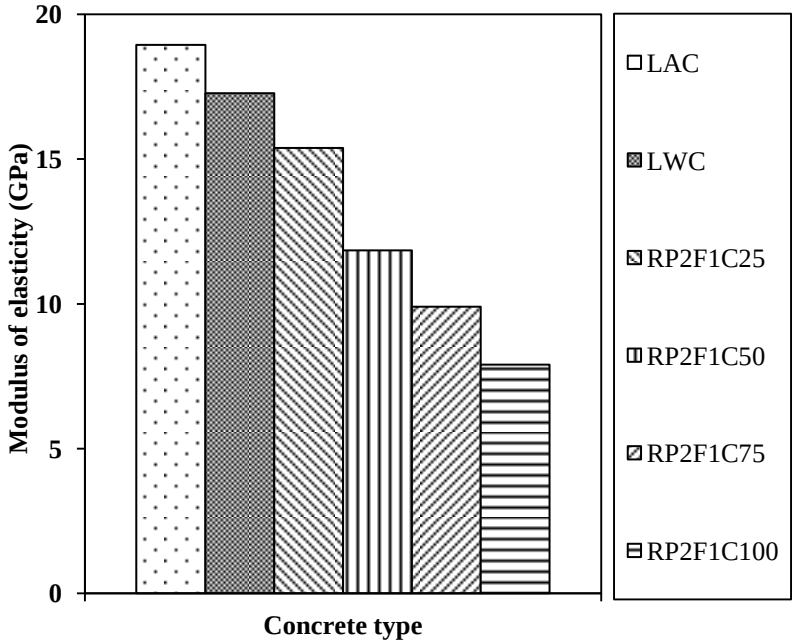


Figure 6.14: Results of 28-day elastic modulus of RP2F1Cs, LWC and LAC

As shown in Figure 6.14, the decrease in the elastic modulus of the RP2F1C mixes compared with that of LWC ranged from 11 to 54% (1.9 to 9.4 GPa), as the replacement level was increased from 25 to 100%. Similarly, the modulus of elasticity of the RP3F3C mixes (Fig.

6.15) was 26-63% (7.2 to 17.7 GPa) lower compared to that of NC due to the increased replacement level from 25 to 100%. Furthermore, RP2F1C100 and RP3F3C100 had an elastic modulus that was 58% (11 GPa) and 43% (7.8 GPa) less than that of LAC, respectively.

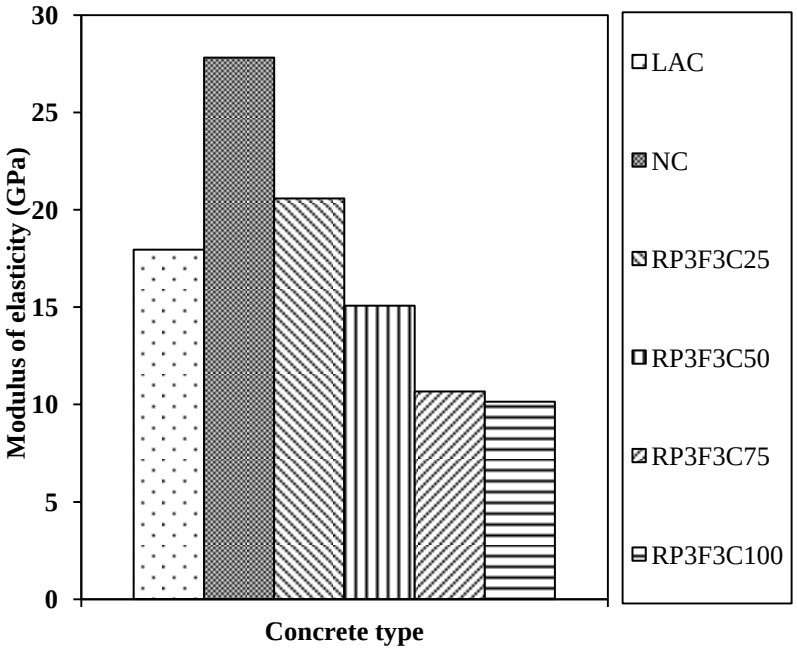


Figure 6.15: Results of 28-day elastic modulus of RP3F3Cs, NC and LAC

Nonetheless, the reduction in the elastic modulus of the RP2F1C and RP3F3C mixes is still lower than those reported in previous studies (Al-Manaseer and Dalal, 1997; Sabaa and Ravindrarajah, 1997; Saikia and de Brito, 2014; Tang et al., 2008); where replacing 15 to 80% of CA with plastic particles yielded significant reductions ranging from 57 to 73%. However, RP2F1C and RP3F3C mixes showed a slightly higher reduction in elastic modulus compared to those of Jansen et al. (2001) and Malloy et al. (2001); who found reductions of 34-42% due to replacing CA totally with plastic based aggregate (i.e. SLA).

The reduction in the elastic modulus of the RP2F1C and RP3F3C mixes can be explained by the incompatibility between the low elastic modulus of recycled plastic aggregate (i.e. RP2F1A and RP3F3A) and the high modulus of elasticity of the cement paste. The low elastic

modulus of RP2F1A and RP3F3A is attributed to the low modulus of elasticity of the plastic present in its matrix. Thus, this leads to an increase in the amount of stress around the aggregate particles which accelerates the failure occurrence, as similarly reported by Kou et al. (2009) and Tang et al. (2008).

6.3.6 Stress-strain behaviour

The stress-strain behaviour of the RP2F1C and RP3F3C mixes made with 25-100% of RP2F1A and RP3F3A as replacement of LWA and NA respectively, are depicted in Figures 6.16 and 6.17 in comparison to those of LAC together with either LWC or NC.

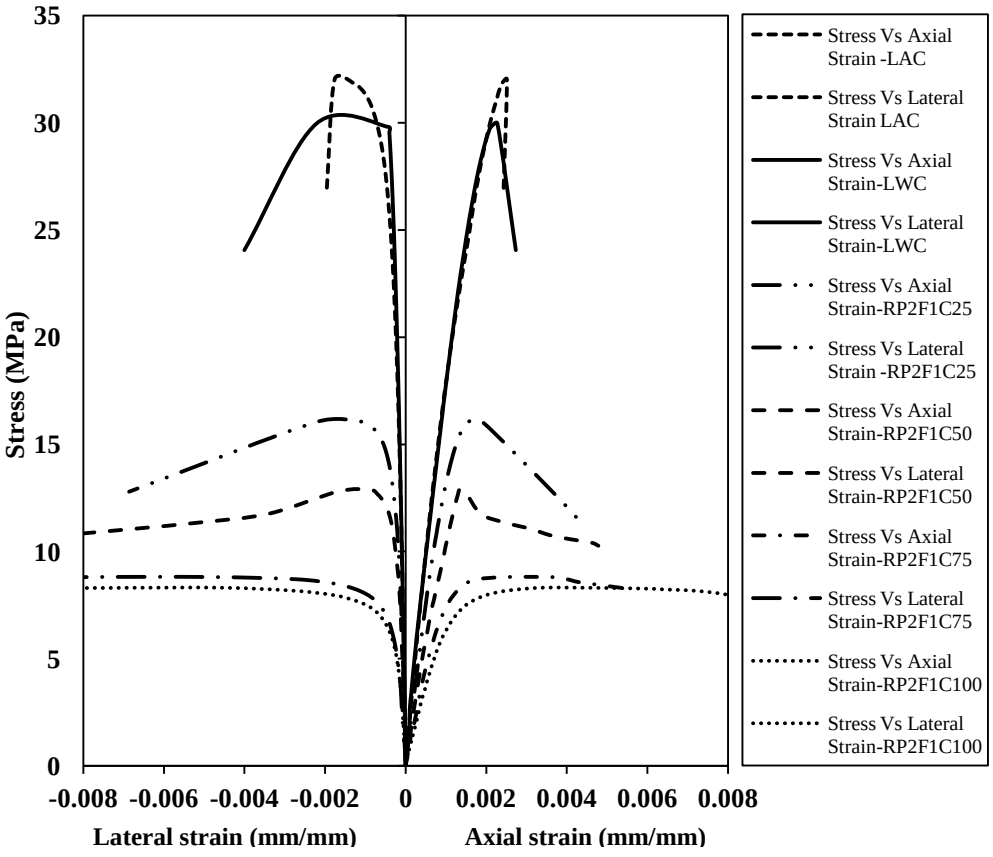


Figure 6.16: Stress-strain curves of RP2F1Cs, LWC and LAC

Figure 6.16 depicts that both LWC and LAC had comparable behaviour where the stress-axial strain response is quasilinear up to the peak stress. The sharp drop in stress is a characteristic of brittle failure. This behaviour is significantly affected by the addition of RP2F1A. For the

RP2F1C mixes, the peak stress decreased; whereas the stress-strain response became more ductile as the replacement level was increased from 25 to 100%.

This finding is consistent with the results of Babu et al. (2005) who observed an increase in the steepness of the stress-strain curve (i.e. became stiffer) with the reduction of the plastic particles' replacement in the mix. As can be seen in Figure 6.16, RP2F1C yielded post-peak deformation where the concrete sample can hold the load for a period of time after failure without full disintegration (i.e. ductile response). A similar finding was reported by Jansen et al. (2001); Kashi et al. (1999) and Malloy et al. (2001); who all observed that concrete made with plastic based aggregate (i.e. SLA) kept deforming at the peak load before fully disintegrating. A possible explanation of this ductility behaviour of the RP2F1C mixes matches that reported by Hannawi et al. (2010) and Ismail and Al-Hashmi (2008); which is accounted for by the high deformation capacity of plastic, since RP2F1A particles have a plasticity nature.

On the other hand, the stress-strain curves presented in Figure 6.17 show that the RP3F3C mixes yielded a similar mode of failure (i.e. brittle failure) to that of NC and LAC. Nonetheless, RP3F3C mixes still achieved maximum stress at higher strain (i.e. axial and lateral) compared to that of NC and LAC. For instance, the increase in axial strain corresponding to the maximum stress of RP3F3C mixes compared with that of NC ranged from 4-59% as the replacement level was increased from 25 to 100%. Additionally, RP3F3C100 had an axial strain that was 58% higher than that of LAC. These results are higher than those reported in previous studies (Jansen et al., 2001; Malloy et al., 2001); where replacing CA totally with plastic based aggregate (i.e. SLA) increased axial strain by 7-30%. The increase in strain capacity of the RP3F3C mixes is most likely due to the presence of

plastic in the RP3F3A matrix, which is consistent with those reported elsewhere (Frigione, 2010; Hannawi et al., 2010; Kashi et al., 1999).

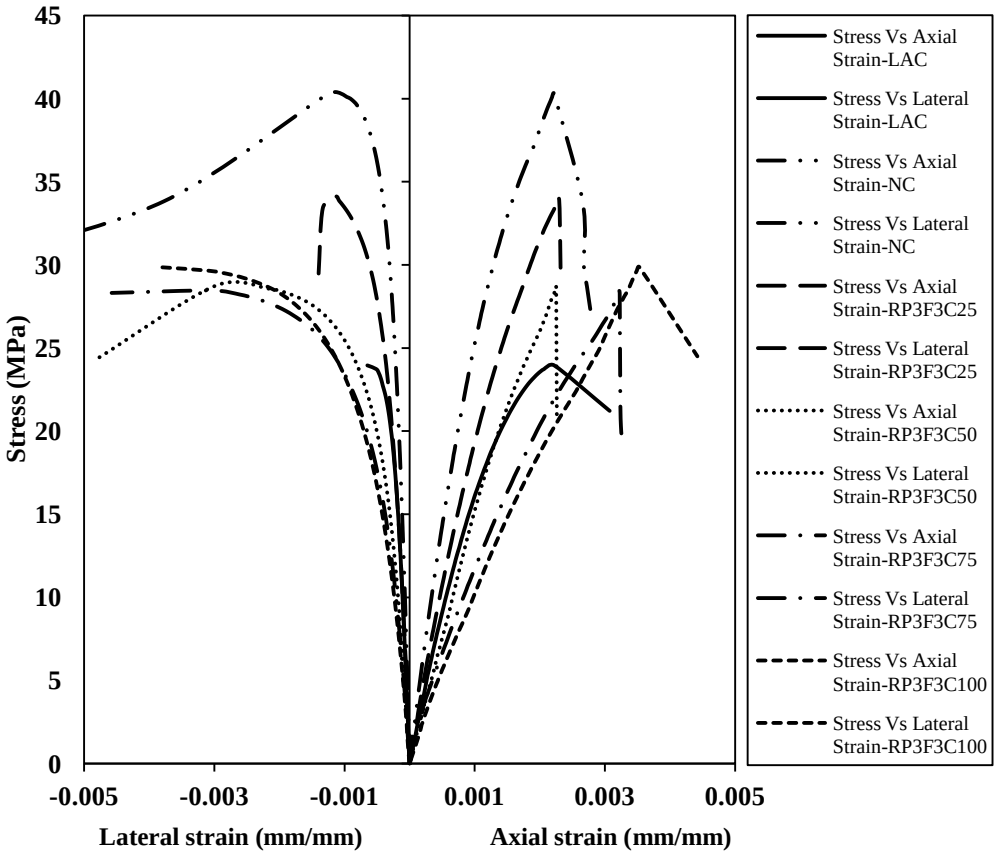


Figure 6.17: Stress-strain curves of RP3F3Cs, NC and LAC

In summary, the reduced brittleness and increased straining observed for RP2F1C and RP3F3C mixes respectively, is a unique feature not shared by conventional lightweight concrete. This feature would prove useful in applications where failure occurs due to repeated loads, e.g. pavements.

6.3.7 Poisson's ratio

The results of the Poisson's ratio of RP2F1C and RP3F3C mixes are respectively shown in Figures 6.18 and 6.19, in comparison with those of LAC and either LWC or NC.

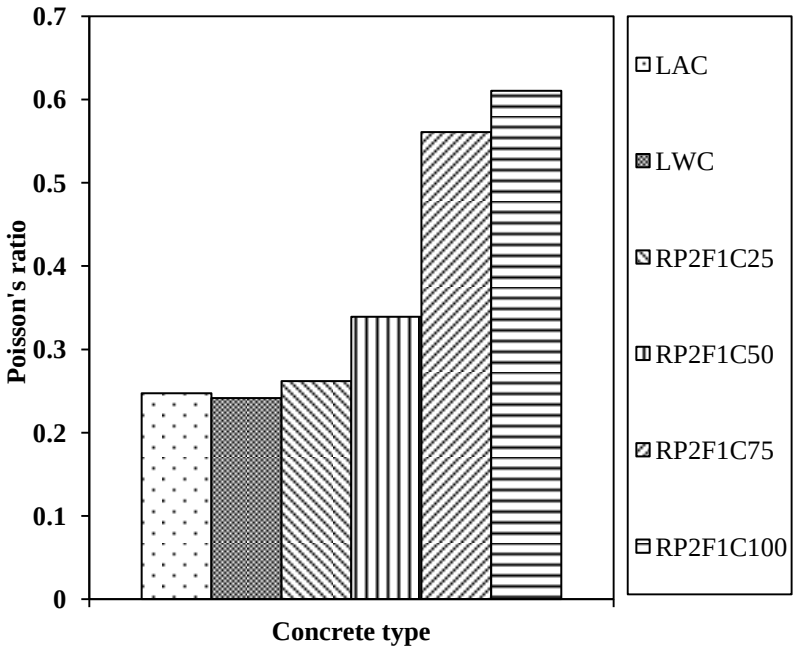


Figure 6.18: Results of 28-day Poisson's ratio of RP2F2Cs, LWC and LAC

As shown in Figure 6.18, there was an increase of 9-41% (0.02 to 0.1) in the Poisson's ratio of RP2F1C mixes compared with that of LWC, as the replacement level was increased from 25 to 50%. While, increasing the replacement level from 75 to 100% yielded an unreasonable increase of 134-154% (0.32 to 0.37), which might be related to an unexpected malfunction or looseness of strain gauges. Similarly, the increase in Poisson's ratio of the RP3F3Cs mixes (Fig. 6.19) compared with that of NC ranged from 12-56% (0.03 to 0.14) as the replacement level was increased from 25 to 100%. Additionally, RP2F1C100 and RP3F3C100 had a 144% (0.36) and 76% (0.17) higher Poisson's ratio than those of the LACs respectively.

The results of the Poisson's ratio of RP2F1C and RP3F3C are in broad agreement with the findings of Kou et al. (2009), observing an increase of 57% in the Poisson's ratio due to the increase in plastic particles' replacement from 0 to 45%. However, the percentage increase in the Poisson's ratio of RP2F1C and RP3F3C is higher than the findings of Jansen et al. (2001); who reported an increase in the Poisson's ratio ranging from 20 to 30% due to replacing CA totally with plastic based aggregate (i.e. SLA).

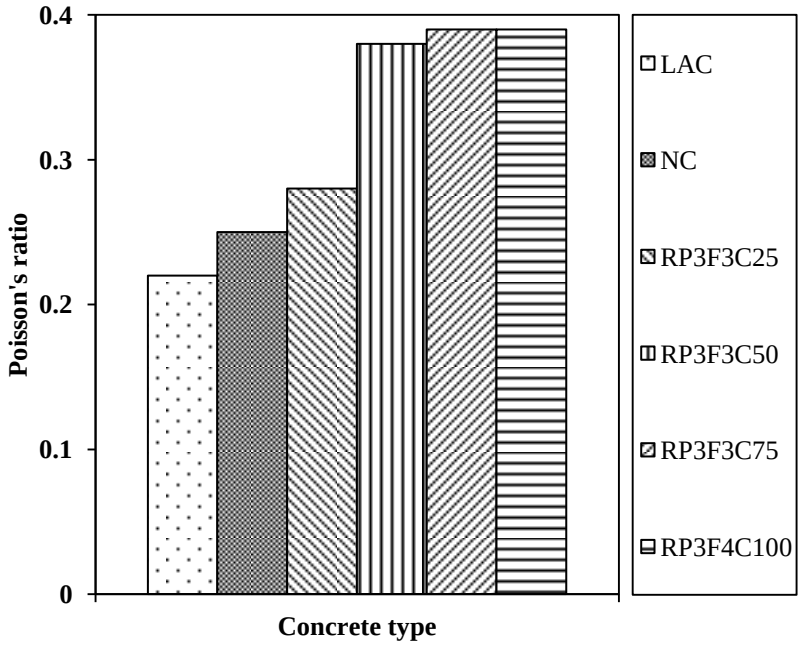


Figure 6.19: Results of 28-day Poisson's ratio of RP3F3Cs, NC and LAC

Overall, the increase in the Poisson's ratio of RP2F1Cs and RP3F3Cs is a strong identification for its ductile behaviour (i.e. gradual failure) which can be linked with the high plasticity or ductility of plastic that exists in the RP2F1A and RP3F3A matrix, as reported by Kou et al. (2009).

6.3.8 Abrasion resistance

Figures 6.20 and 6.21 present the results of the abrasion of RP2F1C and RP3F3C mixes compared with that of either LWC or NC. The LWC and NC had a mass loss of 1.03 and 0.4 gm, respectively. The mass loss of the RP2F1C and RP3F3C mixes ranged from 0.42 to 0.75 gm and from 0.60 to 0.67 gm, respectively.

As shown in Figure 6.20, the reduction in abrasion compared to that of LWC ranged from 29 to 58% (0.28 to 0.61 gm) as the substitution level of LWA with RP2F1A was increased from 25 to 100%. These results are in agreement with the findings of Ferreira et al. (2012) and Saikia and de Brito (2014) who reported an abrasion resistance increase of 28-42% as a result

of replacing 7.5-15% of CA and FA with plastic particles. The explanation of the reduction in abrasion of RP2F1C is consistent with that of Ferreira et al. (2012), which is ascribed to the increase in the resistance of its aggregate particles (i.e. RP2F1A) towards abrasion due to its plasticity nature together with its fibrous surface texture.

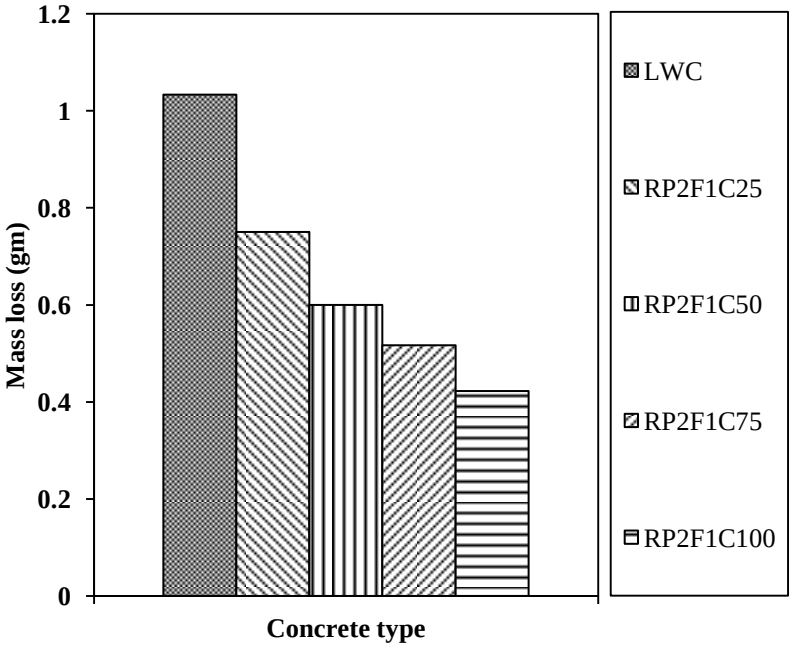


Figure 6.20: Results of mass loss at 6 min of abrasion of RP2F1Cs and LWC at 28 day

On the other hand, there was an increase in the abrasion of RP3F3C (Fig. 6.21) compared to that of NC ranging from 64-112% (0.2 to 0.27 gm), due to increasing the replacement level of NA with RP3F3A from 25 to 100%. This increase is due to the low strength and roughness of its aggregate particles (i.e. RP3F3A) (see section 4.4.1 and 4.4.8) compared to that of normal weight aggregate (i.e. NA), as observed by Kılıç et al. (2008) and Saikia and de Brito (2014).

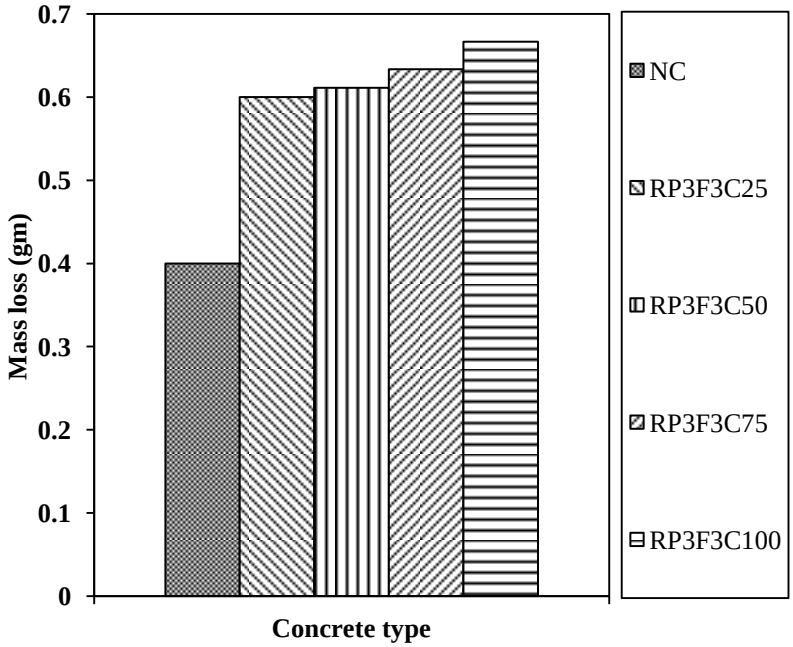


Figure 6.21: Results of mass loss at 6 min of abrasion of RP3F3Cs and NC at 28 day

Although, the abrasion resistance of the RP2F1C mixes increased as the replacement level also increased and vice versa for RP3F3C, the mass loss is comparable for these mixes regardless of the replacement level. Therefore, of these mixes, RP2F1C25 and RP3F3C100 yield a similar mass loss and satisfy the density and strength requirements of ASTM C330/C330M-14 (see Table 6.1). Overall, these two mixes have potential use in structural lightweight applications where high wearing resistance and mechanical performance are required, such as in pavements (Klieger, 1994).

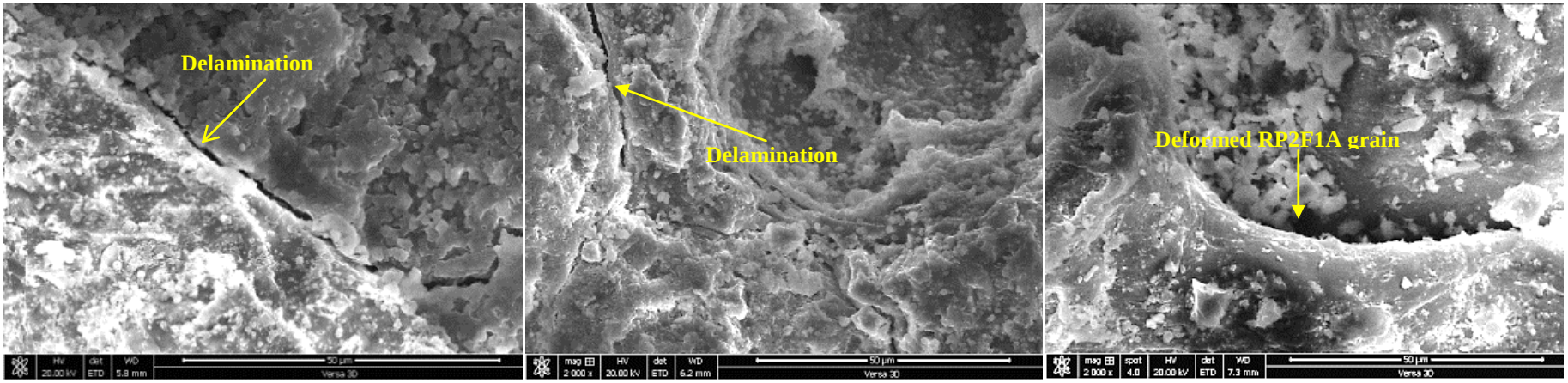
6.3.9 Microscopic investigation

A detailed analysis of the microstructure of LAC, LWC and RP2F1C100 was performed using SEM imaging and an optical microscope, as depicted in Figures 6.22 and 6.23 respectively.

As can be seen in Figure 6.22, the SEM images show delamination and a major crack formation (i.e. brittle failure) in the ITZ of LAC and LWC. However, in the case of

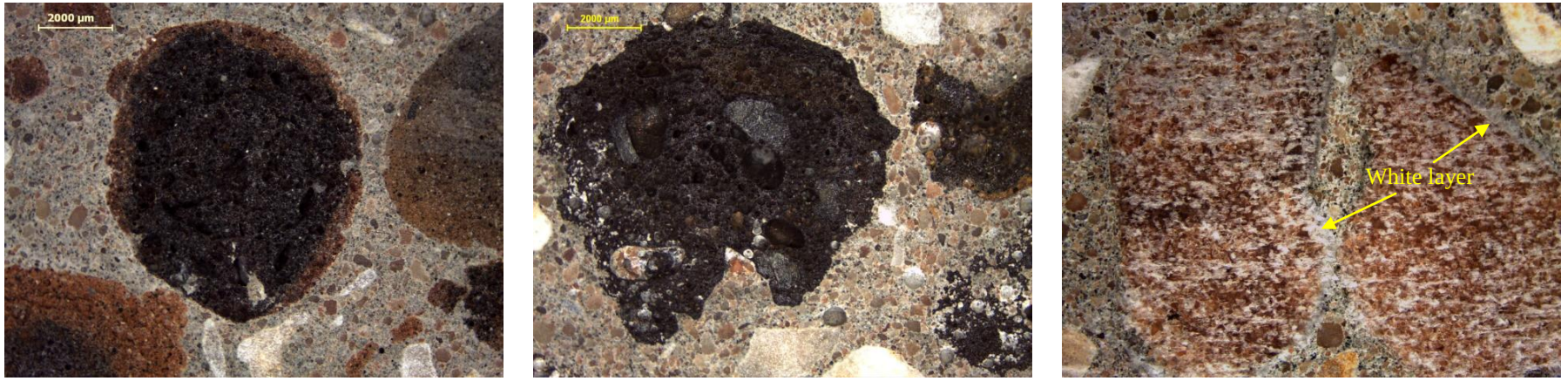
RP2F1C100, the mode of failure changed to ductile behaviour where any major crack formation disappears, due to the relatively high deformability of the RP2F1A particles compared with that of LYA and LWA. Therefore, during load application, stress transfer from the cement matrix to the RP2F1A particles, which have a low modulus of elasticity, results in the higher concentration of stress in the ITZ. This ultimately accelerates the failure occurrence due to weak bonding in the ITZ, which leads to the collapse of the RP2F1A composite (i.e. wider ITZ). This may explain the reason behind the strength deterioration of the RP2F1C mixes compared with that of LWC and LAC.

The microscopic images shown in Figure 6.23 indicate that the LWA and LYA have sharp joint angles/boundaries compared to those diffused boundaries observed in RP2F1A. Additionally, in the case of RP2F1C100, there is a thin white layer around the RP2F1A particles. This phenomenon can be explained by the fact that the impervious nature of RP2F1A hinders the water-cement reaction around the surface of the aggregate, which is consistent with the observation of Choi et al. (2005). This retained water creates a layer at this interface which ultimately prevents good bonding and can also be taken as another justification for the lower strength achieved by the RP2F1C mixes.



a b c

Figure 6.22: SEM images of (a) LAC, (b) LWC and (c) RP2F1C100 (28 days, enlargement: 2000×)



a b c

Figure 6.23: Optical microscopic images of (a) LAC, (b) LWC and (c) RP2F1C100 (28 days)

6.4 Correlation between mechanical properties

In this section, a predictive equation has been deduced using published experimental results. This, together with code equations, has also been used to predict the experimental results. Where possible, improved models have been proposed to predict the mechanical properties of the studied concrete mixes. The correlations developed were amongst compressive strength, splitting tensile strength, flexural strength and modulus of elasticity.

6.4.1 Correlation between splitting tensile strength and compressive strength

Experimental results from the extant literature (Albano et al., 2009; Choi et al., 2005; Juki et al., 2013; Rahmani et al., 2013) were used to examine the correlation between the 28-day splitting tensile strength (f_t) and the 28-day cylinder compressive strength (f_c). Figure 6.24 presents the variation of f_t with f_c for lightweight concrete containing plastic aggregate. Using regression analysis, the relationship between f_t and f_c may be expressed as follows.

$$f_t = 0.50(f_c)^{0.50} \qquad \text{(Eq. 6.1)}$$

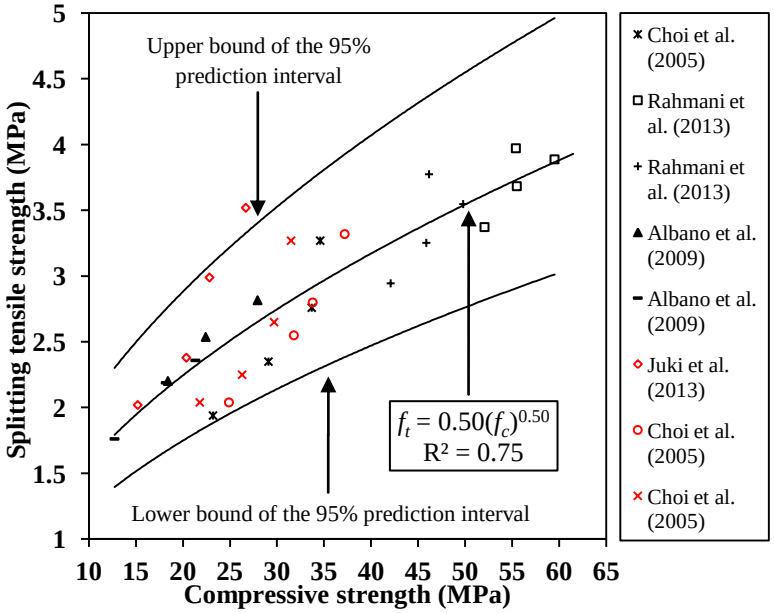


Figure 6.24: Correlation between splitting tensile strength and compressive strength

As can be seen in Figure 6.24, Equation 6.1 shows that f_t is a power function of f_c. This implies that the ratio of f_t to f_c decreases with increasing strength.

Figures 6.25 and 6.26 compare the predictions of Equation 6.1 as well as those of empirical models from the published literature, i.e. ACI 318-99 (Eq. 6.2) and Neville (1995) (Eq. 6.3), with the experimental results of splitting tensile strength of RP2F1C and RP3F3C mixes, respectively.

$$f_t = 0.56(f_c)^{0.50} \qquad \text{(Eq. 6.2)}$$

$$f_t = 0.23(f_c)^{0.67} \qquad \text{(Eq. 6.3)}$$

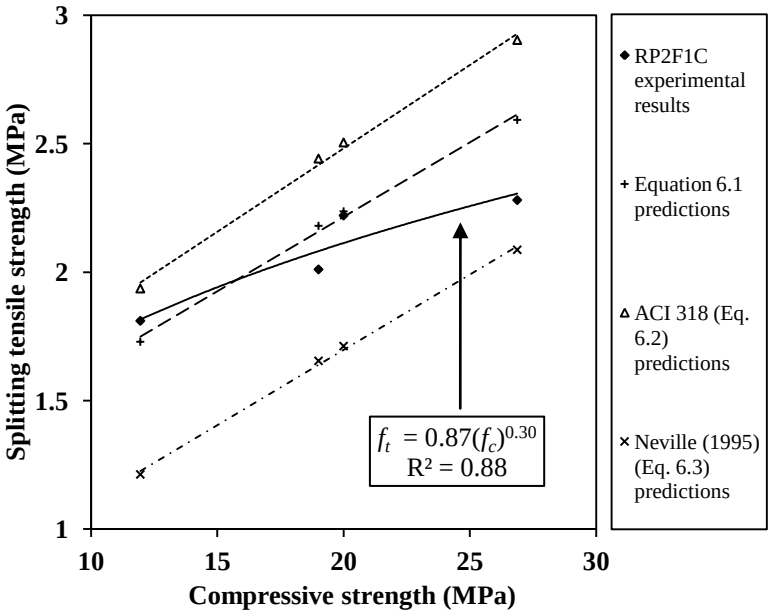


Figure 6.25: Comparison between the experimental results and the predictions of the analytical models relating splitting tensile strength to compressive strength of RP2F1C

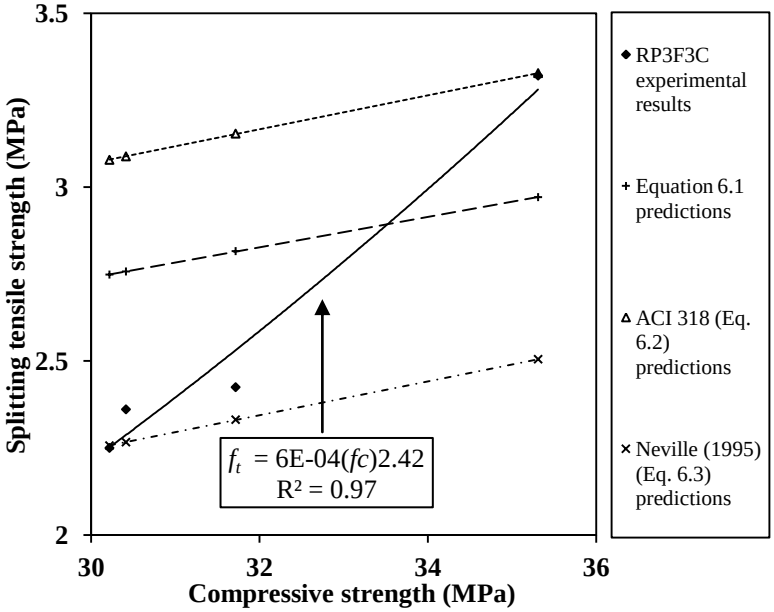


Figure 6.26: Comparison between the experimental results and the predictions of the analytical models relating splitting tensile strength to compressive strength of RP3F3C

As can be seen in Figures 6.25 and 6.26, the predication of Equation 6.1 is considered to be more accurate than those of the ACI 318-99 and Neville models. The ACI 318-99 empirical model overestimates the splitting tensile strength results of RP2F1C and RP3F3C by 7-27.3% and 0.2-36.8%, respectively. However, Neville's model underestimates the experimental results by 8.5-33% and 3.9-24.6% of RP2F1C and RP3F3C, respectively. This is not surprising given that, unlike Equation 6.1, ACI 318-99 and Neville's model were not developed specifically for lightweight concrete containing manufactured plastic aggregate. Figures 6.25 and 6.26 also show that the differences between the predictions of Equation 6.1 and the experimental results of RP2F1C and RP3F3C increase with increasing strength. This reflects the need for a more accurate model. Equations 6.4 and 6.5 are therefore proposed for predicting the splitting tensile strength of the RP2F1C and RP3F3C mixes, respectively.

$$f_t = 0.87(f_c)^{0.30} \qquad \text{(Eq. 6.4)}$$

$$f_t = 6\text{E-}04(f_c)^{2.42} \qquad \text{(Eq. 6.5)}$$

Table 6.2 presents the percentage difference between the predictions of Equations 6.1 to 6.5 and the experimental results. Table 6.2 clearly shows that Equations 6.4 and 6.5 provide excellent estimates, i.e. within ± 5% and ± 6.3 for the splitting tensile strength of the RP2F1C and RP3F3C mixes, respectively.

Table 6.2: Percentage difference in model predictions for the splitting tensile strength

Concrete type	Percentage difference between the predicted and experimental results				
	Eq. 6.1	Eq. 6.2	Eq. 6.3	Eq. 6.4	Eq. 6.5
RP2F1C25	13.7	27.3	-8.5	2.4	-
RP2F1C50	0.7	12.8	-22.9	-3.7	-
RP2F1C75	8.4	21.5	-17.7	4.7	-
RP2F1C100	-4.5	7.0	-33.0	-1.2	-
RP3F3C25	-10.5	0.2	-24.6	-	0.7
RP3F3C50	16.1	30.1	-3.9	-	6.3
RP3F3C75	16.8	30.8	-4.0	-	-1.4
RP3F3C100	22.2	36.8	0.3	-	1.9

6.4.2 Correlation between flexural strength and compressive strength

The experimental results of previous studies described in section 6.4.1 were also used to examine the relationship between the 28-day flexural strength (f_r) and f_c. Figure 6.27 shows the correlation between f_r and f_c for lightweight concrete containing plastic aggregate.

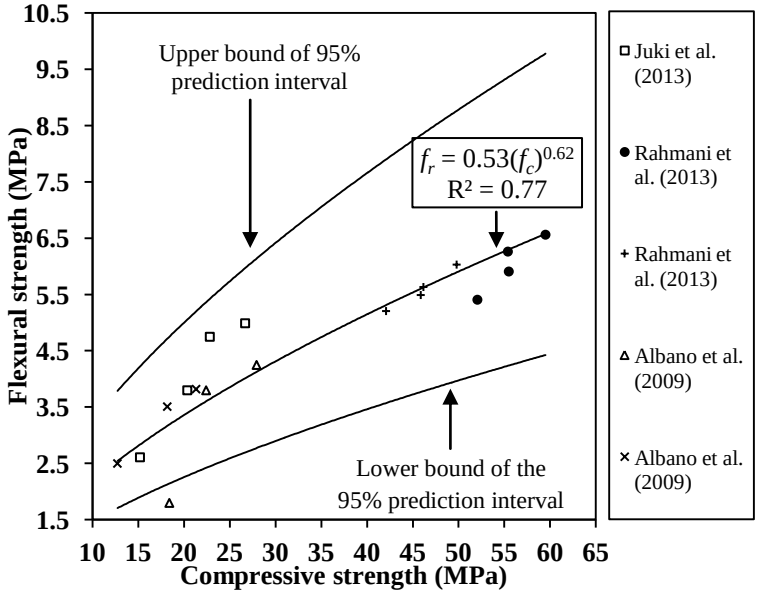


Figure 6.27: Correlation between flexural strength and compressive strength

Equation 6.6, which is based on regression analysis, gives the relationship between f_r and f_c.

$$f_r = 0.53(f_c)^{0.62} \qquad \text{(Eq. 6.6)}$$

Equation 6.6 as well as the empirical models proposed by ACI 318-95 (Eq. 6.7) and Raphael (1984) (Eq. 6.8) were used to predict the flexural strength of the RP2F1C and RP3F3C mixes.

$$f_r = 0.62(f_c)^{0.50} \qquad \text{(Eq. 6.7)}$$

$$f_r = 0.44(f_c)^{0.67} \qquad \text{(Eq. 6.8)}$$

As can be seen in Figures 6.28 and 6.29, both Equation 6.6 and Raphael's empirical models underestimate the flexural strength of the RP2F1C mixes by 6.8 to 13.1% for f_c values ranging from 19.0 to 26.9 MPa. In the same way, these models underestimate the flexural strength of RP3F3C mixes by 1.4 to 12.5% for f_c values ranging from 30.5 to 35.3 MPa. Furthermore, both models significantly underestimate the flexural strength of RP2F1C at f_c = 12.0 MPa, but insignificantly overestimate the flexural strength of RP3F3C mixes at f_c = 30.0 MPa. The ACI 318-95 empirical model significantly underestimates the flexural strength of RP2F1C and RP3F3C mixes, by 23.4 to 38.1% and 14.7 to 30.7%, respectively throughout the tested strength range. This was to be expected because, as explained previously, the ACI 318-95 empirical model was not developed specifically for lightweight concrete containing manufactured plastic aggregate.

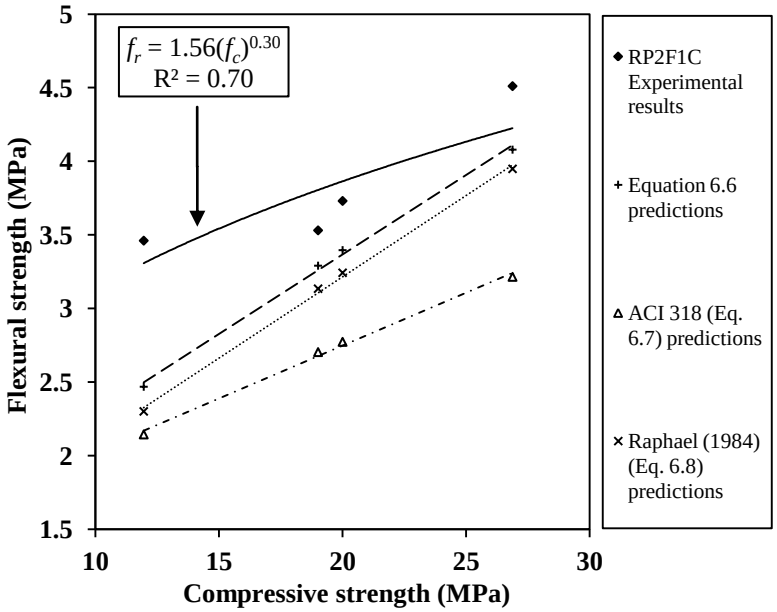


Figure 6.28: Comparison between the experimental results and the predictions of the analytical models relating flexural strength to compressive strength of RP2F1C

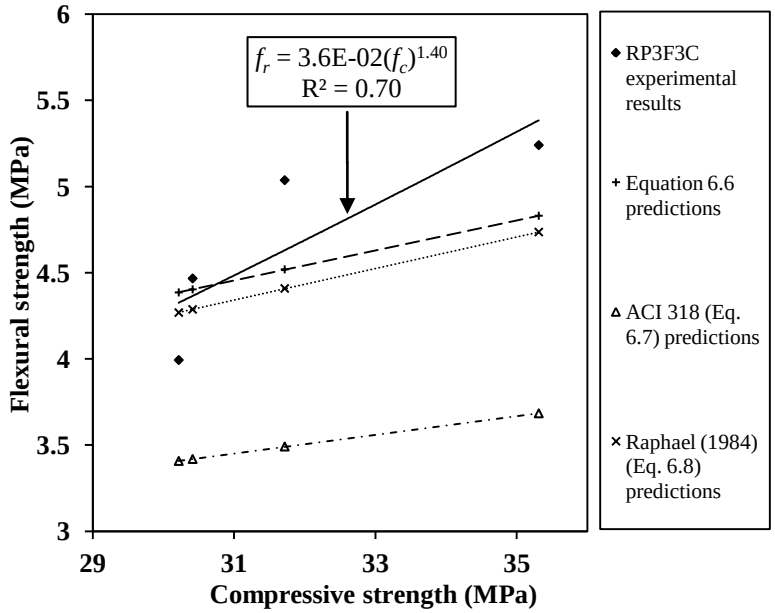


Figure 6.29: Comparison between the experimental results and the predictions of the analytical models relating flexural strength to compressive strength of RP3F3C

The results shown in Figures 6.28 and 6.29 demonstrate the need for improved models. Thus, Equations 6.9 and 6.10 are suggested for predicting the flexural strength of the RP2F1C and RP3F3C mixes, respectively.

$$f_r = 1.56(f_c)^{0.30} \quad \text{(Eq. 6.9)}$$

$$f_r = 3.6\text{E-}02(f_c)^{1.40} \quad \text{(Eq. 6.10)}$$

Table 6.3 compares the percentage difference between the predictions of Equations 6.6 to 6.10 and the experimental results. As can be seen in Table 6.3, Equations 6.9 and 6.10 give the best predictions, i.e. within ± 7.2 and ± 9.6%, for the flexural strength of the RP2F1C and RP3F3C mixes, respectively.

Table 6.3: Percentage difference in model predictions for the flexural strength

Concrete type	**Percentage difference between the predicted and experimental results**				
	Eq. 6.6	**Eq. 6.7**	**Eq. 6.8**	**Eq. 6.9**	**Eq. 6.10**
RP2F1C25	-9.6	-28.7	-12.5	-7.2	-
RP2F1C50	-9.0	-25.7	-13.1	2.7	-
RP2F1C75	-6.8	-23.4	-11.2	6.9	-
RP2F1C100	-28.7	-38.1	-33.5	-5.1	-
RP3F3C25	-7.8	-29.7	-9.6	-	0.9
RP3F3C50	-10.3	-30.7	-12.5	-	-9.6
RP3F3C75	-1.4	-23.5	-4.0	-	-3.9
RP3F3C100	9.8	-14.7	6.9	-	6.5

6.4.3 Correlation between modulus of elasticity and compressive strength

Similar to the cases of the splitting tensile strength and flexural strength, a relationship between the modulus of elasticity (E_c) and f_c was deduced using experimental results from the extant literature (Albano et al., 2009; Choi et al., 2005; Rahmani et al., 2013; Sabaa and Ravindrarajah, 1997). Figure 6.30 illustrates the variation between E_c and f_c for lightweight concrete containing plastic aggregate. Based on regression analysis, the relationship between E_c and f_c may be expressed as follows.

$$E_c = 2.50(f_c)^{0.64} \quad \text{(Eq. 6.11)}$$

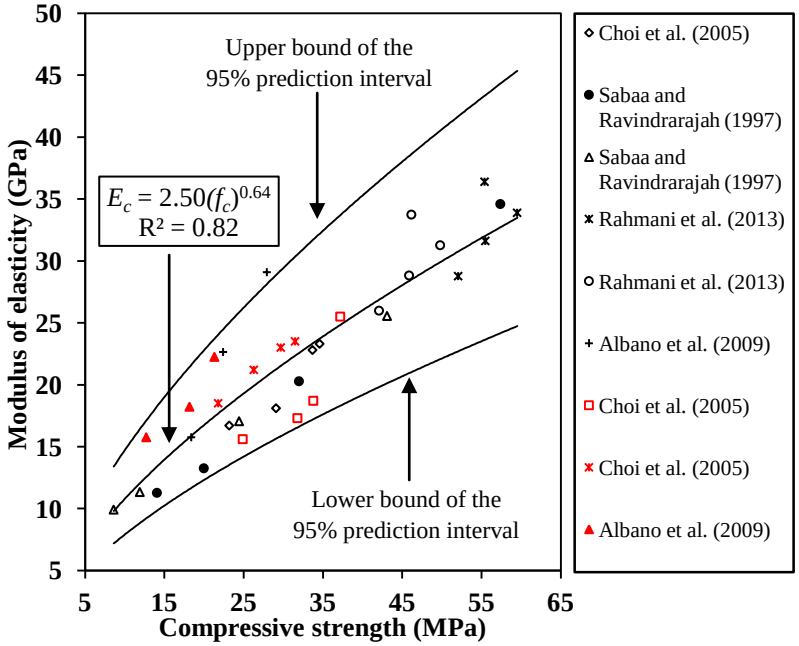


Figure 6.30: Correlation between elastic modulus and compressive strength

Equation 6.11 together with empirical models from the published literature; i.e. ACI 318-05 (Eq. 6.12) and Perry et al. (1991) (Eq. 6.13); were used to predict the elastic modulus of the manufactured plastic aggregate mixes (RP2F1C, RP3F3C).

$$E_c = (\gamma_w)^{1.5} \times (43 \times (10^{-6})) \times (f_c)^{0.50} \qquad \text{(Eq. 6.12)}$$

$$E_c = (\gamma_w)^{1.53} \times (7 \times (10^{-5})) \times (f_c)^{0.25} \qquad \text{(Eq. 6.13)}$$

In Equations 6.12 and 6.13, γ_w is the dry density of concrete in kg/m^3.

Figures 6.31 and 6.32 depict the comparison between the predictions of Equations 6.11 to 6.13 and the experimental results for the elastic modulus of the RP2F1C and RP3F3C mixes, respectively. All models overestimate the elastic modulus of the RP2F1C and RP3F3C mixes. The predictions of Equation 6.11 are 33.6 to 66.4% and 18.9 to 118% higher than the corresponding experimental results of the RP2F1C and RP3F3C, respectively. The remaining two models predicted the elastic modulus of RP2F1C25 and RP3F3C25 with an error ranging from -1 to 6% and from -0.6 to 16.5%, respectively. However, these two models

overestimated the elastic modulus of the remaining RP2F1C and RP3F3C mixes by 26.9 to 55.9% and 23.4 to 76.9%, respectively. Hence it can be concluded that none of the investigated models can be used to accurately predict the elastic modulus of the RP2F1C and RP3F3C concrete mixes.

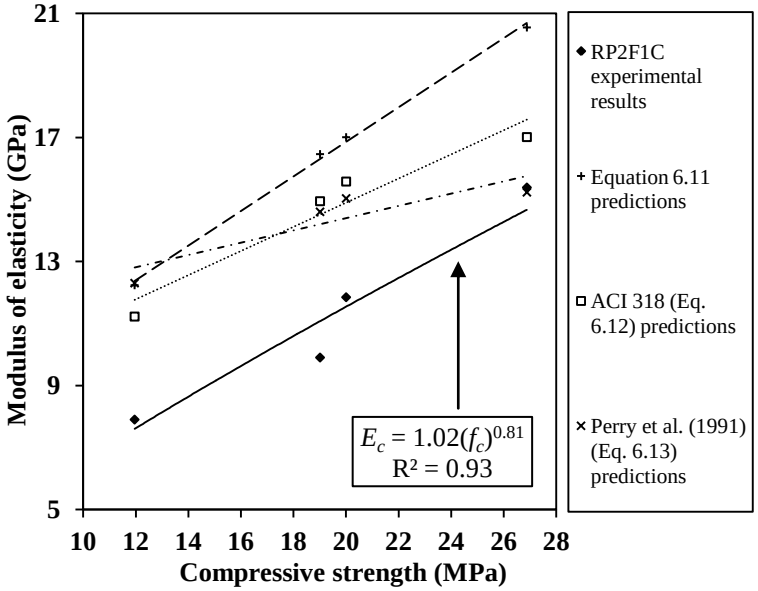


Figure 6.31: Comparison between the experimental results and the predictions of the analytical models relating elastic modulus to compressive strength of RP2F1C

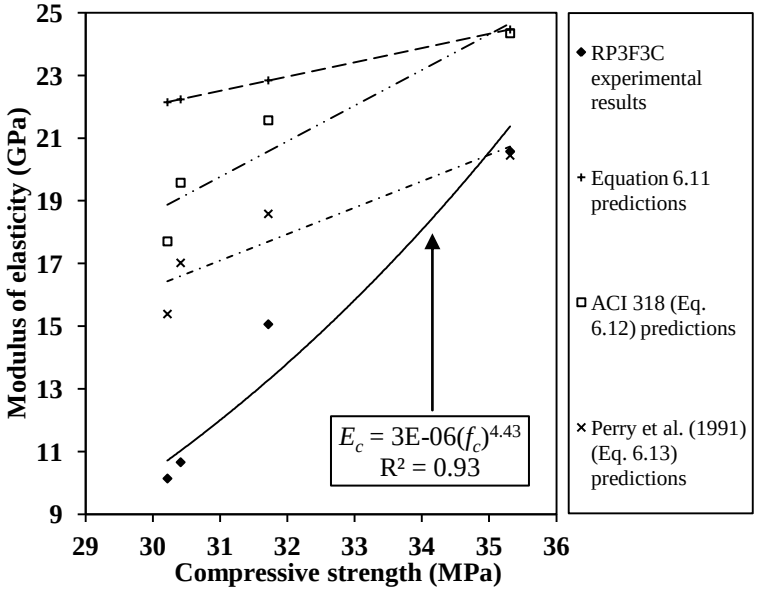


Figure 6.32: Comparison between the experimental results and the predictions of the analytical models relating elastic modulus to compressive strength of RP3F3C

As can be seen in Figures 6.31 and 6.32, regression analysis suggests that the elastic modulus of the RP2F1C and RP3F3C concrete mixes is best given by Equations 6.14 and 6.15, respectively.

$$E_c = 1.02(f_c)^{0.81} \quad \text{(Eq. 6.14)}$$

$$E_c = 3E\text{-}06(f_c)^{4.43} \quad \text{(Eq. 6.15)}$$

Table 6.4 gives the percentage difference between the predictions of Equations 6.11 to 6.15 and the experimental results. As can be seen in Table 6.4, Equations 6.14 and 6.15 yield the best predictions for the elastic modulus of the RP2F1C and RP3F3C concrete mixes with an error ranging from -4.6 to 11.9% and from -10.9 to 6.8%, respectively.

Table 6.4: Percentage difference in model predictions for the elastic modulus

Concrete type	**Percentage difference between the predicted and experimental results**				
	Eq. 6.11	**Eq. 6.12**	**Eq. 6.13**	**Eq. 6.14**	**Eq. 6.15**
RP2F1C25	33.6	6.0	-1.0	-4.6	-
RP2F1C50	43.6	35.2	26.9	-2.5	-
RP2F1C75	66.4	55.8	47.6	11.9	-
RP2F1C100	55	55.8	55.9	-3.6	-
RP3F3C25	18.9	16.5	-0.6	-	4.9
RP3F3C50	51.6	40.5	23.4	-	-10.9
RP3F3C75	108.6	76.9	59.7	-	4.5
RP3F3C100	118.4	63.0	51.7	-	6.8

6.5 Summary

This chapter examines the effect of RP2F1A and RP3F3A, a manufactured plastic aggregate, on the fresh and hardened properties of concrete. The manufactured plastic aggregates (i.e. RP2F1A, RP3F3A) were used as replacement for volcanic lightweight aggregate (LWA) and normal weight aggregate (NA) respectively, between 25-100% on a volumetric basis, at intervals of 25%. It was also used as a full replacement for Lytag aggregate (LYA).

The main findings indicate that there was a significant difference between the slump of manufactured plastic aggregate concrete mixes (i.e. RP2F1Cs, RP3F3Cs) and those of the control mixes (i.e. LWC, NC, LAC). Additionally, the mechanical properties of RP2F1C and RP3F3C mixes were significantly reduced as the replacement level was increased from 25 to 100%. However, RP2F1C and RP3F3C mixes had unique features (i.e. ductile behaviour) compared to the brittle failure observed for the control mixes. The RP2F1C25 (i.e. containing 25% of RP2F1A) and RP3F3C100 (i.e. containing 100% of RP3F3A) meet the requirements of ASTM C330/C330M-14 which confirm the potential of these mixes as lightweight structural mixes. Finally, this chapter presents predictive models for the mechanical properties of the RP2F1C and RP3F3C mixes; where these properties were successfully predicated using the proposed models.

CHAPTER 7: INVESTIGATION OF DURABILITY AND PHYSICAL PROPERTIES OF OPTIMIZED CONCRETE MIXES

7.1 General

As discussed earlier, in Chapter 5, two types of concrete (i.e. RP2F1C, RP3F3C) and their subsequent aggregates (i.e. RP2F1A and RP3F3A) were selected (see section 5.6). The effect of replacing these aggregates on the fresh and hardened properties at various replacement levels was investigated in Chapter 6. However, the influence of including these aggregates on the durability properties and thermal conductivity are described in this chapter; where the replacement levels vary between 25 and 100%. Additionally, the behaviour of RP2F1C and RP3F3C mixes under hot curing (i.e. curing temperature) was also examined.

The results of these tests were analysed and discussed following the same basis as described in Chapter 6. The key points covered in this chapter are listed below:

a) The effect of the replacement level on water absorption, chloride permeability and drying shrinkage of RP2F1C and RP3F3C mixes.
b) The effect on the creep performance of RP3F3C mixes.
c) The effect of implementing RP2F1A on the thermal conductivity of RP2F1C.
d) The influence of hot water curing on the strength performance of the RP2F1C and RP3F3C mixes.
e) Develop analytical correlations amongst durability properties or between mechanical and durability properties of the RP2F1C and RP3F3C mixes.

7.2 Durability related properties of RP2F1C and RP3F3C mixes

7.2.1 Water absorption

The durability or serviceability of concrete is influenced by its permeability or resistance level to chemical attack (ACI 201.2R-01; Zhang and Zong, 2014). Due to this significance, the water absorption of RP2F1C and RP3F3C mixes was measured and results are presented in Figures 7.1 and 7.2 respectively, in comparison with that of LAC and either LWC or NC.

As can be seen in Figure 7.1, LWC had a slightly (i.e. less than 5%) higher water absorption than RP2F1C25 and RP2F1C50 mixes; while, the water absorption of the RP2F1C mixes compared with that of LWC decreased by 19 to 20% at higher replacement levels (i.e. 75 and 100%). These results clearly show that the water absorption of RP2F1C mixes decreases with the increase in the replacement level of LWA with RP2F1A, due to the fact that the water absorption of aggregate (i.e. RP2F1A) is 85% lower than LWA (see section 4.4.5). This observation is consistent with the finding of Babu et al. (2006) who reported water absorption reduction of EPS concrete due to the non-absorbent nature of plastic particles.

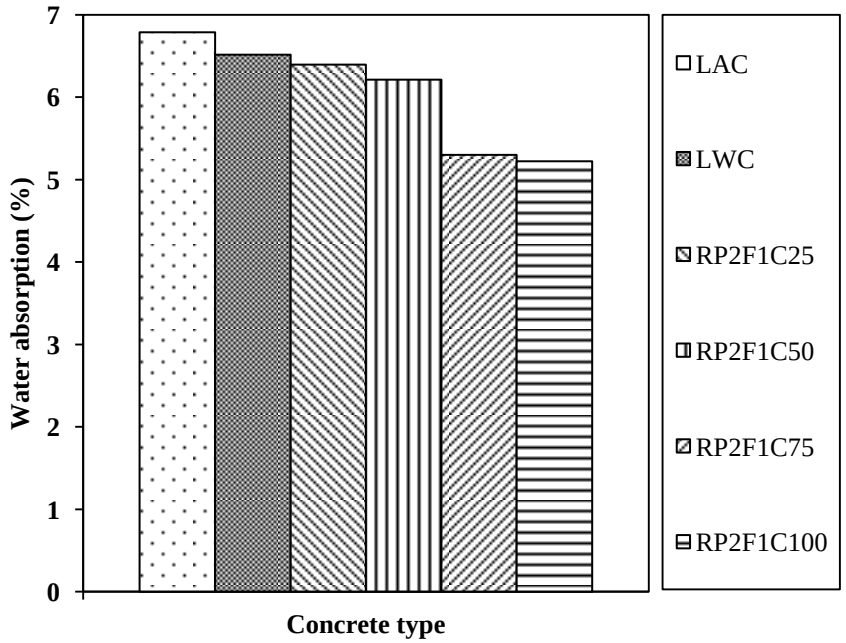


Figure 7.1: Results of 28-day water absorption of RP2F1Cs, LWC and LAC

On the other hand, there was a marginal difference (i.e. less than 3%) between the water absorption of NC and RP3F3C25; whereas, NC had 16 to 21% lower water absorption than the remaining RP3F3C mixes, as shown in Figure 7.2. Nonetheless, the increase in the water absorption of the RP3F3C mixes is still lower than that reported in previous studies (Babu et al., 2006; Saikia and Brito, 2013; Wong, 2010); where replacing 15% and 50 to 80% of CA and both aggregates (CA and FA) with plastic particles increased water absorption by 33% and 55 to 98%, respectively.

This increase in the water absorption of RP3F3C is most likely related to the decrease in the packing level of the mix due to the poorer grading of RP3F3A compared with that of NA, as reported earlier (see section 4.4.2).

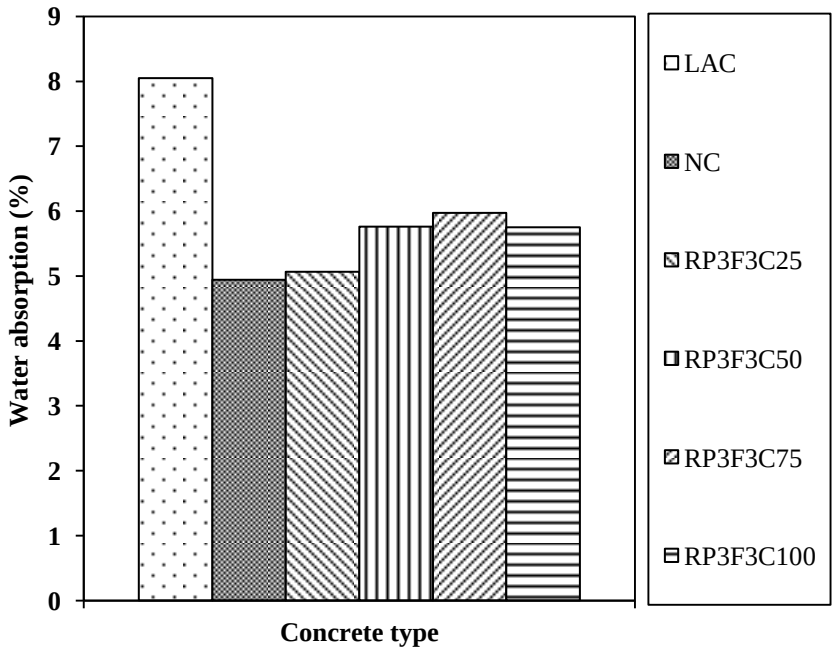


Figure 7.2: Results of 28-day water absorption of RP3F3Cs, NC and LAC

Moreover, RP2F1C100 and RP3F3C100 had a 28-day water absorption that was 23% and 28% less than that of LAC respectively, where all made with 100% manufactured lightweight CA. The high water absorption observed for LAC is related to the high water absorption of its

aggregate (i.e. LYA) which is about 84 and 94% higher compared with that of RP2F1A and RP3F3A, respectively.

Overall, the present study results confirm that RP2F1C and RP3F3C mixes can be produced with up to 100% replacement of LYA and either LWA or NA with relatively low water absorption. However, of these mixes, only RP2F1C25 and RP3F3C100 meet the mechanical requirements (see Table 6.1), as described in Chapter 6. Therefore, these two mixes could potentially be used in structural lightweight applications where relatively low water absorption and moderate strength are required.

7.2.2 Chloride permeability

Figures 7.3 and 7.4 present the results of the chloride permeability of the RP2F1C and RP3F3C mixes respectively, in comparison with that of LAC and either LWC or NC.

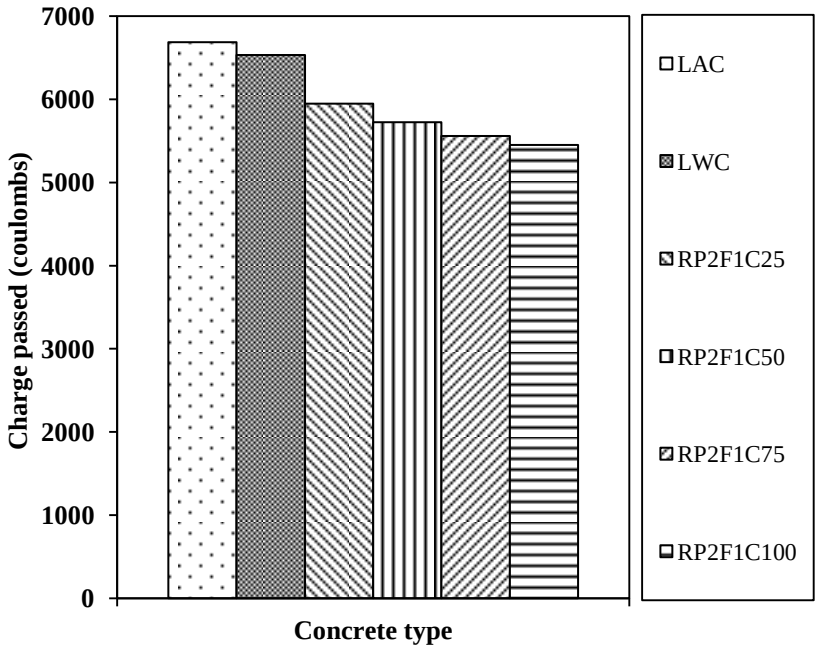


Figure 7.3: Results of 28-day chloride permeability of RP2F1Cs, LWC and LAC

As can be seen in Figure 7.3, the reduction in 28-day chloride permeability of RP2F1C mixes compared with that of LWC ranged from 9 to 17% (584-1080 coulombs) as the replacement

level of LWA with RP2F1A was increased from 25 to 100%. Similarly, as shown in Figure 7.4, the decrease in the 28-day chloride permeability of the RP3F3C mixes compared with that of NC ranged from 23 to 68% (1346-3991 coulombs), as the substitution percentage of NA with RP3F3A was increased from 25 to 100%. The explanation for these reductions is in agreement with Kou et al. (2009), which is related to the lowered ion conductivity and impervious nature of the plastic that exists in the RP2F1A and RP3F3A matrix. Consequently, the passage for ion transfer is disrupted and thereby, chloride ion penetration is reduced.

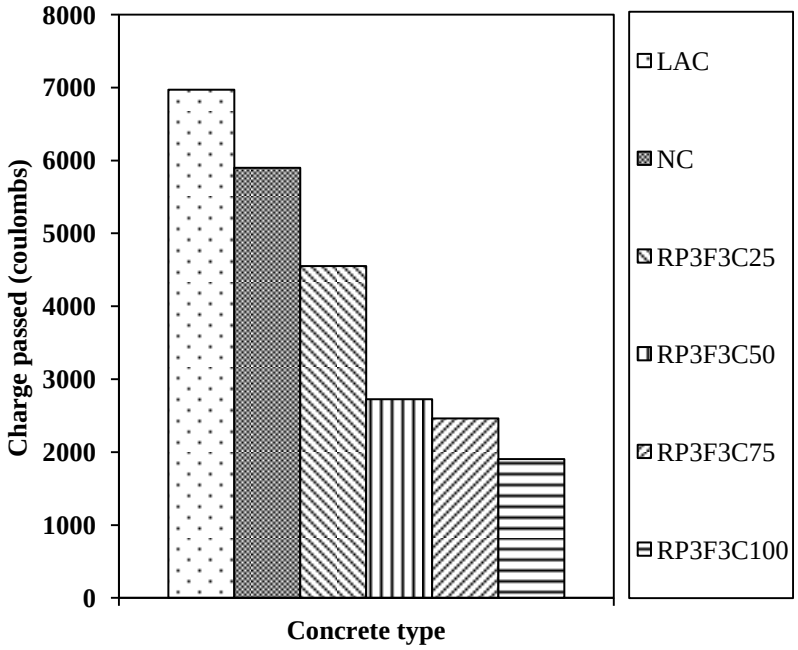


Figure 7.4: Results of 28-day chloride permeability of RP3F3Cs, NC and LAC

Additionally, RP2F1C100 and RP3F3C100 had a 28-day chloride permeability that was 18% (1236 coulombs) and 73% (5062 coulombs) less than that of LAC, respectively; where all contained 100% manufactured lightweight CA. The high chloride permeability observed for LAC may be attributed to the high water absorption of its concrete and subsequent aggregate (i.e. LYA) (see section 7.2.1).

The results of the RP2F1C mixes are in line with the findings of Babu and Babu (2003) and Kou et al. (2009),who reported chloride permeability reductions of 43 and 36% as a result of

substituting 37 and 45% of total aggregates (CA, FA) and FA with plastic particles, respectively. However, the RP3F3C mixes exhibited a higher reduction in the chloride permeability compared with those of either RP2F1C or previous studies (Babu and Babu, 2003; Kou et al., 2009).

The RP2F1C and RP3F3C mixes had a charge passed higher than 2000 coulombs except for the RP3F3C100. Thus, these mixes are classified into medium to high penetrability concrete as specified in the ASTM C1202-12, except for RP3F3C100 which achieved low penetrability.

In summary, RP2F1C25 could be used in structural lightweight applications that have a low exposure level of chloride. However, these results further confirm the potential of RP3F3C100 as a durable lightweight concrete that can be used in structural applications where a high chloride level exists, as it meets both the requirements of chloride permeability (see ASTM C1202-12) and the mechanical properties reported in Chapter 6 (see Table 6.1).

7.2.3 Drying shrinkage

The results of the drying shrinkage of the RP2F1C and RP3F3C mixes made at 50 and 100% replacement levels of LWA and NA with RP2F1A and RP3F3A respectively, are shown in Figures 7.5 and 7.6, in comparison with those of LAC and either LWC or NC.

Figure 7.5 depicts that initially at 7 days (i.e. underwater curing), the maximum expansion was seen with LAC (i.e. 100 % LYA) followed by LWC; while the least was attained by RP2F1C50. However, RP3F3C100 and LAC achieved the highest and lowest expansion at 7 days of underwater curing respectively, amongst the mixes shown in Figure 7.6.

Then, under a drying shrinkage condition, where the samples were removed from the underwater curing and air cured, the length reduction or shrinkage can be divided into two stages due to the rate of the drying shrinkage development. The first stage begins from the 7 days of air curing until about the 49th day; followed by the second stage, which lasts to about 182 days. As can be seen in Figures 7.5 and 7.6, the increment rate in microstrain (μstrain) values obtained in the second stage is about half of those obtained in the first stage.

The increase in the drying shrinkage of the RP2F1C mixes (Fig. 7.5) compared with that of LWC ranged from 36 to 58% (190-302 μstrain), from 17 to 46% (137-363 μstrain) and from 19 to 54% (158-434 μstrain) at 28, 91 and 182 days of air curing respectively, as the replacement level was increased from 50 to 100%.

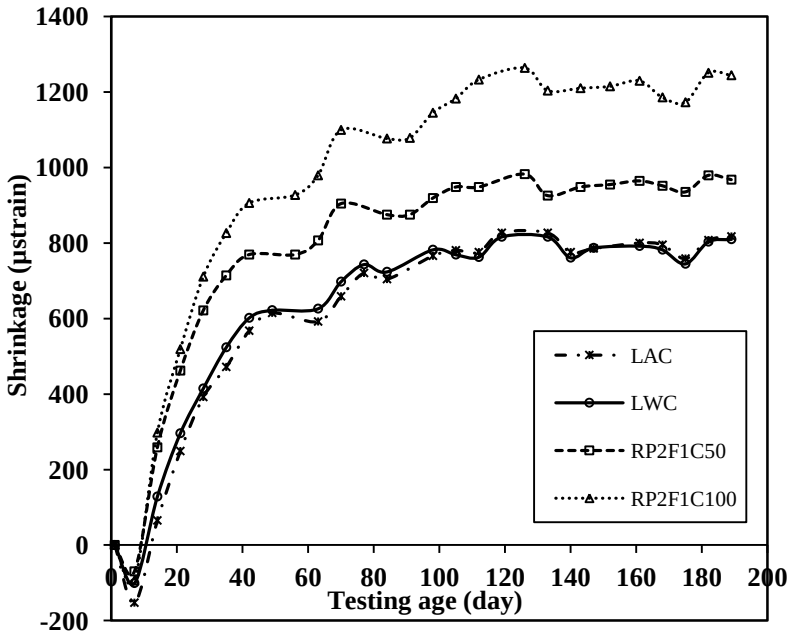


Figure 7.5: Results of drying shrinkage of RP2F1Cs, LWC and LAC

Similarly, the increase in the drying shrinkage of the RP3F3C mixes (Fig. 7.6) compared with that of the NC ranged from 26 to 29% (93-104 μstrain), from 37 to 65% (210-369 μstrain) and from 39 to 72% (259-474 μstrain) at 28, 91 and 182 days of air curing respectively, as the replacement level was increased from 50 to 100%.

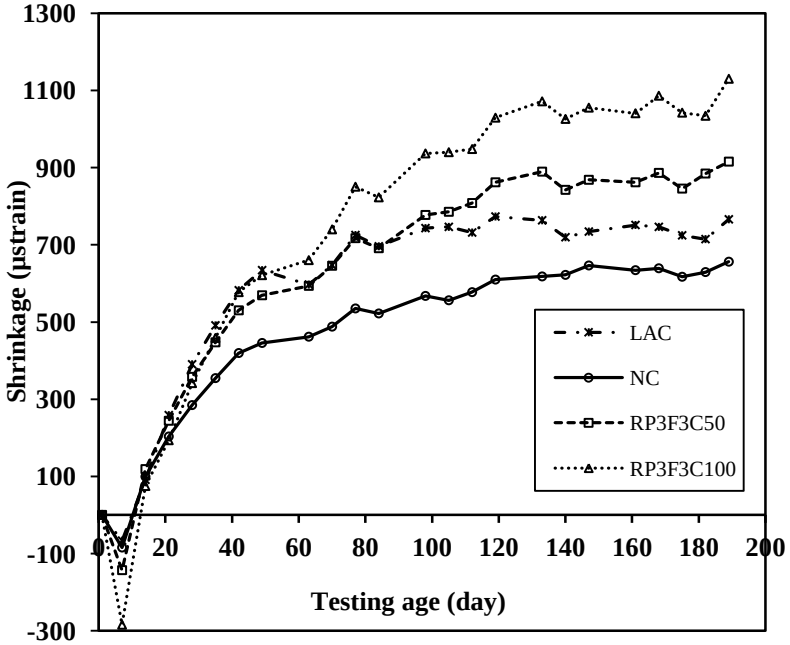


Figure 7.6: Results of drying shrinkage of RP3F3Cs, NC and LAC

Additionally, RP2F1C100 had drying shrinkage that was 75% (354 µstrain), 49% (379 µstrain) and 52% (427 µstrain) higher than that of LAC at 28, 91 and 182 days of air curing respectively. However, RP3F3C100 and LAC had drying shrinkage results that differed by -7 to 47% (-33 to 364 µstrain) at the same period of curing.

The amount of drying shrinkage is normally controlled by water loss (Kwan et al., 2012). However, as only the matrix loses the water, thus the increase in drying shrinkage of RP2F1C and RP3F3C, as compared to the reference mixes, is due to the fact that the elastic modulus of manufactured aggregates (i.e. RP2F1A, RP3F3A) is lower than that of reference aggregates (i.e. LWA, NA, LYA). Therefore, during shrinkage (i.e. change in the length), the manufactured aggregate exhibited low resistance against concrete shrinkage, as reported by (Dhir and Paine, 2007; Silva et al., 2015).

The increase in the drying shrinkage of the RP2F1C and RP3F3C mixes can also be attributed to the low water absorption of its aggregates (i.e. RP2F1A, RP3F3A), which does not

compensate for the water loss from the cement matrix. In contrast, the decrease in the drying shrinkage of LWC and LAC is accounted for by the high absorption of LWA and LYA. Therefore, the water loss from the cement matrix is compensated by the absorbed water released from its aggregates.

Nonetheless, the increase in drying shrinkage of the RP2F1C and RP3F3C mixes is still lower than that reported elsewhere (Chen and Liu, 2004; Fraj et al., 2010); where replacing 45 and 55% of CA and both aggregates (CA, FA) with plastic particles increased the 28 and 90 day drying shrinkage by 149 and 78%, respectively. Furthermore, the drying shrinkage achieved by the RP2F1C and RP3F3C mixes is in agreement with that reported by Hyodo et al. (2013) and Khairallah (2009) for normal weight concrete; where drying shrinkage of 800 to 1000 μstrain was observed at different drying periods (119 to 182 days).

Overall, the drying shrinkage given by the RP2F1C and RP3F3C mixes becomes acceptable with respect to the application of these types of concrete when compared to the normal concrete performance.

7.2.4 Creep

The effect of manufactured plastic aggregate on the creep performance was conducted on selective samples (i.e. RP3F3C mixes) based on their performance in compressive strength. The study of creep for the RP2F1C mixes may be undertaken in a future study. The effect of manufactured aggregate (i.e. RP3F3A) on the time dependent strain is shown in Figures 7.7 to 7.9.

Figures 7.7 to 7.9 depict a rapid increase in the strain immediately after applying load; while, the rate was gradually reduced as the loading age was increased. Figure 7.9 shows that the instantaneous strain of the RP3F3C mixes was significantly higher (i.e. 7 to 100%, 53-734

μstrain) than that of the NC, except for RP3F3C25 which was marginally lower by 9%. Similarly, the increase in the ultimate shrinkage strain of the RP3F3C mixes compared with that of the NC ranged from 28 to 119% (146.7-627.3 μstrain) as the replacement level was increased from 25 to 100%, as shown in Figure 7.8.

Additionally, there was an increase in the ultimate creep strain (see Fig. 7.9) of RP3F3C mixes compared with that of the NC ranging from 3 to 69% (55.2-1681.7 μstrain) as the replacement level was increased from 50 to 100%. However, the RP3F3C mixes made at a replacement level of 25% and NC had ultimate creep strain results that differed marginally by less than 4%.

Generally, creep of concrete behaviour is influenced by the type of aggregate, cement paste, modulus of elasticity and the ITZ between the aggregate and the cement paste (Mehta and Monteiro, 2006). Thus, the increase of creep of the RP3F3C mixes can be attributed to the reduction in the mechanical properties of both the aggregate (i.e. RP3F3A) and subsequent concrete (see sections 6.3.2, 6.3.5). This ultimately would decrease the resistance of the entire composite towards the creep tendency (Mehta and Monteiro, 2006; Sabaa and Ravindrarajah, 1997).

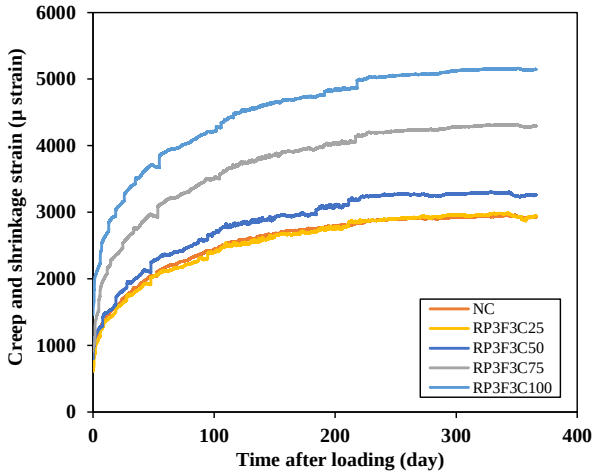


Figure 7.7: Results of time dependent strain for loaded specimens of RP3F3Cs and NC

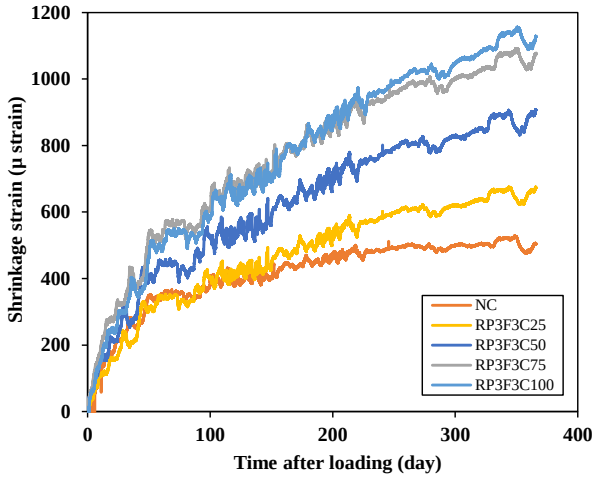


Figure 7.8: Results of shrinkage strain for unloaded specimens of RP3F3Cs and NC

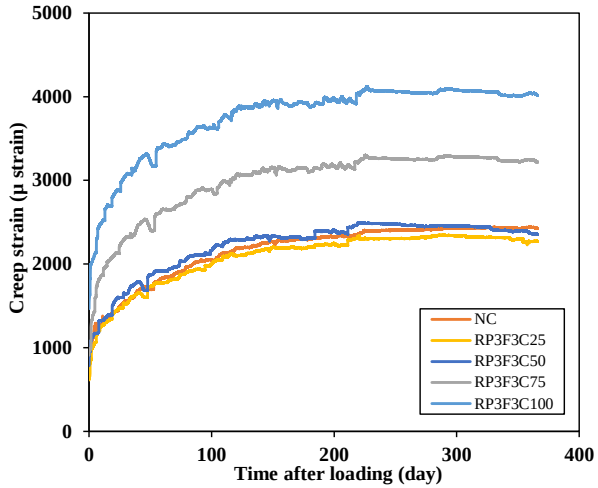


Figure 7.9: Results of creep strain of RP3F3Cs and NC

7.3 Physical properties of RP2F1C and RP3F3C mixes

7.3.1 Thermal conductivity

Thermal conductivity measures the ability of material to transfer heat. Therefore, a material with low thermal conductivity can provide high insulation.

The effect of the manufactured plastic aggregate on the thermal conductivity was only performed for the RP2F1C100 mix due to the shortage in the quantity of the manufactured aggregate. Therefore, the effect of replacing 100 % of LWA with RP2F1A on 28-day thermal conductivity at a saturated and dry condition is presented in Figure 7.10.

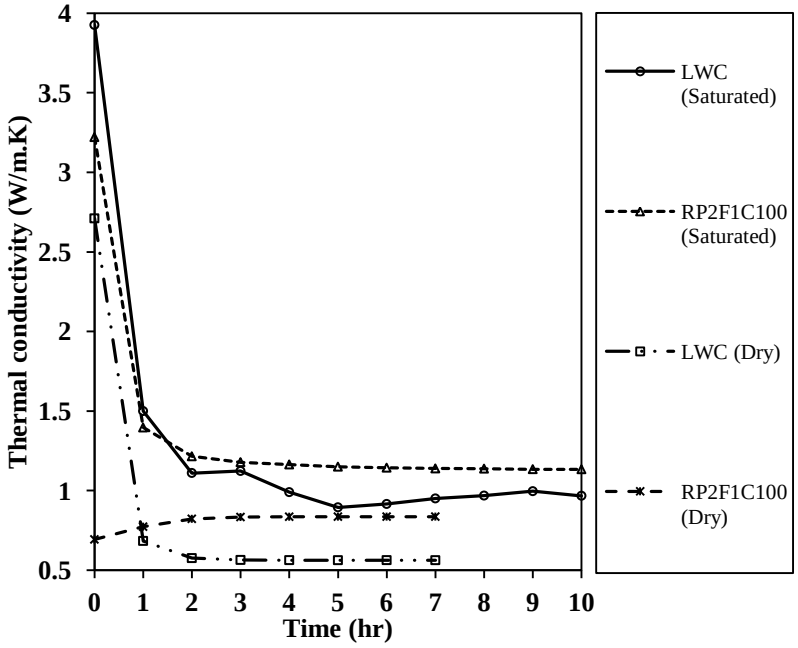


Figure 7.10: Results of 28-day thermal conductivity of RP2F1C100 and LWC in saturated and dry conditions

As it can be seen in Figure 7.10, at the initial time (i.e. 0 hr) thermal conductivity of RP2F1C and LWC mixes is almost 2 to 4 times higher than that measured at later periods (i.e. 7 to 10 hr) except for RP2F1C100 (Dry) which had a marginal difference (i.e. 0.8%).

Additionally, RP2F1C100 had 17% (0.14 W/m.K) and 49% (0.27 W/m.K) higher ultimate thermal conductivity than LWC at the saturated and dry conditions, respectively. Nonetheless, the thermal conductivity of RP2F1C100 are either within or lower than those values reported elsewhere; where manufactured lightweight concrete (i.e. Lytag concrete) or normal weight concrete (i.e. density $\geq$ 2300 kg/m^3) yield a thermal conductivity of 0.80 and 1.63 W/m.K, respectively. The low thermal conductivity of LWC is most likely related to the porous structure of its aggregate (i.e. LWA) together with the existence of entrapped air in its voids, as observed by Al-Jabri et al. (2005).

Moreover, the ultimate thermal conductivity of LWC and RP2F1C100 in a saturated condition was 72 and 36% higher compared with that measured in a dry condition respectively, as shown in Figure 7.10. This was expected because the decrease in moisture of the sample reduces its conductivity; which is in agreement with the findings of Khan (2002), who observed an increase of 70% in thermal conductivity of saturated samples compared with those of dry samples.

Overall, these results suggest that RP2F1C could potentially be used in lightweight applications where low density and high insulation features are required. This yields a novel lightweight concrete with an enhanced insulation property which ultimately would reduce the cost and energy associated with heating and cooling activities.

7.3.2 Curing temperature

The effect of curing temperature (up to 40 °C) on the 28-day compressive strength of RP2F1C and RP3F3C mixes is shown in Figure 7.11, together with results of control mixes (i.e. LWC, NC).

Figure 7.11 indicates that the 28-day compressive strength decreases with increases in the water curing temperature. For instance, the increase in curing temperature from 20 to 30 °C and from 20 to 40 °C reduced the 28-day compressive strength of the RP2F1C mixes by 2 to 8% and 9 to 17% respectively; in comparison with 7 and 13% for the LWC at the same temperatures levels. Similarly, the decrease in compressive strength of the RP3F3C mixes at 30 °C and 40 °C compared with those at 20 °C ranged from 3 to 10% and from 7 to 19% respectively; while, NC had compressive strength results that differed by less than 10% at the same temperature levels.

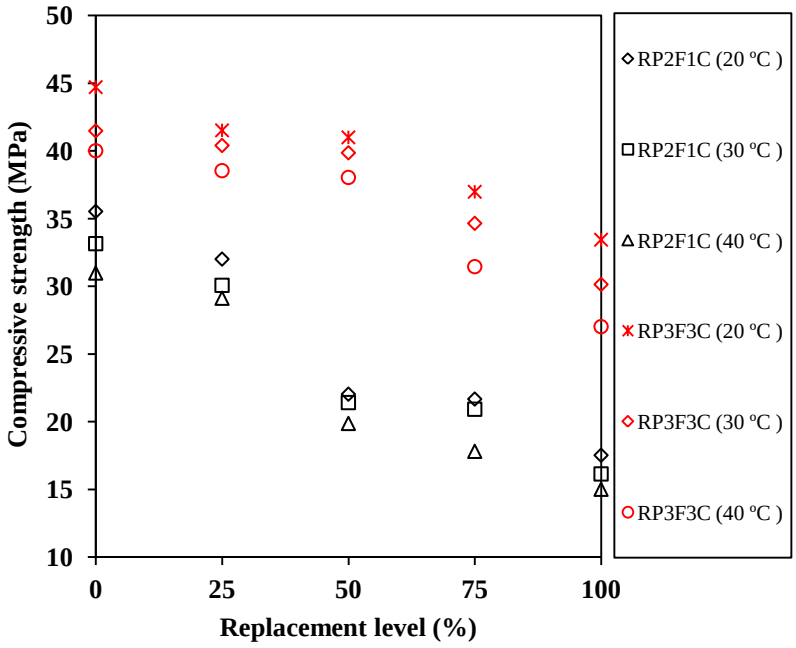


Figure 7.11: Results of 28-day compressive strength of RP2F1Cs, RP3F3Cs, LWC and NC at curing temperatures of 20, 30 and 40 °C

This decrease can be explained by the fact that the increase in curing temperature accelerates the strength gained at the early curing period (i.e. up to 7 days), which ultimately leads to a poorer microstructure containing large pores. This observation is consistent with those reported elsewhere (Ferreira et al., 2012; Silva et al., 2013; Verbeck and Helmuth, 1968). In summary, the present study's results confirm that RP2F1C and RP3F3C can be cured at temperatures up to 30 °C, without significantly affecting compressive strength.

7.4 Correlation of durability properties

7.4.1 Correlation between chloride permeability and compressive strength

The experimental results of the RP2F1C and RP3F3C mixes presented in Figure 7.12, were used to explore the correlation between the charge passed (y) and the cylinder compressive strength (f_c) at 28 days. Results of Kou et al.'s (2009) study were also used to develop a correlation for the sake of comparison (see Fig. 7.12).

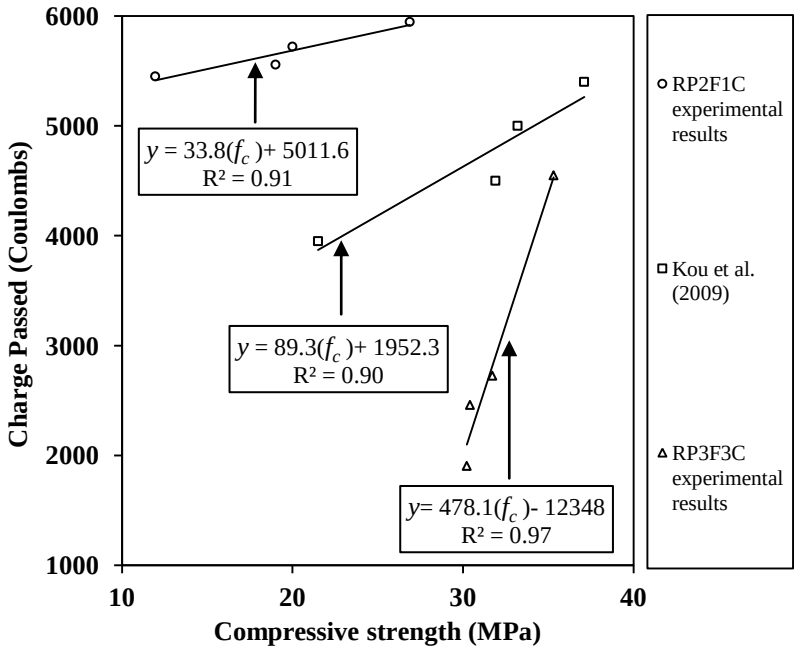


Figure 7.12: Correlation between 28-day chloride permeability and compressive strength

The correlation between y and f_c can be expressed in Eq.7.1, Eq.7.2 and Eq. 7.3 for RP2F1C, RP3F3C and Kou's study respectively, as follows:

$$y = 33.8(f_c) + 5011.6 \quad \text{(Eq. 7.1)}$$

$$y = 478.1(f_c) - 12348 \quad \text{(Eq. 7.2)}$$

$$y = 89.3(f_c) + 1952.3 \quad \text{(Eq. 7.3)}$$

These correlations indicate that the chloride permeability had a proportional relationship with compressive strength, since both decreased as the replacement level was increased (see sections 6.3.2 and 7.2.2).

Table 7.1 presents the percentage difference between the predictions of Equations 7.1 to 7.3 and the experimental results. As shown in Table 7.1, Equation 7.1 exhibits good estimates, i.e. within ± 1.7% for the chloride permeability of the RP2F1C mixes. Similarly, Equation 7.2 yields a good prediction of the chloride permeability of the RP3F3C mixes with an error ranging from -10.9 to 3.4% for f_c values ranging from 30.4 to 35.3 MPa; while the same equation overestimates the chloride permeability for RP3F3C at 100% only.

On the other hand, Kou's model substantially underestimates and overestimates the chloride permeability of the RP2F1C and RP3F3C mixes by 26.8 to 44.6% and 12.2 to 144.3%, respectively. This can be attributed to the difference in the experimental conditions, including all parameters of mixes.

Table 7.1: Percentage difference in model predictions for the chloride permeability

Concrete type	**Percentage difference between the predicted and experimental results**		
	Eq. 7.1	**Eq. 7.2**	**Eq. 7.3**
RP2F1C25	-0.4	-	-26.8
RP2F1C50	-0.6	-	-34.7
RP2F1C75	-1.7	-	-34.3
RP2F1C100	-0.6	-	-44.6
RP3F3C25	-	-0.3	12.2
RP3F3C50	-	3.4	75.6
RP3F3C75	-	-10.9	89.8
RP3F3C100	-	19.1	144.3

7.4.2 Correlation between creep coefficient and time

The creep models of AASHTO (2007) and ACI 209.2R-08 were used to predicate the creep coefficient of the RP3F3C mixes. These models estimate the creep coefficient (φ) at time (t,

t_0) using Equation 7.4. This equation consists of mainly two parts; the former is called the time function for the development of the creep over time; while the latter is the ultimate creep coefficient. The parameters of this equation used in each model are represented in Table 7.2.

$$\varphi(t,t_o) = \underbrace{\frac{(t-t_o)^d}{B+(t-t_0)^d}}_{\text{Time function}} \underbrace{c_u}_{\text{Ultimate creep coefficient}}; \text{ Where } C_u = \lambda\gamma_c \qquad \text{(Eq. 7.4)}$$

Table 7.2: Parameters of creep coefficient in different models

Type of model	
AASHTO LRFD (2007)	**ACI 209.2R-08**
$B = (61 - 0.58\,fc')$	$B = 10$
$d = 1$	$d = 0.6$
$\lambda = 1.9$	$\lambda = 2.35$
$\gamma_c = k_{vs}k_hk_f{t_o}^{-0.118}$	$\gamma_c = \gamma_{la}\gamma_H\gamma_{vs}\gamma_s\gamma_\rho\gamma_\alpha$
$K_{vs} = 1.45 - 0.0051(v/s) \geq 1.0$	$\gamma_{la} = 1.25(t_o)^{-0.118}$
$K_h = 1.56 - 0.008RH$	$\gamma_H = 1.27 - 0.0067RH$
$k_f = \frac{35}{7+fc'}$	$\gamma_{vs} = 2/3[1 + 1.13.e^{-.0213\left(\frac{v}{s}\right)}]$
	$\gamma_s = 0.82 + 0.00264(S_l)$
	$\gamma_\rho = 0.88 + 0.0024(\rho_a)$
	$\gamma_\alpha = 0.46 + 0.09\alpha$

Figure 7.13 compares the predictions of the ACI 209.2R-08 and AASHTO (2007) models, with the experimental results of the creep coefficient of the RP3F3C mixes. As can be seen in Figure 7.13, the predictions of the ACI 209.2R-08 and AASHTO (2007) empirical model underestimates the creep coefficient results of the RP3F3C mixes, except for RP3F3C100 which was in agreement with AASHTO (2007). This is not surprising given that as these models were not developed specifically for lightweight concrete containing manufactured plastic aggregate.

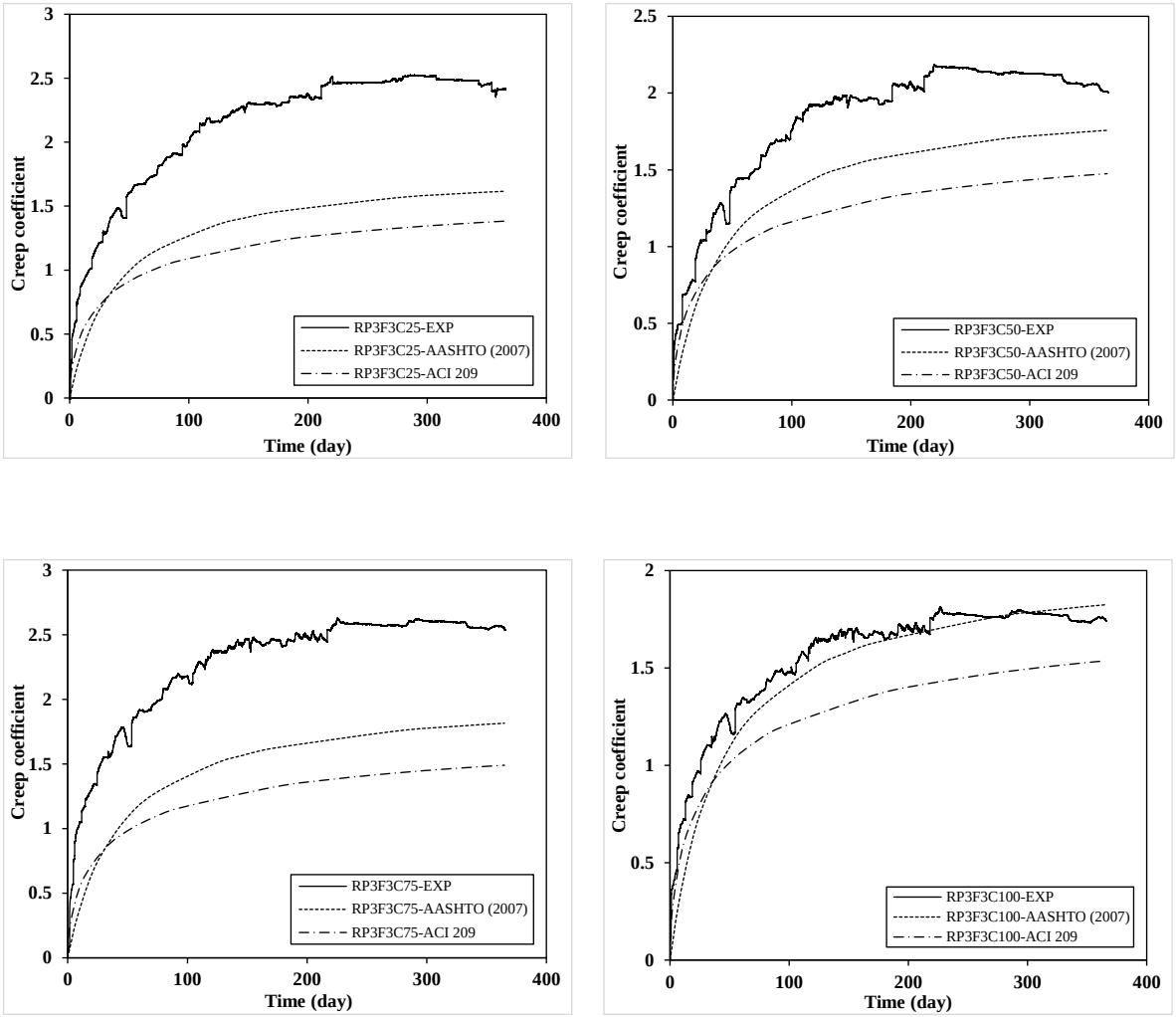


Figure 7.13: Comparison between the experimental results and the predictions of the analytical models relating creep coefficient of RP3F3C mixes

Therefore, the results presented in Figure 7.13 reflect that the equations proposed by ACI209.2R and AASHTO (2007) need to be calibrated based on the existing data. Accordingly, a non-linear regression analysis of the experimental results was performed to calibrate these models for the RP3F3C mixes using Equation 7.4, based on the methodology proposed by Shuraim et al. (2016), which includes the following assumptions:

- In order to get the best fit regression, it was assumed that the parameters *B*, *d* and C_u were unknown.

- In order to calibrate the ACI 209.2R-08 model, it was assumed that the parameter C_u was unknown; while, *B* and *d* follow ACI 209.1R-05 as *B* and *d* both were constant, as given in Table 7.2.
- In order to calibrate the AASHTO (2007) model, it was assumed that the parameter C_u was unknown; while, *B* and *d* follow AASHTO (2007) (see Table 7.2), where *B* was computed while *d* was constant.

Figure 7.14 shows the regression analysis curves (i.e. best fit, ACI 209.2R-08, AASHTO, 2007) of the creep coefficient of the RP3F3Cs mixes, in comparison with the experimental results. The summary of the results of these curves is presented in Table 7.3.

Table 7.3: Regression analysis results of the RP3F3C mixes

Model Type	**Parameter**	**Concrete type**			
		RP3F3C25	**RP3F3C50**	**RP3F3C75**	**RP3F3C100**
Best fit	B	17.72	26.45	12.71	12.46
	d	0.77	0.92	0.76	0.77
	C_u	3.04	2.42	3.03	2.05
	R^2	0.98	0.96	0.98	0.98
AASHTO (2007)	B	40.52	42.60	43.36	43.47
	d	1			
	C_u	2.84	2.47	3.06	2.09
	R^2	0.97	0.96	0.93	0.92
ACI 209.2R-08	B	10			
	d	0.6			
	C_u	3.30	2.83	3.50	2.40
	R^2	0.97	0.94	0.96	0.96

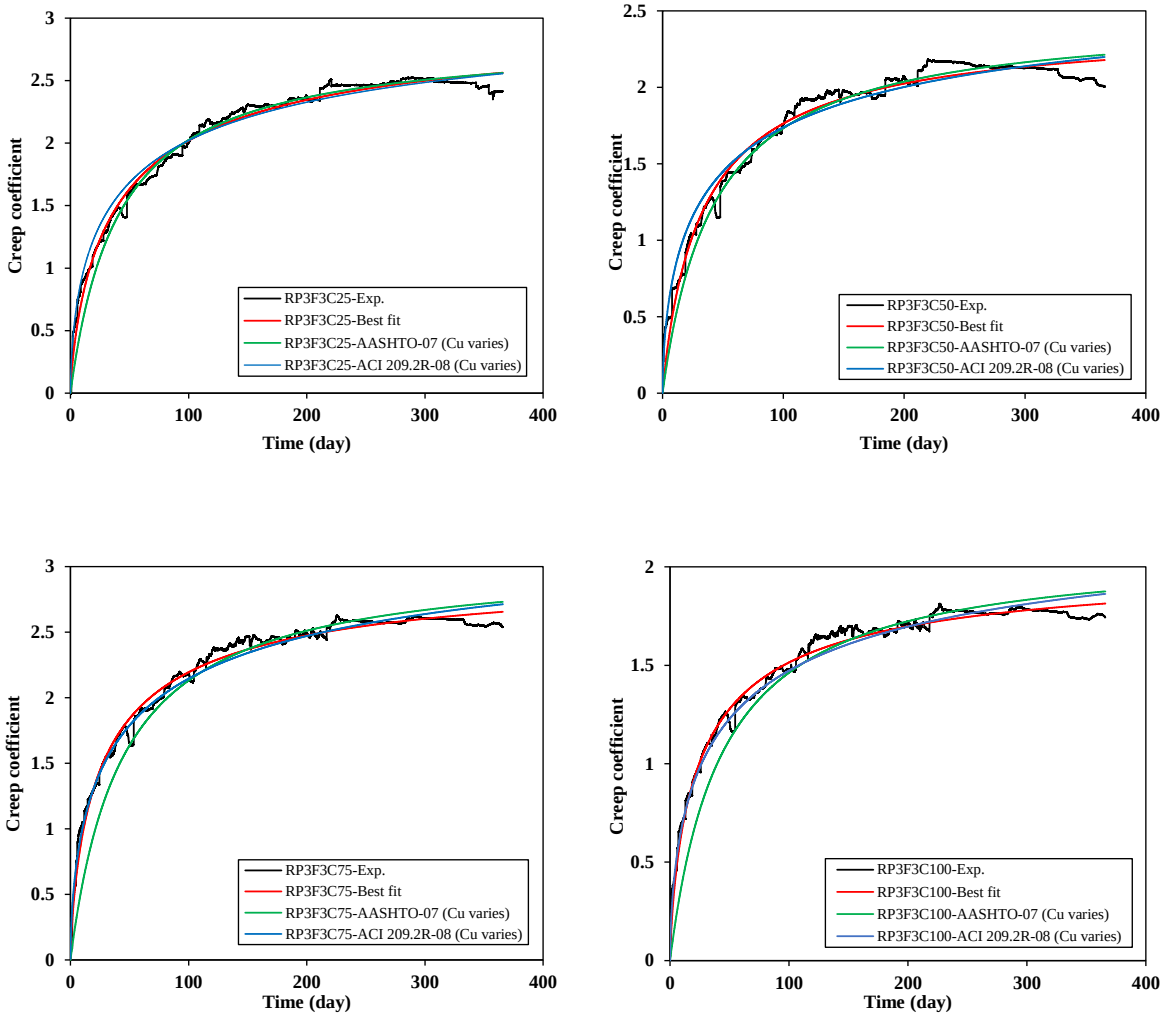


Figure 7.14: Regression and expermental curves for creep coefficients of RP3F3Cs' mixes

As can be seen in Table 7.3, the maximum coefficient of the determination (R^2) was yielded by the "best fit" representation followed by ACI 209.2R-08 and then AASHTO (2007). However, there was a significant difference between the parameter of the best fit regression (i.e. B, d, C_u) for each mix. This reveals that the best fit representation is impractical, as it needs variation of B, d and C_u.

Considering the second best representation in the sense of the R^2 value, the time function of ACI 209.2R-08 has a better capability to represent the experimental results than AASHTO

(2007). Therefore, this study proposed a modification of the current ACI 209.2R-08 model by modifying the ultimate creep coefficient factor (λ_{PA}), as shown in Equation 7.5.

$$\varphi(t,t_o) = \frac{(t-t_o)^{0.6}}{10+(t-t_0)^{0.6}}\lambda_{PA}\gamma_c \qquad \text{(Eq. 7.5)}$$

The proposed value of λ_{PA} takes the value of 3.7, which represents the average values of λ_{PA} resulting from the calibration of the ACI 209.2R-08 model for the RP3F3C mixes, as shown in Table 7.4.

Table 7.4: Calculations for calibrating the ACI models for RP3F3C mixes

Model type	**Parameter**	**Concrete type**			
		RP3F3C25	**RP3F3C50**	**RP3F3C75**	**RP3F3C100**
ACI 209.2R-08	γ_{la}	0.844	0.844	0.844	0.844
	γ_H	1.015	1.015	1.015	1.015
	γ_{vs}	1.158	1.158	1.158	1.158
	γ_s	1.189	1.268	1.282	1.321
	γ_ρ	0.88	0.88	0.88	0.88
	γ_α	0.73	0.73	0.73	0.73
	γ_c	0.759	0.810	0.819	0.844
	C_u	3.30	2.83	3.50	2.40
	$\lambda_{PA} = C_u/\gamma_c$	4.35	3.49	4.27	2.84

Figure 7.15 compares the creep coefficient curves plotted using the proposed model with those observed experimentally, where the proposed model yielded a good capability of representing the experimental results of the RP3F3C mixes. Additionally, the proposed equation was found to correlate well with the experimental data with a coefficient of correlation ranging from 0.96 to 0.98, as shown in Table 7.5. However, it should be noted that the equation proposed (Eq. 7.5) is developed only for the manufactured plastic aggregate used in this study and would need to be calibrated for other types of aggregates.

Table 7.5: Coefficient of correlation of the proposed model for the creep coefficient of RP3F3C mixes

Concrete type	Coefficient of correlation
	Eq. 7.5
RP3F3C25	0.98
RP3F3C50	0.96
RP3F3C75	0.97
RP3F3C100	0.97

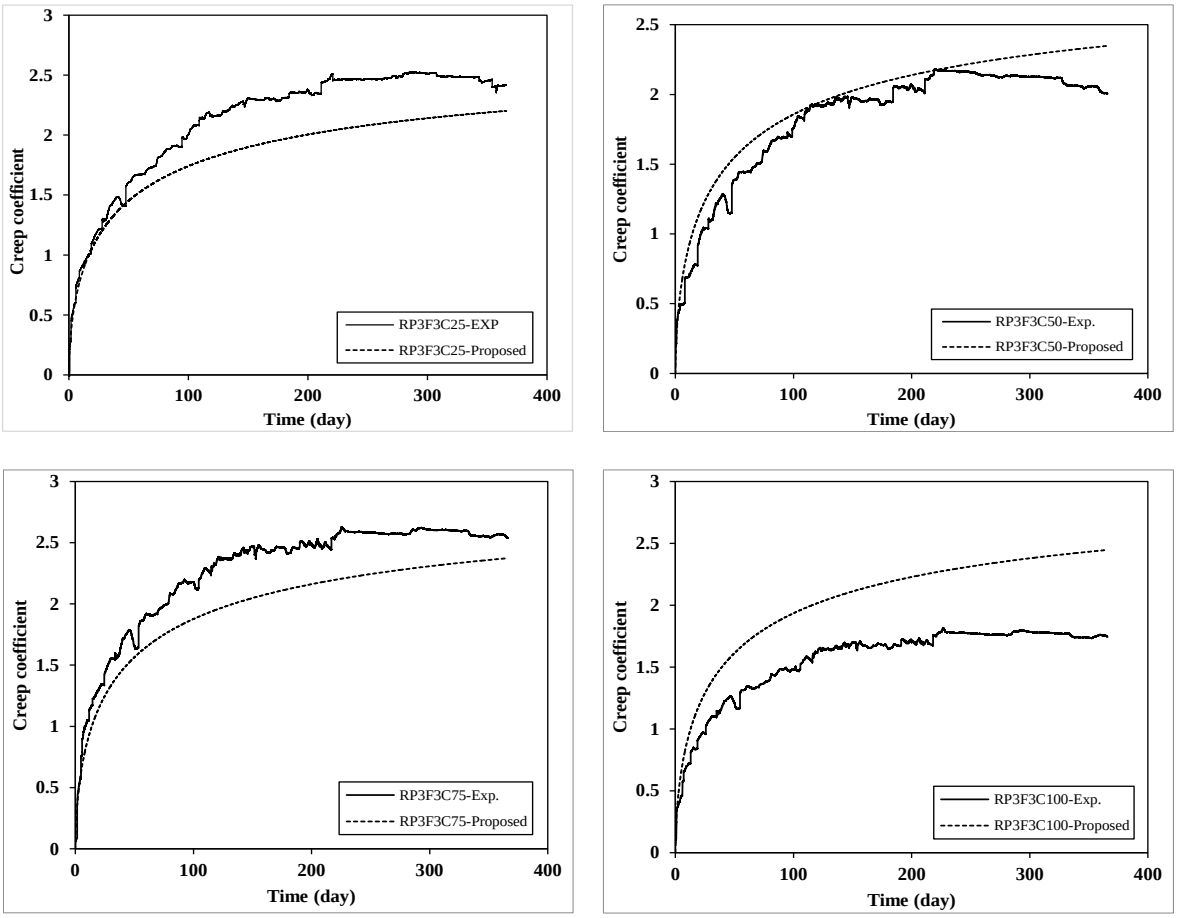


Figure 7.15: Comparison between proposed model and the experimental results for creep coefficient of RP3F3C mixes

7.5 Summary

This chapter investigates the effect of RP2F1A and RP3F3A on the durability properties and thermal conductivity of the produced concrete. Moreover, this chapter examines the influence of temperature curing on the strength performance of RP2F1C and RP3F3C mixes. The

manufactured plastic aggregates (i.e. RP2F1A, RP3F3A) were used as a replacement for volcanic lightweight aggregate (LWA) and normal weight aggregate (NA) respectively, at different replacement levels (25 to 100%) with intervals of 25%. They were also utilized as a total replacement for Lytag aggregate (LYA).

The main findings of this chapter show that the replacement level had a significant effect on the durability properties of concrete. In particular, there was a significant reduction in the chloride permeability of the RP2F1C and RP3F3C mixes; while drying shrinkage and creep strain were increased as the replacement level was increased. Additionally, a significant difference was also observed between the water absorption of the manufactured plastic aggregate concrete mixes (i.e. RP2F1C and RP3F3C) and that of the control mixes (i.e. NC, LWC, LAC). This chapter has also shown that the RP2F1C100 had lower thermal conductivity than normal weight concrete. These results concluded that the RP3F3C100 (i.e. containing 100% RP3F3A) meets the requirements of both ASTM C1202-12 and ASTM C330/C330M-14, which further confirms the potential of RP3F3C100 as a durable lightweight structural mix.

Finally, analytical models for the durability properties of the concrete comprising RP2F1A and RP3F3A were proposed, which show a good capability to represent the experimental results.

CHAPTER 8: CONCLUSIONS AND RECOMMENDATIONS FOR FURTHER STUDIES

8.1 General

The aim of this study consisted of two parts: firstly, to manufacture a novel lightweight aggregate called manufactured recycled plastic aggregate (RPA) that was made from plastic acting as a binder and by-product waste (i.e. fly ash, quarry fines) or granular materials, such as red dune sand acting as a filler. The second part was to produce a viable lightweight concrete containing this aggregate as a partial or full replacement of either normal weight or lightweight coarse aggregate and study its effect on the fresh, hardened, microstructure and durability properties of concrete.

Various types of recycled plastic aggregates were successfully manufactured and subsequently, lightweight concrete was produced. This novel aggregate is promising and exhibited its potential use in lightweight concrete, as it has both relatively low density and absorption together with unique features i.e. ductility. Therefore, the aim of the study was achieved; however, for a better performance the bonding between the recycled plastic aggregate (RPA) and the cement paste needs to be improved by using for example a binding agent.

The main conclusions and recommendations drawn from this research study are presented in the following sections.

8.2 Conclusions

Based on the results presented in each chapter, the conclusions drawn are summarized as follows:

- Recycled plastic aggregate (RPA) was successfully manufactured using the compression moulding press technique at two optimized mix proportions (i.e. 30:70, 50:50 of binder to filler ratio). The particles of the RPAs (Group 2) developed using PET and fillers had better angularity and sharpness than those of the RPAs (Group 1) produced using LLDPE and filler, while the Group 1 RPAs had rougher surface textures (i.e. fibrous) than the Group 2 RPAs. The Group 1 RPAs had relatively better grading than the Group 2 RPAs and LWA, based on the lightweight grading limits. Therefore, the RPAs containing red dune sand filler (i.e. RP1F1A, RP4F1A) were the coarser (i.e. had a large fineness modulus) amongst all the RPAs.
- The water absorption of the Group 2 RPAs (i.e. 0.56 to 1.68%) is lower than that of the Group 1 RPAs (i.e. 2.71 to 9.81%). However, for both groups of RPAs it was 42 to 85% and 90 to 97% lower than that of lightweight aggregates (LWA, LYA), respectively. Similarly, RPAs had relatively low density compared to that of reference aggregates. In addition, the density of the Group 1 RPAs (i.e. 510 to 750 kg/m^3) meets the maximum requirements (i.e. 880 kg/m^3) of lightweight aggregate given in ASTM C330/C330M-14. However, the density of the Group 2 RPAs was higher than the limit by 20-43%. The Group 2 RPAs were 43-61% and 1.1-28.5% stronger than that of LWA and LYA, respectively, since it exhibited better interlocking between binder and filler with fewer voids as confirmed by SEM and optical microscopic images.
- Sustainable lightweight concrete (i.e. had dry density $\leq$ 2000 kg/m^3) was successfully produced using 100% of the RPA. The RPACs-1 (i.e. containing RPAs Group 1) had 52.5 to 80% lower slump than that of volcanic lightweight concrete (i.e. LWC). However, RPACs-2 (i.e. containing RPAs Group 2) and LWC had slump results that differed by -52 to 19%. Additionally, there was a significant difference between

density (i.e. fresh, dry) of RPACs (i.e. RPACs-1, RPACs-2) and normal weight concrete (NC) as the maximum reduction in fresh and dry density of RPACs-1 and RPACs-2 ranged from 18 to 25%. However, the differences were insignificant (less than 10%) compared to those of LWC.

- The RPACs-2 had better mechanical and durability performance than those of RPACs-1 since the highest reduction in the 28-day compressive and flexural strength of RPACs-1 and RPACs-2 compared to that of control concrete (i.e. NC) ranged from 42 to 68% and from 39 to 53%, respectively. Similarly, the decrease in chloride permeability of RPACs-2 compared to that of both NC and LWC varied between 32 to 73%. Thus, these conclusions suggest that the RPACs-2 can potentially be used as structural lightweight concrete mixes, since they meet the requirements of ASTM C330/C330M-14 for dry density, compressive and splitting tensile strength. However, the RPACs-1 mixes can still be used for non-structural lightweight applications where low density and strength are required as they satisfy the requirements of ACI 213R-03. According to the performance of these mixes in terms of fresh, hardened and durability properties, the RP2F1C and RP3F3C mixes were selected from RPACs-1 and RPACs-2, respectively, for a detailed investigation.
- The manufactured plastic aggregates concrete mixes (i.e. RP2F1C, RP3F3C) had lower mechanical performance compared to those of control mixes (i.e. LWC, NC). The compressive strength, flexural strength, splitting tensile strength and elastic modulus of the RP2F1C mixes decreased by 15-62%, 27-44%, 12-31% and 11-54%, respectively, with an increase in the replacement level of the LWA with RP2F1A from 25-100%. The same properties of the RP3F3C were reduced by 15-28%, 3-26%,

7-37% and 26-63%, respectively, as the replacement level of the NA with RP3F3A was increased from 25 to 100%.

- The manufactured plastic aggregates concrete have a unique feature over conventional concrete, as it deforms under load (i.e. ductile behaviour) compared to the brittle mode of failure observed for the control mixes (i.e. LWC, NC, LAC). This conclusion was noted from the increase in the post peak deformation and the strain capacity together with the increase of the Poisson's ratio. The SEM images confirmed that the brittle failure of the control mixes is attributable to a major crack formation in the ITZ. On the other hand, the ductile failure of RPAC-1 including RP2F1C25 can be ascribed to the high deformability of the aggregate (i.e. RP2F1A) particles.
- The inclusion of the manufactured plastic aggregates (i.e. RP2F1A, RP3F3A) substantially increased the drying shrinkage and creep strain values of the manufactured plastic aggregate concrete as compared to those of control mixes (i.e. LWC, NC, LAC). The 182-day drying shrinkage of the RP2F1C and RP3F3C mixes increased by 19-54% and 39-72%, respectively, as the replacement level was increased from 50 to 100%. The RP3F3C mixes had 3 to 69% higher ultimate creep strain than that of NC.
- Significant differences between the manufactured plastic aggregate concrete (i.e. RP2F1C, RP3F3C) and those of control concrete mixes (i.e. LWC, NC, LAC) in terms of abrasion (i.e. mass loss) and water absorption were observed. However, these mixes had better chloride penetration resistance than that of control mixes. The chloride permeability of the RP2F1C and RP3F3C mixes decreased by 9 to 17% and 23 to 68%, respectively, as the replacement level was increased from 25 to 100%. The manufactured plastic aggregate concrete (i.e. RP2F1C) had better insulation features

than the normal weight concrete, while the increase in curing temperature from 20 to 30 °C insignificantly (i.e. ≤ 10%) reduced the 28-day compressive strength of the manufactured plastic aggregates concrete.

- The models were proposed for mechanical and durability properties of RP2F1C and RP3F3C mixes and it was found that the predictions of the proposed models were in good agreement with the experimental results. Until further research is carried out, it is suggested that the proposed models should only be used for the studied type of concrete at a W/C of 0.50.
- The overall findings suggest that the RP2F1C25 and RP3F3C100 meet the dry density, compressive and splitting tensile strength requirements of ASTM C330/C330M-14. However, only the RP3F3C100 satisfies the durability requirements of ASTM C1202-12. This further confirms the potential of RP3F3C100 as a durable lightweight structural mix; while, RP2F1C25 could still be used in structural lightweight applications where a low chloride level exists.

8.3 Recommendations for further works

The findings of this study are encouraging either in terms of aggregate (i.e. RPA) manufacturing or its utilization in structural and non-structural lightweight concrete applications. However, there is still a need to investigate and evaluate the following points:

- A detailed cost effectiveness of the production process of RPA needs to be conducted to verify its feasibility and applicability.
- The water absorption and voids between RPA particles may be measured using another technique to confirm its variability.

- The effect of replacing conventional coarse aggregate with RPA on different durability aspects of concrete, such as sulphate resistance, carbonation, freeze-thaw cycle and leaching tests are recommended for further investigation.
- The effect of pore size distribution on the drying shrinkage behaviour needs to be investigated.
- The effect of using RPA as a replacement for coarse aggregate on the fire resistance and noise insulation need to be examined.
- Predicated models provide excellent predictions for the experimental results of the RP2F1C and RP3F3C mixes. However, further research is required to confirm their applicability to concrete mixes with different manufactured plastic aggregates, W/C ratios and cement contents.
- The fresh, hardened and durability properties of concrete need to be examined for the case of implementing RPA as replacement for fine aggregate or both aggregates (i.e. fine and coarse).
- The potential of using RPA in structural lightweight reinforced elements such as columns, beams and slabs needs to be experimentally investigated in the case of incorporating RPA as replacement for aggregate (i.e. coarse, fine, both). This can be conducted in line with the building code requirements of reinforced concrete (i.e. ACI 318).
- The performance of reinforced lightweight concrete comprised of RPA needs to be numerically evaluated using simulation modelling, for example by using the experiment results of RPA concrete measured in this study.
- The effect of using RPA on the performance of an asphaltic bituminous mix is recommended for study and evaluation.

- The effect of using RPA as a replacement for aggregate (i.e. coarse, fine, both) on the total cost of construction is recommended to be studied.

REFERENCES

AASHTO, 2007. AASHTO LRFD bridge design specifications. Washington, DC.

Abidi, S., Nait-Ali, B., Joliff, Y. and Favotto, C., 2015. Impact of perlite, vermiculite and cement on the thermal conductivity of a plaster composite material: Experimental and numerical approaches. *Composites Part B: Engineering,* 68**,** 392-400.

ACI 201.2R-01, 2001. Guide to Durable Concrete. *American Concrete Institute-ACI Committee 201.* Farmington Hills, MI.

ACI 209.1R-05, 2005. Report on factors affecting shrinkage and creep of hardened concrete. *American Concrete Institute.* Farmington Hills, MI.

ACI 209.2R-08, 2008. Guide for modeling and calculating shrinkage and creep in hardened concrete. *American Concrete Institute.* Farmington Hills, MI.

ACI 211.1-91, 1991. Standard Practice for Selecting Proportions for Normal, Heavyweight, and Mass Concrete (Reapproved 2009). *American Concrete Institute-ACI Committee 211.* Farmington Hills, MI.

ACI 211.2-98, 1998. Standard Practice for Selecting Proportions for Structural Lightweight Concrete (Reapproved 2004). *American Concrete-ACI Committee 211.* Farmington Hills, MI.

ACI 213R-03, 2003. Guide for Structural Lightweight-Aggregate Concrete-ACI Committee 213. *American Concrete Institute.* Farmington Hills, MI.

ACI 213R-03, 2003. Guide for Structural Lightweight-Aggregate Concrete-ACI Committee 213. *American Concrete Institute.*

ACI 301-05, 2005. Specifications for Structural Concrete. *American Concrete Institute.* Farmington Hills, MI.

ACI 318-05, 2005. Building Code Requirements for Structural Concrete (ACI 318-05) and Commentary (ACI 318R-05). *American Concrete Institute (ACI Committee 318).* Farmington Hills, MI.

ACI 318-95, 1995. Building Code Requirements for Structural Concrete (ACI 318-95) and Commentary (ACI 318R-95). *American Concrete Institute (ACI Committee 318).* Farmington Hills, MI.

ACI 318-99, 1999. Building Code Requirements for Structural Concrete (ACI 318-99) and Commentary (ACI 318R-99). *American Concrete Institute (ACI Committee 318),*. Farmington Hills, MI.

Ahmad, S., Sallam, Y. and Al-Hashmi, I., 2013. Optimising dosage of Lytag used as coarse aggregate in lightweight aggregate concretes. *Journal of the South African Institution of Civil Engineering,* 55**,** 80-84.

Ahmaruzaman, M., 2010. A review on the utilization of flyash progress in energy and combustion science. *Volume36 (3)***,** 327-363.

Aigbedion, I. and Iyayi, S. E., 2007. Environmental effect of mineral exploitation in Nigeria. *International Journal of Physical Sciences,* 2**,** 33-38.

Al-Harthy, A., Halim, M. A., Taha, R. and Al-Jabri, K., 2007. The properties of concrete made with fine dune sand. *Construction and Building Materials,* 21**,** 1803-1808.

Al-Jabri, K. S., Hago, A., Al-Nuaimi, A. and Al-Saidy, A., 2005. Concrete blocks for thermal insulation in hot climate. *Cement and Concrete Research,* 35**,** 1472-1479.

Al-Manaseer, A. and Dalal, T., 1997. Concrete containing plastic aggregates. *Concrete International,* 19**,** 47-52.

Al-Sanad, H., Ismael, N. and Nayfeh, A., 1993. Geotechnical properties of dune sands in Kuwait. *Engineering Geology,* 34**,** 45-52.

Al Ansari, M. S., 2012. Improving solid waste management in gulf co-operation council states: developing integrated plans to achieve reduction in greenhouse gases. *Modern Applied Science,* 6**,** 60.

Al Bakri, A. M., Tamizi, S. M., Rafiza, A. and Zarina, Y., 2011. Investigation of HDPE plastic waste aggregate on the properties of concrete. *Journal of Asian Scientific Research,* 1**,** 340.

Albano, C., Camacho, N., Hernandez, M., Matheus, A. and Gutierrez, A., 2009. Influence of content and particle size of waste pet bottles on concrete behavior at different w/c ratios. *Waste Management,* 29**,** 2707-2716.

Alhozaimy, A., Jaafar, M., Al-Negheimish, A., Abdullah, A., Taufiq-Yap, Y., Noorzaei, J. and Alawad, O., 2012. Properties of high strength concrete using white and dune sands under normal and autoclaved curing. *Construction and Building Materials,* 27**,** 218-222.

Alhumoud, J. M., Al-Ghusain, I. and Al-Hasawi, H., 2004. Management of recycling in the Gulf Co-operation Council states. *Waste Management,* 24**,** 551-562.

Alqahtani, F. K., Ghataora, G., Khan, M. I. and Dirar, S., 2017. Novel lightweight concrete containing manufactured plastic aggregate. *Construction and Building Materials,* 148**,** 386-397.

Alqahtani, F. K., Khan, M. I. and Ghataora, G., 2014. Synthetic aggregate for use in concrete. *U.S. Patent 8,921,463.*

Alqahtani, F. K., Khan, M. I., Ghataora, G. and Dirar, S., 2016. Production of Recycled Plastic Aggregates and Its Utilization in Concrete. *Journal of Materials in Civil Engineering***,** 04016248.

Andrady, A. L., 1994. Assessment of environmental biodegradation of synthetic polymers. *Journal of Macromolecular Science, Part C: Polymer Reviews,* 34**,** 25-76.

ASTM C29/C29M-16, 2016. Standard Test Method for Bulk Density ("Unit Weight") and Voids in Aggregate. *ASTM International.* West Conshohocken, PA, USA.

ASTM C33/C33M-16, 2016. Standard Specification for Concrete Aggregates. *ASTM International.* West Conshohocken, PA, USA.

ASTM C39/C39M-16, 2016. Standard Test Method for Compressive Strength of Cylindrical Concrete Specimens. *ASTM International.* West Conshohocken, PA, USA.

ASTM C127-15, 2015. Standard Test Method for Relative Density (Specific Gravity) and Absorption of Coarse Aggregate. *ASTM International.* West Conshohocken, PA, USA.

ASTM C128-15, 2015. Standard Test Method for Relative Density (Specific Gravity) and Absorption of Fine Aggregate. *ASTM International.* West Conshohocken, PA, USA.

ASTM C136/C136M-14, 2014. Standard Test Method for Sieve Analysis of Fine and Coarse Aggregates. *ASTM International.* West Conshohocken, PA, USA.

ASTM C138/C138M-16, 2016. Standard Test Method for Density (Unit Weight), Yield, and Air Content (Gravimetric) of Concrete. *ASTM International.* West Conshohocken, PA, USA.

ASTM C143/C143M-15, 2015. Standard Test Method for Slump of Hydraulic-Cement Concrete. *ASTM International.* West Conshohocken, PA, USA.

ASTM C150/C150M-16, 2016. Standard Specification for Portland Cement. *ASTM International.* West Conshohocken, PA, USA.

ASTM C157/C157M-14, 2008. Standard Test Method for Length Change of Hardened Hydraulic-Cement Mortar and Concrete. *ASTM International.* West Conshohocken, PA,USA.

ASTM C177-13, 2013. Standard Test Method for Steady-State Heat Flux Measurements and Thermal Transmission Properties by Means of the Guarded-Hot-Plate Apparatus. *ASTM International.* West Conshohocken, PA, USA.

ASTM C192/C192M-16, 2016. Standard Practice for Making and Curing Concrete Test Specimens in the Laboratory. *ASTM International.* West Conshohocken, PA, USA.

ASTM C330/C330M-14, 2014. Standard Specification for Lightweight Aggregates for Structural Concrete. *ASTM International.* West Conshohocken, PA, USA.

ASTM C469/C469M-14, 2014. Standard Test Method for Static Modulus of Elasticity and Poisson's Ratio of Concrete in Compression. *ASTM International.* West Conshohocken, PA, USA.

ASTM C496/C496M-11, 2011. Standard Test Method for Splitting Tensile Strength of Cylindrical Concrete Specimens *ASTM International.* West Conshohocken, PA, USA.

ASTM C512/C512M-15, 2015. Standard Test Method for Creep of Concrete in Compression. *ASTM International, .* West Conshohocken, PA, USA.

ASTM C579-02, 2012. Standard Test Methods for Compressive Strength of Chemical-Resistant Mortars, Grouts, Monolithic Surfacings, and Polymer Concretes. *ASTM International.* West Conshohocken, PA, USA.

ASTM C580-02, 2012. Standard Test Method for Flexural Strength and Modulus of Elasticity of Chemical-Resistant Mortars, Grouts, Monolithic Surfacings, and Polymer Concretes. *ASTM International.* West Conshohocken, PA, USA.

ASTM C617/C617M-15, 2015. Standard Practice for Capping Cylindrical Concrete Specimens. *ASTM International.* West Conshohocken, PA, USA.

ASTM C618-15, 2015. Standard Specification for Coal Fly Ash and Raw or Calcined Natural Pozzolan for Use in Concrete. *ASTM International.* West Conshohocken, PA, USA.

ASTM C944/C944M-12, 2012. Standard Test Method for Abrasion Resistance of Concrete or Mortar Surfaces by the Rotating-Cutter Method. *ASTM International.* West Conshohocken, PA, USA.

ASTM C1202-12, 2012. Standard Test Method for Electrical Indication of Concrete's Ability to Resist Chloride Ion Penetration. *ASTM International.* West Conshohocken, PA, USA.

ASTM D2584-11, 2011. Standard Test Method for Ignition Loss of Cured Reinforced Resins. *ASTM International.* West Conshohocken, PA, USA.

ASTM D4703-15, 2015. Standard Practice for Compression Molding Thermoplastic Materials into Test Specimens, Plaques, or Sheets. *ASTM International.* West Conshohocken, PA, USA.

Aznar, M. P., Caballero, M. A., Sancho, J. A. and Francés, E., 2006. Plastic waste elimination by co-gasification with coal and biomass in fluidized bed with air in pilot plant. *Fuel Processing Technology,* 87**,** 409-420.

Babu, D. S., Babu, K. G. and Tiong-Huan, W., 2006. Effect of polystyrene aggregate size on strength and moisture migration characteristics of lightweight concrete. *Cement and Concrete Composites,* 28**,** 520-527.

Babu, D. S., Babu, K. G. and Wee, T., 2005. Properties of lightweight expanded polystyrene aggregate concretes containing fly ash. *Cement and concrete research,* 35**,** 1218-1223.

Babu, K. G. and Babu, D. S., 2003. Behaviour of lightweight expanded polystyrene concrete containing silica fume. *Cement and concrete research,* 33**,** 755-762.

Babu, K. G. and Babu, D. S., 2004. Performance of fly ash concretes containing lightweight EPS aggregates. *Cement and Concrete Composites,* 26**,** 605-611.

Bai, Y., Ibrahim, R. and Basheer, P. M., 2004. Properties of lightweight concrete manufactured with fly ash, furnace bottom ash, and lytag. *International workshop on sustainable development and concrete technology.*

Barth, H.-J., 1999. Desertification in the eastern province of Saudi Arabia. *Journal of Arid Environments,* 43**,** 399-410.

Batayneh, M., Marie, I. and Asi, I., 2007. Use of selected waste materials in concrete mixes. *Waste Management,* 27**,** 1870-1876.

BBC, 2014. *Ocean Cleanup concept* [Online]. Available: http://www.bluebird-electric.net/oceanography/Ocean_Plastic_International_Rescue/Boyan_Slat.htm [Accessed 22 March 2017].

Bedick, R., 1995. Report to Congress—Barriers to the increased utlization of coal combustion/desulfurization byproducts by governmental and commercial sectors. *Supplemental Proceedings: 11th International Symposium on Use and Management of Coal Combustion By-Products (CCB's).* American Coal Ash Association and Electric Power Research Institute Symposium.

Bethanis, S., 2007. Value-added utilisation of municipal waste incinerator bottom ash as lightweight aggregate in concrete. *WIT Transactions on Ecology and the Environment,* 102.

Birckhead, R., Impact of changing state and federal regulations on ash management at Virginia power. Proceedings: 11th International Symposium on Use and Management of Coal Combustion By-Products (CCB's), 1995. 15-19.

Block, D. G., 2016. *Recycled Resin Prices Likely To Follow Same Pattern as 2015* [Online]. Plastic Technology. Available: http://www.ptonline.com/articles/recycled-resin-prices-likely-to-follow-same-pattern-as-2015 [Accessed 18 June 2016].

Bremner, T. and Holm, T., 1986. Elastic compatibility and the behavior of concrete. *Journal Proceedings,* 83**,** 244-250.

BS 812-112:1990, 1990, Methods for determination of aggregate impact value (AIV). *British Standards Institution.* London, UK.

BS 1881-122:2011, 2011. Testing concrete: Method for determination of water absorption. *British Standards Institution.* London, UK.

BS EN 12390-7:2009, 2009. Testing hardened concrete:Density of hardened concrete. *British Standards Institution.* London, UK.

BS EN 12664:2001, 2001. Thermal performance of building materials and products-Determination of thermal resistance by means of guarded hot plate and heat flow meter methods-Dry and moist products of medium and low thermal resistance. *British Standards Institution.* London, UK.

Chandra, S. and Berntsson, L., 2002. *Lightweight aggregate concrete-Science, Technology, and Applications*, NOYES PUBLICATIONS.

Chaudhary, M., Srivastava, V. and Agarwal, V., 2014. Effect of waste low density polyethylene on mechanical properties of concrete. *Journal of Academia and Industrial Research (JAIR),* 3**,** 123-126.

Chen, B. and Liu, J., 2004. Properties of lightweight expanded polystyrene concrete reinforced with steel fiber. *Cement and concrete research,* 34**,** 1259-1263.

Choi, Y.-W., Moon, D.-J., Chung, J.-S. and Cho, S.-K., 2005. Effects of waste PET bottles aggregate on the properties of concrete. *Cement and Concrete Research,* 35**,** 776-781.

Choi, Y. W., Moon, D. J., Kim, Y. J. and Lachemi, M., 2009. Characteristics of mortar and concrete containing fine aggregate manufactured from recycled waste polyethylene terephthalate bottles. *Construction and Building Materials,* 23**,** 2829-2835.

Clark, J. H. and Hardy, J. J., 2004. Towards sustainable chemical manufacturing: polylactic acid–a sustainable polymer. *Sustainable Development in Practice: Case Studies for Engineers and Scientists, first ed. Wiley***,** 250-282.

Clarke, J. L., 2005. *Structural lightweight aggregate concrete*, Taylor & Francis e-Library.

Collins, R. J. and Ciesielski, S. K., 1994. Recycling and use of waste materials and by-products in highway construction:Synthesis of Highway Practice 199. NATIONAL ACADEMY PRESS,Washington, D.C. 1994.

Curlee, T. R., 1986. *The economic feasibility of recycling: a case study of plastic wastes*, Praeger Publishing, New York

Deccan Chronicle, C. G. a. S. S., 2016. *Dump. Burn. Pollute. Who cares in indifferent Bengaluru?* [Online]. Available: http://www.deccanchronicle.com/nation/current-affairs/170516/dump-burn-pollute-who-cares-in-indifferent-bengaluru.html [Accessed 26 November 2016].

Dehdezi, P. K., Erdem, S. and Blankson, M. A., 2015. Physico-mechanical, microstructural and dynamic properties of newly developed artificial fly ash based lightweight aggregate–Rubber concrete composite. *Composites Part B: Engineering,* 79**,** 451-455.

Demirboğa, R., Örüng, İ. and Gül, R., 2001. Effects of expanded perlite aggregate and mineral admixtures on the compressive strength of low-density concretes. *Cement and concrete research,* 31**,** 1627-1632.

Dhir, R., Jones, M. and Munday, J., 1985. A practical approach to studying carbonation of concrete. *Magazine of Concrete,* 19**,** 32-34.

Dhir, R. and Paine, K., 2007. Performance related approach to use of recycled aggregates. *WRAP Aggregate Research Programme, project AGG,* 74.

Domone, P. and Illston, J., 2010. *Construction materials: their nature and behaviour*, CRC Press.

El-Newehy, M., 2016. *Plastic Waste Management* [Online]. King Saud University. Available: http://fac.ksu.edu.sa/sites/default/files/plastic_waste_management.pdf [Accessed 28 November 2016].

Elzafraney, M., Soroushian, P. and Deru, M., 2005. Development of energy-efficient concrete buildings using recycled plastic aggregates. *Journal of architectural engineering,* 11**,** 122-130.

EPA, 2014. *Municipal Solid Waste Generation, Recycling, and Disposal in the United States-Tables and Figures for 2012* [Online]. U.S. Environmental Protection Agency. Available: https://www.epa.gov/sites/production/files/2015-09/documents/2012_msw_dat_tbls.pdf [Accessed 02 December 2016].

EPA, 2015. *Advancing Sustainable Materials Management: 2013 Fact Sheet* [Online]. Environmental Protection Agency (EPA). Available: https://www.epa.gov/sites/production/files/2015-09/documents/2013_advncng_smm_fs.pdf [Accessed 21 June 2016].

Ettu, L., Ibearugbulem, O., Ezeh, J. and Anya, U., 2013. A reinvestigation of the prospects of using periwinkle shell as partial replacement for granite in concrete. *International Journal of Engineering Science Invention,* 2**,** 54-59.

Ferreira, L., de Brito, J. and Saikia, N., 2012. Influence of curing conditions on the mechanical performance of concrete containing recycled plastic aggregate. *Construction and Building Materials,* 36**,** 196-204.

Formosa, J., Haurie, L., Chimenos, J., Lacasta, A. M. and Rosell, J. R., 2008. Comparative study of magnesium by-products and vermiculite formulations to obtain fire resistant mortars. *Materials Science Forum,* 587**,** 898-902.

Fraj, A. B., Kismi, M. and Mounanga, P., 2010. Valorization of coarse rigid polyurethane foam waste in lightweight aggregate concrete. *Construction and Building Materials,* 24**,** 1069-1077.

Francis, R., 2016. *Recycling of Polymers: Methods, Characterization and Applications*, John Wiley & Sons.

Fredonia, 2012. *Global Demand for Construction Aggregates in 2015, Demand and Sales Forecasts* [Online]. Available: http://www.freedoniagroup.com/industry-study/world-construction-aggregates-2838.htm [Accessed 23 May 2015].

Fredonia, 2017. *Global Demand for Construction Aggregates* [Online]. Available: http://www.freedoniagroup.com/Search.aspx?searchTerm=Global+Demand+for+Construction+Aggregates+&searchType=TitleSearch [Accessed 30 March 2017].

Frigione, M., 2010. Recycling of PET bottles as fine aggregate in concrete. *Waste Management,* 30**,** 1101-1106.

Frye, J. A., 1994. Small particle size lightweight aggregate. Google Patents.

Galetakis, M. and Soultana, A., 2016. A review on the utilisation of quarry and ornamental stone industry fine by-products in the construction sector. *Construction and Building Materials,* 102, Part 1**,** 769-781.

Galvão, J. C. A., Portella, K. F., Joukoski, A., Mendes, R. and Ferreira, E. S., 2011. Use of waste polymers in concrete for repair of dam hydraulic surfaces. *Construction and Building Materials,* 25**,** 1049-1055.

Gambhir, M. L., 2013. *Concrete Technology: Theory and Practice*, Tata McGraw-Hill Education.

Garzanti, E., Vermeesch, P., Andò, S., Vezzoli, G., Valagussa, M., Allen, K., Kadi, K. A. and Al-Juboury, A. I., 2013. Provenance and recycling of Arabian desert sand. *Earth-Science Reviews,* 120**,** 1-19.

Gu, L. and Ozbakkaloglu, T., 2016. Use of recycled plastics in concrete: A critical review. *Waste Management,* 51**,** 19-42.

Guettala, A., Melkmi, S. and Tibermacine, N., A study of mechanical characteristics for sand concrete (Rolled sand concrete and dune sand concrete). 7th Arab structural engineering conference, Kuwait, 1997.

Gunasekaran, K., Annadurai, R. and Kumar, P., 2012. Long term study on compressive and bond strength of coconut shell aggregate concrete. *Construction and Building Materials,* 28**,** 208-215.

Haghi, A., Arabani, M. and Ahmadi, H., 2006. Applications of expanded polystyrene (EPS) beads and polyamide-66 in civil engineering, Part One: Lightweight polymeric concrete. *Composite Interfaces,* 13**,** 441-450.

Hakami, B. A. and Seif, E.-S. S. A., 2015. Household solid waste composition and management in Jeddah City, Saudi Arabia: a planning model. *International Research Journal of Environment Sciences,* 4**,** 1-10.

Haktanir, T. and Altun, F., 2002. Structural lightweight concrete with pumice aggregates of erciyes region. *Innovations and Developments In Concrete Materials And Construction: Proceedings of the International Conference held at the University of Dundee, Scotland, UK on 9–11 September 2002***,** 587-596.

Hamad, A. J., 2015. Size and shape effect of specimen on the compressive strength of HPLWFC reinforced with glass fibres. *Journal of King Saud University-Engineering Sciences*.

Hannawi, K., Kamali-Bernard, S. and Prince, W., 2010. Physical and mechanical properties of mortars containing PET and PC waste aggregates. *Waste Management,* 30**,** 2312-2320.

Heidrich, C., Feuerborn, H.-J. and Weir, A., Coal combustion products: a global perspective. Proceedings of the World of Coal Ash Conference, 2013. 22-25.

Herki, A., Khatib, J. and Negim, E., 2013. Lightweight concrete made from waste polystyrene and fly ash. *World Applied Sciences Journal,* 21**,** 1356-1360.

Hopewell, J., Dvorak, R. and Kosior, E., 2009. Plastics recycling: challenges and opportunities. *Philosophical Transactions of the Royal Society of London B: Biological Sciences*, 364**,** 2115-2126.

Hossain, K. and Lachemi, M., 2007. Mixture design, strength, durability, and fire resistance of lightweight pumice concrete. *ACI materials journal*, 104**,** 449-457.

Hossain, K. M. A., 2004. Properties of volcanic pumice based cement and lightweight concrete. *Cement and concrete research*, 34**,** 283-291.

Huffman, M., Limestone pond fines case study: Subtitle D landfill soil infiltration layer and other applications. International Center for Aggregates Research 9th Annual Symposium: Aggregates-Concrete, Bases and Fines, 2001.

Hyodo, H., Tanimura, M., Sato, R. and Kawai, K., Evaluation of effect of aggregate properties on drying shrinkage of concrete. Third International Conference on Sustainable Construction Materials and Technologies, Kyoto, Japan, 2013.

IEEP, 2011. European Commission DG ENV-PLASTIC WASTE IN THE ENVIRONMENT. Institute for European Environmental Policy.

Irvin, E., 2010. *A Kentucky Community Surrounded by Coal Ash* [Online]. Available: http://sierraclub.typepad.com/compass/2010/09/a-kentucky-community-surrounded-by-coal-ash.html [Accessed 24 March 2017].

Ismail, Z. Z. and Al-Hashmi, E. A., 2008. Use of waste plastic in concrete mixture as aggregate replacement. *Waste Management*, 28**,** 2041-2047.

Jambeck, J. R., Geyer, R., Wilcox, C., Siegler, T. R., Perryman, M., Andrady, A., Narayan, R. and Law, K. L., 2015. Plastic waste inputs from land into the ocean. *Science*, 347**,** 768-771.

Jansen, D., Kiggins, M., Swan, C., Malloy, R., Kashi, M., Chan, R., Javdekar, C., Siegal, C. and Weingram, J., 2001. Lightweight fly ash-plastic aggregates in concrete. *Transportation Research Record: Journal of the Transportation Research Board***,** 44-52.

Joshua, O., Ogunde, A., Omuh, I., Ayegba, C. and Olusola, K., 2015. Exploring The Pozzolanic Potential of Blend of Palm Kernel Nut Ash (Pkna) With Cement Towards a Sustainable Construction.

Juki, M. I., Awang, M., Annas, M. M. K., Boon, K. H., Othman, N., Roslan, M. A. and Khalid, F. S., 2013. Relationship between compressive, splitting tensile and flexural strength of concrete containing granulated waste Polyethylene Terephthalate (PET) bottles as fine aggregate. *Advanced Materials Research,* 795**,** 356-359.

Kan, A. and Demirboğa, R., 2009. A novel material for lightweight concrete production. *Cement and Concrete Composites,* 31**,** 489-495.

Kashi, M., Swan, C., Holmstrom, O. and Malloy, R., 1999. Innovative lightweight synthetic aggregates developed from coal Flyash. *13 th International Symposium on Management and Use of Coal Combustion Products,* 1**,** 5-1.

Kayali, O., 2008. Fly ash lightweight aggregates in high performance concrete. *Construction and Building Materials,* 22**,** 2393-2399.

Kearsley, E. P. and Wainwright, P. J., 2001. Porosity and permeability of foamed concrete. *Cement and Concrete Research,* 31**,** 805-812.

Khairallah, R. S., 2009. *Analysis of Autogenous and Drying Shrinkage of Concrete.*

Khan, M., 2002. Factors affecting the thermal properties of concrete and applicability of its prediction models. *Building and Environment,* 37**,** 607-614.

Kılıç, A., Atiş, C. D., Teymen, A., Karahan, O., Özcan, F., Bilim, C. and Özdemir, M., 2008. The influence of aggregate type on the strength and abrasion resistance of high strength concrete. *Cement and Concrete Composites,* 30**,** 290-296.

Klieger, P., 1994. *Significance of tests and properties of concrete and concrete-making materials,* ASTM International.

Koide, H., Tomon, M. and Sasaki, T., 2002. Investigation of the use of waste plastic as an aggregate for lightweight concrete. *Sustainable Concrete Construction: Proceedings of the International Conference held at the University of Dundee, Scotland, UK on 9–11 September 2002,* 5**,** 177-185.

Koksal, F., Gencel, O. and Kaya, M., 2015. Combined effect of silica fume and expanded vermiculite on properties of lightweight mortars at ambient and elevated temperatures. *Construction and Building Materials,* 88**,** 175-187.

Kosmatka, S. H., Panarese, W. C. and Kerkhoff, B., 2002. *Design and control of concrete mixtures,* Portland Cement Association Skokie, IL.

Kou, S., Lee, G., Poon, C. and Lai, W., 2009. Properties of lightweight aggregate concrete prepared with PVC granules derived from scraped PVC pipes. *Waste Management,* 29**,** 621-628.

Kozul, R. and Darwin, D., 1997. Effects of aggregate type, size, and content on concrete strength and fracture energy. University of Kansas Center for Research, Inc.

Kwan, W. H., Ramli, M., Kam, K. J. and Sulieman, M. Z., 2012. Influence of the amount of recycled coarse aggregate in concrete design and durability properties. *Construction and Building Materials,* 26**,** 565-573.

Laukaitis, A., Žurauskas, R. and Kerien, J., 2005. The effect of foam polystyrene granules on cement composite properties. *Cement and Concrete Composites,* 27**,** 41-47.

Lima, P. R. L., Leite, M. B. and Santiago, E. Q. R., 2010. Recycled lightweight concrete made from footwear industry waste and CDW. *Waste Management,* 30**,** 1107-1113.

Luo, F. J., He, L., Pan, Z., Duan, W. H., Zhao, X. L. and Collins, F., 2013. Effect of very fine particles on workability and strength of concrete made with dune sand. *Construction and Building Materials,* 47**,** 131-137.

LYTAG, 2016. *What is Lytag* [Online]. Available: http://www.lytag.com/about [Accessed 20 June 2016].

Madandoust, R., Ranjbar, M. M. and Mousavi, S. Y., 2011. An investigation on the fresh properties of self-compacted lightweight concrete containing expanded polystyrene. *Construction and Building Materials,* 25**,** 3721-3731.

Maier, P. L. and Durham, S. A., 2012. Beneficial use of recycled materials in concrete mixtures. *Construction and Building Materials,* 29**,** 428-437.

Malloy, R., Desai, N., Wilson, C., Swan, C., Jansen, D. and Kashi, M., 2001. High Carbon Fly Ash/Mixed Thermoplastic Aggregate for Use in Lightweight Concrete (859). *Technical Papers of the Annual Technical Conference-Society of Plastics Engineers Incorporated,* 3**,** 2743-2752.

Malloy, R., Kashi, M. G. and Swan, C. W., 2003. *Fly ash/mixed plastic aggregate and products made therefrom-U.S. Patent 6,669,773.*

Manning, D., 2004. Exploration and Use of Quarry Fines. Mineral Solutions. Report No. 087/MIST2/DACM/01, MIST project reference: MA/2/4/003, Manchester, Published in 2004.

Marzouk, O. Y., Dheilly, R. and Queneudec, M., 2007. Valorization of post-consumer waste plastic in cementitious concrete composites. *Waste Management,* 27**,** 310-318.

Mastellone, M. L., 1999. *Thermal treatments of plastic wastes by means of fluidized bed reactors.* PhD, Second University of Naples:Italy.

Mathew, P., Varghese, S., Paul, T. and Varghese, E., 2013. Recycled plastics as coarse aggregate for structural concrete. *International Journal Of Innovative Research In Science, Engineering And Technology,* 2**,** 687-690.

Mattigod, S., Rai, D., Eary, L. and Ainsworth, C., 1990. Geochemical factors controlling the mobilization of inorganic constituents from fossil fuel combustion residues: I. Review of the major elements. *Journal of environmental quality,* 19**,** 188-201.

MDB, 2003. *Materials Data Book,* Cambridge University-Engineering Department.

Mehta, P. K. and Aïtcin, P.-C., 1990. Principles underlying production of high-performance concrete. *Cement, concrete and aggregates,* 12**,** 70-78.

Mehta, P. K. and Monteiro, P. J. M., 2006. *Concrete Microstructure, Properties, and Materials,* United States of America, McGraw-Hill.

Melo, M. O. B., da Silva, L. B., Coutinho, A. S., Sousa, V. and Perazzo, N., 2012. Energy efficiency in building installations using thermal insulating materials in northeast Brazil. *Energy and Buildings,* 47**,** 35-43.

Mitchell, C., 2009. Quarry fines and waste. *Quarries & Mines***,** 63-67.

Mitchell, C., 2016. Mineral waste in the UK : innovation, optimisation and recycling. [Lecture] In: 4th Fujairah International Forum for Industrial Rocks & Mining, Expo 2016, Fujairah, United Arab Emirates, 23-25 Feb 2016.

Mladenovič, A., Šuput, J., Ducman, V. and Škapin, A. S., 2004. Alkali–silica reactivity of some frequently used lightweight aggregates. *Cement and concrete research,* 34**,** 1809-1816.

Mounanga, P., Gbongbon, W., Poullain, P. and Turcry, P., 2008. Proportioning and characterization of lightweight concrete mixtures made with rigid polyurethane foam wastes. *Cement and Concrete Composites,* 30**,** 806-814.

Muthusamy, K., Nordin, N., Vesuvapateran, G., Ali, M., Harun, H. and Ullap, H., 2014. Exploratory Study of Rubber Seed Shell as Partial Coarse Aggregate Replacement in Concrete. *Research Journal of Applied Sciences, Engineering and Technology* 7**,** 1013-1016

Naik, T. R., Singh, S. S., Huber, C. O. and Brodersen, B. S., 1996. Use of post-consumer waste plastics in cement-based composites. *Cement and concrete research,* 26**,** 1489-1492.

Neville, A. M., 1995. *Properties of Concrete,* Essex, England, Pearson Education Limited.

Neville, A. M., 2011. *Properties of concrete,* Pearson Education Limited, Essex, England, UK.

Nizami, A.-S., Rehan, M., Ouda, O. K., Shahzad, K., Sadef, Y., Iqbal, T. and Ismail, I. M., 2015. An argument for developing waste-to-energy technologies in Saudi Arabia. *Chem. Eng,* 45**,** 337-342.

O'Flynn, M., 2000. Manufactured sands from hardrock quarries: environmental solution or dilemma for southeast Queensland. *Australian Journal of Earth Sciences,* 47**,** 65-73.

Ouda, O. K. and Cekirge, H. M., 2014. Potential environmental values of waste-to-energy facilities in Saudi Arabia. *Arabian Journal for Science and Engineering,* 39**,** 7525-7533.

Ouda, O. K. M., Raza, S. A., Nizami, A. S., Rehan, M., Al-Waked, R. and Korres, N. E., 2016. Waste to energy potential: A case study of Saudi Arabia. *Renewable and Sustainable Energy Reviews,* 61**,** 328-340.

Partanen, J. E., Ellis, S. W. and Bartell, D., 2010. *Incorporation of plastic scrap in asphalt compositions-U.S. Patent 7,772,302 B2.*

Perry, S., Bischoff, P. and Yamura, K., 1991. Mix details and material behaviour of polystyrene aggregate concrete. *Magazine of Concrete Research,* 43**,** 71-76.

Phillips, P. and Richards, G., 2004. The use of mixed polymer waste products to produce paving grade asphalt. *Proceedings of the 3rd Eurasphalt and Eurobitume Congress,* . Vienna.

Pinto, J., Vieira, B., Pereira, H., Jacinto, C., Vilela, P., Paiva, A., Pereira, S., Cunha, V. M. and Varum, H., 2012. Corn cob lightweight concrete for non-structural applications. *Construction and Building Materials,* 34**,** 346-351.

PlasticsEurope, 2015. *Plastics – the Facts 2015:An analysis of European plastics production, demand and waste data* [Online]. Brussels – Belgium: European Association of Plastic Recycling & Recovery Orginization. Available: http://www.plasticseurope.org/documents/document/20151216062602-plastics_the_facts_2015_final_30pages_14122015.pdf [Accessed 04 December 2016].

PlasticsEurope, 2016. *Plastics – the Facts 2016: An analysis of European plastics production, demand and waste data* [Online]. Available: http://www.plasticseurope.org/documents/document/20161014113313-plastics_the_facts_2016_final_version.pdf [Accessed 20 November 2016].

Prusty, J. K. and Patro, S. K., 2015. Properties of fresh and hardened concrete using agro-waste as partial replacement of coarse aggregate–A review. *Construction and Building Materials,* 82**,** 101-113.

Psomopoulos, C., Bourka, A. and Themelis, N. J., 2009. Waste-to-energy: A review of the status and benefits in USA. *Waste Management,* 29**,** 1718-1724.

Quiroga, P. N. and Fowler, D. W., 2004. Guidelines for proportioning optimized concrete mixtures with high microfines. International Center for Aggregates Research Report 104-2, Austin, TX.

Rached, M. M., De Moya, M. and Fowler, D. W., 2009. Utilizing aggregates characteristics to minimize cement content in portland cement concrete.

Rahman, M. M., Islam, M. A. and Ahmed, M., 2012. Recycling of waste polymeric materials as a partial replacement for aggregate in concrete. *International Conference on Chemical, Environmental and Biological Sciences.*

Rahmani, E., Dehestani, M., Beygi, M., Allahyari, H. and Nikbin, I., 2013. On the mechanical properties of concrete containing waste PET particles. *Construction and Building Materials,* 47**,** 1302-1308.

Rai, B., Rushad, S. T., Kr, B. and Duggal, S., 2012. Study of waste plastic mix concrete with plasticizer. *ISRN Civil Engineering*.

Rankin, S., 2017. *Aerial view of the fly ash landfill at Dominion's Chesapeake Energy Center in Chesapeake* [Online]. Available: http://www.metronews.ca/news/world/2017/03/23/coal-ash-why-in-the-world-would-we-be-importing-it.html [Accessed 31 March 2017].

Raphael, J. M., Tensile strength of concrete. ACI Journal Proceedings, 1984. 158-165.

Ravindrarajah, R. S., 1999. Bearing strength of concrete containing polystyrene aggregate. *Proceedings of the RILEM 8th International Confrence: Durability of Building Materials and Components,* 1**,** 505-514.

Ravindrarajah, R. S. and Tuck, A., 1994. Properties of hardened concrete containing treated expanded polystyrene beads. *Cement and Concrete Composites,* 16**,** 273-277.

Rebeiz, K. S. and Craft, A. P., 1995. Plastic waste management in construction: technological and institutional issues. *Resources, Conservation and Recycling,* 15**,** 245-257.

Reddy, B. D., Jyothy, S. A. and Shaik, F., 2014. Experimental analysis of the use of coconut shell as coarse aggregate. *J. Mech. Civil Eng,* 10**,** 6-13.

Reddy, M. M., .B, A. and .R, B., 2012. Melt-Densified Post Consumer Recycled Plastic Bags Used As Light Weight Aggregate In Concrete. *International Journal of Engineering Research and Applications (IJERA),* 2**,** 1097-1101.

Remadnia, A., Dheilly, R., Laidoudi, B. and Quéneudec, M., 2009. Use of animal proteins as foaming agent in cementitious concrete composites manufactured with recycled PET aggregates. *Construction and Building Materials,* 23**,** 3118-3123.

Rochman, C. M., Browne, M. A., Halpern, B. S., Hentschel, B. T., Hoh, E., Karapanagioti, H. K., Rios-Mendoza, L. M., Takada, H., Teh, S. and Thompson, R. C., 2013. Policy: Classify plastic waste as hazardous. *Nature,* 494**,** 169-171.

Rodrigues, F., Evangelista, L. and Brito, J. d., 2013. A new method to determine the density and water absorption of fine recycled aggregates. *Materials Research,* 16**,** 1045-1051.

Roy, W. R., Thiery, R. G., Schuller, R. M. and Suloway, J. J., 1981. Coal fly ash: a review of the literature and proposed classification system with emphasis on environental impacts. Illinois State Geological Survey, Urbana (USA).

Russell, B. W. and Freyne, S. F., 1998. High Performance Concrete for Transportation Structures. Oklahoma Department of Transportation.

RWDI, 2017. *Wind-Blown Sand or Snow* [Online]. Available: http://rwdi.com/expertise/all-services/windblown-sand-snow [Accessed 24 March 2017].

Sabaa, B. and Ravindrarajah, R. S., 1997. Engineering properties of lightweight concrete containing crushed expanded polystyrene waste. *Proceedings of the Symposium MM: Advances in Materials for Cementitious Composites***,** 1-3.

Sabic, 2009. Datasheet for Linear Low Density Polyethylene for Blown Film. *Saudi Arabia for Basic polymer International company.*

Sabic, 2013. Satasheet for Polyethylene terephthalate. *Saudi Arabia for Basic polymer International company.*

Safiuddin, M., Raman, S. and Zain, M., 2007. Utilization of quarry waste fine aggregate in concrete mixtures. *Journal of Applied Sciences Research,* 3**,** 202-8.

Saikia, N. and Brito, J. d., 2013. Waste polyethylene terephthalate as an aggregate in concrete. *Materials Research,* 16**,** 341-350.

Saikia, N. and de Brito, J., 2014. Mechanical properties and abrasion behaviour of concrete containing shredded PET bottle waste as a partial substitution of natural aggregate. *Construction and Building Materials,* 52**,** 236-244.

Sakr, K. and El-Hakim, E., 2005. Effect of high temperature or fire on heavy weight concrete properties. *Cement and concrete research,* 35**,** 590-596.

Sawyers, J. P., 1995. *Method for recycling plastic into cementitions building products. United States Patent and Trademark Office-US 5422051 A.*

Schackow, A., Effting, C., Folgueras, M. V., Güths, S. and Mendes, G. A., 2014. Mechanical and thermal properties of lightweight concretes with vermiculite and EPS using air-entraining agent. *Construction and Building Materials,* 57**,** 190-197.

Seif, E.-S. S. A., 2013. Assessing the engineering properties of concrete made with fine dune sands: an experimental study. *Arabian Journal of Geosciences,* 6**,** 857-863.

Seif, E.-S. S. A., Sonbul, A. R., Hakami, B. A. H. and El-Sawy, E., 2016. Experimental study on the utilization of dune sands as a construction material in the area between Jeddah and Mecca, Western Saudi Arabia. *Bulletin of Engineering Geology and the Environment,* 75**,** 1007-1022.

Shafigh, P., Jumaat, M. Z., Mahmud, H. B. and Hamid, N. A. A., 2012. Lightweight concrete made from crushed oil palm shell: tensile strength and effect of initial curing on compressive strength. *Construction and Building Materials,* 27**,** 252-258.

Shannag, M. J., 2011. Characteristics of lightweight concrete containing mineral admixtures. *Construction and Building Materials,* 25**,** 658-662.

Shuraim, A. B., Aslam, F., Rizwan Hussain, R. and Alhozaimy, A. M., 2016. Coupled Effect of Coarse Aggregate Type and Silica Fume on Creep Coefficients of High-Strength Concrete. *Journal of Materials in Civil Engineering,* 28**,** 04016159.

Shutterstock, 2017. *Plastic waste dumping site* [Online]. Available: https://www.shutterstock.com/image-photo/plastic-waste-dumping-site-448263469 [Accessed 22 March 2017].

Siddique, R., 2004. Performance characteristics of high-volume Class F fly ash concrete. *Cement and Concrete Research,* 34**,** 487-493.

Siddique, R. and Khan, M. I., 2011. *Supplementary cementing materials*, Springer Science & Business Media.

Siddique, R., Khatib, J. and Kaur, I., 2008. Use of recycled plastic in concrete: A review. *Waste Management,* 28**,** 1835-1852.

Silva, R. V., de Brito, J. and Dhir, R. K., 2015. Prediction of the shrinkage behavior of recycled aggregate concrete: A review. *Construction and Building Materials,* 77**,** 327-339.

Silva, R. V., de Brito, J. and Saikia, N., 2013. Influence of curing conditions on the durability-related performance of concrete made with selected plastic waste aggregates. *Cement and Concrete Composites,* 35**,** 23-31.

Slabaugh, S., Swan, C. and Malloy, R., 2007. Development and properties of Foamed synthetic Lightweight Aggregates. *World of Coal Ash (WOCA) Conference.*

SoilSolutions, 2017. *drifting sand causing dangerous driving conditions* [Online]. Available: https://www.soilsolutions.com/solutions/sand-stabilization/ [Accessed 23 March 2017].

SpecialChem, 2015. *Water Absorption 24 hours* [Online]. Available: http://omnexus.specialchem.com/polymer-properties/properties/water-absorption-24-hours [Accessed 02 May 2015].

Sriningsih, W., Saerodji, M. G., Trisunaryanti, W., Armunanto, R. and Falah, I. I., 2014. Fuel production from LDPE plastic waste over natural zeolite supported Ni, Ni-Mo, Co and Co-Mo metals. *Procedia Environmental Sciences,* 20**,** 215-224.

Swan, C. and Sacks, A., 2005. Properties of synthetic lightweight aggregates for use in pavement systems. *Advances in Pavement Engineering.*

Tang, W., Lo, Y. and Nadeem, A., 2008. Mechanical and drying shrinkage properties of structural-graded polystyrene aggregate concrete. *Cement and Concrete Composites,* 30**,** 403-409.

Tanyildizi, H. and Coskun, A., 2008. Performance of lightweight concrete with silica fume after high temperature. *Construction and Building Materials,* 22**,** 2124-2129.

Tolle, D., Arthur, M. and Pomeroy, S., 1982. Fly ash use for agriculture and land reclamation: a critical literature review and identification of additional research needs. RP-1224-5. Columbus, Ohio: Battelle Columbus Laboratories.

Topçu, I. l. B. and Uğurlu, A., 2003. Effect of the use of mineral filler on the properties of concrete. *Cement and Concrete Research,* 33**,** 1071-1075.

Trucost, 2016. Plastics and Sustainability: A Valuation of Environmental Benefits, Costs and Opportunities for Continuous Improvement.

USGS, 2015. Mineral commodity summaries 2015. U.S. Geological Survey (USGS).

Verbeck, G. J. and Helmuth, R. H., 1968. Structures and physical properties of cement paste. *Proceedings of the Fifth International Symposium on the Chemistry of Cement,* 3**,** 1-32.

Wainwright, P., Cresswell, D. and Van der Sloot, H., 2002. The production of synthetic aggregate from a quarry waste using an innovative style rotary kiln. *Waste Management & Research,* 20**,** 279-289.

Wainwright, P. and Robery, P., 1997. Structural performance of reinforced concrete made with sintered ash aggregate. *Studies in environmental science,* 71**,** 411-419.

Weinecke, M. and Faulkner, B., 2002. Production of lightweight aggregate from waste materials. *Mining engineering,* 54**,** 39-43.

Wong, S., 2010. Use of recycled plastics in a pavement system. *35th Conference on Our World in Concrete and Structures.* Singapore.

XIAOPENG, L., 2005. *Structural lightweight concrete with pumice aggregate.* Master Thesis, Msc Thesis, Department of Civil Engineering, National University of Singapore.

Xu, Y., Jiang, L., Xu, J. and Li, Y., 2012. Mechanical properties of expanded polystyrene lightweight aggregate concrete and brick. *Construction and Building Materials,* 27**,** 32-38.

Yao, Z., Ji, X., Sarker, P., Tang, J., Ge, L., Xia, M. and Xi, Y., 2015. A comprehensive review on the applications of coal fly ash. *Earth-Science Reviews,* 141**,** 105-121.

Yesilata, B., Isıker, Y. and Turgut, P., 2009. Thermal insulation enhancement in concretes by adding waste PET and rubber pieces. *Construction and Building Materials,* 23**,** 1878-1882.

Zhang, G., Song, J., Yang, J. and Liu, X., 2006. Performance of mortar and concrete made with a fine aggregate of desert sand. *Building and Environment,* 41**,** 1478-1481.

Zhang, L., 2011. Fundamental mechanical properties of Lytag concrete. *2011 International Conference on Multimedia Technology (ICMT).* IEEE.

Zhang, S. and Zong, L., 2014. Evaluation of relationship between water absorption and durability of concrete materials. *Advances in Materials Science and Engineering,* 2014.

APPENDICES

Appendix A1: Tests conducted on coarse aggregate

Coarse aggregates were investigated in terms of the physical, mechanical and morphological properties. The physical properties include particle size distribution, shape and texture, unit weight, specific gravity, water absorption, voids and fineness modulus. However, mechanical performance was evaluated by measuring the aggregate's impact value. Table A1.1 presents the standards used for the coarse aggregate tests.

Table A1.1: Test standards used for coarse aggregate tests

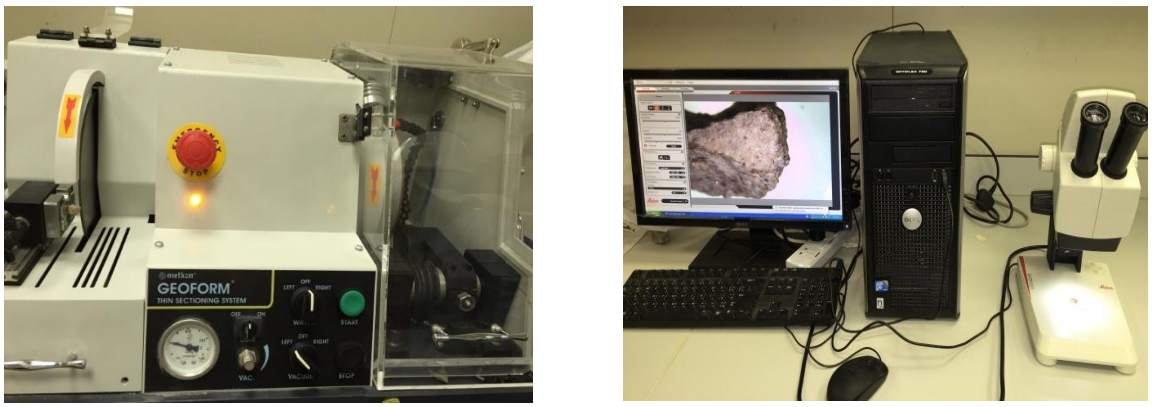
Test	Standard for normal weight aggregate	Standard for lightweight aggregate
Particle size distribution and fineness modulus	ASTM C136	ASTM C136 cited in (ASTM C330/C330M-14)
Unit weight and voids	ASTM C29/C 29M	ASTM C29/C 29M-16 cited in (ASTM C330/C330M-14)
Specific gravity	ASTM C127-15	(ASTM C127-15) cited in (ASTM C330/C330M-14)
Water absorption	ASTM C127-15	(ASTM C127-15) cited in (ASTM C330/C330M-14)
Impact value test	BS 812-112:1990	BS 812-112:1990
Ash test	-	ASTM D2584

Moreover, microscopic investigation of coarse aggregate particles was examined using scanning electron and optical microscopes. Therefore, aggregate particles were prepared for surface and cross-sectional morphology examination and elemental content determination by scanning electron microscopy (SEM) and energy dispersive X-ray (EDX). However, in the case of the optical microscope, the aggregate samples were prepared and tested in the following procedures. Firstly, aggregate particles were glued over sliding glass. Then, a flat surface of aggregate particle (see Fig. A1.1) was prepared using a diamond cutter device as

shown in Figure A1.2a. After that, the particle was washed with distilled water to prevent any contamination caused and then dried at a low temperature (less than 50 °C) for 30 min. Finally, the sample was fixed in the optical microscope and images were taken of the surface of the particles at different zoom levels, as shown in Figure A1.2b. Furthermore, the ash remaining after the test was observed in line with the test procedures explained in ASTM D2584. This test was conducted to assess the homogeneity between plastic and filler in the RPA composite.



Figure A1.1: Coarse aggregate particle after surface preparation



a b

Figure A1.2: (a) diamond cutter device and (b) optical microscope set-up

It should be noted that the required number of samples for each test is one representative sample in accordance with the ASTM C330/C330M-14. However, in this study an average of three samples was used for each test to ensure good repeatability.

Appendix A2: Tests conducted on concrete

A2.1 General

The properties of concrete containing RPAs were further investigated after evaluating the RPAs' properties, and were compared with those of NC, LWC and LAC. The concrete tests include the fresh, hardened and durability properties together with some other properties. The fresh properties comprise slump and fresh density. However, the hardened properties include dry density, compressive strength, indirect splitting tensile strength, flexural strength, modulus of elasticity and Poisson's ratio, and the abrasion test. The durability properties were examined using water absorption, chloride permeability, drying shrinkage and creep tests. Additionally, thermal conductivity and temperature curing were also examined.

It should be noted that, an average of three samples was taken at each age test as specified in the ASTM C192/C192M-16a in order to ensure good repeatability of the concrete's results. The average of three results yielded a variation within ±5% of the mean values (i.e. compressive strength for LWC0.5 at 28 days was 29.02, 31.34, 29.91, so the mean is equal to 30.09, variance is equal to 1.17, standard deviation of the mean is equal to 0.6755; so the results for compressive strength of LWC0.5 is equal to 30.09 ± 0.7).

Full details of the procedures of these tests is given in the following sections.

A2.2 Fresh properties

A2.2.1 Slump test

The workability of concrete was measured using the slump cone method in accordance with test procedures explained in the ASTM C143/C143M-15a (equivalent to BS EN 12350-2:2009). The slump cone was filled in three layers. Each layer was tamped 25 times with a tamping rod. The cone was then lifted vertically to let the concrete flow under its own weight.

Finally, the drop of concrete from an initial height was measured in mm which represents the slump of concrete, as shown in Figure A2.1.



Figure A2.1: Slump measurement using cone test method

A2.2.2 Fresh density

The fresh density of concrete is defined as the mass over volume of the fresh concrete. The fresh density was measured in line with the test method specified in the ASTM C138/C138M-16 (equivalent to BS EN 12350-6:2009). Therefore, a cylindrical mould was filled with fresh concrete in two layers. Each layer was vibrated for three seconds using a vibrating table. Subsequently, the weight of the mould filled with concrete (Fig. A2.2a) was noted. Then, the net weight of the concrete was calculated by finding the difference between the weight of the mould filled with concrete and the pre-determined empty weight of the mould.

Similarly, the volume occupied by the concrete, which is equivalent to that of water, was measured in the following manner. Firstly, the weight of the cylindrical mould filled with water (Fig. A2.2b) was noted. Then, the net weight of the water was calculated by finding the difference between the weight of the mould filled with water and the pre-determined empty

weight. Consequently, the volume occupied by the water was calculated by knowing the weight and density of the water (i.e. 998 Kg/m^3).

Finally, the fresh density of the concrete was calculated using the weight and volume of fresh concrete; where the volume occupied by concrete is equivalent to that of water.



a b

Figure A2.2: Steel mould filled with (a) concrete and (b) water

A2.3 Hardened properties

A2.3.1 Dry density

The dry density test of the concrete was conducted in line with BS EN12390-7:2009. Therefore, on the day of testing (i.e. the 28th day), cube specimens of 50 by 50 by 50 mm in dimension were taken from the curing tank and dried in the oven for 24 hrs at 105±10 °C. The next day, the specimens were taken from the oven and cooled in an airtight vessel to room temperature. Subsequently, the dry weight and the actual measurements (i.e. length, width, height) of each specimen were measured. Then, the actual volume of each specimen was computed using the actual measurements. Finally, the dry density was calculated using the dry weight and the actual volume of each cube specimen.

A2.3.2 Compressive strength

The cube and cylinder compressive strength was conducted in accordance with test procedures given in ASTM C579-01 (equivalent to BS EN 1354:2005) and ASTM C39/C39M-16b, respectively.

Therefore, the load and strength at which the cubes and cylinder failed were obtained for cube specimens of 50 by 50 by 50 mm and cylinder specimens of 100 by 200 mm, respectively. The load was applied under a constant rate of loading of 0.2 MPa/s using a compressive machine (i.e. Toni tech). Figure A2.3 shows the Toni tech machine used to measure the cube compressive strength.

Although, the cube dimensions are consistent with the size requirements described in the ASTM C579−01, the size reduction effect was investigated as the dimensions of the cube specimen does not satisfy the size requirement of BS EN 12390-3:2009 for normal concrete. The results show that the compressive strength of the 50-mm cube was relatively higher (i.e. less than 14%) than that of a standard cube (100 mm), as explained in detail in Appendix A4.

A2.3.3 Flexural strength

The flexural strength test was conducted in line with test procedures explained in the ASTM C580-02 (equivalent to ASTM C293/C293M-16). However, the specimen dimensions meet those specified in the ASTM C580-02 only.

Therefore, the flexural load at failure was observed for prismatic specimens of 40 by 40 by 160 mm using a Toni tech machine (see Fig. A2.3); where the load was applied at the centre of the specimen under a continuous rate of 0.6 mm/min. Subsequently, the flexural strength was calculated using the formula given in ASTM C293/C293M-16 or ASTM C580-02.



Figure A2.3: Toni tech loading machine

A2.3.4 Splitting tensile strength

In the case of splitting tensile strength, the test was performed in accordance with the test method described in ASTM C496/C496M-11 (equivalent to BS EN 12390-6:2000). Accordingly, a cylinder specimen of 50 by 100 mm was placed between two wooden plates in a compression machine (see Fig. A2.4); where the load was applied under a constant rate of 1 MPa/min. Finally, splitting load at failure was observed and splitting tensile strength was calculated using the formula described in the ASTM C496/C496M-11 standard.



Figure A2.4: Compression load machine (Toni tech)

A2.3.5 Modulus of elasticity and Poisson's ratio

The modulus of elasticity and Poisson's ratio of concrete under compression was assessed in line with test procedures explained in the ASTM C469/C469M-14; where a cylinder specimen of 100 by 200 mm was used. Therefore, the test was performed in the following manner.

Initially, the specimens were sulphate capped at least two hours prior to the test as specified in the ASTM C617/C617M-15. Then, the specimen was fixed in the compressometer; where two linear variable displacement transformer (LVDT) wires were connected to the data acquisition instrument to record the change in the length associated with load increase. Similarly, the compression machine was also connected to the same instrument to record the applied load.

Subsequently, the compressometer set-up was placed in the compression machine (see Fig. A2.5); where load was applied under a rate of loading of 0.2 MPa/s. The stress and axial strain were calculated; where the stress is equal to the load over area, while axial strain is equal to the average of change in length over the effective gauge length (100 mm). Finally, stress-axial strain was graphically presented and the modulus of elasticity was calculated as the slope of the stress-strain curve using the two main points. These two main points were the loads corresponding to 50 microstrain and the strain corresponding to 40 % of the ultimate load.



Figure A2.5: Set-up for modulus of elasticity and Poisson's ratio test

On the other hand, in the case of Poisson's ratio, two electrical strain gauges were attached horizontally (laterally) in the middle of the same specimen used for the modulus of elasticity; where the lateral strain was recorded. Consequently, Poisson's ratio was calculated as specified in the ASTM C469/C469M-14.

A2.3.6 Abrasion test

The abrasion test of a concrete specimen of 200 by 200 by 50 mm was conducted by following the ASTM C944/C944M-12. Therefore, the test was performed in the following procedures. Firstly, the weight of each specimen was noted to the nearest 0.1 g prior to testing and then mounted in the abrasion device (Fig. A2.6a). Then, the specimen was subjected to three cycles of normal load (i.e. 98 N) at three different representative locations; where each cycle lasted for two minutes. This abrasion cycle was performed using a dressing wheel (Fig. A2.6b) which rotates at a speed of 200 r/min. Finally, the difference in the weight before and after each abrasion cycle was noted in (g) as the weight loss.

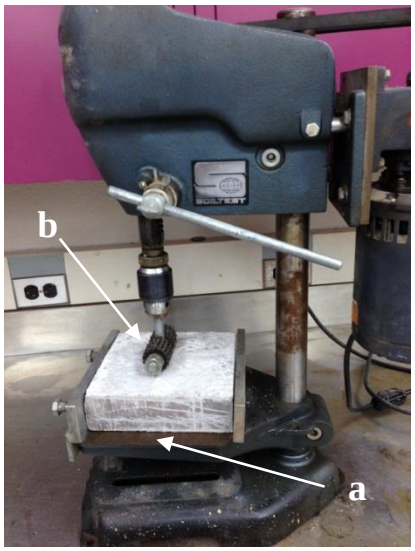


Figure A2.6: Abrasion test device comprised (a) sample plate and (b) dressing wheel

A2.3.7 Microscopic investigations

The morphological analysis of the concrete was performed using a scanning electron microscope (SEM) and an optical microscope. The microscopic investigation was performed on small thin sections of concrete samples, as shown in Figure A2.7. These samples were taken from the un-fractured side of the flexural strength specimens using a diamond cutter under running water without applying mechanical force (see Appendix A1).



Figure A2.7: Thin section of different concrete samples prepared using diamond cutter device

A2.4 Durability properties

A2.4.1 Water absorption

The 28-day water absorption of concrete was conducted in line with test procedures described in the BS EN 1881-122:2011. Therefore, the weight of the specimens in the saturated surface dry (SSD) and oven dry (OD) conditions was measured. Then, the amount of water inside the sample was calculated as the difference between the weights of saturated surface dry (SSD) and the oven dry (OD). Finally, the water absorption was expressed in % as the ratio between the weights of water inside the specimen to its OD weight.

A2.4.2 Chloride permeability

The resistance of concrete to the chloride ion penetration was performed for concrete 100 × 50 mm cylinders in accordance with ASTM C1202-12. Thus, the test was conducted in four stages (i.e. preparation, suction, saturation, testing), according to the following procedures.

Initially, the preparation stage was performed on the day of testing (i.e. 28 day); where the periphery of the specimens was glued except the top and bottom sides. Then suction and saturation processes were performed, as shown in Figure A2.8. The specimens were placed in the desiccators; where they were subjected to a suction process (i.e. air vacuum) for 3 hrs using a vacuum pump. After that, the saturation process was started immediately; where the water inlet was opened until the specimens were fully submerged. Finally, the specimens were subjected to air vacuuming for another hour and then kept in the water for 18 hrs.

The charge passed through the samples was then measured as follows. Firstly, the sample was fixed between two cells (Fig. A2.9); where one side was filled with sodium chloride (NaCl), while the other side was filled with sodium hydroxide (NaOH). Then, two power cables (Fig. A2.9) were connected to these cells; where the negative terminal was connected to the NaCl cell, whereas the positive terminal was connected to the NaOH cell. Finally, the charge passing through the samples within 6 hrs was observed; where the current was connected to the cells using a power supply device.

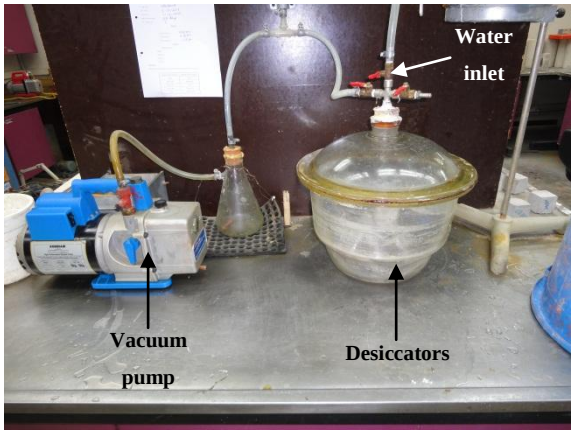


Figure A2.8: Desiccators, water inlet, and vacuum pump used in suction and saturation processes

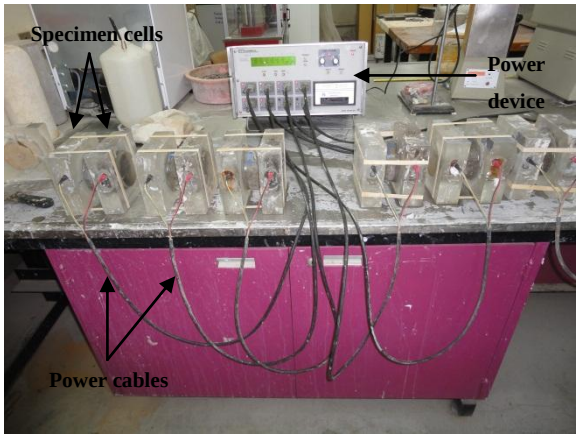


Figure A2.9: Chloride ion penetration test set-up i.e. specimen cells, power cables, and power device

A2.4.3 Drying shrinkage

Drying shrinkage of a concrete specimen was conducted in accordance with test procedures explained in ASTM C157/C157M-08. Therefore, the change in the linear dimension of concrete prisms of 75 by 75 by 285 mm was measured in the following manner. Firstly, concrete prisms were cast in steel moulds having metallic studs at the ends, in two layers with a vibration of 15 seconds per layer. Then, the surface was smoothed, and the screws were loosened and properly covered by the plastic sheet to avoid any moisture loss. Specimens were demoulded after 24±4 hrs and immersed in curing tanks for 45 to 60 minutes. Then the samples were removed from the curing tanks and the initial comparator dial gauge readings were noted for both the reference bar (Fig. A2.10a) and concrete sample (Fig. A2.10b). After that, specimens were returned back to the curing tanks; where they were cured for 7 days. On the 7^{th} day of curing, the samples were removed from the curing tanks and gauge readings for the reference bar and concrete sample were immediately noted. Finally, the concrete samples were then stored or cured, in the air environment; where a weekly reading were observed for specimens up to 182-day.



a b

Figure A2.10: Drying shrinkage set-up with (a) reference bar and (b) concrete sample

A2.4.4 Creep test

The creep test was conducted for concrete 100 by 200 mm cylinders in line with ASTM C512/C512M-10. Figure A2.11 shows the creep test set-up; where the specimens were prepared and tested as follows. Initially, samples used for time dependent strain (i.e. samples subjected to load) were prepared with sulphate capping; while those used for shrinkage strain measurements (i.e. unloaded sample) were not capped . Then, electrical strain gauges having 60 and 1 mm length and width, respectively were fixed vertically in the middle of each specimen's sides, as shown in Figures A2.11 and A2.12. After that, samples used for time dependent strain were placed in a series in the loading frame, as shown in Figure A2.12a; where these frames together with unloaded samples (i.e. shrinkage samples) (Fig. A2.12b) were placed in a controlled chamber with relative humidity and temperature of 38±4% and 23±2 °C, respectively. Subsequently, the electrical strain gauges for both loaded and unloaded samples were connected to the data acquisition instrument, to record strain readings.

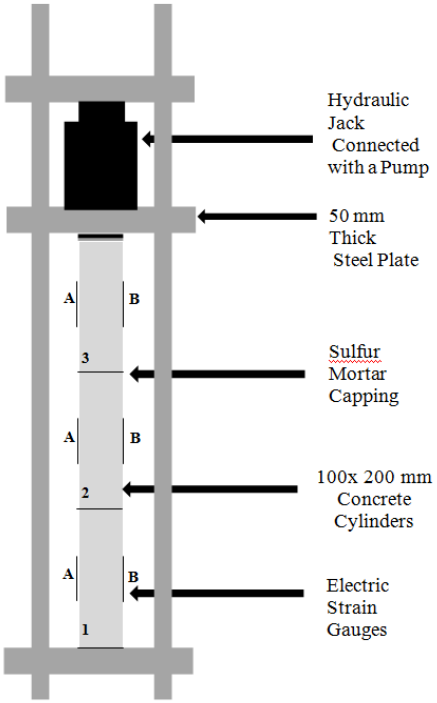


Figure A2.11: Creep test setup



a b

Figure A2.12: Creep setup with (a) loaded sample and (b) unloaded samples

At loading, specimens were loaded at a pressure equivalent to 40% of the ultimate compressive strength using a hydraulic jack that was placed on each frame (see Fig. A2.11, A2.12). This pressure was frequently maintained as it should not exceed 2% lower than that of the initial reading. The reading of the initial strain (instantaneous strain) was noted immediately after the loading and was continuously recorded for over 1 year. The data

reading intervals were automatically programmed to be taken every 15 min which is more than those specified in ASTM C 512.

Consequently, the strain induced by shrinkage was calculated at any time as the average of the strain readings of the unloaded samples. However, the time dependent strain induced by creep and shrinkage was calculated at any time as the average of the strain readings of the loaded samples.

Moreover, the strain induced by creep only was calculated at any time as the difference between the time dependent strain (i.e. for loaded samples) and shrinkage strain (i.e. for unloaded samples). Finally, the creep coefficient was computed at any time as follows:

$$Creep\ coeffiecent = \frac{Creep\ strain - \ Instantaneous\ strain}{Instantaneous\ strain}$$

A2.5 Physical properties

A2.5.1 Thermal conductivity

There are different test methods used to measure the thermal conductivity in steady and non-steady states, such as hot guarded plate and hot weir (ASTM C177-13; BS EN 12664:2001). In this study, thermal conductivity was conducted for a concrete 50 by 50 by 5 cm slab, using the guarded hot plate technique in accordance with ASTM C177-13. Figures A2.13 and A2.14 depict the test set-up; where thermal conductivity was observed in two different conditions as follows. Firstly, in the case of the saturated condition, a sample was taken from the curing tank and visible water only was removed using a soft cloth until an SSD state was achieved. The sample was then placed in the measurement system (Fig. A2.14a) and was insulated from four sides using insulation foam (Fig. A2.14b) to prevent heat flow from the periphery. After that, the sheet and its sensors were placed on the upper side of the specimen in order to record

the heat passing through the specimen, as shown in Figure A2.14c. Finally, the test measurement system was closed in order to start the test. The heat flow measured in the previous step was continuously recorded using programme software (i.e. Lambda 2010 software) until heat flow became constant.

However, in the case of the dry condition, the sample used previously in the wet condition was removed from the measurement system and oven dried for 72 hrs. After that, the specimen was air cooled at room temperature for 1 hr. Then, thermal conductivity in the dry condition was measured using the same procedures used earlier in the saturated condition.

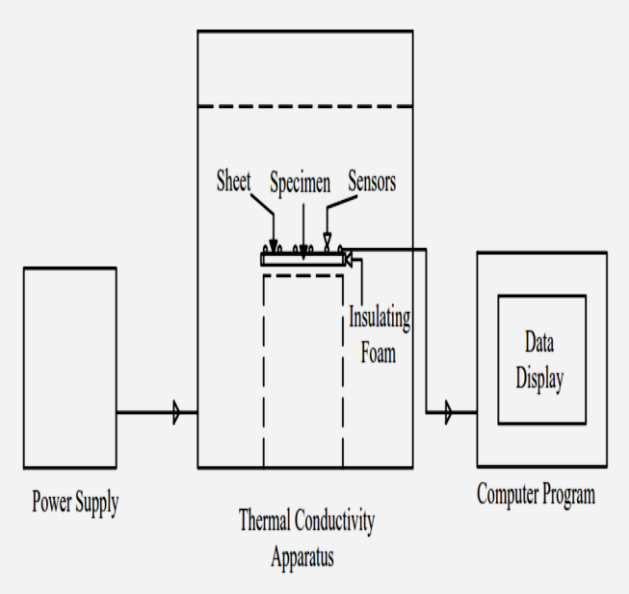


Figure A2.13: Thermal conductivity setup



a b c

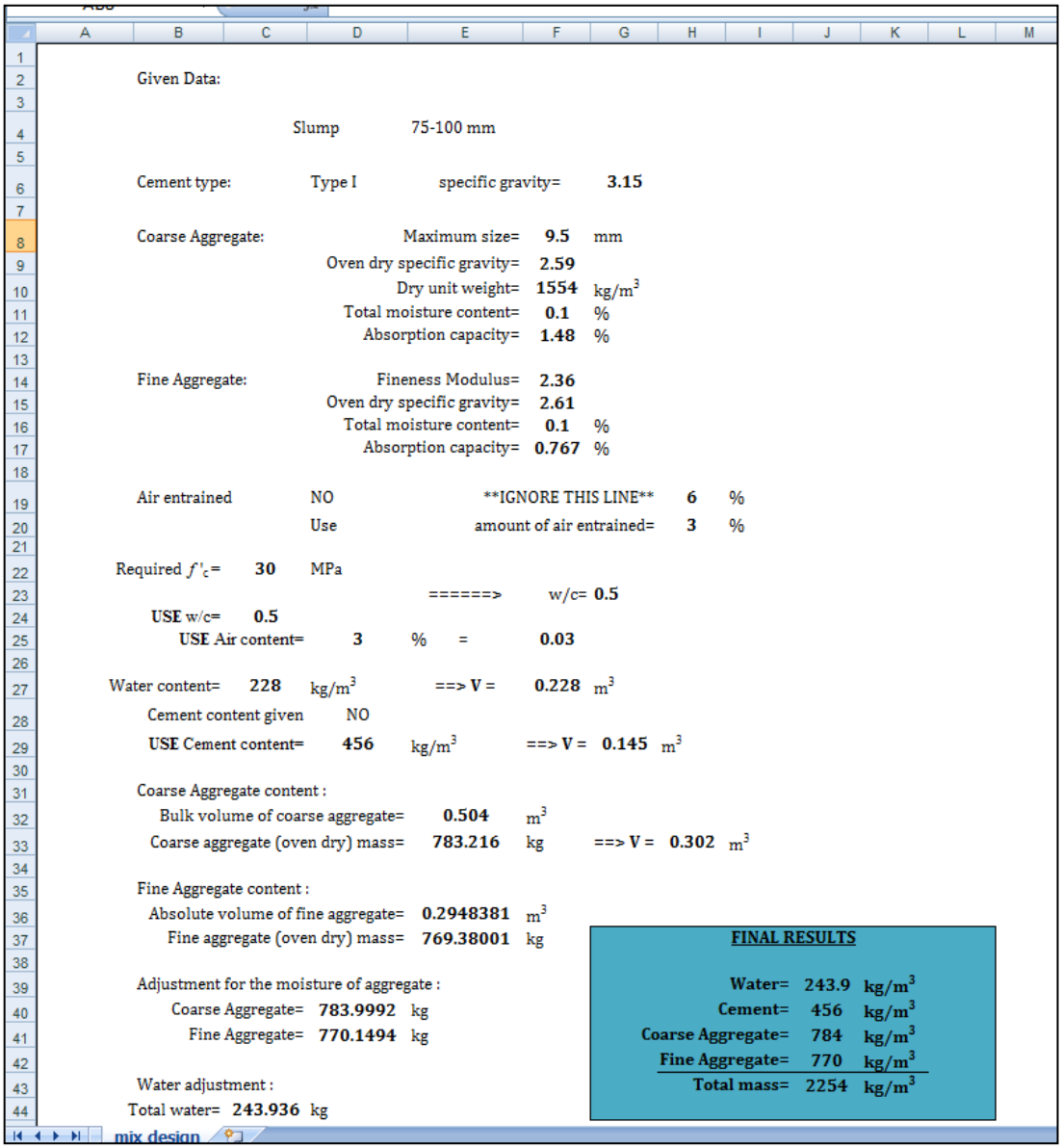
Figure A2.14: Measurement system of thermal conductivity

A2.5.2 Temperature curing

The effect of temperature curing on the compressive strength was investigated using a concrete 50 by 50 by 50 mm cube. Therefore, concrete specimens were prepared using the same procedures used in the compressive strength tests. Then, after 24 hr, specimens were demoulded and cured in a controlled curing tank at two different temperature levels (i.e. 30±2 °C, 40±2 °C) until the day of testing. On the day of testing (i.e. 28 day), the specimens were taken from the curing tanks; where the compressive strength was observed in the same way as explained earlier in section A2.3.2. Finally, these values were compared with 28-day compressive strength measured at standard curing (i.e. 20±2 °C).

Appendix A3: Sample calculations of mix design

1-Mix design of NC (as control mix) using ACI 211.1



Given Data:

Slump 75-100 mm

Cement type: Type I specific gravity= **3.15**

Coarse Aggregate: Maximum size= **9.5** mm
Oven dry specific gravity= **2.59**
Dry unit weight= **1554** kg/m^3
Total moisture content= **0.1** %
Absorption capacity= **1.48** %

Fine Aggregate: Fineness Modulus= **2.36**
Oven dry specific gravity= **2.61**
Total moisture content= **0.1** %
Absorption capacity= **0.767** %

Air entrained NO **IGNORE THIS LINE** **6** %
Use amount of air entrained= **3** %

Required f'_c= **30** MPa
=======> w/c= **0.5**
USE w/c= **0.5**
USE Air content= **3** % = **0.03**

Water content= **228** kg/m^3 ==> **V** = **0.228** m^3
Cement content given NO
USE Cement content= **456** kg/m^3 ==> **V** = **0.145** m^3

Coarse Aggregate content :
Bulk volume of coarse aggregate= **0.504** m^3
Coarse aggregate (oven dry) mass= **783.216** kg ==> **V** = **0.302** m^3

Fine Aggregate content :
Absolute volume of fine aggregate= **0.2948381** m^3
Fine aggregate (oven dry) mass= **769.38001** kg

Adjustment for the moisture of aggregate :
Coarse Aggregate= **783.9992** kg
Fine Aggregate= **770.1494** kg

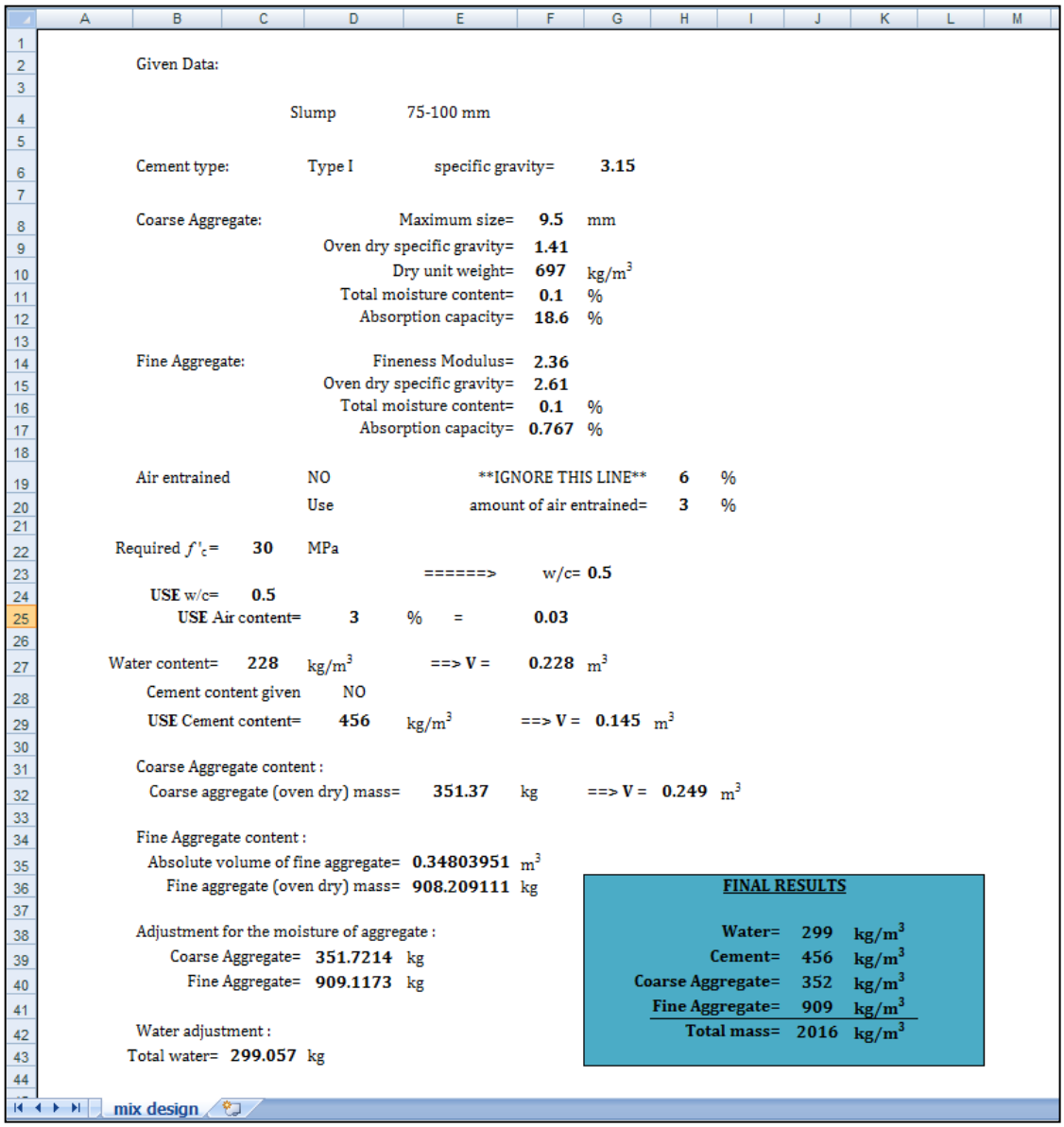
Water adjustment :
Total water= **243.936** kg

FINAL RESULTS

Water=	**243.9**	**kg/m^3**
Cement=	**456**	**kg/m^3**
Coarse Aggregate=	**784**	**kg/m^3**
Fine Aggregate=	**770**	**kg/m^3**
Total mass=	**2254**	**kg/m^3**

mix design

2-Mix design of LWC (as control mix) using ACI 211.2-98



Given Data:

Slump 75-100 mm

Cement type: Type I specific gravity= **3.15**

Coarse Aggregate:
Maximum size= **9.5** mm
Oven dry specific gravity= **1.41**
Dry unit weight= **697** kg/m^3
Total moisture content= **0.1** %
Absorption capacity= **18.6** %

Fine Aggregate:
Fineness Modulus= **2.36**
Oven dry specific gravity= **2.61**
Total moisture content= **0.1** %
Absorption capacity= **0.767** %

Air entrained NO **IGNORE THIS LINE** **6** %
Use amount of air entrained= **3** %

Required f'_c= **30** MPa
=======> w/c= **0.5**
USE w/c= **0.5**
USE Air content= **3** % = **0.03**

Water content= **228** kg/m^3 ==> V = **0.228** m^3
Cement content given NO
USE Cement content= **456** kg/m^3 ==> V = **0.145** m^3

Coarse Aggregate content :
Coarse aggregate (oven dry) mass= **351.37** kg ==> V = **0.249** m^3

Fine Aggregate content :
Absolute volume of fine aggregate= **0.34803951** m^3
Fine aggregate (oven dry) mass= **908.209111** kg

Adjustment for the moisture of aggregate :
Coarse Aggregate= **351.7214** kg
Fine Aggregate= **909.1173** kg

Water adjustment :
Total water= **299.057** kg

FINAL RESULTS

Water=	**299**	**kg/m^3**
Cement=	**456**	**kg/m^3**
Coarse Aggregate=	**352**	**kg/m^3**
Fine Aggregate=	**909**	**kg/m^3**
Total mass=	**2016**	**kg/m^3**

mix design

3-Mix design of RP2F1C0.5

	A	B	C	D	E
1	Mix design of RP2F1C0.5				
2	Properties of coarse aggregate of reference aggregate			Calculations	
3	Dry unit weight of reference aggregate	697.00		1- Amount of free mixing water (kg/m3)	228
4	Specific Gravity (OD Basis) of reference aggregate	1.41		Volume of water (m3)	0.228
5	Absorption(%) of reference aggregate	18.60		2-Amount of air (%)	3.00
6	Moisture content (%) of reference aggreate	0.10		Volume of air (m3)	0.03
7	Maximum aggregate size (mm)	9.50		3-W/C	0.50
8	Amount of reference aggregate(kg/m3)	351.37		4-Amount of cement (kg/m3)	456
9	Replacement level (%)	0.00		Volume of cement (m3)	0.1448
10				5-Coarse aggregates calculations	
11	Properties of coarse aggregate of RPA			Amount of coarse aggregate of RPA (kg/m3)	378.09
12	Dry unit weight of RPA	750.00		Amount of coarse aggregate of reference aggregate (kg/m3)	0.00
13	Specific Gravity (OD Basis) of RPA	1.48		Volume of coarse aggregate of RPA (m3)	0.2555
14	Absorption (%) of RPA	2.75		Volume of coarse aggregate of reference aggregate (m3)	0.00
15	Moisture content (%) of RPA	0.10		6-Fine aggregate calculations	
16	Maximum aggregate size (mm)	9.50		Volume of fine aggregate (m3)	0.3418
17	Replacement level (%)	100.00		Amount of fine aggregate (kg/m3)	891.857
18				7-Adjutment for the moisture of aggregates	
19	Properties of normal weight fine aggregate			Amount of coarse aggregate of RPA (kg/m3)	378
20	Specific Gravity (OD Basis) of red sand	2.62		Amount of coarse aggregate of reference aggregate (kg/m3)	0.00
21	Specific Gravity (OD Basis) of crushed sand	2.59		Amount of fine aggregate (kg/m3)	893
22	Absorption (%) of red sand	0.28		8-Total water calculations	
23	Absorption(%) of crushed sand	1.67		Amount of total water (kg/m3)	244.0
24	Moisture content (%) of red sand	0.10			
25	Moisture content (%) of crushed sand	0.10			
26					
27	Properties of cement				
28	Cement Specific Gravity	3.15			

4-Mix design of RP3F3C0.5

	A	B	C	D	E
1	Mix design of RP3F3C0.5				
2	Properties of coarse aggregate of reference aggregate			Calculations	
3	Dry unit weight of reference aggregate	697.00		1- Amount of free mixing water (kg/m3)	228
4	Specific Gravity (OD Basis) of reference aggregate	1.41		Volume of water (m3)	0.228
5	Absorption(%) of reference aggregate	18.6		2-Amount of air (%)	3.00
6	Moisture content (%) of refrence aggreate	0.10		Volume of air (m3)	0.03
7	Maximum aggregate size (mm)	9.50		3-W/C	0.50
8	Amount of reference aggregate (kg/m3)	351.37		4-Amount of cement (kg/m3)	456
9	Replacement level (%)	0.00		Volume of cement (m3)	0.1448
10				5-Coarse aggregates calculations	
11	Properties of coarse aggregate of RPA			Amount of coarse aggregate of RPA (kg/m3)	564.11
12	Dry unit weight of RPA	1119.00		Amount of coarse aggregate of reference aggregate (kg/m3)	0.00
13	Specific Gravity (OD Basis) of RPA	1.79		Volume of coarse aggregate of RPA (m3)	0.3151
14	Absorption (%) of RPA	0.95		Volume of coarse aggregate of reference aggregate (m3)	0.00
15	Moisture content (%) of RPA	0.10		6-Fine aggregate calculations	
16	Maximum aggregate size (mm)	9.50		Volume of fine aggregate (m3)	0.2821
17	Replacement level (%)	100.00		Amount of fine aggregate (kg/m3)	736.125
18				7-Adjutment for the moisture of aggregates	
19	Properties of normal weight fine aggregate			Amount of coarse aggregate of RPA (kg/m3)	565
20	Specific Gravity (OD Basis) of red sand	2.62		Amount of coarse aggregate of reference aggregate (kg/m3)	0.00
21	Specific Gravity (OD Basis) of crushed sand	2.59		Amount of fine aggregate (kg/m3)	737
22	Absorption (%) of red sand	0.28		8-Total water calculations	
23	Absorption(%) of crushed sand	1.67		Amount of total water (kg/m3)	237.7
24	Moisture content (%) of red sand	0.10			
25	Moisture content (%) of crushed sand	0.10			
26					
27	Properties of cement				
28	Cement Specific Gravity	3.15			

5-Mix design of LAC

	A	B	C	D	E
1	Mix design of LAC				
2	Properties of coarse aggregate of reference aggregate			Calculations	
3	Dry unit weight of reference aggregate	697.00		1- Amount of free mixing water (kg/m3)	225
4	Specific Gravity (OD Basis) of reference aggregate	1.41		Volume of water (m3)	0.225
5	Absorption(%) of reference aggregate	18.60		2-Amount of air (%)	3.00
6	Moisture content (%) of reference aggreate	0.10		Volume of air (m3)	0.03
7	Maximum aggregate size (mm)	9.50		3-W/C	0.50
8	Amount of reference aggregate(kg/m3)	351.37		4-Amount of cement (kg/m3)	450
9	Replacement level (%)	0.00		Volume of cement (m3)	0.1429
10				5-Coarse aggregates calculations	
11	Properties of coarse aggregate of LYA			Amount of coarse aggregate of LYA (kg/m3)	448.51
12	Dry unit weight of RPA	889.69		Amount of coarse aggregate of reference aggregate (kg/m3)	0.00
13	Specific Gravity (OD Basis) of LYA	1.44		Volume of coarse aggregate of LYA (m3)	0.3115
14	Absorption (%) of LYA	16.82		Volume of coarse aggregate of reference aggregate (m3)	0.0000
15	Moisture content (%) of LYA	0.70		6-Fine aggregate calculations	
16	Maximum aggregate size (mm)	9.50		Volume of fine aggregate (m3)	0.2907
17	Replacement level (%)	100.00		Amount of fine aggregate (kg/m3)	758.526
18				7-Adjutment for the moisture of aggregates	
19	Properties of normal weight fine aggregate			Amount of coarse aggregate of LYA(kg/m3)	452
20	Specific Gravity (OD Basis) of red sand	2.62		Amount of coarse aggregate of reference aggregate (kg/m3)	0
21	Specific Gravity (OD Basis) of crushed sand	2.59		Amount of fine aggregate (kg/m3)	759
22	Absorption (%) of red sand	0.28		8-Total water calculations	
23	Absorption(%) of crushed sand	1.67		Amount of total water (kg/m3)	302.4
24	Moisture content (%) of red sand	0.10			
25	Moisture content (%) of crushed sand	0.10			
26					
27	Properties of cement				
28	Cement Specific Gravity	3.15			

6-Mix design of RP2F1C25

	A	B	C	D	E
1	Mix design of RP2F1C25				
2	Properties of coarse aggregate of reference aggregate			Calculations	
3	Dry unit weight of reference aggregate	697.00		1- Amount of free mixing water (kg/m3)	225
4	Specific Gravity (OD Basis) of reference aggregate	1.41		Volume of water (m3)	0.225
5	Absorption(%) of reference aggregate	18.60		2-Amount of air (%)	3.00
6	Moisture content (%) of reference aggreate	0.10		Volume of air (m3)	0.03
7	Maximum aggregate size (mm)	9.50		3-W/C	0.50
8	Amount of reference aggregate(kg/m3)	351.37		4-Amount of cement (kg/m3)	450
9	Replacement level (%)	75.00		Volume of cement (m3)	0.1429
10				5-Coarse aggregates calculations	
11	Properties of coarse aggregate of RPA			Amount of coarse aggregate of RPA (kg/m3)	94.52
12	Dry unit weight of RPA	750.00		Amount of coarse aggregate of reference aggregate (kg/m3)	263.53
13	Specific Gravity (OD Basis) of RPA	1.48		Volume of coarse aggregate of RPA (m3)	0.0639
14	Absorption (%) of RPA	2.75		Volume of coarse aggregate of reference aggregate (m3)	0.1869
15	Moisture content (%) of RPA	0.10		6-Fine aggregate calculations	
16	Maximum aggregate size (mm)	9.50		Volume of fine aggregate (m3)	0.3514
17	Replacement level (%)	25.00		Amount of fine aggregate (kg/m3)	916.920
18				7-Adjutment for the moisture of aggregates	
19	Properties of normal weight fine aggregate			Amount of coarse aggregate of RPA (kg/m3)	95
20	Specific Gravity (OD Basis) of red sand	2.62		Amount of coarse aggregate of reference aggregate (kg/m3)	264
21	Specific Gravity (OD Basis) of crushed sand	2.59		Amount of fine aggregate (kg/m3)	918
22	Absorption (%) of red sand	0.28		8-Total water calculations	
23	Absorption(%) of crushed sand	1.67		Amount of total water (kg/m3)	282.4
24	Moisture content (%) of red sand	0.10			
25	Moisture content (%) of crushed sand	0.10			
26					
27	Properties of cement				
28	Cement Specific Gravity	3.15			

Appendix A4: Investigating of specimen size effect

The effect of the specimen size on the compressive strength was investigated using a 50-mm cube and a 100-mm cube in accordance with test procedures explained in ASTM C579-02 and BS EN 12390-3:2009, respectively. Figure A4.1 compares the 28-day compressive strength of LWC, RP3F1C, RP3F3C and RP4F2C using the 50-mm cube with those of the 100-mm cube.

As can be seen in Figure A4.1, the 28-day compressive strength of the 50-mm cube was higher than that of the 100-mm cube by 15, 8, 12 and 13 % for LWC, RP3F1C, RP3F3C and RP4F2C respectively. Therefore, these results suggest that the increase in compressive strength due to the reduction in the specimens' size was less prominent in RPA concrete as compared to LWA concrete.

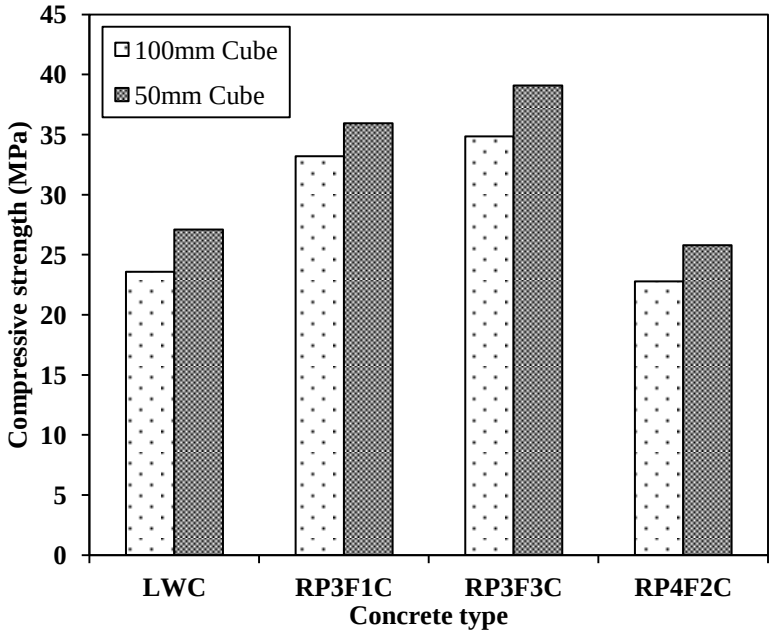


Figure A4.1: Compressive strength for standard and proposed specimens sizes